



SAPIENZA
UNIVERSITÀ DI ROMA

FACOLTA' DI SCIENZE MATEMATICHE, FISICHE E NATURALI

PhD Thesis in Chemical Sciences

XXVI Cycle (2010-2013)

**NONCOVALENT BIFUNCTIONAL ORGANOCATALYSIS
APPLIED TO THE ACHIEVEMENT OF CHIRAL EPOXIDES
AND 1,2-DIOLS**

Chiara Palumbo

Supervisor

Prof. M. Antonietta Loreto

Head of PhD School

Prof. Lucio D'Ilario

TABLE OF CONTENTS

LIST OF SYMBOLS AND ABBREVIATIONS	iv
1. INTRODUCTION	6
1.1 The concept of Symmetry	7
1.2 Chirality	8
1.3 Formation of chiral compounds	10
1.3.1 The three approaches	10
1.3.2 Chiral pool	11
1.3.3 Chiral resolution	12
1.3.4 Enantioselective synthesis	15
1.3.5 Asymmetric catalysis	17
1.5 Enantioselective Organocatalysis	19
1.5.1 A new concept	19
1.5.2 The history of Organocatalysis	20
1.5.3 Covalent or Noncovalent Organocatalysis	21
1.5.4 Noncovalent organocatalysis	22
1.5.5 Hydrogen bonding organocatalysis	23
1.5.6 Brønsted acids organocatalysis	25
2. OBJECTIVE OF THE THESIS	29
3. ENANTIOSELECTIVE NUCLEOPHILIC EPOXIDATION OF 3-YLIDENEOXINDOLES	32
3.1 Organocatalysis for the epoxidation of electron-deficient olefins	33
3.2 Target molecules	41
3.2.1 Spiro oxindoles	41
3.2.2 Asymmetric synthesis of spiroepoxy oxindoles	43
3.3 Results and discussion	46
3.3.1 A foreword and first experiments	46
3.3.2 Screening of the catalyst and of reaction conditions	48
3.3.3 Structural and stereochemical assignment	51
3.3.4 Mechanistic considerations	57
3.3.5 Substrate scope	61
3.3.6 In-depth catalyst screening	65
3.3.7 Synthesis of 3-ylidenoxindoles	74

3.3.8 Enlargement of the substrate scope	79
3.4 Conclusions	86
4. KINETIC RESOLUTION OF DIOLS BEARING A QUATERNARY STEREOCENTER <i>VIA</i> ASYMMETRIC ACETALIZATION	91
4.1 Confined Brønsted acids Organocatalysis applied to acetalization	92
4.2 Vicinal diols bearing a quaternary stereocenter	93
4.3 Results and discussion	94
4.3.1 Sharpless approach to optically active vicinal diols: catalytic asymmetric dihydroxylation	94
4.3.2 Strategy and first experiments	96
4.3.3 Catalyst screening	98
4.3.4 Reaction conditions optimization	103
4.3.5 Synthesis of the diols	108
4.3.6 Substrate scope	110
4.3.7 Mechanism hypothesis and considerations on the stereochemistry assignment	114
4.4 Conclusions	115
EXPERIMENTAL PART	119
General experimental	120
General procedure for preparing 1-methyl-indole-2,3-diones 172, 173.	122
Characterization of 1-methyl-indole-2,3-diones 172, 173.	122
General procedure for preparing 1-methylindol-2,3-diones 131, 168-171, 175, 178	123
Characterization of 1-methylindol-2,3-diones 131, 168-171, 175, 178	123
General procedure for preparing 3-ylidenoxindole 180	125
Characterization of 3-ylidenoxindole 180	126
General procedure for preparing 3-ylideneoxindoles 132, 146-150, 154-156, 181	
Characterization of 3-ylideneoxindoles 132, 146-150, 154-156, 181, 210-215	127
General procedure for preparing 3-ylideneoxindoles 151, 152	138
Characterization of 3-ylideneoxindoles 151, 152	138
General procedure for preparing 3-ylideneoxindoles 153, 232	139
Characterization of 3-ylideneoxindoles 153, 232	139
General procedure for preparing 3-ylideneoxindoles 233-237	140
Characterization of 3-ylideneoxindoles 233-237	141
Procedure for preparing 3-ylideneoxindole 239	143
Characterization of 3-ylideneoxindole 239	143
Procedure for preparing 3-ylideneoxindole 224	144
Characterization of 3-ylideneoxindole 224	144

General procedure for the Asymmetric Epoxidation	145
Characterization of epoxides 133, 182-193, 240-260	145
General procedure for the synthesis of 1,2-diols 277, 284-290 (procedure 1)	179
General procedure for kinetic resolution of diols (procedure 2)	180
Characterization of diols 277, 284-290	181
Characterization of acetals 281, 291, 296	183
General procedure for preparing catalyst H	185
Characterization of 209 and H	186
Assignment of configurations of epoxides	187
References	194

LIST OF SYMBOLS AND ABBREVIATIONS

*	Designating chiral moiety
Ac	Acetyl
Ar	Aryl, aromatic
Aq.	aqueous
BA	Brønsted acid
Boc	<i>tert</i> -butyloxycarbonyl
Calcd	calculated
BINOL	1,1'-bi-2-naphthol
Bn	Benzyl
Cat.	catalyst/catalytic
Conv.	conversion
d	doublet
DCM	Dichloromethane
DMF	Dimethylformamide
DMSO	Dimethylsulfoxide
dr	diastereomeric ratio
EI	Electron Impact
equiv	equivalent(s)
<i>ee</i>	enantiomeric excess
<i>er</i>	enantiomeric ratio
Et	ethyl
ESI	electrospray ionization
GC (GC-MS)	gas chromatography (gas chromatography coupled with mass detection)
HOMO	highest occupied molecular orbital
HPLC	high performance liquid chromatography
HRMS	high resolution mass spectrometry
HX*	designating chiral Brønsted acids, e.g. chiral phosphoric acid diesters
L	ligand (abbreviation used in schemes)
LA	Lewis acid
LDA	lithium diisopropylamide
LUMO	lowest unoccupied molecular orbital
<i>m</i>	<i>meta</i>
M	multiplet
M	molar (concentration)
Me	methyl
MTBE	methyl <i>tert</i> -butyl ether
MW	molecular weight
<i>m/z</i>	atomic mass units per charge
NMR	nuclear magnetic resonance spectroscopy
NOESY	nuclear Overhauser effect spectroscopy
NuH/Nu	nucleophile

<i>o</i>	<i>ortho</i>
<i>p</i>	<i>para</i>
Ph	phenyl
PG	protecting group
Pr	propyl
quint	quintet
<i>rac.</i>	racemic
r.t.	room temperature
t	triplet
TFA	trifluoroacetic acid
THF	tetrahydrofuran
TLC	thin layer chromatography
TMS	trimethylsilyl
TRIP	3,3'-bis(2,4,6-triisopropylphenyl)-1,1'-binaphthyl-2,2'-diyl hydrogen phosphate

1. INTRODUCTION

“ Dans la vie, rien n'est à craindre, tout est à comprendre”^a

Marie Curie

^a “ In life, nothing has to be feared, everything has to be understood” Marie Curie

1.1 The concept of Symmetry

“*Naturalis potestas ita architectata est*”^b

Marcus Vitruvius Pollio

Ad pulchritudinem tria requiruntur...

...et debita proportio sive consonantia”

Thomas Aquinas^c

The term ‘symmetry’ derives from the Greek word ‘συμμετρεῖν’ (symmetreín) which is the sum of ‘σύν’ (‘syn’, meaning ‘with’) and μέτρον (‘metron’, meaning ‘measure’). Moreover this word was frequently invoked in ancient greek texts that dealt with the beauty and the good and originally meant a relation of commensurability. However its meaning has changed during the centuries. Its subsequent Latin transliteration, *symmetria* was adopted by Vitruvius in the influential theory of architecture (Vitruvius *praecepta symmetriarum*, in *De Architectura*), in which he wrote about symmetry as the proportion of the body and the buildings. In book III he wrote: ‘*Symmetry is a proper agreement among the members of the work itself, and relation between the different parts and the whole general scheme, in accordance with a certain part selected as standard.*’ And then: ‘*in perfect buildings the different members must be in exact symmetrical relations to the whole general scheme*’. In fact here Vitruvius meant proportion, assigning to this characteristic charm and harmony; moreover he did not even call attention to the correspondence of the limbs, thus he was far away from the concept of relationship between mirror images. Saint Thomas Aquinas in the *Summa Theologiae*, stated the correlation between beauty and “consonantia”, meaning proportion as well.

Throughout some centuries symmetry kept this meaning until the 1436, when the Italian artist Alberti in his *De picture* wrote about symmetry of a human body, clearly differentiating it from proportion. At that time the concept was still not clear and explicit.

In fact during the Renaissance a transformation occurred and this concept finally changed: in the 1794 the mathematician Legendre adopted the term symmetry without

^b “The architect was the power of Nature” Marcus Vitruvius Pollio, *De Architectura*

^c St. Thomas Aquinas, *Summa Theologiae*

the aesthetic sense, thus bestowing the scientific community and effectively introducing the modern meaning of symmetry. Indeed this was a revolution.^d

1.2 Chirality

“All the rigid regularities are inherently revolting to the taste, because their observation do not offer lasting pleasures”

“I shall call a body which is exactly equal and similar to another, but which cannot be enclosed in the same limits as that other, its incongruent counterpart”

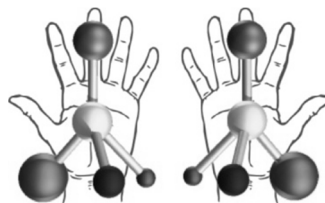
Immanuel Kant

The observation of symmetry and asymmetry in bodies and in general in the whole universe is an ancient matter, even though it has not been rationalized for a long time. In the 18th century Kant was the first philosopher to find something interesting in mirror images of asymmetric objects and he called them ‘incongruent counterparts’, taking advantage of some examples related to human bodies, as the right and left hands. In discordance to the classical concept of beauty, he attributed to ‘rigid regularities’ a feeling of boredom and a sense of ugliness.^e The matter of this dissertation is related to those that Kant called incongruent counterparts, that in chemistry are the enantiomers of a molecule, the left-handed and the right-handed; the easiest way to understand this concept is comparing our hands, as Kant mentioned in his pioneering considerations, that are mirror images but not superimposable, like the enantiomers (Figure 1).

^d Goldstein, B., *From Summetria to Symmetry: the making of a Revolutionary Concept*, Springer, **2008**;
Heilbronner, E. *Reflections on symmetry: In Chemistry and elsewhere*, Wiley, **1993**.

^e Hall, B., *The Arguments of Kant’s Critique of Pure Reason*, Lexington Books, **2010**.

Figure 1: right and left hands compared to two enantiomers



In fact this feature is observed in molecules having a specific property, chirality. The word, firstly introduced in 1904, derives from Greek ‘ $\chi\epsilon\iota\rho$ ’ (‘kheir’, meaning ‘hand’). A chiral molecule is not superimposable on its mirror image. The discovery of chirality happened in 1815, with the observation of Jean Baptiste Biot that some molecules could rotate the polarized light plane.¹

The occurrence of only one enantiomer of a molecule in nature is connected to the evidence that enantiomers have different biological activity and in general that they have a different behaviour in a chiral environment, despite they have the same physical/chemical properties. Thus enzymes, receptors and biologically occurring chiral molecules behave in a different way towards the left-handed or the right-handed enantiomer of a chemical or drug. For instance some different fragrances are isomers of the same molecule, for example (*S*)-limonene (**1**) smells like pine, instead (*R*)-limonene (**2**) smells like lemon (Figure 2). One can distinguish the two fragrances because of our nasal receptors, made of chiral molecules able to recognise the difference between the two enantiomers.

Figure 2: limonene enantiomers and respective different fragrances: pine and lemon.

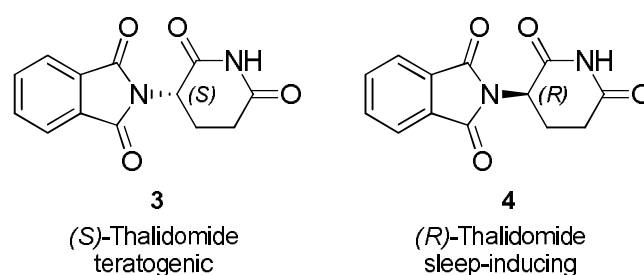


Other examples are molecules used by insects as sexual attractors, pheromones, as well as most of the commercialized drugs. Biochemical processes are strongly affected by stereochemical differences, because of the chirality of the involved molecules. A tragic example is Thalidomide, a sedative drug which was broadly prescribed to pregnant women to avoid nausea because it did not cause dependence (Figure 3); unfortunately

one of the two enantiomers was responsible for foetus deformities as teratogen agent. Moreover, in this particular case, an additional problem is *in vivo* racemization of (*R*)-Thalidomide into the (*S*)-Thalidomide; so even if the drug had been commercialized as a single enantiomer, it would have been risky because of racemisation process.

In the light of these considerations, it appears undeniable the importance of producing only one enantiomer of a given molecule, as pure as possible and in large scale.¹

Figure 3: Thalidomide, the two enantiomers



1.3 Formation of chiral compounds

“ On ne fait jamais attention à ce qui a été fait ; on ne voit que ce qui reste à faire ”^f

Marie Curie

1.3.1 The three approaches As just depicted, it is very important for both academic and industrial purposes to get important synthetic target molecules as single enantiomer or enantioenriched mixture, in the easiest and cheapest way. This goal can be achieved choosing among three different approaches:¹

- 1) Chiral pool: use of enantiopure starting material provided by nature
- 2) Resolution: separation of enantiomers by chemical or physical means
- 3) Enantioselective synthesis: preparation from nonchiral precursors using chiral reagents or catalysts

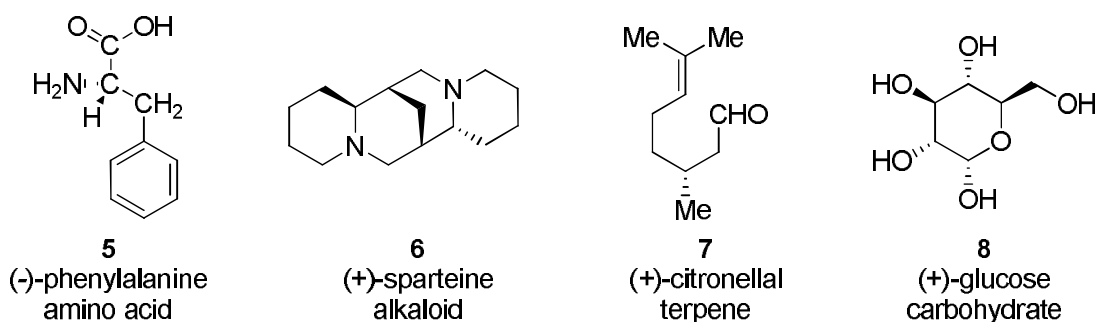
Each of the above mentioned strategies presents pros and cons, depending on the purpose, and choosing a suitable method is often not easy; several aspects should be taken into account, for example reagent costs and hazards, scale, waste generation, number of steps.²

^f “We never look at what has been done; we just look at what has to be done” Marie Curie

1.3.2 Chiral pool

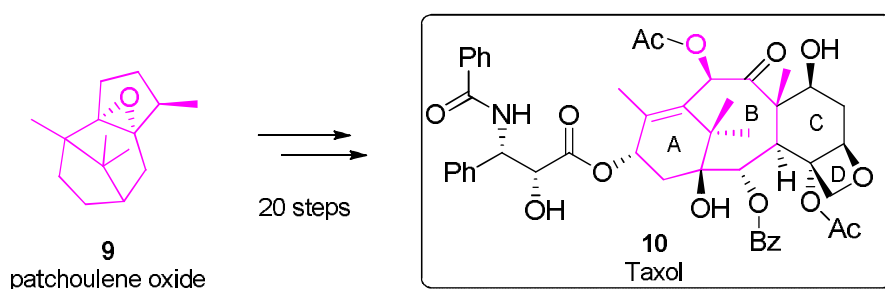
The chiral pool strategy is the synthesis of a chiral compound starting from naturally occurring molecules then modifying the structure in chemical steps towards the target molecule; throughout the steps, the stereocentres required for the target molecule will generally not be involved and indeed racemisation has to be avoided.¹ Noteworthy examples of such compounds are amino acids, alkaloids, terpenes, and carbohydrates such as compounds displayed in Figure 4; definitely, these building blocks should be cheap and readily available in high enantiomeric purity to be useful to the purpose. In fact chemists usually opt for this method only if the objective molecule contains a structural chiral scaffold, which is easily obtainable from a commercially available natural product, whose synthesis would be difficult or too expensive.

Figure 4: examples of naturally occurring chiral compounds.



One example of convenient chiral pool approach is the Holton first total synthesis of paclitaxel (10), the anti-cancer agent known as Taxol; Holton's group achieved this important molecule in twenty steps, starting from the commercially available natural product patchoulene oxide (9, Scheme 1).³ The depicted synthesis is in fact easier and cheaper than other ones which take advantage of other approaches.⁴

Scheme 1: Holton's synthesis of Taxol starts from patchoulene oxide



Unfortunately, even though in many cases chiral pool strategy can be suitable, nature does not provide such a broad scope of easily accessible chiral scaffolds, therefore alternative approaches to asymmetric synthesis are quite often preferred.⁴

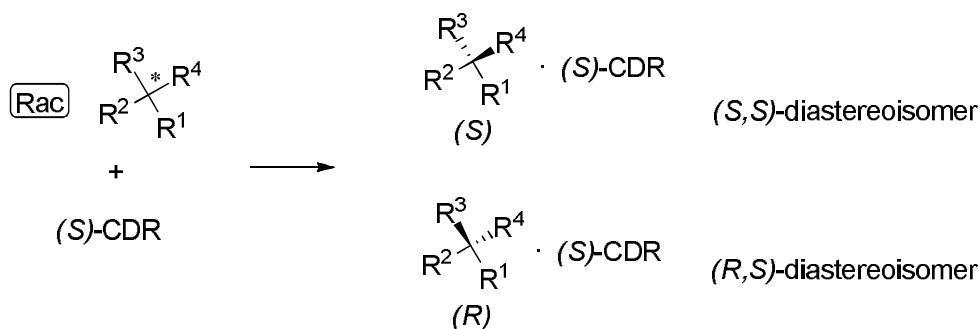
1.3.3 Chiral resolution

Resolution, namely the separation of the two enantiomer, has been widely used in industry as well as in academia since it displays great advantages; accessing directly to the racemate is very often much cheaper, rather than trying to get an asymmetric induction. In many industrial protocols this is still the elected technique, despite there being the half yield disadvantage; sometimes the by-products can be reconverted into the desired optically active product, increasing even more the advantages of this method, which in the last decades has been very often criticized because of the above mentioned disadvantage and considered “not elegant”.⁵

The three main types of resolutions are: (a) *classical resolution*, (b) *chiral chromatography*, (c) *kinetic resolution*.

(a) The *classical resolution* is the so-called indirect approach and implies the derivatization with an optically active compound to give diastereoisomers which may be easily separated either by normal chromatography or via other techniques and then reconverted into the desired product. The applicability of this methods depends on (i) the energy difference between the two diastereomers, (ii) the availability of optically pure chiral derivatizing reagents (CDR), (iii) the presence on the substrate molecule of moieties that could be covalently derivatized or that could make a diastereomeric salt with the CDR that could be crystallized.⁶

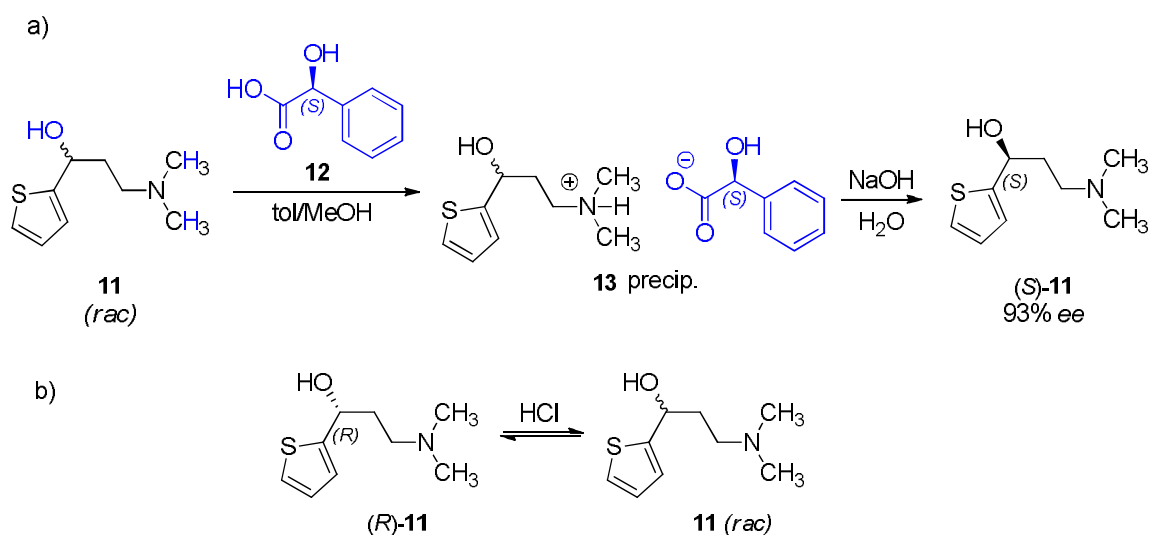
Scheme 2: classical approach to resolution, diastereoisomers formation with an optically pure chiral derivatizing agent (CDR)



A modern example of this evergreen approach is the industrial preparation of Duloxetine, a serotonin-norepinephrine reuptake inhibitor, which is used to cure major

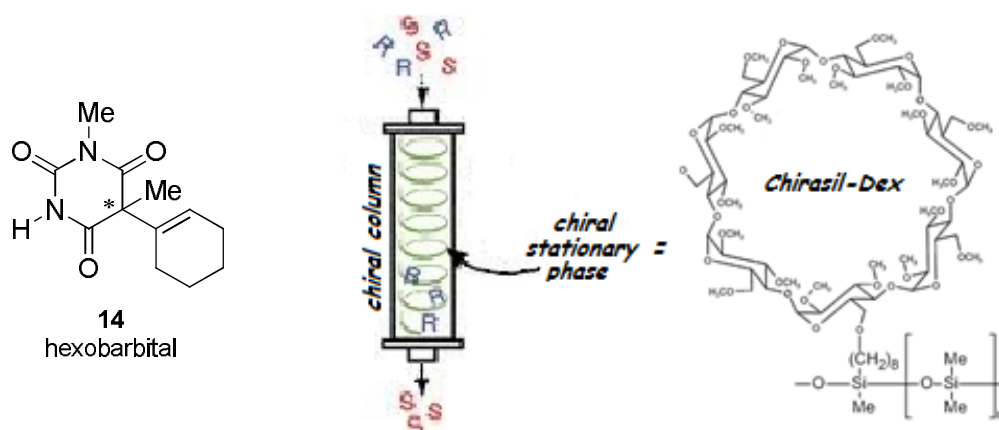
depressive disorders and many other diseases.⁷ As depicted in Scheme 3, the racemic alcohol is dissolved in toluene and methanol in the presence of (*S*)-mandelic acid; the optically active mandelic acid forms a diastereomeric salt with one of the two enantiomers of the alcohol. The salt, which is insoluble and precipitate, is filtered and treated with sodium hydroxide easily affording the (*S*)-enantiomer of the desired product. The pros of this technique, called RRR (resolution racemisation recycle) results in limited wastes because the unreacted (*R*)-enantiomer, still in solution, treated with HCl epimerizes and is recycled back.⁸

Scheme 3: a) optical resolution of Duloxetine via diastereomeric derivatization with (*S*)-mandelic acid; b) the (*R*) enantiomer is epimerized and recycled back.



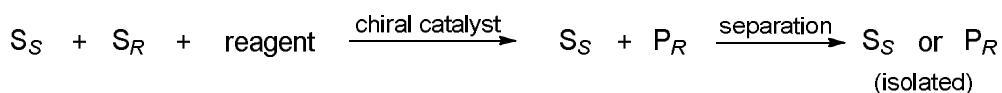
(b) The second type of resolution, well known as direct approach, take advantage of *Chiral Chromatography* techniques. This is a variant of column chromatography, in which generally the stationary phase is chiral and has different affinity with the two enantiomers, which therefore are recovered at the end of the column at different times. An advantage of this direct method is that the synthesis of diastereomers is not required.⁹ Several different chiral stationary phases have been developed over the years, many of them based on oligosaccharides such as cellulose or cyclodextrin scaffold. For instance a number of non-steroidal anti-inflammatory drugs and barbiturates, such as hexobarbital (**14**), have been effectively separated by cyclodextrines linked via an octamethylene spacer to a dimethylpolysiloxane (Scheme 4).¹⁰ The main disadvantage of this approach is the high cost of the preparative chiral columns.

Scheme 4: cyclodextrine chiral phase Chirasil-Dex was used to separate hexobarbital enantiomers



(c) *Kinetic Resolution* performs an important role. This method involves a chiral catalyst or reagent to promote selective reaction of one enantiomer over the other giving a mixture of enantioenriched starting material and product. The desired component is then isolated (Scheme 5). The theoretical yields for such resolutions are usually 50%; if the undesired material can be racemized, those yields can be brought to very high values and this is the case of dynamic kinetic resolution (DKR).²

Scheme 5: Catalytic Kinetic Resolution

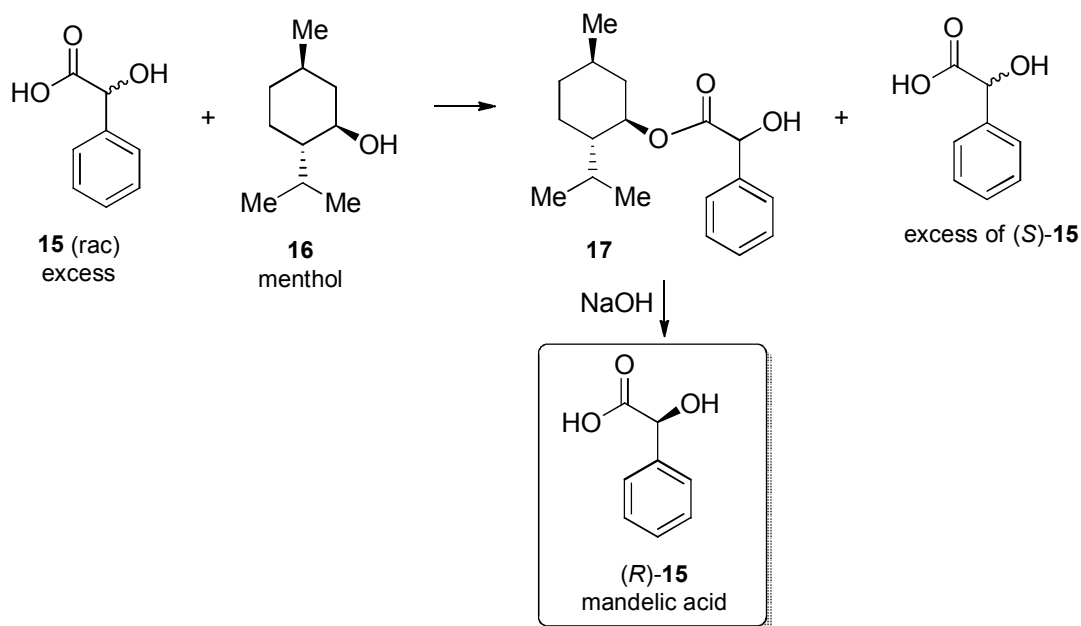


The first example of chemical kinetic resolution (KR) was presented by Marckwald and McKenzie in 1899, when they found the esterification of (*R*)-mandelic acid (**15**) with (*S*)-menthol (**16**) to be faster than the reaction of the (*S*)-enantiomer (Scheme 6).¹¹ Kinetic resolution can be conducted with the use of chemical reagents and catalysts or taking advantage of enzyme catalysis. A noteworthy example of enzymatic KR is the Degussa's methodology for preparing natural and unnatural amino acids employing acylases: they synthesized the racemic mixtures of *N*-acetyl amino acids by Strecker synthesis and used acylases to obtain enantiomerically pure L-amino acids (Scheme 7).¹²

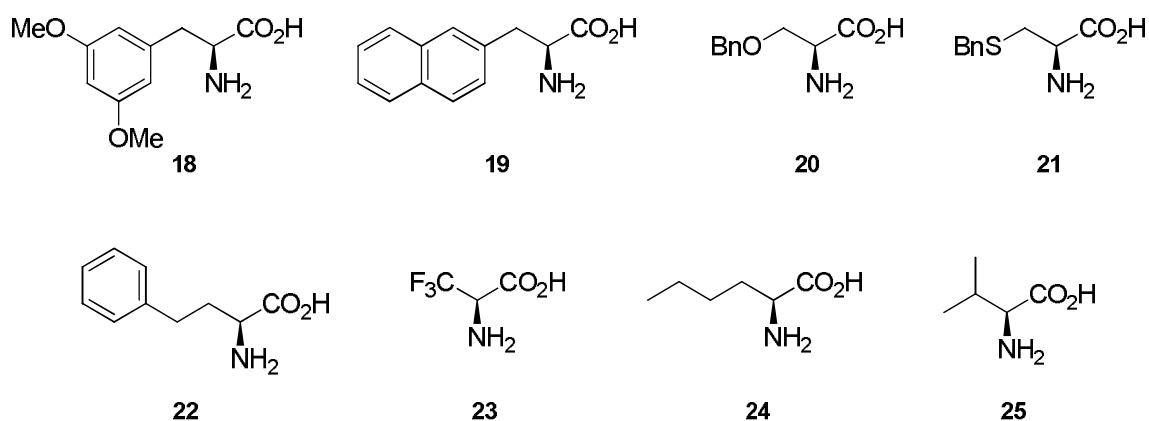
Thus kinetic resolution, especially DKR, can be very practical and many companies have opted for this convenient methodology. Indeed, there are some conditions that must be met, in order to consider the KR approach:

- racemate is cheap
- catalyst is very selective at low loading
- catalyst is cheap and recoverable
- the resolved starting material and product are easily separable
- ideally both starting material and product are valuable

Scheme 6: (*R*)-mandelic acid resolution by (*S*)-menthol



Scheme 7: Examples of natural and unnatural amino acids resolved by Degussa's enzymatic KR



1.3.4 Enantioselective synthesis

The third way to achieve chiral compounds is traditionally called “asymmetric synthesis” (IUPAC, 1996)¹³ and can be described as “a chemical reaction (or reaction sequence) in

which one or more new elements of chirality are formed in a substrate molecule and which produces the stereoisomeric (enantiomeric or diastereoisomeric) products in unequal amounts. In fact, enantioselective synthesis is probably the most fascinating and intriguing approach to optically pure molecules that a chemist could think about. The first definition of asymmetric synthesis was given by Marckwald in 1904:

*“Asymmetrische Synthesen sind solche, welche aus symmetrisch konstituirten Verbindungen unter intermediärer Benutzung optisch aktiver Stoffe, aber unter Vermeidung jedes analytischen Vorganges, optisch aktive Substanzen erzeugen”*⁸

This definition specifies that asymmetric synthesis allows chemists to avoid any analytical separation technique to have enantiopure products. Indeed, high levels of asymmetry can be reached by the use of a chiral reagent or catalyst; these compounds have the power to induce asymmetry in a chemical transformation by interacting with other nonchiral reagents.¹⁴ Concisely, the known methods for asymmetric synthesis can be conveniently divided into four major classes, depending on how the influence of the chiral group is exerted, as follows:¹

- I. *First generation or substrate-controlled method*
Reaction is driven intramolecularly by a stereogenic centre already present in the chiral substrate.
- II. *Second generation or auxiliary-controlled methods*
The difference with the first generation is that the chiral auxiliary, that initially binds the substrate, is removed after it has served its purpose.
- III. *Third generation or reagent controlled methods*
The chiral reagent does not bind the substrate therefore does not need to be removed.
- IV. *Fourth generation or catalyst-controlled methods*
The final refinement is to use a chiral catalyst to direct the conversion of an achiral molecule directly to a chiral product with an achiral reagent.

Among the four strategies towards enantioselective synthesis, the first three require stoichiometric amounts of an enantiomerically pure compound, the fourth one instead

⁸ “Asymmetric synthesis are those that produce optically active substances from symmetrically constituted compounds with the intermediate use of optically active materials, but with the avoidance of any separations.” Marckwald

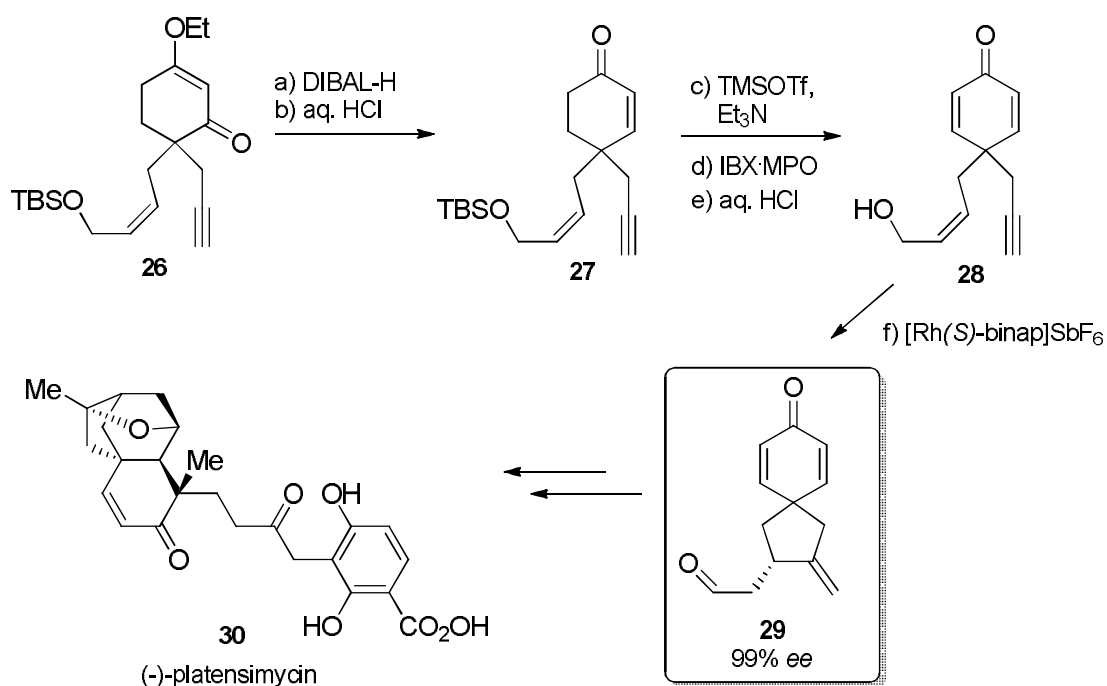
takes advantage of a catalyst, which is thus used in lower quantities, and can sometimes be recovered as well. There are some criteria to judge an asymmetric synthesis and to choose one of the possible methods:¹⁵

- a. the high stereoselectivity;
- b. if a chiral catalyst is employed, low catalyst loadings are preferable, and the catalyst must be easily separable from the product;
- c. if a chiral auxiliary is used, it should be both removable without compromising the newly formed stereocenter and recoverable in good yield without racemisation;
- d. the chiral auxiliary or catalyst should be readily and inexpensively available, preferably as both enantiomer.

1.3.5 Asymmetric catalysis

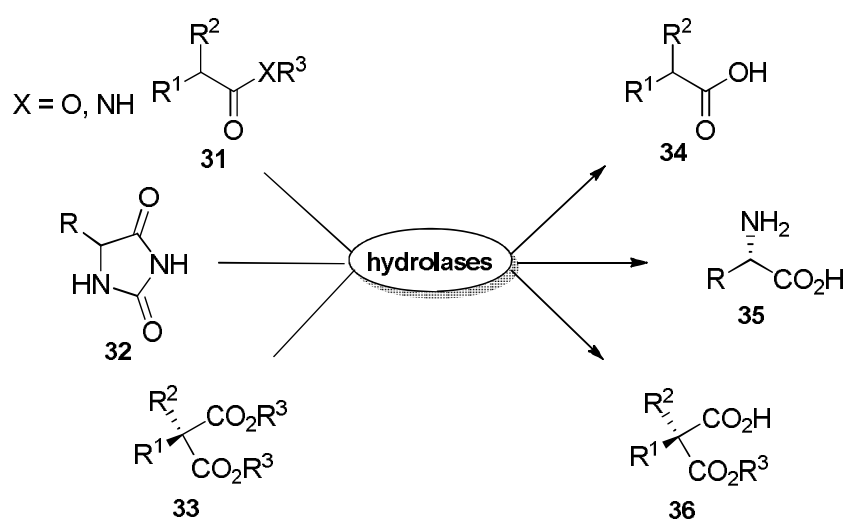
As just depicted, the fourth generation method for asymmetric synthesis presents some advantages: the catalyst is used at low loading, the choice of the starting material is far wider, since it need no longer to come from the chiral pool, and there is no need to dedicate two extra steps to the installation and removal of chiral auxiliary. For these reasons the chiral catalyst approach has been extensively exploited in the last decades.

For asymmetric catalysis the three eligible methods are transition-metals complex catalysis, enzymatic catalysis and organocatalysis; those strategies are complementary to each other, nevertheless, the chemistry community, for many years, has believed that only the first two types of catalysts could be efficient and selective. In fact in the last decades enantioselective synthesis by metal-catalysis has been broadly explored; a noteworthy example of highly efficient asymmetric synthesis is the rhodium-catalyzed asymmetric enyne cycloisomerization of terminal alkynes towards the formal total synthesis of (-)-platensimycin (**30**), presented by Nicolau in 2009 (Scheme 8).¹⁶

Scheme 8: enantioselective formal synthesis of (S)-plantensimycin via Rhodium catalysis

Although the use of metal catalysts brings many advantages, it represents a polluting, expensive catalytic methodology, with respect for instance to enzymatic processes.

Due to the enormous progresses in the field of enzyme discovery and enzyme engineering, in the recent years numerous examples of organic synthesis with enzymes have been developed. Enzymes represent a useful and cheap way to obtain different reactions and each class of enzymes can cover a broad range of chemical transformations. A significant example are the hydrolases, which are probably the most popular and frequently used enzymes; among them, representative examples are proteases, lipases, and esterases; typical transformations catalyzed by hydrolases include hydrolysis of esters and amides, and Scheme 9 give an overview of reactions scope.¹⁷

Scheme 9: examples of reactions catalyzed by hydrolases

The use of enzymes presents some disadvantages, as limited stability of enzymes under organic reaction conditions and low efficiency when using wild-type strains. Organocatalysis, the third and more recently developed approach to asymmetric catalysis, can overcome those problems together with the costs and environmental issues that are intrinsic of organometallic catalysis.¹⁸

1.5 Enantioselective Organocatalysis

*“..What's in a name? that which we call a rose
 By any other name would smell as sweet..”*
 William Shakespeare, “Romeo and Juliet”

1.5.1 A new concept

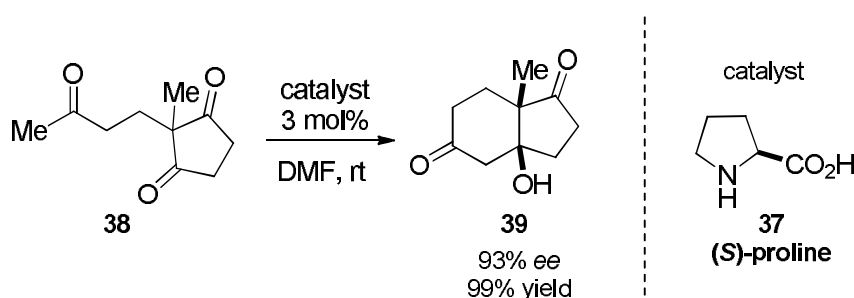
The term “organocatalysis” has been introduced in the scientific community in 2000 by D. MacMillan,¹⁹ one of the pioneers of this field. It means: the use of small organic molecules to catalyse organic transformations, even though some recent examples of organocatalysis combined with metal catalysis have been included in the organocatalysis branch as well.²⁰ During the last decades, organocatalysis has been included among the most important and successful concepts in asymmetric catalysis and it has been used for the enantioselective construction of C-C, C-N, C-O, C-S, C-P, and C-halide bonds. Furthermore, this new branch experienced a fast rise in the first eight years from its advent with more than 2000 manuscripts published in the field, in which more than 150 discrete reactions are reported. In one of his masterpieces, MacMillan proposed that this big power of attraction could be attributed to the name: he suggested

that the term Organocatalysis provided a strong identity and helped to unify the field. Indeed this fast rise could be possible thanks to some pioneering studies concerning non-metal catalysis and to the previously highlighted importance of asymmetric synthesis of valuable molecules.

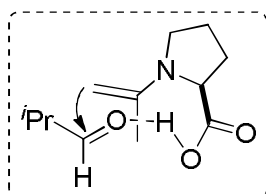
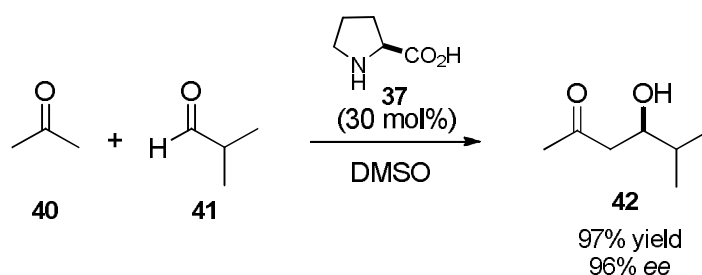
1.5.2 The history of Organocatalysis

The history of organocatalysis has the special characteristic of being started more than a hundred years ago and actually being ignored as such an important field until the year 2000. In fact in 1912 Bredig and Fiske reported that cinchona alkaloid promoted the addition of hydrogen cyanide to benzaldehyde with low enantioselectivity²¹ and in 1960 Pracejus found a cinchona alkaloid catalyzed asymmetric addition of methanol to ketenes.²² Afterwards, in 1971, Hajos's and Wiechert's groups reported independently the (*S*)-proline catalysed asymmetric aldol reaction, without a satisfying mechanistic study and without recognising the important novelty (Scheme 10).²³

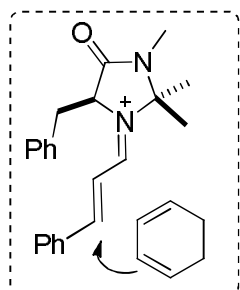
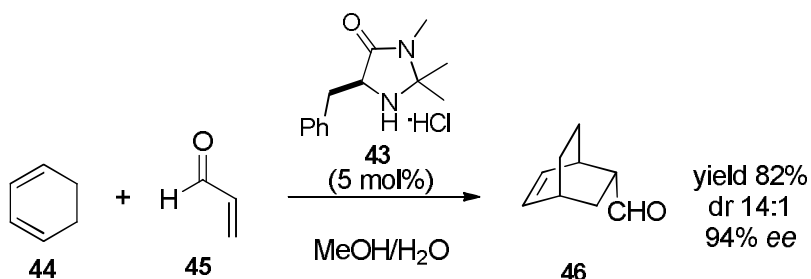
Scheme 10: Hajos reaction catalyzed by (*S*)-proline



Only in 2000, B. List reported an asymmetric (*S*)-proline (**37**) catalysed aldol reaction between acetone and some aldehydes, leading to the corresponding aldols with very high enantiomeric excesses and high yields. The hypothesised mechanism involves the formation of the enamine between (*S*)-proline and acetone, a stronger nucleophile than the corresponding enol; (*S*)-proline is able to increase the HOMO energy and thus the reactivity of the nucleophile.¹⁸ Moreover in the reaction intermediate, the catalyst interacts with the aldehyde through the protonation of the carbonyl (Scheme 11). In the same year, D. MacMillan presented a direct Diels-Alder reaction catalysed by a new chiral imidazolidinone catalyst (**43**); in his paper he verified that his catalyst could direct the addition of a diene to enals, by lowering the energy of the LUMO, thus activating the electrophile towards the nucleophilic addition (Scheme 12).^{19a}

Scheme 11: direct aldol reaction catalysed by (*S*)-proline

In the intermediate (*S*)-proline interacts with both compounds, by covalent activation (enamine) and noncovalent activation (partial protonation of the carbonyl)

Scheme 12: direct Diels-Alder reaction catalysed by MacMillan imidazolidinone

MacMillan imidazolidinone activates the aldehyde *via* iminium ion, lowering the LUMO energy

These recently developed organocatalytic reactions paved the way to many groups that started to work in the same field, thus developing many different catalysts types and contributing to the growth of organocatalysis scope.^{19b, 24}

1.5.3 Covalent or Noncovalent Organocatalysis

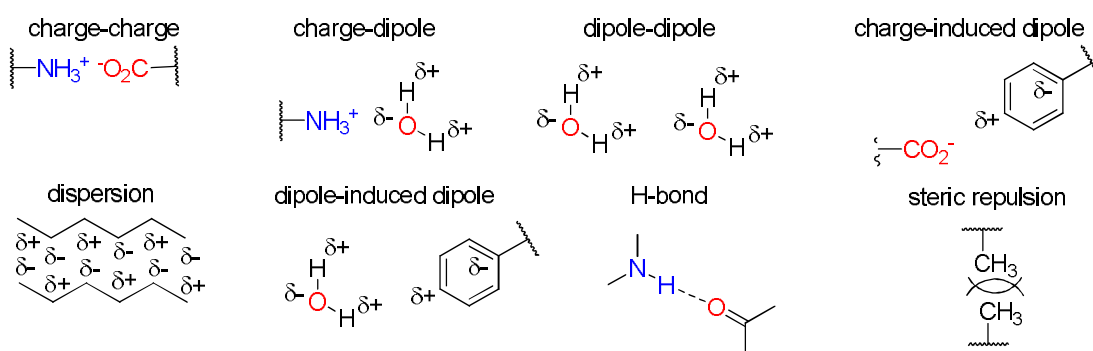
Among the various organocatalytic methodologies there are different types of activation and two main areas can be identified on the mechanistic basis: (i) “covalent organocatalysis” and (ii) “noncovalent organocatalysis”. In the former case, within the catalytic cycle, the catalyst covalently binds the substrate, in the latter case only noncovalent interactions, such as hydrogen bonding or the formation of ion pairs,

activate the molecule towards the asymmetric transformation. Typical examples of covalent organocatalysis are proline-catalyzed aldol reactions which proceed via enamine intermediates (see Scheme 11).¹⁸ However, noncovalent organocatalysis has recently been explored by many research groups and a vigorous development in this area has been achieved as well.²⁴⁻²⁵

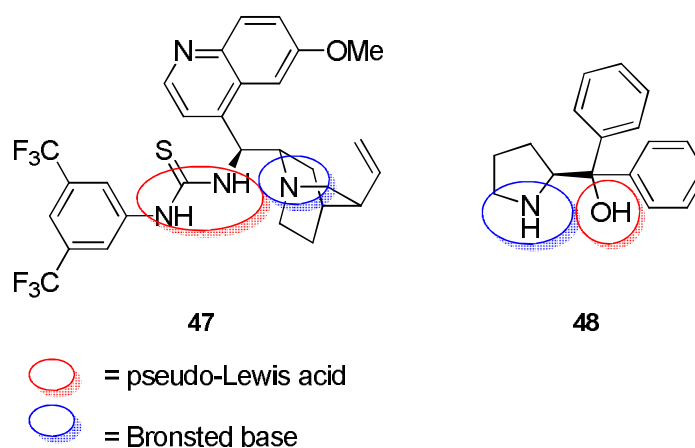
1.5.4 Noncovalent organocatalysis

Noncovalent organocatalysis is often attributed mainly to either hydrogen bond network or ion pairs formation. As recently elucidated by E. N. Jacobsen, many different kinds of interactions are often cooperating within the reaction mechanism in order to lead to high enantioselectivities.²⁶ The known noncovalent interactions scope includes charge-charge, charge-dipole, dipole-dipole, charge-induced dipole, dipole-induced dipole forces, steric repulsion and H-bond (Figure 5).

Figure 5: noncovalent interactions



Indeed noncovalent interactions are weaker and less directional with respect to covalent bonding; thus in order to get the same results in terms of stereoselectivity, more than one interaction is requested in order to have an effective spatial constraints. In fact, catalysts for this type of activation bear few H-bond donor or acceptors or acid/basic sites, capable of generating multiple, but in concert operating, weak interactions. Many catalysts are also called “bifunctional” as they bear more than one function. Noteworthy examples of bifunctional noncovalent organocatalysts are the Soós thiourea (**47**) and diphenyl prolinol (**48**), depicted in Figure 6. Both of these catalysts bear a pseudo-Lewis acids function and a Brønsted base function.²⁷ The different functions work in concert within many reaction mechanisms, activating both electrophile and nucleophile.²⁸

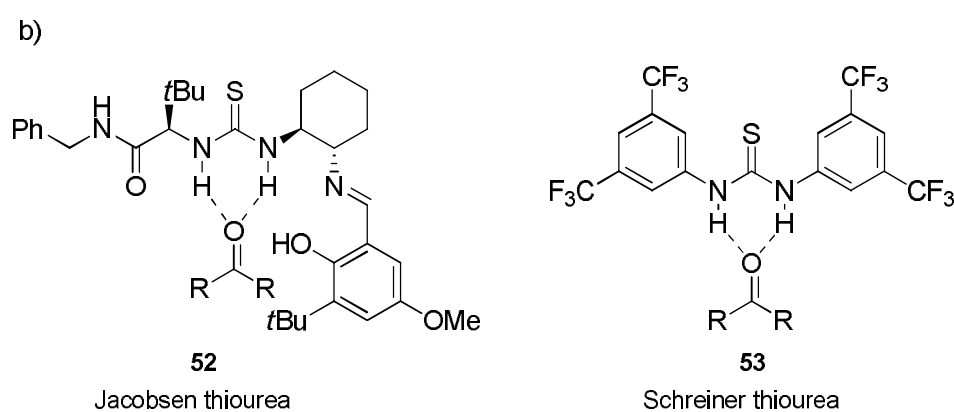
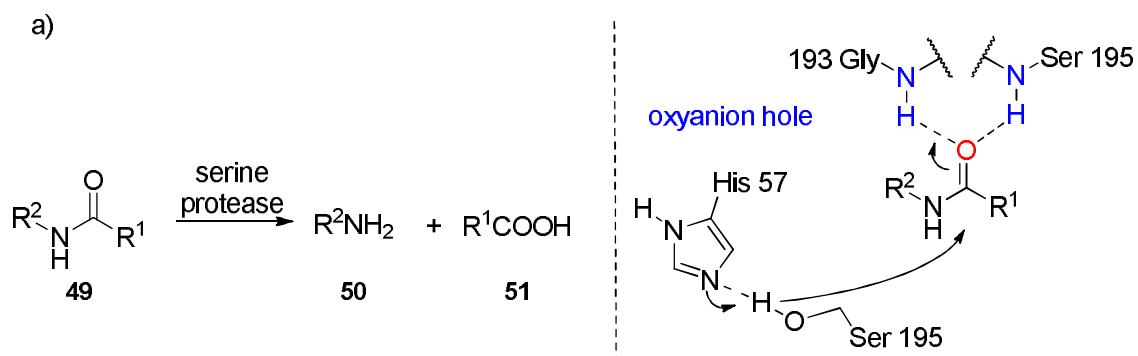
Figure 6: examples of bifunctional – noncovalent organocatalysts

Among the different kinds of noncovalent asymmetric catalysis, H-bonding and Brønsted acid catalysis are so far the most investigated.

1.5.5 Hydrogen bonding organocatalysis

Hydrogen bond organocatalysis clearly relies on H-bond interactions, even though other secondary interactions usually cooperate with them. For instance, milestones such as Jacobsen's²⁹ and Schreiner's thioureas (**52**, **53**, Scheme 13b),²⁷ clearly resemble the enzymatic pocket of serine proteases in the activation of the amide carbonyl towards the serine nucleophilic attack. Within what is called the “oxyanion hole”, the amide carbonyl is coordinated and activated by two NH groups so favouring the serine nucleophilic attack with the formation of a tetrahedral intermediate stabilized by H-bonding in the oxyanion hole (Scheme 13a).³⁰

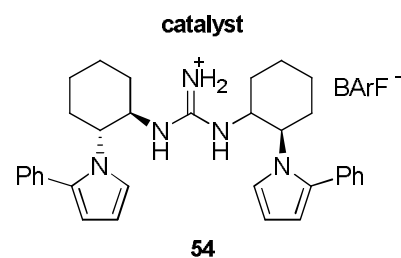
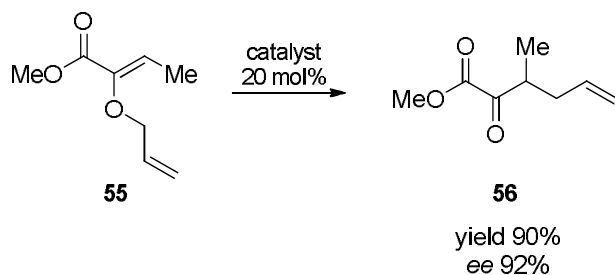
Scheme 13: a) oxyanion hole in serine protease activating a carbonyl; b) hydrogen bonding organocatalysts activating a carbonyl



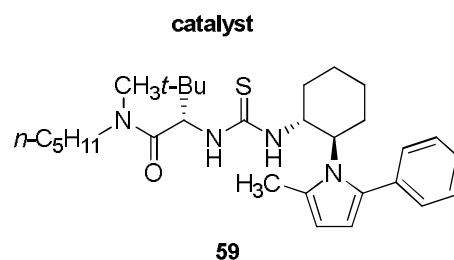
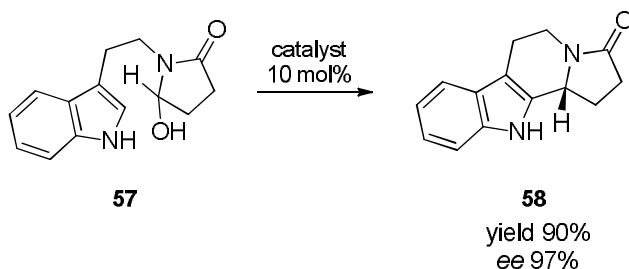
A variety of electrophiles can be activated towards nucleophilic asymmetric addition with the same action mode and a series of reactions have so far been investigated.³¹ Moreover, H-bonding catalysts can promote enantioselective reactions by stabilizing anionic fragments, as in Claisen rearrangement,³² by binding an anion, as in Pictet-Spengler cyclization³³ and hydrocyanation of imines (Scheme 14).³⁴

Scheme 14: examples of reactions catalyzed by H-bonding catalysts

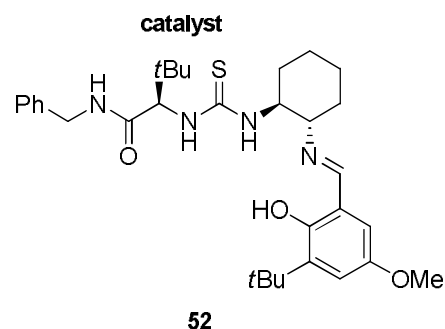
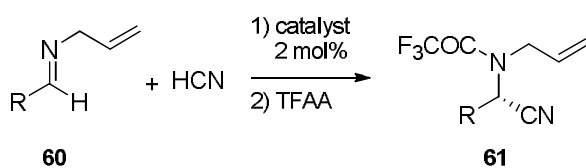
a) Claisen rearrangement



b) Pictet-Spengler cyclization



c) imine hydrocyanation



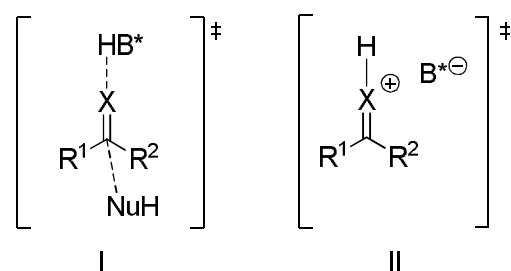
Regarding the classification of hydrogen-bonding catalysts within the Lewis/Brønsted acid/base catalysis branches, the Shreiner's group carried out some studies concerning thioureas have been conducted, by the use of NMR, IR and computational techniques, as well as some reactivity comparisons between well-known Lewis acids (aluminium trichloride, titanium tetrachloride). These studies proved that there are many similarities between Lewis acids and hydrogen bonding additives; this is the reason why some hydrogen bonding catalysts can be classified as Lewis acids.²⁷

1.5.6 Brønsted acids organocatalysis

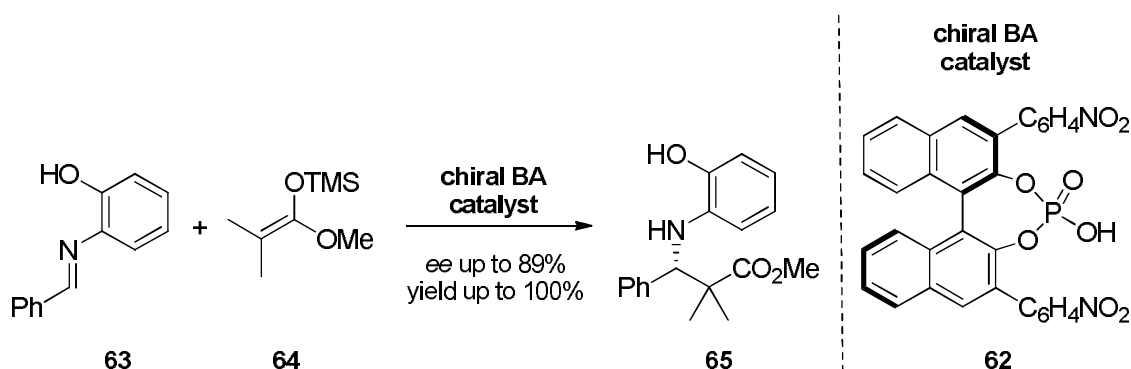
Substrate activation by Brønsted acids (BA) is related to, but different from, hydrogen bonding catalysis, since in the former case, proton transfer from the catalyst to the substrate occurs. The terms “specific Brønsted acid catalysis” and “general Brønsted acid catalysis” are used, depending on whether proton transfer occurs to the substrate in

its ground state or in the transition state. In specific Brønsted acid catalysis, the electrophilic substrate is reversibly protonated in a pre-equilibrium step, prior to the nucleophile attack (II, Scheme 15), instead in general acid catalysis the proton is (partially or fully) transferred in the transition state of the rate-determining step (I, Scheme 15). In transition state I the hydrogen on the acidic centre interacts with the substrate via hydrogen bond, instead in transition state II the substrate is protonated. This activation mode is related to H-bonding, since clearly the formation of a hydrogen bond precedes proton transfer;²⁵ moreover some recent studies by Rueping's group suggested that in some cases the activation mode is in between the two mentioned ones.³⁵

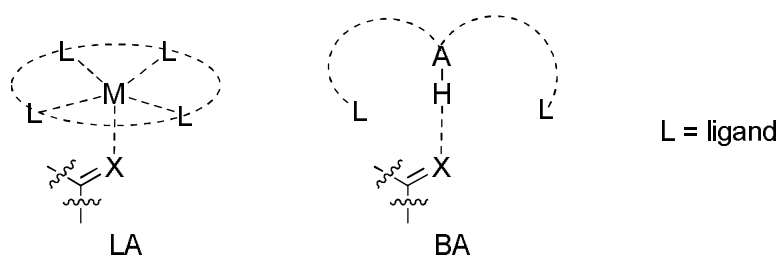
Scheme 15: transition states in general acid catalysis (I) and in specific acid catalysis (II)



Chiral BA catalysis has had a breakthrough in 2004, when Terada and Akiyama independently presented an enantioselective Mannich-type reaction catalyzed by new metal-free phosphoric acid, BINOL-derived compounds (Scheme 16).³⁶ These pioneering studies already showed how powerful could be the use of BA catalysis for asymmetric synthesis; in fact the BINOL derived catalysts were designed in order to get an environment both sterically demanding, to achieve good enantioselectivity, and moderately acid, to protonate the imine's nitrogen.

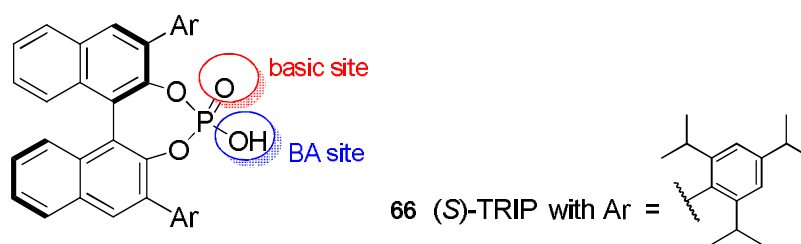
Scheme 16: Enantioselective Mannich-Type reaction presented by Akiyama's group in 2004

While the first studies did not elucidate the specific mechanistic pathway (even though suggesting the protonation of the imide by the phosphoric acidic site), later on, the BA catalytic activity came up. First of all in the activation of a compound, i.e. carbonylic derivative, towards chemical transformations, for example a carbonylic compound, BA differ in the catalytic centre from the well known Lewis Acids (LA): LA). Indeed, in BA the centre is a proton instead of a metal or metalloid and this is actually the simplest centre an organic chemist could think about (Scheme 17). Furthermore, proton has only one valence orbital and the interactions number is limited with respect to LA catalysts. As a consequence, the sterically hindering groups of the BA catalyst scaffold should be bulkier.³⁷

Scheme 17: Lewis Acid (LA) vs Brønsted Acid (BA) catalysts

Moreover, BA are bifunctional catalysts, since they bear an acidic site and a basic site (Figure 7); thanks to these characteristics in the last ten years many different types of chiral phosphoric acids have been synthesized and used as catalysts in a broad scope of enantioselective reactions. For instance, the bulky (*S*)-TRIP, developed by List's group, can efficiently catalyze enantioselective transacetalizations,³⁸ Povarov reactions,³⁹ O-alkylations,⁴⁰ Pictet-Spengler reactions,⁴¹ and many other transformations (Figure 7).

Figure 7: chiral BINOL-derived phosphoric acids, particularly (*S*)-TRIP



This dissertation is mainly focused on H-bonding and Brønsted acids organocatalysis and in the next chapters some successful applications of these activation modes will be presented.

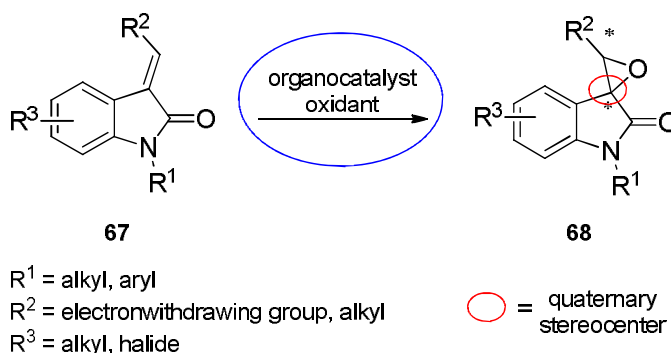
2. OBJECTIVE OF THE THESIS

The importance of organocatalysis in the asymmetric synthesis panorama has been previously described. Moreover, in the light of the interesting perspectives in the field of noncovalent organocatalysis and of the importance of optically pure compounds as intermediates and building blocks in fine organic synthesis, this PhD work has been centred on applications of noncovalent organocatalysis to the synthesis of enantiomerically enriched valuable molecules. In particular, among the different aspects of noncovalent organocatalysis, bifunctional hydrogen bonding catalysis and Brønsted acids catalysis have been exploited. Within these field, two different kinds of approaches towards optically pure molecules have been investigated, namely asymmetric catalysis and kinetic resolution, which have already been depicted in Chapter 1.

Thus, the results and discussions of this thesis are divided into two sections and reported in two different Chapters.

The first part, reported in Chapter 3, deals with H-bonding bifunctional organocatalysis applied to the enantioselective epoxidation of electron deficient olefins, in particular 3-ylidenoxindoles **67** (Scheme 18). The goal was developing an efficient, cheap and easy asymmetric synthesis of epoxides **68** bearing a quaternary stereocenter. This subject has been studied under the supervision of Prof. Maria Antonietta Loreto (University “La Sapienza”, Rome).

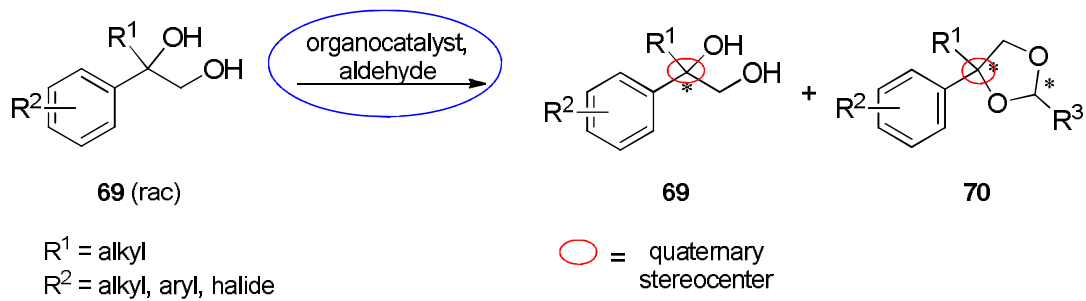
Scheme 18: organocatalytic epoxidation of 3-ylidenoxindoles



The second part of this dissertation, reported in Chapter 4, is about Brønsted acids (BA) organocatalysis employed for a kinetic resolution of racemic 1,2-diols **69** bearing a quaternary stereocenter, *via* asymmetric acetalization (Scheme 19). In particular the purpose was developing a new methodology that could lead to both enantiomerically enriched products **69** and acetal **70**. Moreover, the applicability and the scope of the

reaction have been investigated, during an internship in Prof. Dr. Benjamin List's laboratories (Max-Planck-Institut für Kohlenforschung, Mülheim an der Ruhr).

Scheme 19: organocatalytic kinetic resolution of 1,2-diols

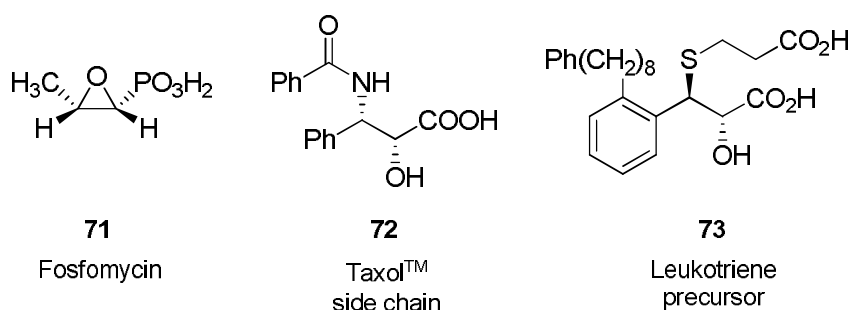


**3. ENANTIOSELECTIVE NUCLEOPHILIC
EPOXIDATION
OF 3-YLIDENEOXINDOLES**

3.1 Organocatalysis for the epoxidation of electron-deficient olefins

Chiral epoxides are among the most valuable intermediates and building blocks in fine organic synthesis. The oxirane ring easily undergoes to a number of stereoselective chemical transformations that directly led to more elaborate enantiopure compounds which are precursors of natural products or biologically active molecules.⁴² In Scheme 20 a few examples are presented: a well-known epoxide, such as the antibiotic Fosfomycin **71**, and some epoxide-derived molecules, such as the side chain of the famous anticancer agent TaxolTM **72** and a Leukotriene precursor **73**.⁴³

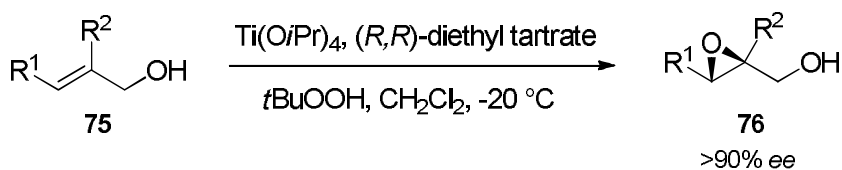
Scheme 20: examples of epoxides-derived compounds



For the aforementioned reasons, asymmetric synthesis of epoxides is a hunted goal for organic chemists and the enantioselective epoxidation of olefins represents a powerful strategy for the synthesis of enantiomerically enriched epoxides.

Katsuki and Sharpless paved the way to the epoxide asymmetric synthesis, introducing a practical method for the enantioselective epoxidation of non-activated olefins, though limited to allylic alcohols (**75**). The $\text{Ti}(\text{iPrO})_4$ -(*R,R*)-DET^h catalyzed epoxidation, brings to the oxidized products in high yields and high enantioselectivities for a very broad scope of such kind of compounds (Scheme 21); these appealing features have made Sharpless epoxidation one of the most exploited asymmetric transformations.⁴⁴

Scheme 21: the first practical asymmetric epoxidation

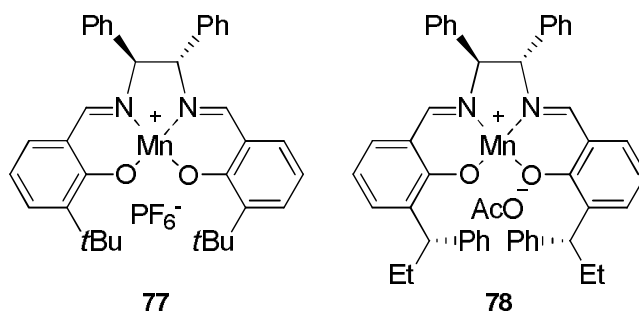


Many efforts have been made in this field, to afford catalytic asymmetric epoxidation of unfunctionalized olefins. In 1990 Katsuki et al. and Jacobsen et al. independently

^h Diethyl tartrate (DET)

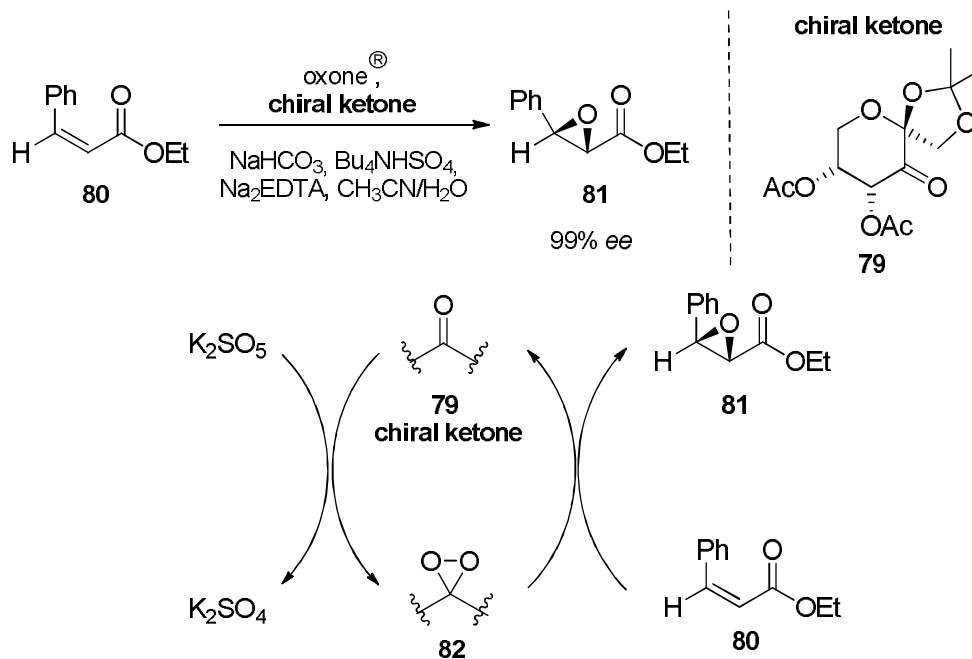
reported enantioselective epoxidation using chiral Mn(salen) complexes (**77** and **78**) as catalysts (Scheme 22). Complex **78** is the first example of the C_2 -symmetric salen catalyst consisting of two chiral subunits. This strategy has achieved wide scope of catalytic performance, as well as high enantioselectivity (up to 95% *ee*).⁴⁵ Afterwards, with some new complexes, the same research groups were able to reach excellent results (90- \rightarrow 99% *ee*) by introducing some new salen-complexes;⁴⁶ moreover, Berkessel et al. have recently developed an efficient epoxidation taking advantage of a similar catalyst type.⁴⁷

Scheme 22: Mn(salen) complexes used as initial chiral catalysts for enantioselective epoxidation reactions



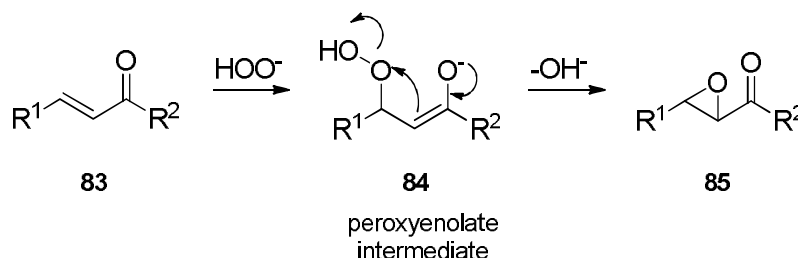
Apart from the well established metal-catalysis, some other methods have been disclosed for the enantioselective epoxidation which take advantage of the cheaper and environmentally friendly organocatalysis. The oxidant for such reactions may be either electrophilic or nucleophilic, although electrophilic oxidants are often not sufficiently efficient for a broad scope epoxidation of olefins. In particular, they are not strong enough to oxidize electron-deficient olefins. A noteworthy example of efficient organocatalytic enantioselective electrophilic epoxidation was presented by Shi in 2002; this methodology takes advantage of the action of Oxone[®], which converts a chiral sugar-derived ketone (**79**) into the oxirane electrophilic reactive species (**82**). The reaction leads to a relatively broad scope of epoxides with interesting *ee*s (up to 99%) (Scheme 23), but is still strictly substrate-dependent, even though represents the only example of organocatalytic epoxidation of α,β -unsaturated esters (**80**).⁴⁸ Nevertheless, the reaction mixture results to be quite complex as well the reaction pathway which easily gives undesired byproducts.

Scheme 23: Shi epoxidation



In fact, despite the usefulness of α,β -epoxycarbonyl compounds and of epoxides bearing electron withdrawing group (EWG), no system for the asymmetric epoxidation of electron-deficient olefins has achieved widespread popularity among synthetic organic chemists.⁴⁹ Only over the last few years systems which allow the epoxidation of alkenes bearing an electron withdrawing group (EWG) and a number of methodologies involving different types of catalyst-reagent combination have been established.⁵⁰ Most of the reported methods are essentially asymmetric modification of the Weitz-Sheffer reaction⁵¹ in which one of the oxygen atoms in the nucleophilic oxidant is transferred to the α,β -unsaturated precursor (**83**) through the α -peroxyenolate intermediate (**84**) formation (Scheme 24).

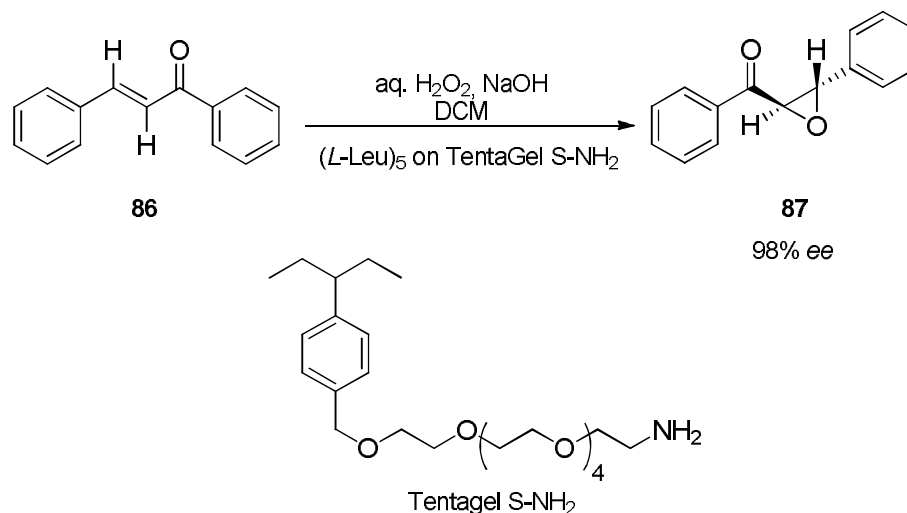
Scheme 24: Weitz-Sheffer epoxidation



Based on this model, some peptide-catalyzed organocatalytic approaches have been developed during the last few years; among them, the Juliá-Colonna epoxidation,⁵² whose mechanism has been studied by Berkessel et al,⁵³ requires poly-amino acids to

activate enones towards nucleophilic attack of hydrogen peroxide *via* H-bonds. Berkessel et al. furthermore showed that, for aminoacidic poli-Leucyne TentaGelⁱ-bound catalysts, high enantioselectivities (> 95% *ee*) can be achieved with just five *L*-Leu residues (Scheme 25).

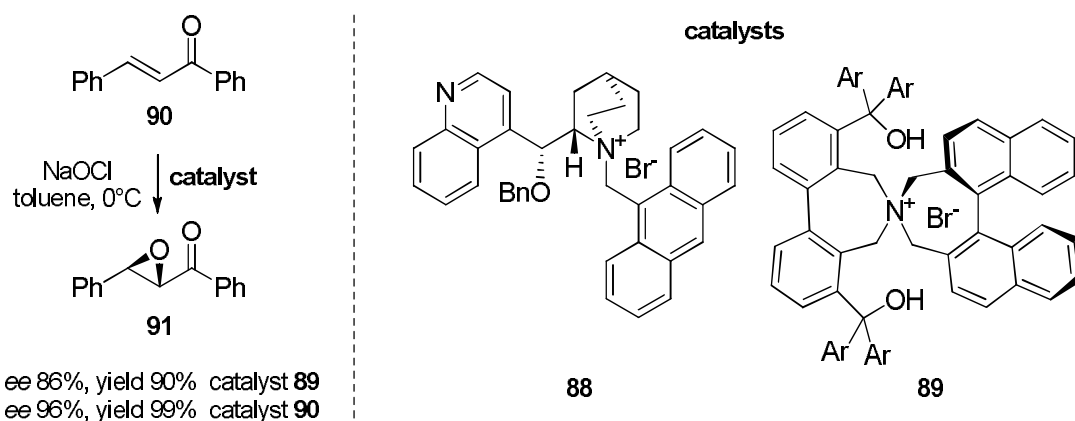
Scheme 25: Berkessel epoxidation of enones



Among organocatalytic approaches to Weitz-Sheffer-type epoxidation of enones, a noteworthy method is a phase transfer catalytic reaction (PTC), which take advantage of Cinchona alkaloids derivatives (**88**) or quaternary ammonium salts (**89**) (Scheme 26); to this purpose *t*-butyl hydroperoxide (TBHP), hydrogen peroxide or NaOCl are used as oxidants.⁵⁴ Although the scope of the substrates is narrow, this method has been successfully employed for the epoxidation of calchone (**90**), since good enantioselectivities are achieved (96% *ee*).

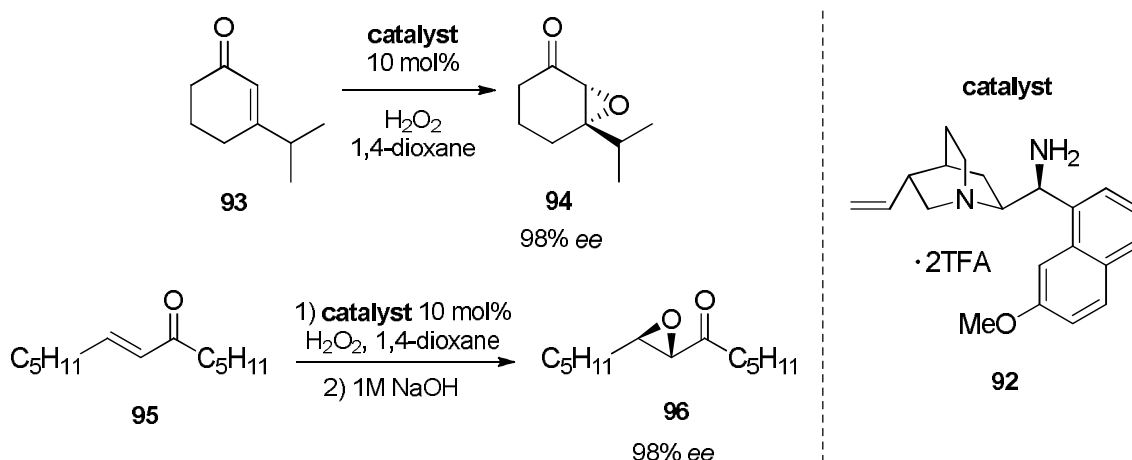
ⁱ Poli-Leucyne catalyst is bound to a poliethylen glicol – polistirene resin, TentaGel S-NH₂

Scheme 26: PTC in the epoxidation of enones

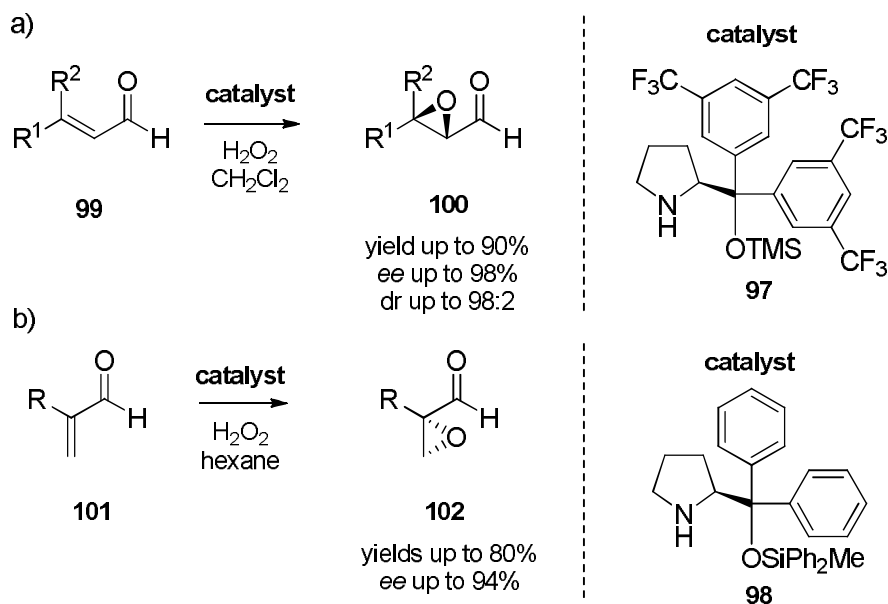


In this context, the List group recently developed an interesting asymmetric variant of the Weitz-Sheffer reaction; the use of bifunctional Cinchona alkaloid derivative **92** as catalysts and hydrogen peroxide as oxidant, allowed them to obtain the oxidation of various cyclic and non-cyclic enones with excellent enantioselectivities (up to 98% *ee*) (Scheme 27).⁵⁵

Scheme 27: List enones epoxidation

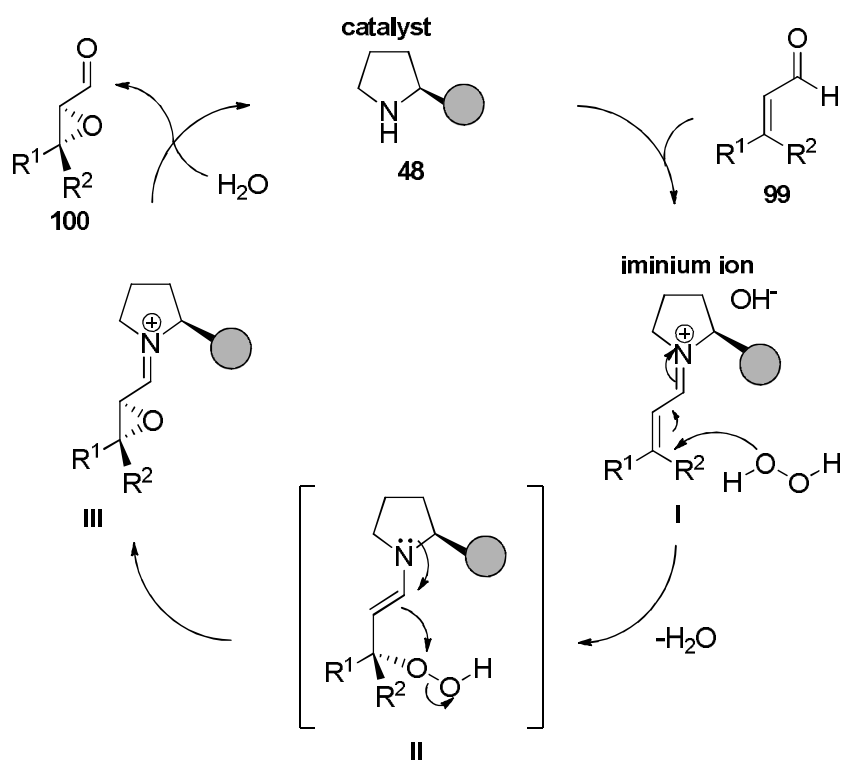


For the enantioselective epoxidation of \square and \square -branched enals, Hayashi's and Jørgensen's groups independently disclosed the dreadful potential of α,α -diaryl prolinol silyl ethers (**97** and **98**) catalysis (Scheme 28), obtaining the desired epoxide in high enantioselectivities (up to 98% *ee*) and excellent yields (up to 90%).⁵⁶

Scheme 28: catalytic enantioselective epoxidation of enals a) by Jørgensen et al. b) by Hayashi et al.


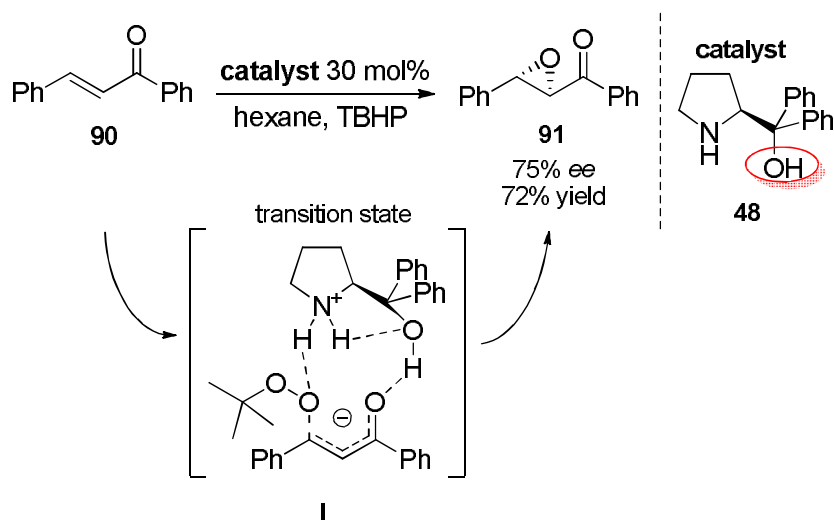
Furthermore, both groups investigated on the reaction mechanism, hypothesizing an iminium ion covalent catalysis. In fact, within the catalytic cycle, the key intermediate is an iminium ion, which lowers the LUMO energy of the electrophilic double bond of enal. The subsequent stereoselective addition of the peroxide anion, followed by the cyclization, led to the enantioenriched epoxide (Scheme 29).

Scheme 29: proposed mechanism for epoxidation of enals



In the same field, Lattanzi and Zhao have independently developed the enantioselective epoxidation of α,α -unsaturated ketones, exploiting the peculiarity of α,α -diphenyl prolinol (**48**) as catalyst and using TBHP as the oxidant.⁵⁷ The mechanistic hypothesis for the calchone (**90**) epoxidation postulates that the α,α -diphenyl prolinol, which bears the free hydroxyl function, could act as bifunctional, H-bonding catalyst. The catalyst is supposed to be both involved in an ionic couple with the oxidant, and to coordinate the carbonylic oxygen *via* H-bond, thus facilitating the peroxide attack in the α -position of the enone function (Scheme 30).

Scheme 30: Lattanzi enones epoxidation



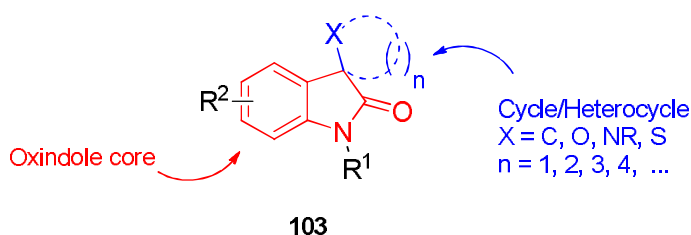
The so far reported examples deal with the enantioselective epoxidation of enones and enals. Other few cases of asymmetric oxidations of these kind of compounds are described in the recent literature,⁵⁸ whereas not much is reported about unsaturated esters and amides.⁵⁹ The scarcity of specific bibliography probably does not reflect a lack of interest, but rather a difficulty to handle these less reactive molecules. However, this field is still almost unexplored and is yet to be realized on a wide range of α,β -unsaturated carboxylic derivatives. Consequently the urgency for an efficient and effective stereoselective epoxidation of electron-poor alkenes remains a challenging endeavour of great interest.

3.2 Target molecules

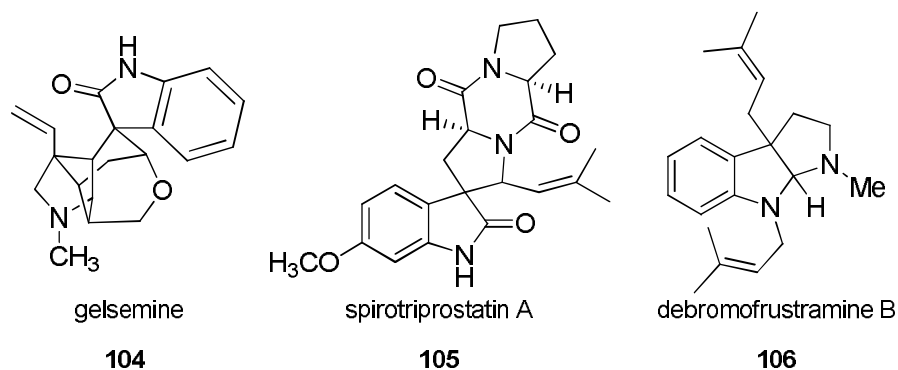
3.2.1 Spiro oxindoles

In 1900, Adolf Von Baeyer proposed the nomenclature “spiro compound” for a particular class of bicyclic molecules: “A spiro compound has two rings which have only one atom in common and the two rings are not linked by a bridge. The rings may form part of other ring systems (fused ring, bridged fused ring, system named by von Baeyer nomenclature). The common atom is known as a spiro atom.”⁶⁰ Among such molecules, spiro-oxindoles in the last decades strengthened their importance in organic chemists priorities; the reasons behind this attention are the growing awareness of the biological activity of this molecules as well the synthetic ongoing challenge of building quaternary stereocenters.⁶¹ Particularly, spiro oxindoles (**103**) are characterized by an oxindole core, one of the most recurring moieties in natural products, which is spiro-fused with cycles or heterocycles of various dimensions and kinds (Scheme 31).

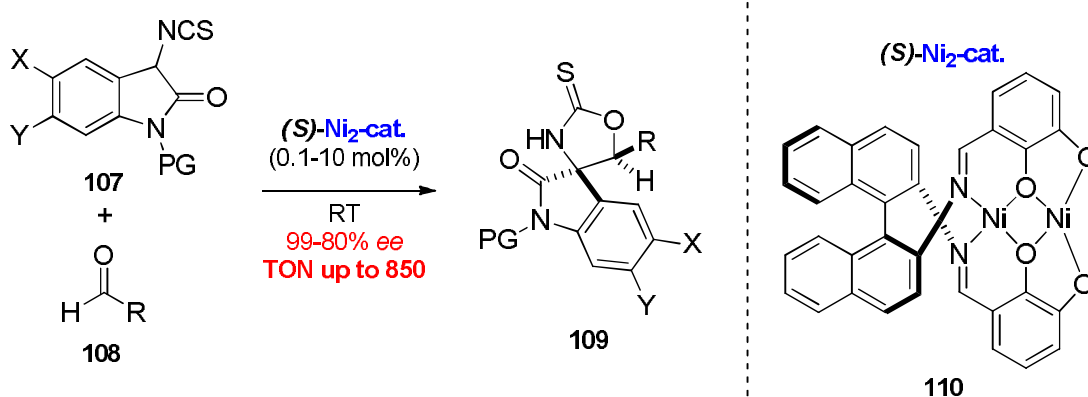
Scheme 31: spiro-oxindole frame



Many examples exist of naturally occurring alkaloid-type products and synthetic molecules,⁶² containing oxindole core, well known for their remarkable pharmacological activity, as anti-bacterial, anti-cancer, and anti-malaria agents; often these molecules have inspired chemists to total synthesis endeavour.⁶³ Noteworthy spiro-oxindolic compounds are the natural alkaloids gelsemine **104**, spirotriprostatine A **105**, and defrustramine B **106**, which have shown interesting biocide activity and whose syntheses, during the last decades, have been addressed by a number of research groups (Scheme 32).⁶⁴ These spiro compounds often contain some quaternary stereocenters in addition to the spiro center; therefore asymmetric synthesis of such type of molecules represents a great goal, because of the depicted features and above all because of the challenge of the simultaneous creation of those multiple quaternary stereocenters.⁶⁵

Scheme 32: noteworthy examples of oxindole-derived spiro compounds


The majority of the asymmetric syntheses of spiro oxindoles reported in literature, requires enantiopure reagents (chiral pool approach) or metal complexes as either chiral ligands or catalysts; furthermore these approaches often consist of multi-steps reactions, or involve difficult methodologies that very often have a narrow substrate scope.⁶⁶ For instance, Matsunaga *et al.* recently presented an addition of oxindoles **107** bearing an isothiocyanato group to aldehydes **108** under dinuclear Nickel Schiff base **110** catalysis (Scheme 33). The homodinuclear metal catalyst provides an easy one step access to spirocyclic oxindole compounds, in one step, leading to high enantioselectivity (up to 99% *ee*) with a high catalyst turnover number (TON, up to 850), at room temperature.⁶⁷

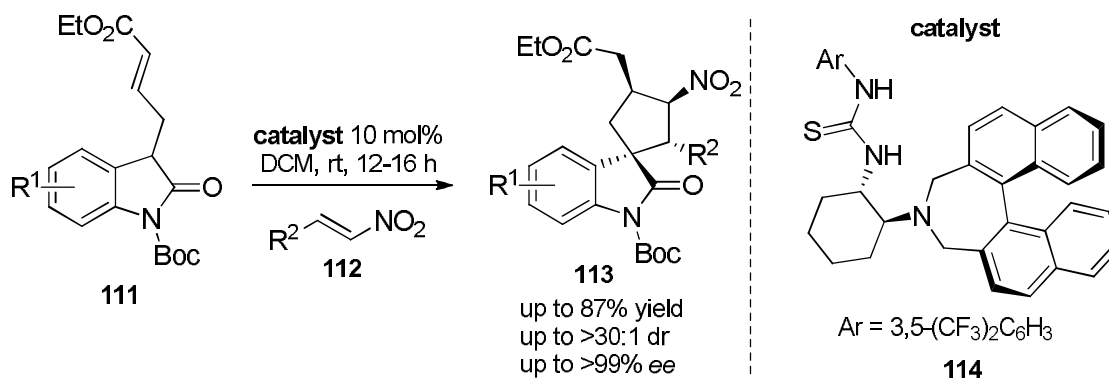
Scheme 33: dinuclear Ni Schiff base catalysis towards spiro-oxindoles


In this panorama, organocatalysis has recently had its breakthrough, thus in the last few years many groups focused their attention to organocatalytic enantioselective synthesis of spiro-oxindoles.

A noteworthy example was reported in 2011 by Shao's group that has developed an organocatalytic asymmetric double Michael addition of nitroalkenes **112** to 3-

substituted spiro-oxindoles **111**; this transformation, catalyzed by a thiourea catalyst (**114**) in mild conditions, leads to spirocyclopentaneoxindoles (**113**) with quite good diastereoselectivity and enantioselectivity (up to >30:1 dr; up to >99% *ee*) (Scheme 34).⁶⁸

Scheme 34: enantioselective synthesis by Shao *et al.*

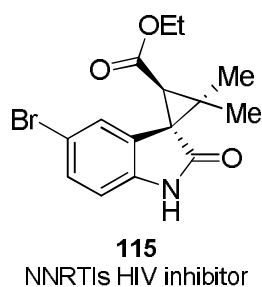


Several other examples of organocatalytic asymmetric synthesis of spirocyclopentane and spirocyclohexane oxindoles have recently been presented, whereas not much attention has so far been addressed to oxindoles spiro fused with three-membered rings.⁶⁶

3.2.2 Asymmetric synthesis of spiroepoxy oxindoles

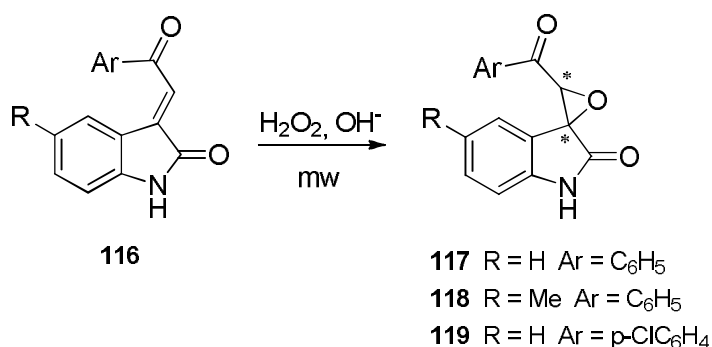
The field of symmetric and nonsymmetric synthesis of highly strained three-membered-cycle, spiro-fused oxindoles has not been broadly investigated so far, even though these include some examples of biologically relevant compounds, such as cyclopropyl oxindole scaffolds, like **115**, that have shown powerful activity as HIV transcriptase inhibitors.⁶⁹

Scheme 35: cyclopropyl oxindole



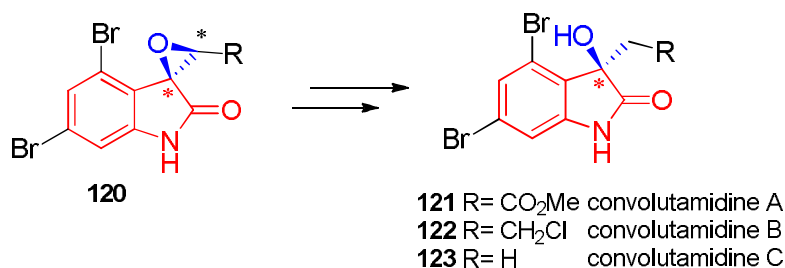
Among three-membered ring spiro-fused oxindoles, spiro-epoxy oxindoles are also considered pharmacologically interesting compounds; this interest is due to the presence of the oxirane moiety, which, because of its high reactivity, is often related to anti-viral or cytotoxic activity. Although in the 60's Anthony firstly envisioned the spiro-epoxy oxindoles high reactivity under various conditions,⁷⁰ only far more recently other research groups have reported about the symmetric synthesis of many interesting biocide spiroepoxy-oxindoles. Some of such compounds (**117-119**) were synthesised as racemates by Dandia *et al.* through nucleophilic epoxidation of the 3-alkenyl oxindoles **116**, using hydrogen peroxide as oxidant, under basic conditions, with microwaves irradiation (Scheme 36).⁷¹ Many other approaches to spiroepoxy-oxindoles are reported in literature, but none of them achieve enantioenriched compounds.⁷²

Scheme 36: Dandia synthesis of spiro-epoxy oxindoles; **117** and **118** have anti-fungal and anti-tubercular properties, **119** is active against melanoma



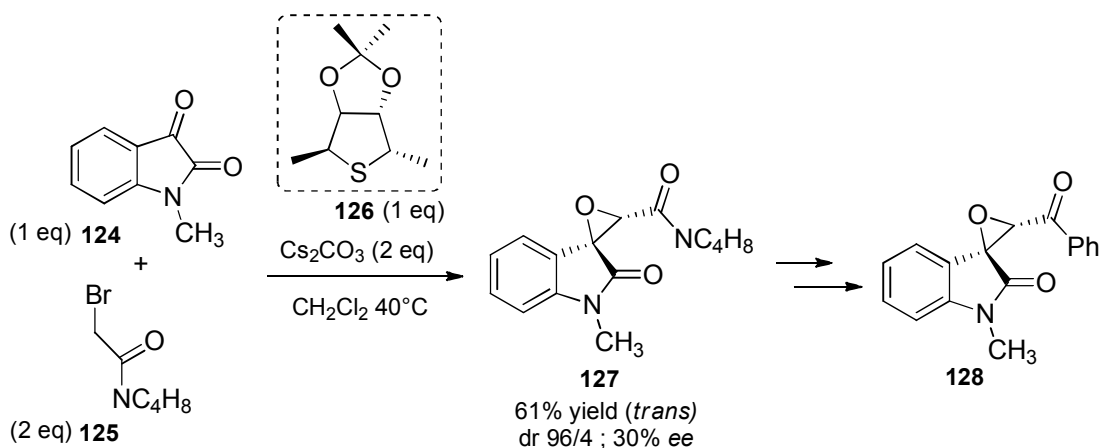
Furthermore, spiroepoxy oxindoles can be considered direct precursors of the corresponding alcohols, *via* the opening of the oxirane ring (Scheme 37). Such compounds are among biologically active molecules, such as convolutamidine A, B, and C (**121-123**) that are alkaloids isolated from a marine organism and are known to stop leukaemia promyelocytic (AML) cells growth.

Scheme 37: epoxy oxindoles as direct precursors of convolutamidines



Indeed, an asymmetric and possibly organocatalytic approach to these interesting molecules, is a desired goal. The past few years have witnessed a rapid progress in the asymmetric organocatalytic construction of various spirocyclic oxindoles, nevertheless the literature concerning asymmetric synthesis of these molecules, spiro-fused with an oxirane ring is surprisingly poor.⁶⁶ An example was presented in 2007 by Metzner *et al.* in which a chiral sulfide (**126**) afforded a promising and straightforward entry to the nonracemic epoxyoxindole **127** with poor enantioselectivity (30% *ee*) (Scheme 38). The product could be easily converted in the anticancer agent **128**, *via* phenyllithium chemoselective addition to the amide.⁷³

Scheme 38: Shulz et al. presented an asymmetric synthesis of spiroepoxyoxindoles



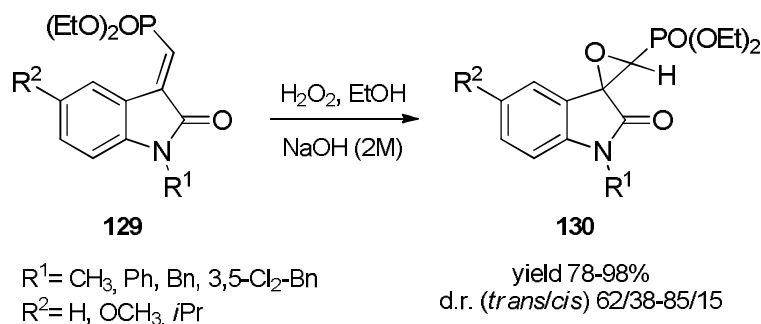
3.3 Results and discussion

3.3.1 A foreword and first experiments

As a consequence of the oxindole-derived compounds relevance, Loreto's research group in the last few years has addressed many efforts to study both synthesis of 3-ylideneoxindoles and their use for the construction of three-membered ring spiro-fused oxindoles. In 2009 they presented the facile synthesis of spiroaziridine-oxindoles, starting from the corresponding alkenes.⁷⁴ In 2011 the same group reported about a Weitz-Sheffer-type nucleophilic epoxidation of 3-(oxyphosphonylmethylene)-oxindoles (**129**) which allowed them to obtain racemic compounds (for example **130**) bearing a phosphonate moiety on the epoxidic ring (Scheme 39).⁷⁵ The reaction showed to be highly diastereoselective (up to 85/15 dr), since, starting from the *E* isomer (**129**), almost only the isomer **130-trans** was always isolated.

The phosphonate moiety in 3-ylideneoxindoles **129** represents a second electron withdrawing group (EWG) on the exocyclic double bond, which is then more electrophilic and is thus activated towards nucleophilic attack; moreover phosphonate group indeed represents an appealing function because it is endowed in many anti-viral and anti-bacterial agents, such as phosphomycin.⁷⁶

Scheme 39: diastereoselective nucleophilic epoxidation of ylidenoxindoles

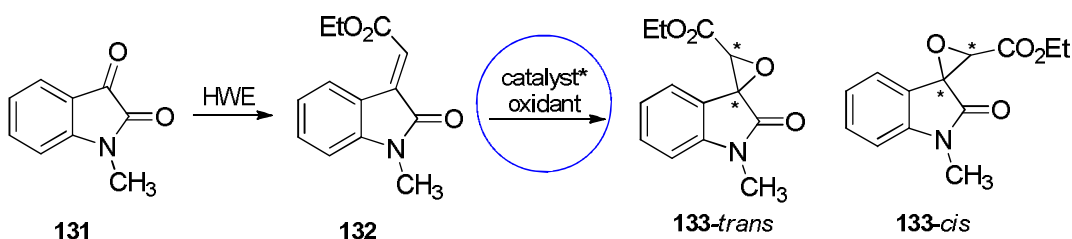


In the light of these interesting studies and of the potential interest of an enantioselective approach to the appealing spiroepoxy-oxindoles, the possibility of synthesizing optically active spiro-epoxyoxindole esters was taken into account.

On these grounds and in the light of the lack of efficient methodologies for enantioselective epoxidation of electron-poor olefins, the main purpose of this thesis is the development of an efficient, general, organocatalytic asymmetric modification of the nucleophilic epoxidation of electron-poor 3-ylideneoxindoles, that could afford the

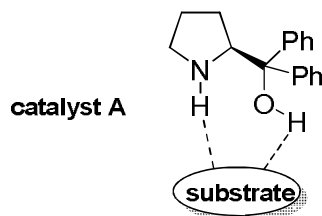
corresponding spiroepoxyoxindoles with high diastereisomeric ratios and high enantiomeric excesses. At variance with the above studies,⁷⁵ the initial investigations were performed on the ylidenoxindole **132**, carrying a carboxy-ethyl group, more potent than the phosphonate group, as a second EWG. Substrate **132** was easily prepared, following the procedure reported in literature, from 1-methyl isatin (**131**) via a Horner-Wadsworth-Emmons reaction (HWE) (Scheme 40). The epoxidation of *E*-olefin **132** could in principle lead to two diastereoisomers, **133-trans** and **133-cis**, even though an excess of *trans* was expected, because of the *E*-configuration of the substrate's double bond.

Scheme 40: epoxidation of carbethoxy derivative **132** and the four epoxy isomers. Stereochemistry is re



In order to choose a chiral organocatalysts, since a number of chiral secondary amines exhibit different action mode with respect to the employed substrate, we started to try the (*S*)-1,1'-bi-2-phenylprolinol (catalyst **A**) in view of the great potential previously showed in catalyzing epoxidation of α,β -unsaturated ketones.⁷⁷ Indeed, the so-called “chameleon” catalyst, is endowed with two functionalities, a hydroxyl and an amine, that makes diphenylprolinol included in the bifunctional catalysts class; for these reasons it can establish non-covalent interactions with suitable substrates (Scheme 41).

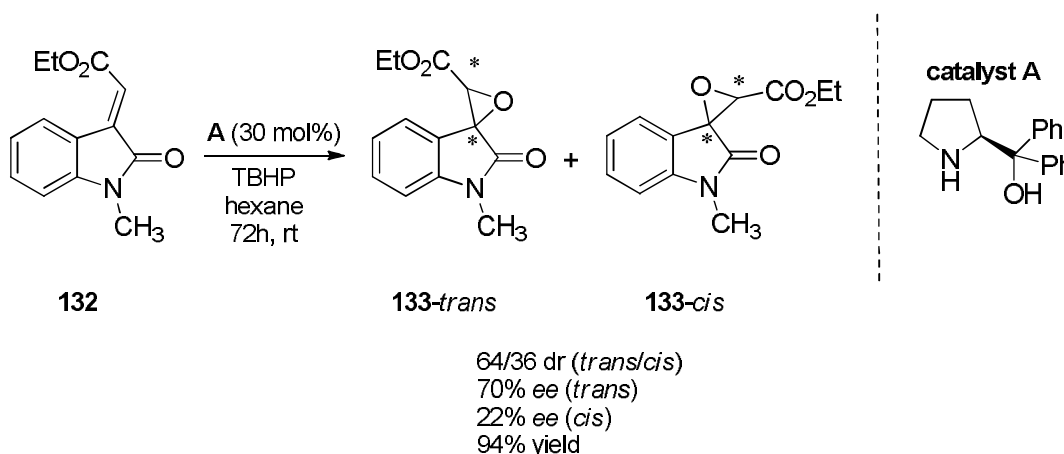
Scheme 41: diphenylprolinol (**48**, catalyst **A**) as a noncovalent catalyst, creates an hydrogen bond net with suitable substrates



Taking into account what previously reported about the epoxidation of α,β -unsaturated ketones,⁷⁸ the first reaction on **132** was performed with 30 mol% of **A**. *Tert*-butylhydroperoxide (TBHP) was employed as oxidizing agent and the reaction was

performed in HPLC grade hexane, even though both the substrate and products were barely soluble in such a medium. This first attempt was successful. Despite the starting material having the *E* configuration, after purification of the reaction crude *via* flash chromatography, two products were isolated and identified as *trans* and *cis* spiro-oxiranes (**133-trans**, **133-cis**), whose characterization and configuration assignment is reported in section 3.3.3. The reaction resulted to be diastereoselective, with a diastereomeric ratio of 64/36 in favour of the *trans* isomer, and enantioselective, since for the *trans* isomer a 70% *e.e.* was observed. A lower *ee* was measured for the *cis* (22% *ee*) (Scheme 42).⁷⁹

Scheme 42: first organocatalytic experiment was performed in presence of 1.1 equivalents of TBHP, 30 mol% of catalyst A, in hexane for HPLC (0.38 M solution).



3.3.2 Screening of the catalyst and of reaction conditions

In the light of the first good result, achieved *via* diphenylprolinol catalysis, further investigation of the reaction conditions were planned, by studying the effects of different catalysts, oxidizing agents, solvents, reagents concentration and temperature. Starting with a catalyst screening, a few pyrrolidine derivatives, in particular commercially available catalysts **B-E**, were tested under the same conditions (Scheme 44). Results are reported in Table 1. Catalysts **B** and **C**, respectively the methyl- and the trimethylsilyl-ether of diphenylprolinol **A**, led to very poor enantioselectivity (Table 1, entries 2,3), probably because of the lack of a pseudo-Lewis acid function that prevents the formation of a strong H-bond network. This results strongly suggested the key role of the free OH group in the catalyst **A**, able to establish an H-bond network.

Subsequently, the reaction was performed with pyrrolidine derivatives **D**, **E**, bearing both Brønsted basic and Lewis acid sites, but bringing some substituents on phenyl

rings.⁸⁰ Particularly, the bulkier catalyst **D**, endowed with two 3,5-dimethylphenyl substituent, led to lower ee_s and slower reactivity, with respect to catalyst **A**. Furthermore, catalyst **E**, which bears the electron withdrawing trifluoromethyl substituents on both phenyl rings, led to similar enantioselectivity already observed with catalyst **A**, but both in lower yields and lower reactivity (Table 1, entries 4,5). Thus, the less expensive diphenylprolinol **A** appeared to be the best choice for our reaction so far. Afterwards, going on with the optimization of the reaction, some variations in the reaction conditions were devised, exploring oxidizing agents different from TBHP (Scheme 44). However, the use of both hydrogen peroxide, already used by Loreto *et al.* in the diastereoselective epoxidation of ylidenoxindoles,⁷⁵ and the bulkier cumene hydroperoxyde, did not improve ee_s . In the former case a sharp drop in ee_s was observed, although accompanied by a marked increase in dr , while, in the latter case, the same enantioselectivity as with catalyst **A** was observed, but with a great drop in reactivity, since the reaction time for complete conversion changed from 72 to 400 hours (Table 1, entries 6, 7).

Scheme 43: reaction to be optimized; catalysts tested for the initial screening of the reaction conditions

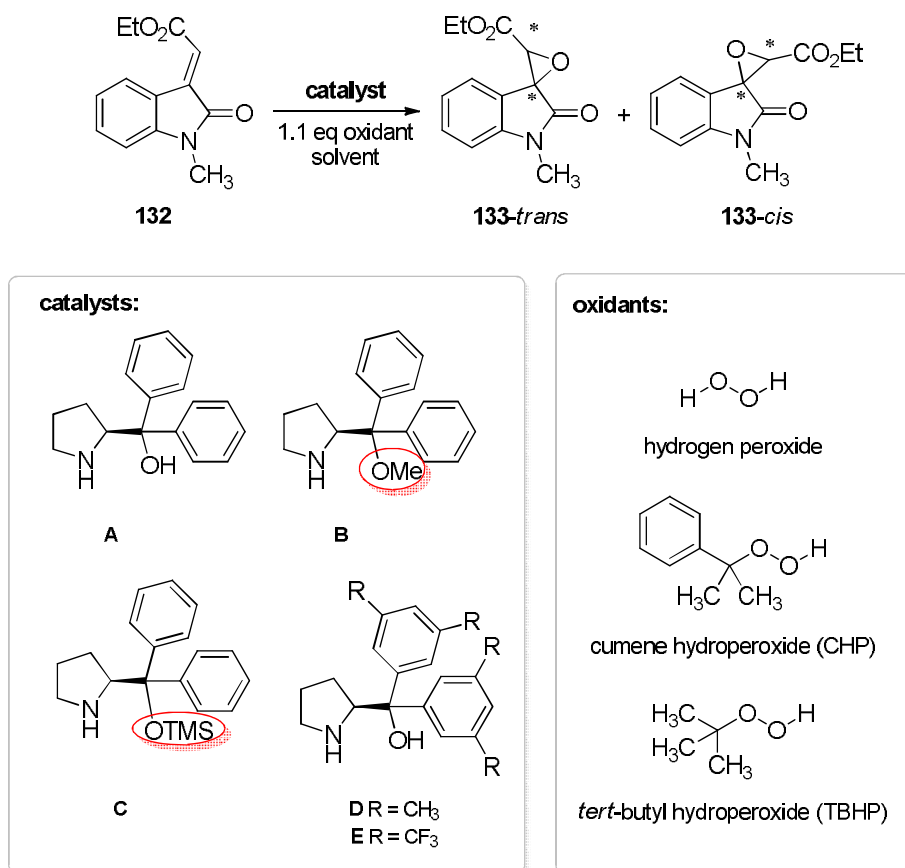


Table 1: screening of reaction conditions (catalyst, oxidant, solvent, concentration, temperature) Reaction conditions: N-methyl- α -ylideneoxindole **132** (0.5 mmol), TBHP (0.6 mmol), catalyst (0.15 mmol) in 1.3mL HPLC grade hexane, at RT. ^Yields of the isolated products are expressed as the sum of the diastereomers. d.r. were determined by ^1H NMR of the crude reaction mixture. ee_s were determined by chiral-phase HPLC analysis. ^aH₂O₂ (30% in water, 0.15 mmol) was employed as the oxidant. ^bCumene hydroperoxide (CHP, 0.15 mmol) was employed as the oxidant.

entry	catalyst	time (h)	yield (%)	dr (<i>trans/cis</i>)	<i>e.e. trans</i> (%)	<i>e.e. cis</i> (%)
1	A	72	94	64/36	70	22
2	B	40	83	25/75	37	2
3	C	140	95	36/64	58	1
4	D	110	89	64/36	72	36
5	E	360	75	66/34	38	22
6^a	A	36	84	96/4	2	1
7^b	A	400	80	66/34	70	22

Furthermore, the reaction was performed in different solvents, polar and nonpolar, such as chloroform, acetonitrile, ethanol, dimethyl sulfoxide, tetrahydrofuran, and toluene (see Table 2). Performing the reaction in toluene or chloroform, did not lead to an increased stereoselectivity, but instead it decreased the reactivity, even though the reaction mixture was completely soluble in such media. The use of polar solvents lowered both rate and selectivity. Thus hexane appeared to be the best solvent, in terms of selectivity and efficiency, in spite of the poor solubilising power. This evidence could be ascribable to phase transfer effects. Later on, the effect of the concentration, was explored, by performing the reaction with a different amount of solvent. Higher dilution was found to lead to better enantioselectivity (82% *ee* for **133-trans**, Table 2, entry 4) with the same reaction rate.

Moreover, varying the experimental temperature did not seem to affect our reaction, since performing the reaction at 4°C similar results were obtained (Table 2, entry 5).

Thus the best conditions for the enantioselective epoxidation required catalyst **A** 30 mol%, in hexane, at room temperature, with TBHP as oxidising agent (Table 2, entry 4).

Scheme 44: reaction to be optimized; catalysts tested for the initial screening of the reaction conditions

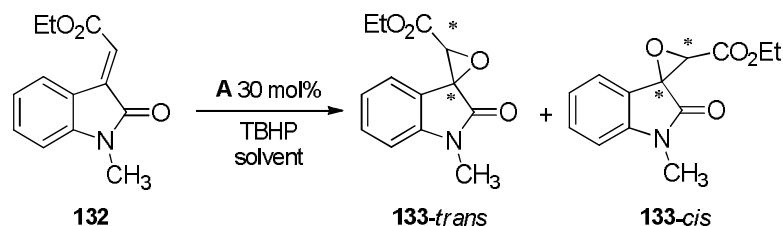


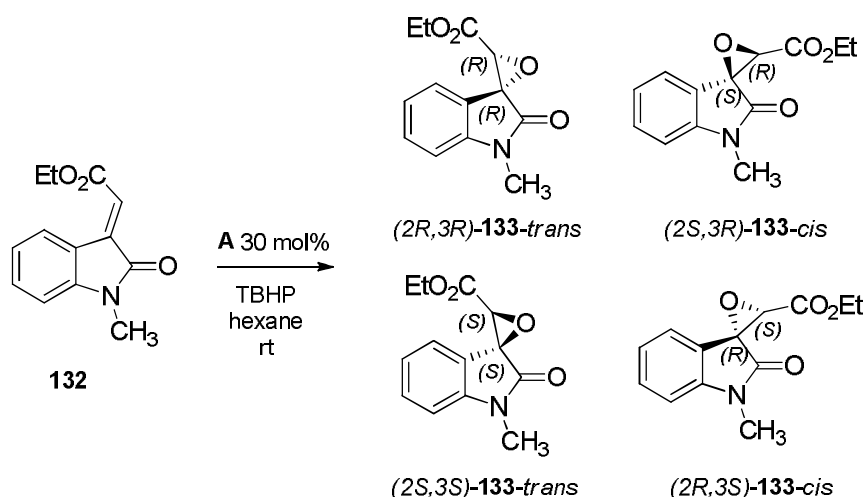
Table 2: Reaction conditions: N-methyl- α -ylideneoxindole **132** (0.5 mmol), TBHP (0.6 mmol), catalyst **A** (0.15 mmol) and solvent at RT. Yields of the isolated products are expressed as the sum of the diastereomers. d.r. were determined by ^1H NMR of the crude reaction mixture. ee_s were determined by chiral-phase HPLC analysis. *reaction was performed at 4°C .

entry	solvent	mL	time (h)	yield (%)	dr (<i>trans/cis</i>)	<i>ee</i> <i>trans</i> (%)	<i>ee</i> <i>cis</i> (%)
1	hexane	0.5	12	96	68/32	45	14
2	hexane	1.0	48	95	67/33	67	20
3	hexane	2.0	68	87	64/36	74	26
4	hexane	2.7	72	95	64/36	82	19
5*	hexane	2.7	72	92	66/34	64	36
6	hexane	4.0	120	90	55/45	80	25
7	CHCl_3	0.6	240	55	66/34	71	16
8	CH_3CN	0.6	192	90	68/32	46	40
9	EtOH	1.3	192	70	61/39	48	39
10	DMSO	1.3	96	83	78/22	33	40
11	THF	0.6	192	85	68/42	57	29
12	toluene	0.6	120	73	59/41	69	18

3.3.3 Structural and stereochemical assignment

After the first optimization of the reaction conditions was done, a structural and stereochemical assignment for the products was accomplished, since the epoxidation led to new products, namely two diastereoisomers, each one including two enantiomers [(*2R,3R*)-**133-trans**, (*2S,3S*)-**133-trans**, (*2S,3R*)-**133-cis**, (*2R,3S*)-**133-cis**], Scheme 45).

Scheme 45: epoxidation products

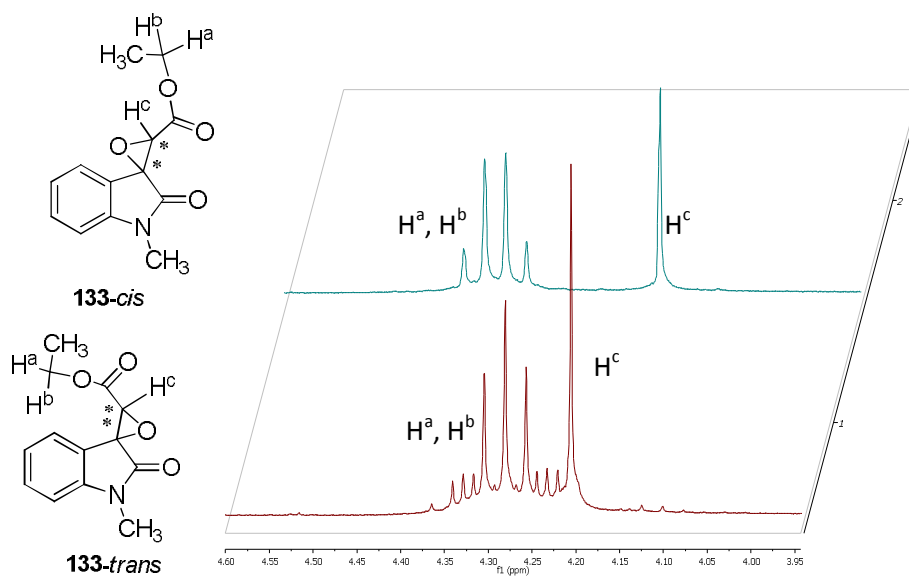


$^1\text{H-NMR}$ and NOESY data

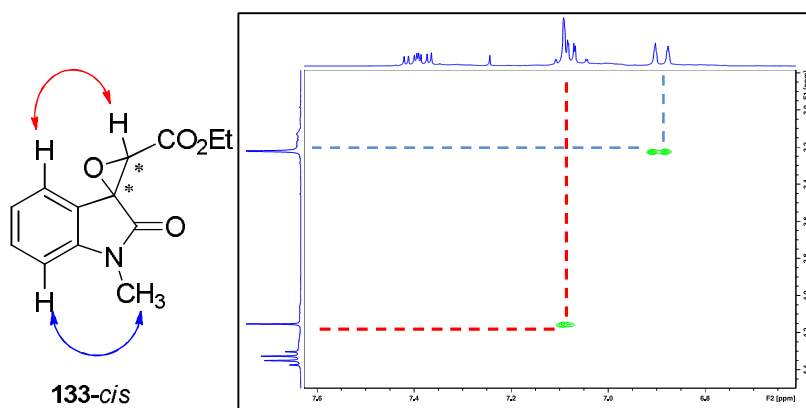
The *trans/cis* configuration of the epoxidation products, **133-trans** and **133-cis**, was assigned by $^1\text{H-NMR}$ and NOESY analysis. In the $^1\text{H-NMR}$ spectra, the differences were the shift of the H^c singlet and the shape of the H^a - H^b system, which in one spectrum shows the expected multiplet while in the other appears as a quartet (Scheme 46). In fact protons H^a and H^b are diastereotopic, because of the chiral centres. In the light of these evidences, NOESY experiments, whose data are reported below, appeared necessary to unambiguously elucidate the configurations (Scheme 47, Scheme 48). Indeed:

- in the NOESY spectrum of **133-cis** (Scheme 47) cross-peaks were found between the aromatic 4-H atom [δ 7.04-7.14 (m, 2H, CH_{arom}) ppm] and the epoxide proton [δ 4.15 (s, 1H, OCH) ppm], due the spatial proximity of these nuclei, unequivocally proving the *cis* configuration of the minor diastereoisomer **133-cis**. Moreover, further cross-peaks are generated by the spatial interaction between the H atom belonging to the N-CH_3 [δ 3.22 (s, 3H, CH_3N) ppm] group and 7-H atom on the aromatic ring [δ 6.89 (dd, $J = 7.8\text{Hz}$, 0.5Hz , 1H, CH_{arom}) ppm].
- conversely, no NOESY cross peaks for the epoxide proton were found in the major **133-trans** isomer (Scheme 47).

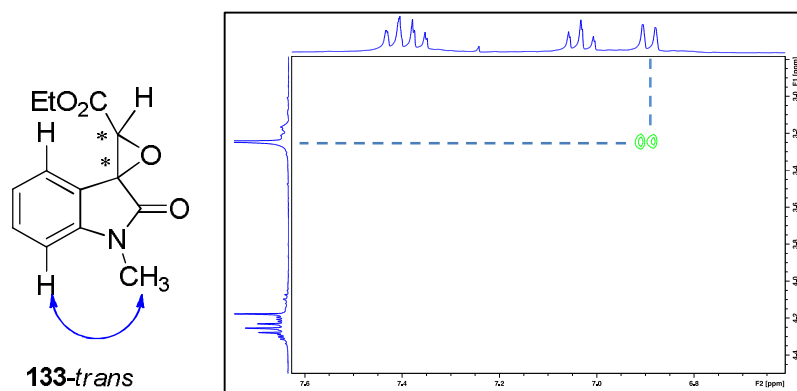
Scheme 46: $^1\text{H-NMR}$ segment of the methylene and oxiranic protons



Scheme 47: segment of the NOESY spectrum of the **133-cis** isomer



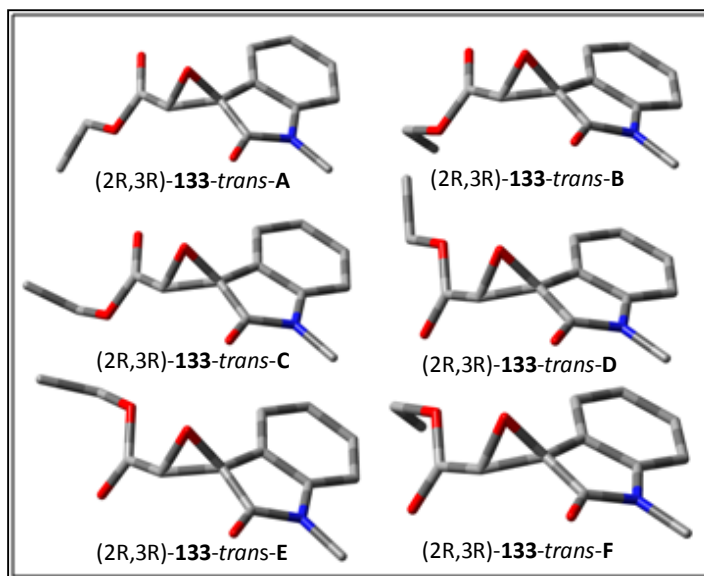
Scheme 48: segment of the NOESY spectrum of the **133-trans** isomer



Optical Rotation Dispersion Data: assignment of absolute configurations to products 133 by comparison between calculated and experimental values.

The absolute configurations for the two diastereoisomers **133**, are based on a thorough comparison of the aforementioned experiments, analytical data and a quantum mechanical *ab initio* calculation of chiroptical properties. Indeed, once it is unambiguously determined *via* ^1H NMR and NOESY experiments, the *trans/cis* configuration of the obtained diastereomers (**133-trans** and **133-cis**) was used to simulate the optical rotation dispersion (ORD). This calculation was performed, by means of the Time-Dependent Density Functional Theory (TDDFT) method,^j using an arbitrarily fixed absolute configuration (*2R,3R*) for the major enantiomer of **133-trans**. In fact, molecular mechanics provided six conformers (**133-trans-A** - **133-trans-F**, Figure 8), which were then fully optimized;^k calculated conformers free energies were used to carry out Boltzmann's populations distribution. All optimized conformers differ each other by the orientation of the ester moiety (Figure 8). In Figure 9 the most stable conformer (*2R,3R*)-**133-trans-A** structure is reported.

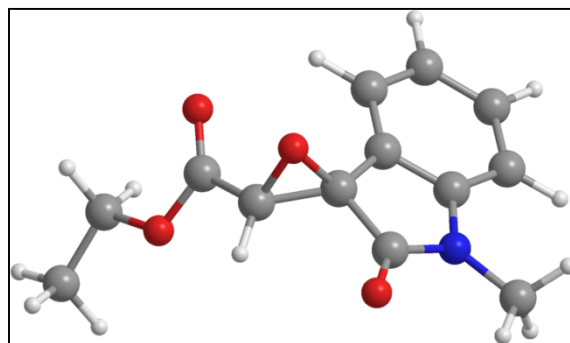
Figure 8: structures of the most stable conformers of (*2R,3R*)-**133-trans** optimized at the DFT/B3LYP/6-31G* level of theory



^j Calculations performed by Giuseppe Mazzeo, Università della Basilicata

^k Molecular mechanics provided six conformers, then fully optimized at DFT/B3LYP/6-31G* level of calculation.

Figure 9: The most stable conformer (*2R,3R*)-**133-trans-A** calculated at DFT/B3LYP/6-31G* level of theory



The calculated optical rotatory power at four different wavelengths (589.3, 546, 435 and 405 nm), relative free energies, Boltzmann populations for all optimized conformers of (*2R,3R*)-**133-trans** were compared with the experimental ORD and are shown in Table 3.

Table 3: Relative-free energies with respect to the most stable conformer (**133-trans-A**), populations and calculated ORD values ($\text{deg [dm g/cm}^3\text{]}^{-1}$) obtained at TDDFT/B3LYP/6-31G* level for each conformer (**133-trans-A** - **133-trans-F**) at four different wavelengths. Comparison between the total calculated and the experimental ORD values in CH_2Cl_2 ($c = 0.55 \text{ g/cm}^3$ in CH_2Cl_2).

Conformers	ΔG (kcal/mol)	% pop	$[\alpha]_D$	$[\alpha]_{546}$	$[\alpha]_{435}$	$[\alpha]_{405}$
133-trans-A	0.0	45.9	-101	-127	-294	-419
133-trans -B	0.4	24.3	-51	-64	-153	-220
133-trans -C	0.5	21.4	-75	-92	-193	-262
133-trans -D	1.4	4.7	-15	-18	-37	-50
133-trans -E	1.7	2.7	-7	-8	-18	-25
133-trans -F	2.2	1.0	-2	-2	-6	-8
Total						
Calculated			-250	-312	-701	-984
ORD values						
Experimental			-101	-134	-295	-395
ORD values						

Data in Table 3 show that the sign, the order of magnitude and the uniform trend in the experimental ORD have been correctly reproduced by the calculations, despite the fact

that the Boltzmann averaged ORD values are about twice higher than the experimental ones. Such differences may result from basis set calculation errors in overestimating ORD. Nevertheless, it is important to notice that all calculated conformers OR are negative. In fact, problems may arise in the case of flexible molecule having many conformers with opposite-signed OR in order to get a more accurate geometries, populations and OR computational analysis achieving a reliable absolute configuration assignment. In any case the conformers geometry optimization and the ORD calculation were performed with other methods (Table 4), in order to check if significantly changes may occur in the theoretical predictions of respective conformers and/or in the conformational distribution, which could become more significant as in the present case where several conformers are involved. Then no significantly differences were found (Table 4).

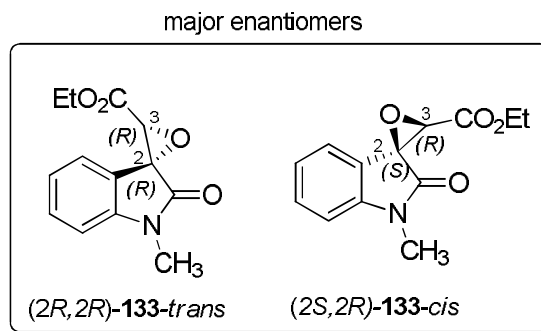
Table 4: Relative-free energies with respect to the most stable conformer (**133-trans-A**), populations and calculated ORD values ($\text{deg} [\text{dm g/cm}^3]^{-1}$) obtained at TDDFT/B3LYP/6-31++G(2d,2p) level for each conformer (**133-trans-A** - **133-trans-F**) at four different wavelengths. Comparison between the total calculated and the experimental ORD values in CH_2Cl_2 ($c = 0.55 \text{ g/cm}^3$ in CH_2Cl_2).

Conformers	ΔG (kcal/mol)	% pop	$[\alpha]_D$	$[\alpha]_{546}$	$[\alpha]_{435}$	$[\alpha]_{405}$
133-trans-A	0.0	53.9	-115	-145	-337	-478
133-trans -B	0.6	18.6	-39	-49	-116	-167
133-trans -C	0.7	17.2	-57	-71	-149	-202
133-trans -D	1.3	6.4	-20	-25	-51	-68
133-trans -E	1.8	2.7	-6	-8	-17	-24
133-trans -F	2.3	1.1	-2	-3	-6	-9
Total						
Calculated ORD values			-240	-301	-677	-948
Experimental ORD values			-101	-134	-295	-395

In conclusion a satisfactory agreement between experimental and calculated ORD was found; these evidences strongly support the (2*R*,3*R*) configuration for the **133-trans** epoxide (Scheme 48). Likewise, the (2*S*,3*R*) configuration to the major enantiomer of

133-cis has been assigned by exploiting the same quantum mechanics protocol. In particular, the experimental optical rotation value at $\lambda = 589.3$ nm for the (2'S,3'R)-**133-cis-A** is $[\alpha]_D = -105$ ($c = 0.035$ g/cm³ in CHCl₃); this value has to be compared with the *ab initio* calculated one $[\alpha]_D = -258$ [deg (dm g/cm³)⁻¹].⁸⁰

Scheme 49: assigned configurations of the major enantiomers



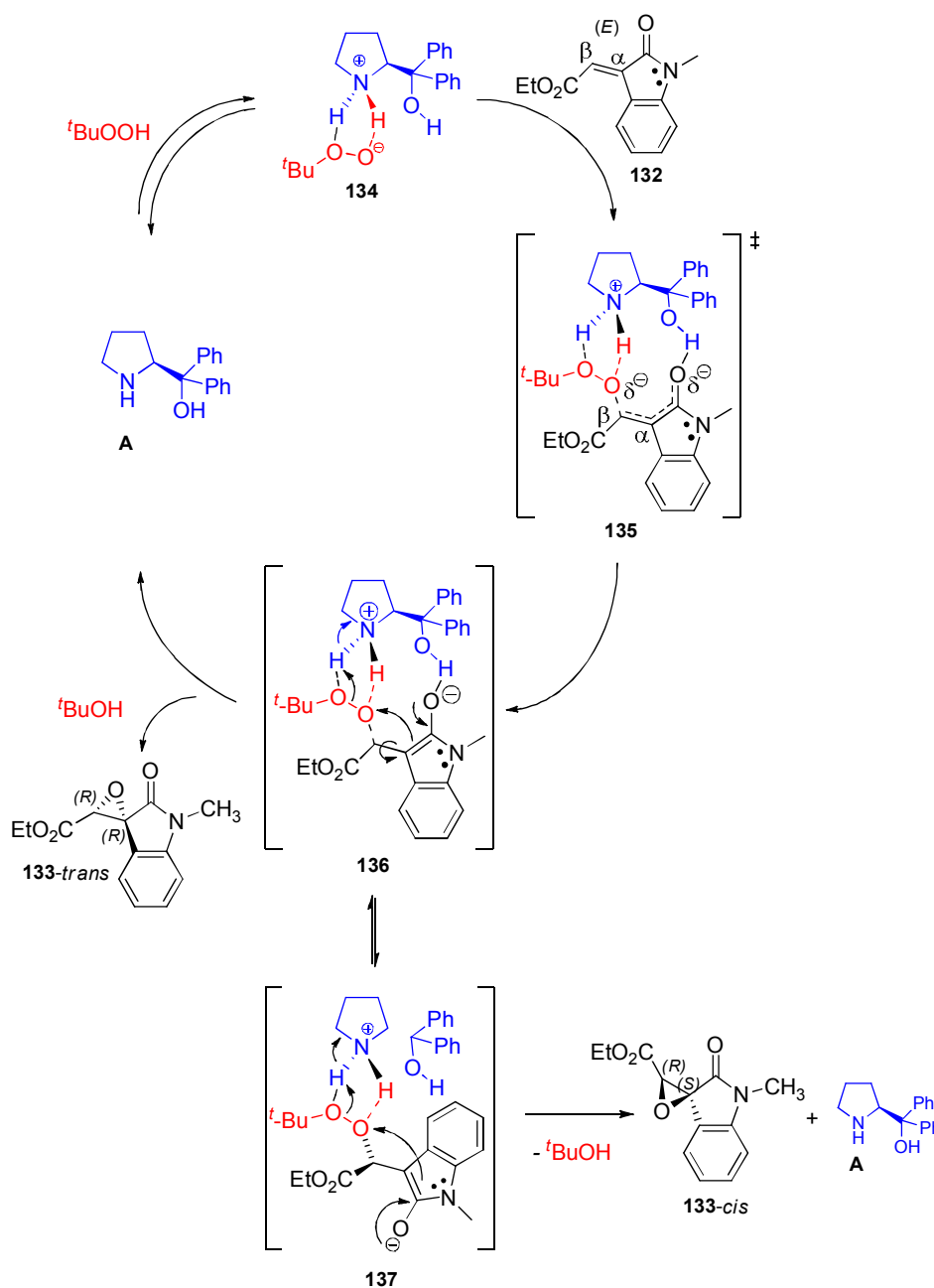
3.3.4 Mechanistic considerations

Initial hypothesis

In the light of the experimental evidences and of the calculated configuration (2R,3R) of the major stereoisomer (**133-trans**), a mechanism hypothesis was formulated, which agreed with the recent statements regarding the asymmetric epoxidation of α,β -unsaturated ketones.⁷⁸ This hypothesized catalytic pathway, depicted in Scheme 50, proposes the following: (i) the interaction between TBHP and the catalyst activates the oxidizing agent, leading to the tight ion pair **134**; (ii) the first regioselective attack of **134** at the C _{β} carbon¹ of the substrate is promoted by both the intermediate aromatization and formation of a stabilizing H-bond between the OH in the catalyst and the partial negative charge on the lactam carbonyl moiety;⁸¹ (iii) thus, the reagent approach is preferentially driven toward the less-hindered *re*-face of the double bond, resulting in the aromatic and long-living **136** intermediate; and (iv) two alternative evolutions of **136** may result in either the oxirane (2R,3R)-**133-trans** (*via* irreversible direct ring closure) or the diastereomer (2S,3R)-**133-cis** (*via* intramolecular H-bond breaking and the rapid subsequent rotation around the C _{α} -C _{β} σ bond to produce the **137** intermediate).⁸⁰

¹ α and β positions are referred to the lactamic carbonyl group.

Scheme 50: initial mechanism hypothesis



Further mechanistic considerations

Our initial mechanism hypothesis has been reconsidered in the light of some DFT calculations performed by Prof. Shiina;^m these calculations suggest a slightly different reaction mechanism, which is depicted in Scheme 51. Some key steps can be elucidated:

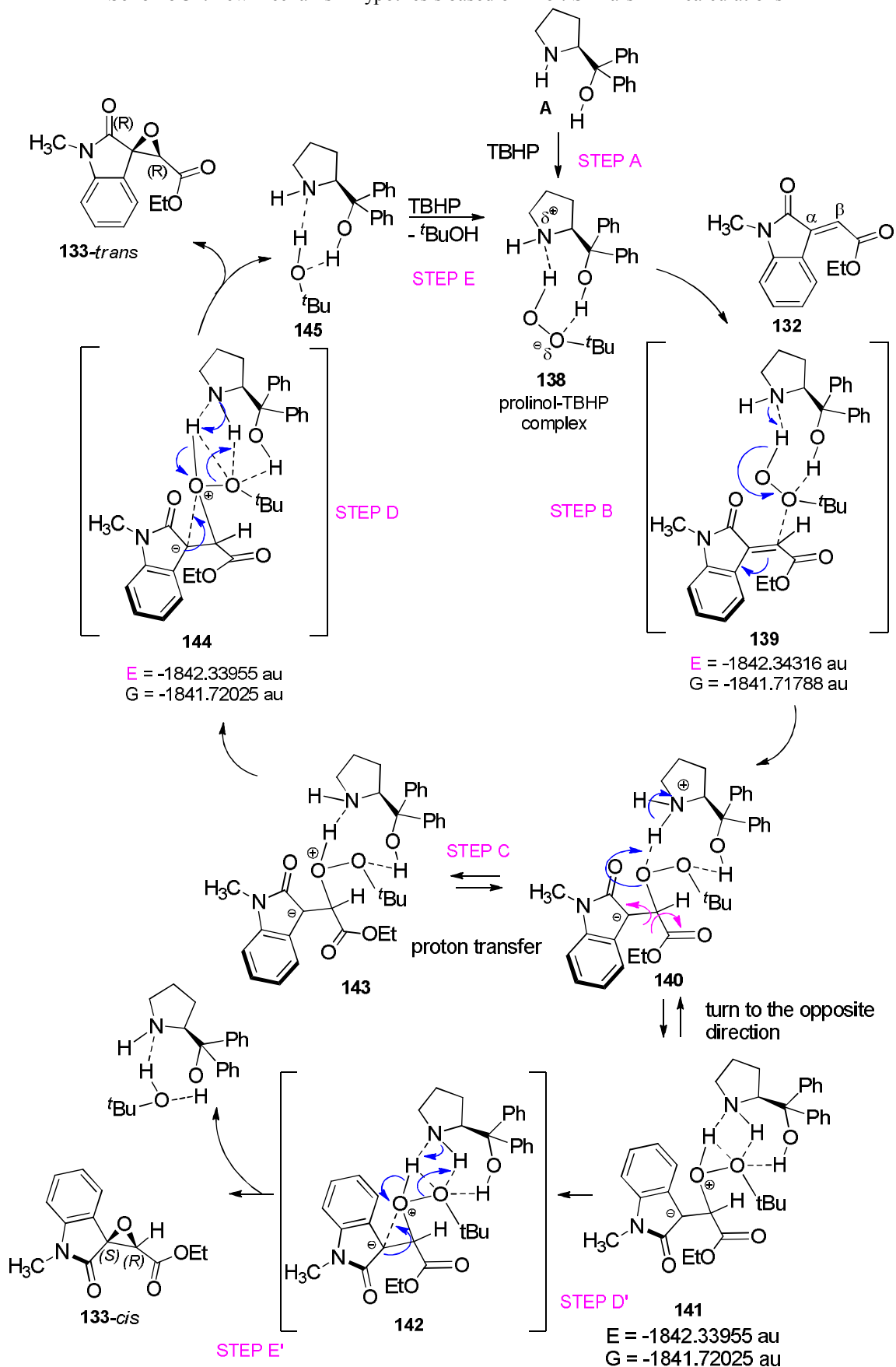
1. first step (Scheme 51, step A) is the formation of the prolinol-oxidant complex (138), which already differs from our initial hypothesis, since it envisages two

^m Tokyo University of Science

H-bonds between TBHP and the base site of **A** without deprotonation of the oxidant;

2. in the second step (step B), the nucleophilic attack of **138** at the substrate α -position and the deprotonation of the oxidant simultaneously gives rise to the transition state **139**, in which there is no H-bond interaction between the carbonyl in the substrate and the catalyst's hydroxyl. Therefore, substrate aromatization is no more conceived as a stabilizing process.
3. subsequent evolution of the transition state **139** into the intermediate **140** occurs with some charge transfers;
4. afterwards either a proton transfer (step C) or the rotation around the C $_{\alpha}$ -C $_{\beta}$ σ bond can occur, leading to intermediates **143** or **141**, respectively;
5. then, the repositioning of the negative charge in the transition states **144** (from **143**; step D) and **142** (from **141**; step D') facilitates the ring closures (steps E and E') to give the *trans*- or the *cis*-epoxides, regenerating the catalyst.

Scheme 51: new mechanism hypothesis based on Prof. Shina's DFT calculations

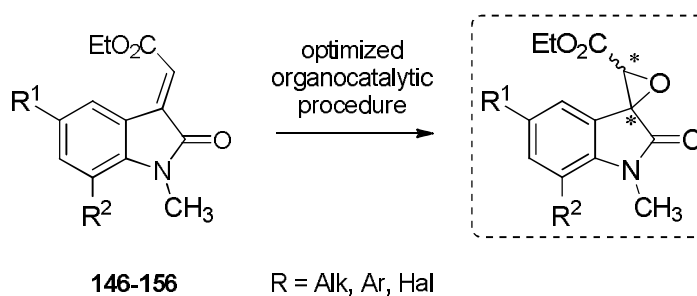


3.3.5 Substrate scope

Synthesis of the starting materials

The above described optimized procedure for the epoxidation of the model ylidenoindole **132** was tested with other substrates in order to check the generality of the methodology. In fact, a procedure, to be considered a good one, should be useful for a broad scope of compounds. Indeed the evaluation has to be done in terms of enantioselectivity, yield and reaction time. Thus a substrate scope was planned bearing various substituents on the aromatic ring, such as alkyl or aryl groups and halides (Scheme 52). Studying the effect of electron withdrawing or electron donating groups, the effect of bulky substituents on different positions of the oxindole ring, could have allowed us to give further insights on the reaction mechanism.

Scheme 52: Plan for the substrate scope



The synthesis of ylidenoindoles (**146** to **156**) was accomplished starting from the corresponding isatines *via* methylation of the oxyndole nitrogen followed by a Horner-Wadsworth-Emmons (HWE) 3-ylidenation (Scheme 53), following the procedures reported in literature.^{74, 80} Reaction times and yields for the HWE reaction are reported in Table 5. The starting olefins, some of which had not been previously synthesized, have been fully characterized by proton and carbon NMR spectrometry, IR and HRMS.

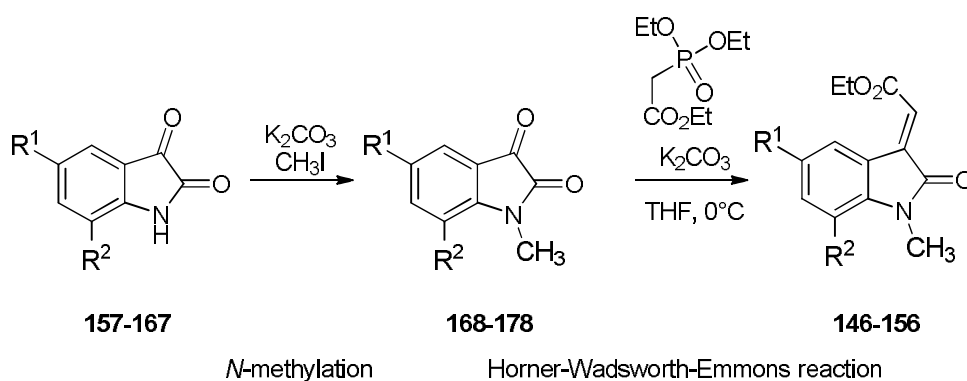
Scheme 53: Synthesis of *N*-methylated carboxylates


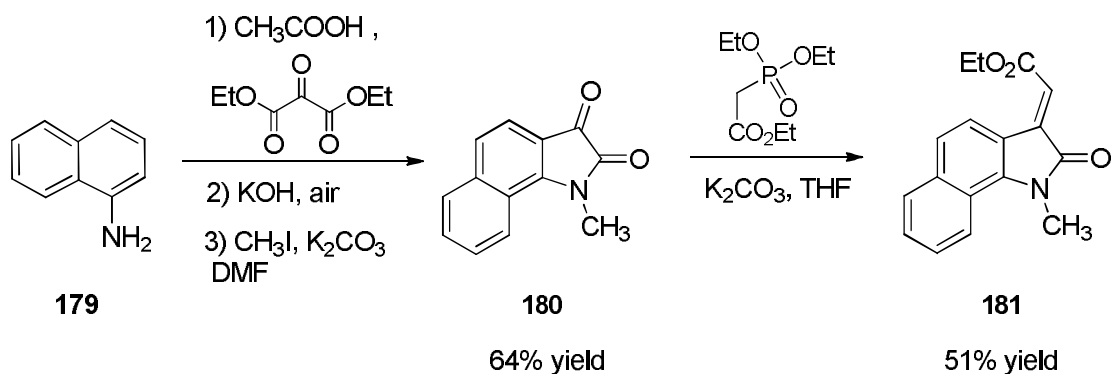
Table 5: Unless otherwise stated, compounds were synthesized following procedures reported in Scheme 53. *for entries 7, 8 and 9 a Wittig reaction was performed instead of the HWE reaction. Detailed procedures are reported in the experimental part. ^olefin obtained starting directly from commercially available methyl-isatine.

entry	product	R ¹	R ²	<i>N</i> -methylation		HWE	
				yield	time	yield	time
1	132	H	H	98%	12 h	80%	12 h
2	146	F	H	95%	30 min	60%	5 h
3	147	Cl	H	99%	20 h	76%	5 h
4	148	I	H	94%	1 h	21%	6 h
5	149	OCF ₃	H	95%	1 h	67%	5 h
6	150	<i>i</i> -Pr	H	84%	overnight	63%	48 h
7*	151	NO ₂	H	89%	30 min	58%	3 h
8*^	152	OCH ₃	H	90%	12 h	90%	12 h
9*	153	Cl	Cl	95%	1 h	89%	2 h
10	154	H	F	96%	30 min	71%	1 h
11	155	H	Cl	98%	30 min	61%	1 h
12	156	H	Br	98%	30 min	56%	1 h

Compound **181** (Scheme 54) was instead obtained through a one pot reaction where an acid catalyzed Friedel-Crafts alkylation with diethyl ketomalonate was followed by the intramolecular amidation.^{81(a)} Subsequent saponification and *N*-methylation gave the isatin **180** which was converted into the 3-yliden-derivative **181** by the usual HWE

reaction. Intermediate **180** and the new product were fully characterized and the *E*-configuration of the double bond was assigned by comparison with the known 3-ylidenoxindoles.

Scheme 54: Synthesis of compound **181** by Friedel-Crafts alkylation, followed by saponification, N-methylation and final HWE ylidation



Organocatalytic epoxidation on the synthesized compounds

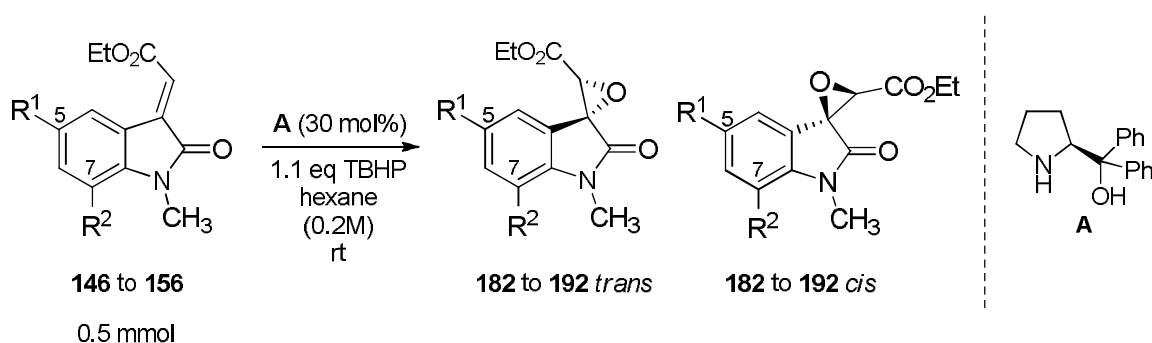
With the optimized epoxidation procedure in our hands, the reaction was tested on the other new *N*-methyl olefins (Scheme 55, **132-156**, **181**) and results are reported in Table 6. The epoxidation reaction always led to the two diastereomers, (Scheme 55, **182-192-trans**, **182-192-cis**), which were isolated from the reaction crude *via* flash chromatography. Moreover, all the obtained epoxides have not been previously synthesized, thus complete characterization was necessarily done for every *trans* and *cis* isomer. The epoxidation of compounds endowed with halides in positions 5 or 7 (Table 6, entries **2-4**, **9-12**) resulted in good enantiomeric excess for the *trans* product, except for the epoxide bearing a iodine, which instead showed a lower *ee* (Table 6, entry **4**). The presence of a bromine (entry **12**) or two chlorine atoms (entry **9**), led to the highest enantioselectivities for the *trans* product (respectively 88% *ee* and 85% *ee*) together with an higher *ee* for the *cis* isomers too (respectively 53% *ee* and 58% *ee*) and a faster reaction if compared with that performed on the model unsubstituted 3-ylidenoxindole. In addition, in all reported cases, including isopropyl, nitro and trifluoromethoxy compounds (entries **5-6**), an inversion of the diastereomeric ratio was observed, in favour of the *cis* products.

These effects could be ascribable to some supplementary interactions between the halide and the catalyst able to stabilize the transition state that precedes the *cis* isomer

formation. It appeared clear that these organocatalytic nucleophilic epoxidation outcomes are influenced by halide substituents.

Furthermore, the naphthyl-derived olefin **181** was as well successfully epoxidized, even though products (Scheme 56, **193-trans**, **193-cis**) resulted to be unstable after some hours from purification. This interesting derivatives showed similar enantioselectivity (82% *ee* for the *trans* isomer), reaction time and yield (entry **13**, Table 6). This results suggest that the steric hindrance on the aromatic ring does not strongly affect either the enantioselectivity or the overall reactivity of the reaction.

Scheme 55: epoxidation of the 3-ylidenoxindoles **146-156**. Results are reported in Table 6.



Scheme 56: epoxidation of the naphthyl-derived 3-ylidenoxindole **181**. Results are reported in Table 6.

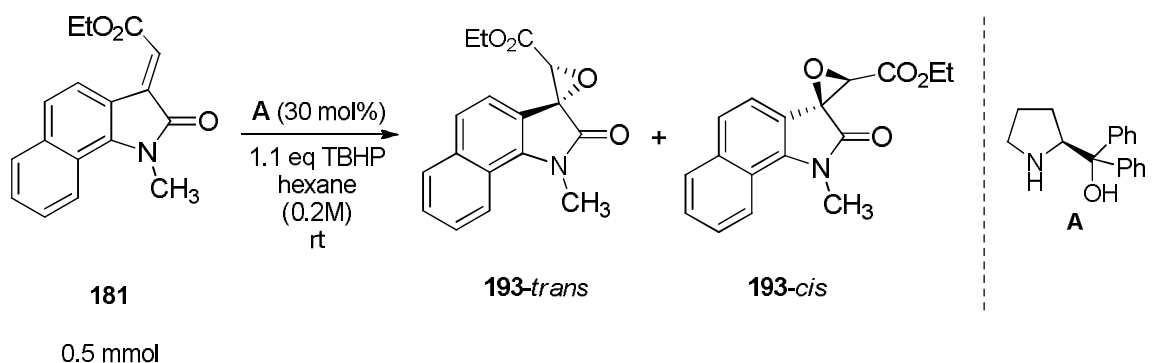


Table 6: the epoxidation was performed on 3-ylidenoxindoles **146-156**, **181**, following the optimized procedure, which requires **A** 30 mol%, 1.1 eq of TBHP, 0.2M in HPLC hexane, at rt.

entry	compound	R ¹	R ²	yield	time (h)	dr (trans/cis)	ee% (trans)	ee% (cis)
1	133	H	H	95%	72	63/36	82	19
2	182	F	H	75%	30	48/52	84	30
3	183	Cl	H	92%	42	40/60	76	42
4	184	I	H	97%	24	33/67	60	32
5	185	OCF ₃	H	36%	144	40/60	78	30
6	186	<i>i</i> -Pr	H	90%	96	42/58	78	27
7	187	NO ₂	H	72%	48	27/73	70	12
8	188	OCH ₃	H	98%	48	51/49	80	24
9	189	Cl	Cl	79%	33	37/73	85	53
10	190	H	F	85%	36	34/66	80	27
11	191	H	Cl	88%	38	25/75	81	32
12	192	H	Br	71%	48	30/70	88	58
13	193	naphtyl derivative		98%	24	51/49	82	10

3.3.6 In-depth catalyst screening

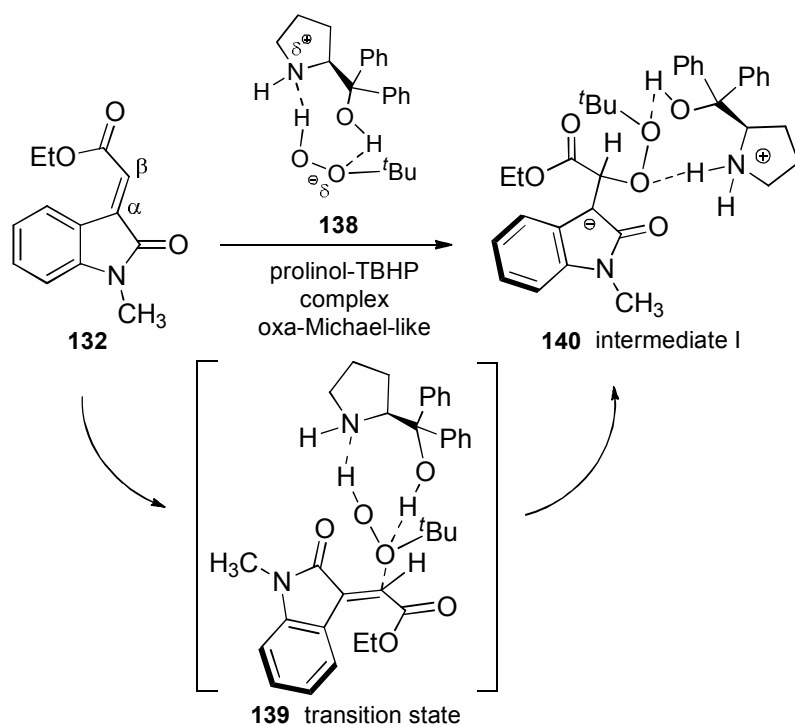
In the light of preliminary results⁸⁰ and of the initial reaction conditions screening, further efforts were directed to an in-depth variation of the catalyst structure, in order to improve the nucleophilic epoxidation in terms of stereoselectivity, efficiency and generality of the scope. In fact one of the points that had been disclosed so far is the importance of the free OH for the reaction rate and enantioselectivity; according to the initial mechanism hypothesis, this pseudo-Lewis acidic function is essential to establish an effective H-bond network among the catalyst, the oxidant and the substrate. In the light of these considerations, two different ways were envisioned in order to mutate the catalyst structure: keeping the pyrrolidinic skeleton and changing the Lewis acidic

group or changing the skeleton and both of the functionalities. In both cases the free hydroxyl function had to be preserved.

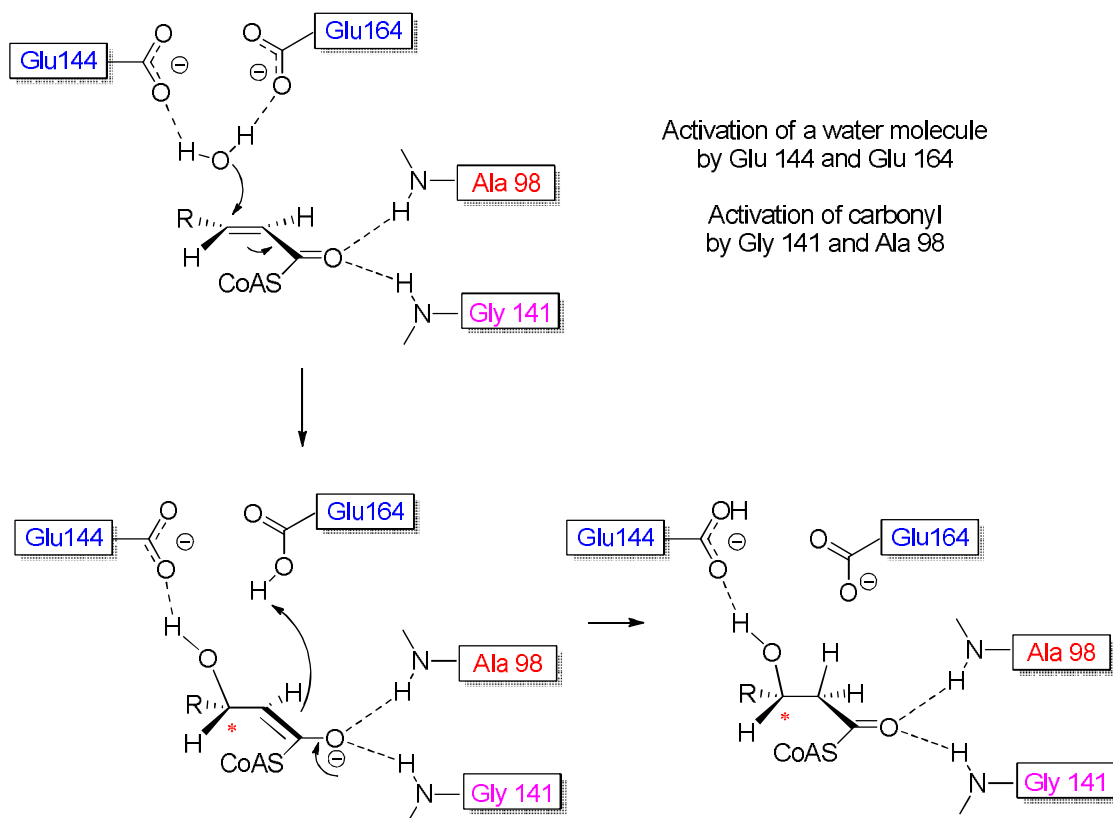
Analogy between the organocatalytic nucleophilic epoxidation and a biological system: enoyl-CoA hydratase

The first step of the nucleophilic epoxidation is supposed to be the oxa-Michael-like addition of the t -BuOO $^-$ species to the electrophilic double bond (Scheme 57). Generally speaking, the oxa-Michael reactions, *i.e.* addition reactions of oxygen nucleophiles to conjugated systems, have traditionally received much less attention from the scientific community compared to the addition of carbon nucleophiles to conjugate acceptor systems (Michael reaction). This was mainly due to the lack of reactivity and selectivity of these reactions.⁸² Moreover, the naturally occurring oxa-Michael reaction, which is fundamental step in fatty acids metabolism, catalyzed by enoyl-CoA hydratase, requires the activation of a water molecule towards the nucleophilic Michael addition to the activated acyl-CoA unsaturated thioester. In this specific enzymatic catalytic pathway (Scheme 58), the substrate's carbonyl is activated by an alanine (Ala 98) and a glycine (Gly 141) residues, while water molecule is activated by two glutamate residues (Glu 144 and Glu 164).

Scheme 57: oxa-Michael-like attack, which led to the first reaction intermediate (intermediate I)



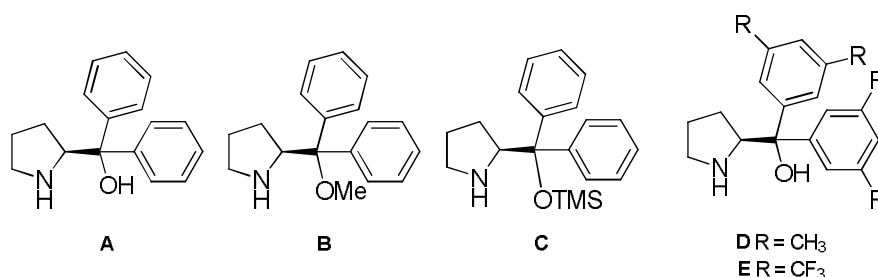
Scheme 58: enoyl-CoA hydratase catalyzes an oxa-Michael



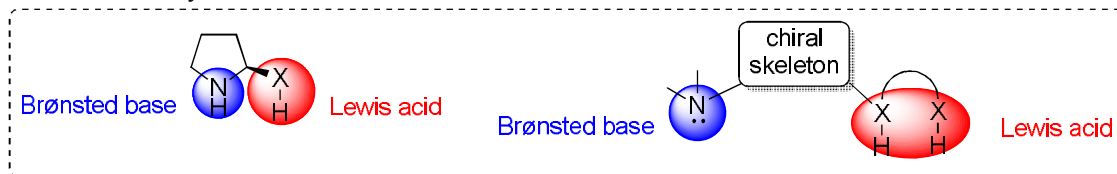
Plan of the catalysts screening

It is well-known how nature inspire chemists in particular in designing catalyst's scaffolds; thus, in the light of the analogy between the epoxidation, which is the objective of this thesis, and the oxa-Michael promoted by enoyl-CoA hydratase, some syntheses of new catalysts syntheses were planned, in order to better activate the substrate, and probably stabilizing the transition state that brings to the desired epoxy isomer. Results for catalysts **B**, **C**, **D**, and **E**, which have been previously discussed, showed that catalysts bearing a protected hydroxyl function, failed in leading any improvement of the enantioselectivity (Scheme 59). Thus, testing different pyrrolidine-derived catalysts could have probably facilitated the analysis of stereo-electronic effects involved in the reaction. Moreover, the use of catalysts bearing two hydrogen donor groups could lead to an increase of the substrate reactivity (the α,β -unsaturated bond would be more electrophilic) and could have led to higher stereoselectivity thanks to a stronger hydrogen bond network among the substrate/catalyst/oxidant (Scheme 60).

Scheme 59: Catalysts which had already been tested



Scheme 60: catalyst's Brønsted basic and Lewis acid sites seem to be influential for the reaction outcome

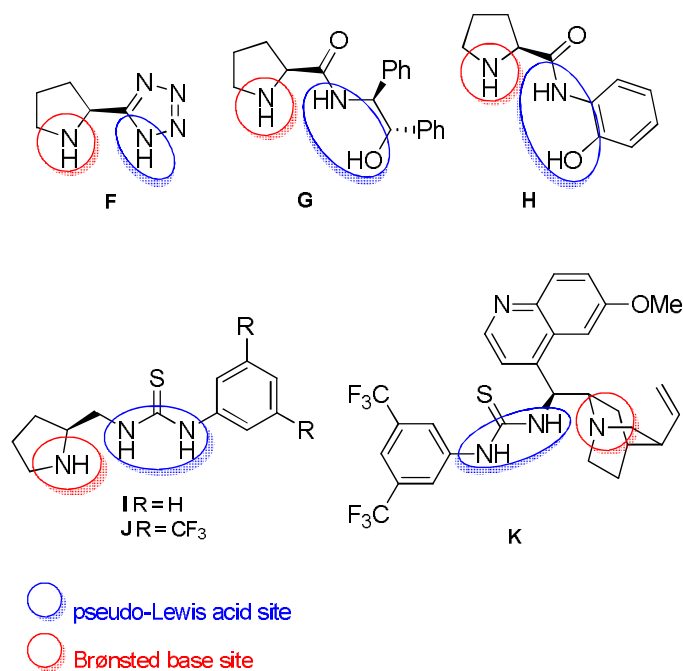


Thus the initial scope of the catalyst (Scheme 61, catalysts **A-E**)^{77, 80, 83} was enlarged to other compounds, in which:

- i. the Brønsted basic site was preserved whereas the Lewis acidic site was changed to a tetrazolic ring (pirrolidine derivative **F**)
- ii. the Brønsted basic site was preserved and two hydrogen bond donor were added: an hydroxyl group and an amide (pirrolidine derivative **G**, **H**)⁸⁴
- iii. the Brønsted basic site was preserved, linked to a thiourea through a methylene (catalysts **I**, **J**)⁸⁵
- iv. the chiral skeleton was changed to an *epi*-quinine, in which the basic site is a tertiary amine and the lewis acid group is a thiourea (Soos catalyst, **K**)^{28a}

Catalysts **A** to **G** were commercially available, catalysts **H**, **I**, **J** and **K** were instead synthesized, following the reported procedures.^{28a, 84b, 84c, 85}

Scheme 61: Catalysts **F** and **G** were commercially available; catalysts **H** - **K** have been synthesized.



Synthesis of the catalysts

Once established the structure of the catalysts that could hypothetically be beneficial to the purpose, molecules which resulted not to be commercially available (Scheme 61, **H**, **I**, **J**, **K**), were easily synthesized suiting the following routes:

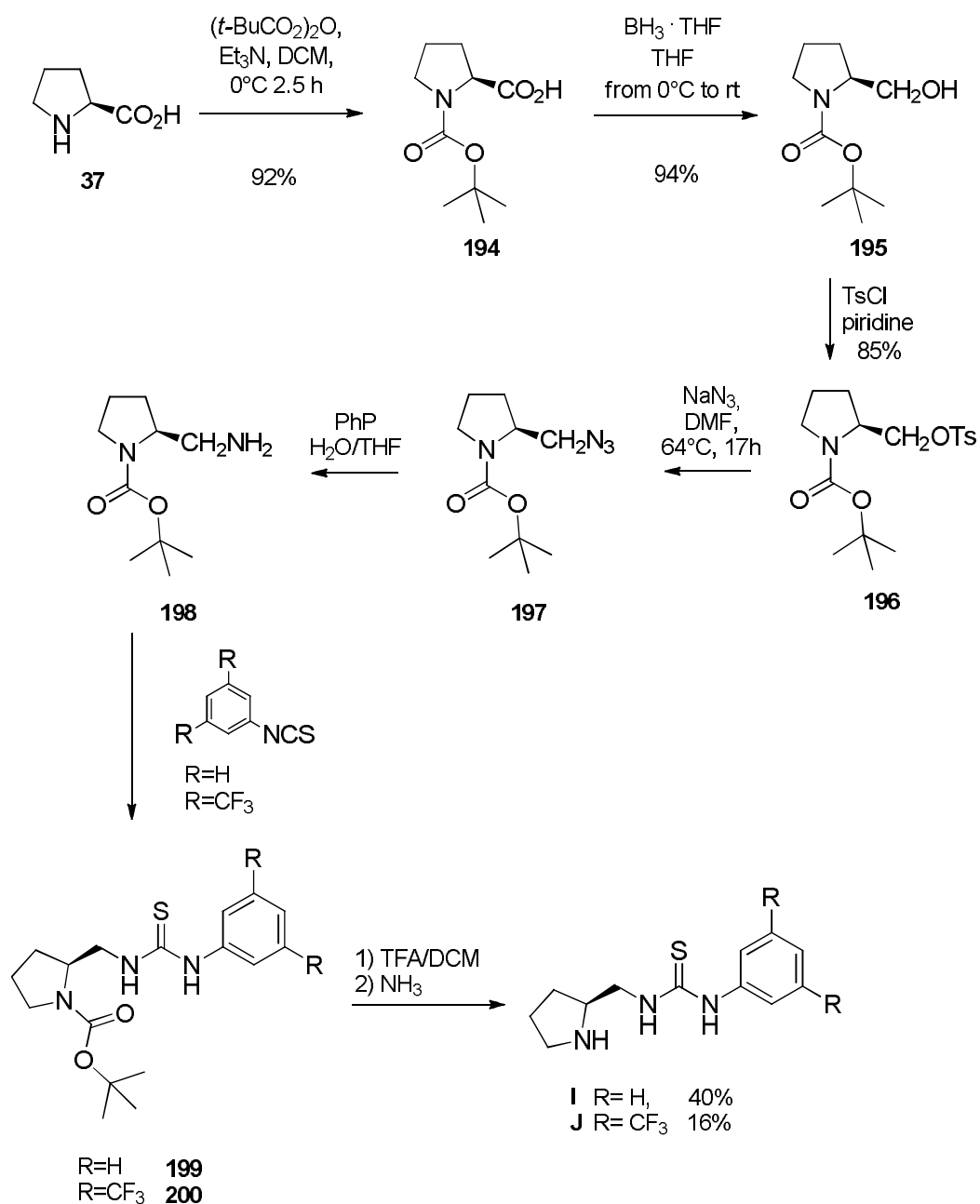
*i. Synthesis of 1-aryl-3-pyrrolydin-2-yl-thioureas, catalysts **I**, **J***

Synthesis of catalysts **I** and **J** was accomplished starting from (*S*)-proline, **37**, suiting procedures previously reported,⁸⁶ which are depicted in Scheme 62.

The commercially available (*S*)-proline, was protected as *t*-butyl carbamate using di-*tert*-butyl anhydride activated by base, in DCM. After crystallization, desired product **194** was obtained in 92% yield. The following reduction of the carboxyl moiety to primary alcohol was accomplished by means of borane solution in THF. Column chromatography led to **195** in high yield. Then the oxydrilic function was transformed in a better leaving group *via* pyridine catalysed tosylation. The desired product, **196**, was isolated in 85% yield after chromatography. Afterwards **196** was converted in the azide **197** through an S_N2 reaction with sodium azide; the crude was sufficiently pure to be used in the following step without any further purification. Then compound **197** was reduced to amine *via* Staudinger reaction, with triphenyl phosphine, leading to **198**, which was used as crude for the following transformation. The reaction with aryl

thioisocyanates led to the two intermediates thioureas, **199** and **200**. These compounds were then deprotected in presence of TFA, giving the free pyrrolidines, which were then purified, yielding to catalysts **I** and **J**, respectively in 40% and 16% overall yield. Final products, **I** and **J**, were fully characterized and the structures of the desired catalysts were confirmed.

Scheme 62: synthesis of 1-aryl-3-pyrrolidin-2-yl-thioureas, catalysts **I** and **J**



ii.

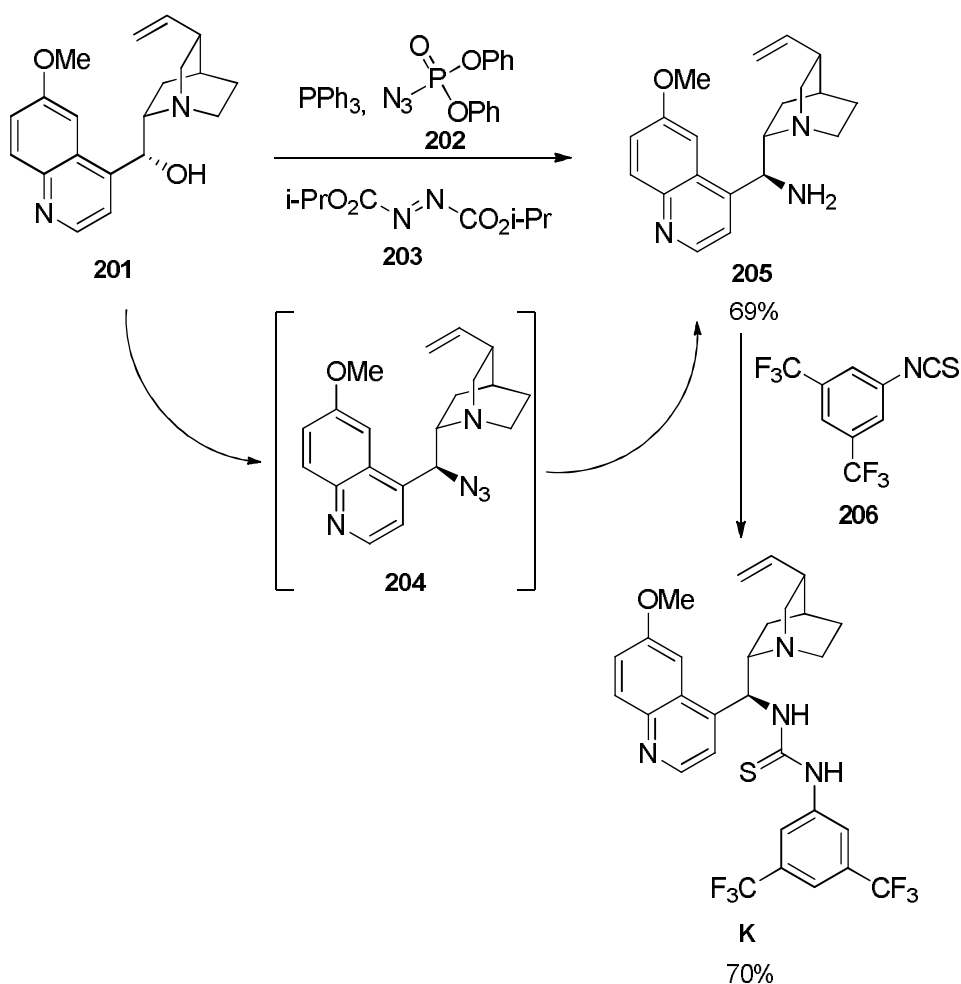
iii.

iv. *Synthesis of the Soós thiourea, catalyst K*

Catalyst **K**, the Soós thiourea, was synthesized in a two step synthesis (Scheme 63) starting from (-)-quinine (**201**), a commercially available alkaloid from the species *cinchona*.⁸⁷

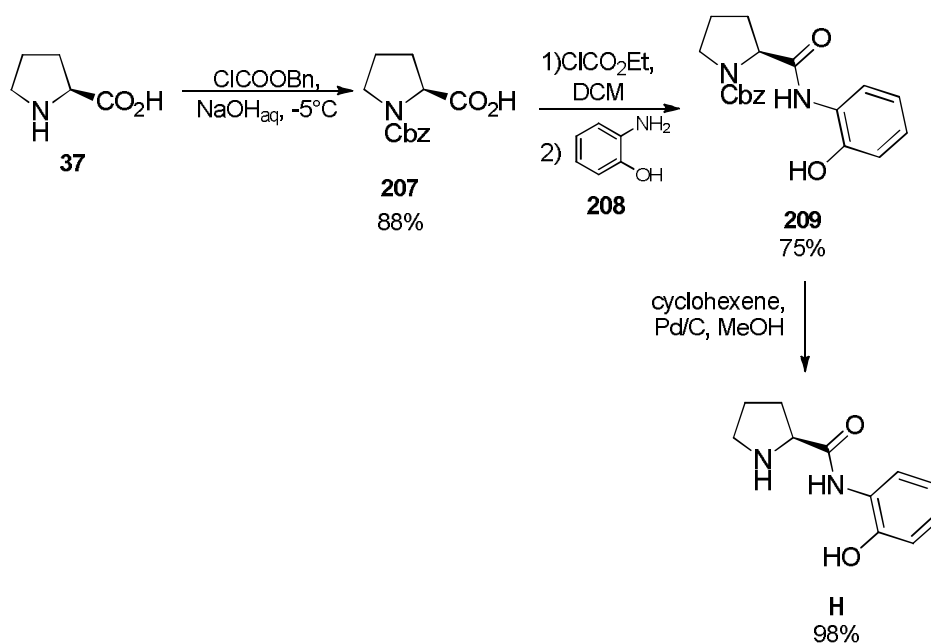
First step of the synthesis was a Mitsunobu reaction, which transforms the alcoholic function into an azide (**202**). Then the azide was reduced to amine *via* Staudinger reaction, with PPh_3 , leading to product **205** in 69% overall yield. Then, the second step was the reaction with isothiocyanate **206**, that led to the desired catalyst **K**, which was analyzed by NMR spectroscopy, confirming the expected structure.

Scheme 63: synthesis of Soós thiourea, catalyst **K**



iii. *Synthesis of catalysts H*

Catalyst **H**, as well, was synthesized starting from (*S*)-proline (Scheme 64).⁸⁸ First step of the synthesis was the protection of (*S*)-proline with Cbz group, leading to the protected pyrrolidine **207**, which was used in the next step without further purification. Then, the reaction with ethyl chloroformate and amino-phenol **208**, brought to compound **209** in good yield (75%). The following deprotection of the amine was accomplished in reducing conditions, by means of cyclohexene on Pd/C, thus avoiding the acidic conditions and formation of the ammonium salt.

Scheme 64: Synthesis of catalyst **H****Catalyst screening**

Afterwards, all the new catalysts were used for a wider catalyst screening. To this aim, the epoxidation reaction was performed under the previously optimized conditions, which required TBHP as oxidizing agent, hexane as solvent, in presence of catalysts **F** - **K** and at room temperature (Scheme 65). Results are disclosed in Table 7. Tetrazolic catalyst **F**, characterized by the presence of an NH function instead of the free hydroxyl, gave interesting results: the enantioselectivity for the *trans* isomer was similar to the one obtained with catalyst **A**, but for the *cis* isomer an inversion of sign was observed in the *ee* (Table 7, entry **6**); unfortunately, a great decrease of reactivity was observed and reaction time increased from 72 to 240 hours.

The use of other amidic catalysts was envisioned: **G**, **H**, in which the OH function is sustained by a NH function, and thioureas **I**, **J**, **K**, in which the OH function is substituted by two NH. These were tested and results did not show any increment in enantioselectivity. On the contrary, lower ee_s were observed (entries **7-10**, Table 7). The only case in which an increment in selectivity was observed is with the use of Soos catalyst (entry **11**), which gave the *trans* isomer in 88% ee , even though with a reversed diastereomeric ratio, in favour of the *cis* isomer, and with very poor yield.

Scheme 65: reaction conditions for the in-depth catalyst screening; catalysts are depicted in Scheme 61.

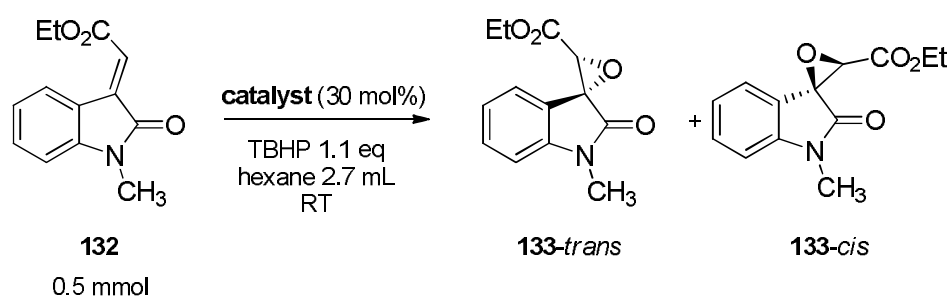


Table 7: Reagents and conditions (Scheme 65) were the previously optimized: starting material 0.2 mmol, TBHP 1.1, hexane 1ml, 0.06 mmol catalyst, rt. Catalysts are depicted in Scheme 61. [^]Measured by ¹H-NMR; ^{^^}measured by chiral phase HPLC.

entry	catalyst	time (h)	yield (%)	dr (<i>trans/cis</i>) [^]	ee <i>trans</i> (%) ^{^^}	ee <i>cis</i> (%) ^{^^}
1	A	72	92	64/36	82	19
2	B	40	83	25/75	37	2
3	C	140	95	36/74	58	1
4	D	110	89	64/36	72	36
5	E	360	75	66/34	38	22
6	F	240	4	79/21	83	-22
7	G	72	20	60/40	-0.7	11
8	H	48	27	85/15	2	1
9	I	168	87	60/40	20	34
10	J	72	10	65/35	33	42
11	K	144	36	40/60	88	15

After this wide catalyst screening, including some further changes in the catalyst structure with respect to the previously tested (**A-D**), some conclusions have been drawn:

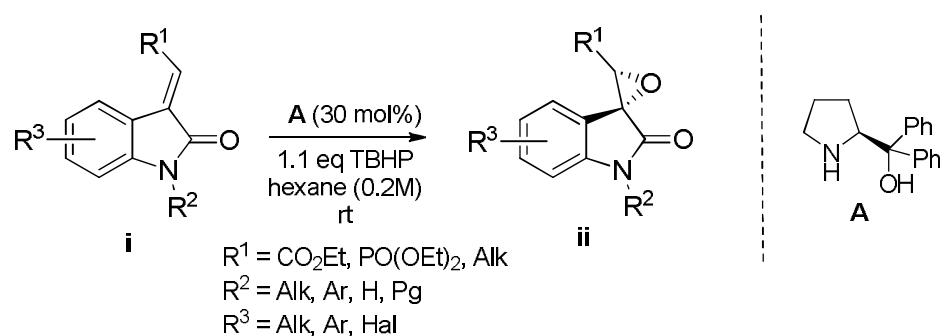
- i. the reaction seems not to benefit of the substitution of the hydroxyl with other functions;
- ii. a change of the catalysts scaffold does not bring to an improvement of the enantioselectivity so far;
- iii. an additional H-bonding site does not lead to better results;
- iv. the conclusion was that catalyst **A** was still the best one so far.

3.3.7 Synthesis of 3-ylidenoxindoles

The good results achieved for the reaction on *N*-methylated substrates, suggested the possibility of reaching better enantioselectivities by changing the starting material. Furthermore, the generality of the reaction had to be tested extensively, by enlarging the substrate scope to diversely substituted 3-ylidenoxindoles **i** (Scheme 66). Moreover, such enlargement could be beneficial to a better analysis of the reaction mechanism. For the above reasons, a new, wider substrate scope was planned (Scheme 66), including compounds **i** bearing:

- i. a different group at the nitrogen (**i**, $R^1 = \text{CO}_2\text{Et}$, $R^2 = \text{aryl group or BOC}$, $R^3 = \text{H}$) or both at the nitrogen and at the aromatic ring (**i**, $R^1 = \text{CO}_2\text{Et}$, $R^2 = \text{aryl group}$, $R^3 = \text{alkyl, halide}$) to check the effect of steric hindrance and electronic effects on the reaction outcomes;
- ii. different substituents at the aromatic ring, with the free NH group (**i**, $R^1 = \text{CO}_2\text{Et}$, $R^2 = \text{H}$, $R^3 = \text{alkyl, halide}$), to check the NH effect and the possibility of a further H-bond between the substrate and the catalyst-oxidant complex;
- iii. a different EWG at the exocyclic double bond [**i**, $R^1 = \text{PO(OEt)}_2$, $R^2 = \text{CH}_3$, phenyl, aryl, $R^3 = \text{alkyl, H}$], to check the effect of the electronwithdrawing force on the reactivity;⁷⁵
- iv. an electron releasing group at the exocyclic double bond (**i**, $R^1 = \text{alkyl}$, $R^2 = \text{CH}_3$, $R^3 = \text{H}$), to check whether the second EWG is necessary for the epoxidation.

Scheme 66: Plan for the broader substrate scope



Syntheses of starting 3-ylidenoxindoles, which in most of the cases had not been previously synthesized, were accomplished following different procedures,^{75, 80} starting from corresponding isatines, depending on the reactivity and on the commercial availability of starting material.

*Synthesis of 3-ylidenoxindoles *N*-substituted and bearing groups on the aromatic ring*

3-Ylidenoxindoles **210-215**, bearing different groups at the nitrogen and on the aromatic ring, were synthesised from commercially available isatines **216-221**, by means of a Horner-Wadsworth-Emmons (HWE) reaction, taking advantage of potassium carbonate as base able to deprotonate the triethyl-phosphonoacetate. The formation of the products (**210-215**) shifted the initial acid-base equilibrium towards the deprotonated species. The depicted procedure was followed by flash chromatography purification, which led to the desired *E*-olefins in good yields (up to 98%). Results are disclosed in Table 8. All products had not been synthesized before, apart from **211**, and were fully characterized by NMR spectrometry and HRMS.⁸⁰

Scheme 67: Synthesis of *N*-alkylated 3-ylidenoxindoles, *via* HWE reaction, starting from commercially available isatines.

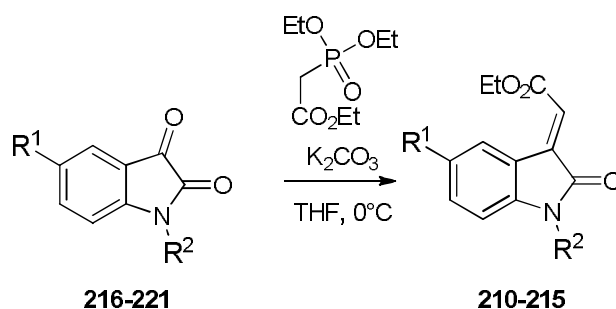
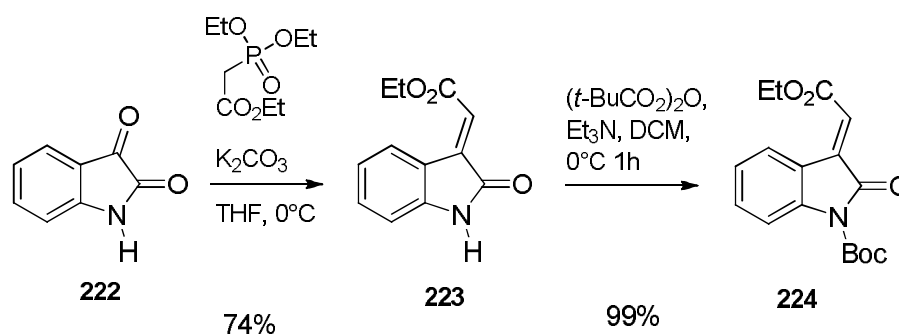


Table 8: results corresponding to Scheme 67; detailed procedures are reported in the experimental section.

entry	isatine	product	R ¹	R ²	time (h)	yield
1	216	210	H	Ph	42	40%
2	217	211	H	Bn	48	80%
3	218	212	H	2,4-Cl ₂ -Bn	48	88%
4	219	213	<i>i</i> -Pr	Bn	48	67%
5	220	214	OCH ₃	Bn	48	98%
6	221	215	OCH ₃	2-NO ₂ -Bn	48	80%

Moreover, a *tert*-butoxy carbonyl *N*-protected substrate was synthesized, as depicted in Scheme 68. Compound **223** was obtained in good yield, through HWE reaction, in presence of potassium carbonate as base. Subsequently, the protection of the nitrogen was easily accomplished using di-*tert*-butyl dicarbonate. Final product **224** was isolated after flash chromatography in quantitative yield and fully characterized.⁶⁹

Scheme 68: *N*-Boc protection and HWE reaction

Synthesis of 3-ylidenoxindoles bearing the free NH and substituents on the aromatic ring

Compounds **223**, **225-232**, endowed with a free NH, and bearing different substituents on the aromatic ring, were taken into account. This selection of substrates included: (i) olefin **225**, without any further substitution on the aromatic ring;⁸⁹ (ii) substrates **225-227**, **229-231**, bearing a halide in position 5 or 7; (iii) compound **232**, with two chlorides in positions 5 and 7; (iv) compound **228**, bearing an OCF₃ at 5 position.

All substrates were easily prepared, in good yields, by means of HWE reaction, under conditions **a** (Scheme 69). Results are reported in Table 9. For compound **232**, the use of a Wittig reaction was necessary,⁹⁰ in acetic acid, and led to the wanted *E*-olefin in good yields and short reaction times (Scheme 69, Table 9). All compounds were purified through flash chromatography and fully characterized by NMR; the double bond configuration for compounds that had not been previously synthesized, was assigned by analogy with similar known molecules.

Scheme 69: synthesis of compounds bearing a free NH. Yields and reaction times are depicted in Table 6.

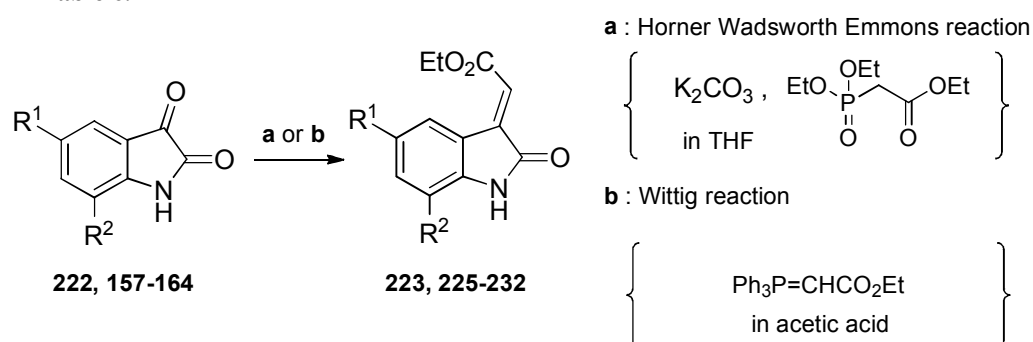
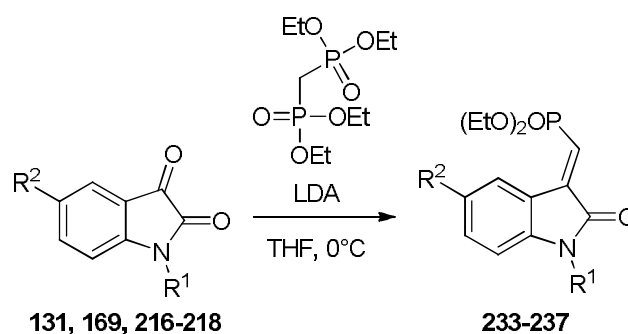


Table 9: Reactions were performed in conditions **a**, Scheme 69. ^reaction was performed in conditions **b**, Scheme 69

entry	isatine	product	R ¹	R ²	time (h)	yield (%)
1	222	223	H	H	22	74
2	157	225	F	H	19	54
3	158	226	Cl	H	18	80
4	159	227	I	H	24	40
5	160	228	OCF ₃	H	12	44
6	165	229	H	F	18	80
7	166	230	H	Cl	16	42
8	167	231	H	Br	19	50
9 [^]	164	232	Cl	Cl	3	60

Synthesis of phosphonates 233-237, bearing PO(OEt)₂ as a second EWG

As aforementioned, in the last few years Loreto's laboratories have directed their attention and efforts to the synthesis of phosphonate derivatives, namely spiroepoxyoxindoles bearing a phosphonate on the oxirane ring.⁷⁵ Those compounds have been previously synthesized by this research group in a diastereoselective way, but not any organocatalytic enantioselective procedure had been developed so far, even though this particular epoxides could have a potential as biocidal agents. In the light of these considerations, this kind of substrates was taken into account for a further substrate scope extension. Therefore, compounds **233-237** were synthesized by HWE reaction following the reported procedure,⁷⁵ which requires the LDA as a base and tetraethyl-diphosphonate as alkylating agent (Scheme 70, Table 10). The same method was employed as well to achieve the new compound **237**, which bears a chloride in position 5 on the aromatic ring. Such compound was obtained in moderate yield and short reaction time. Results for compounds **233-237** are reported in Table 10.

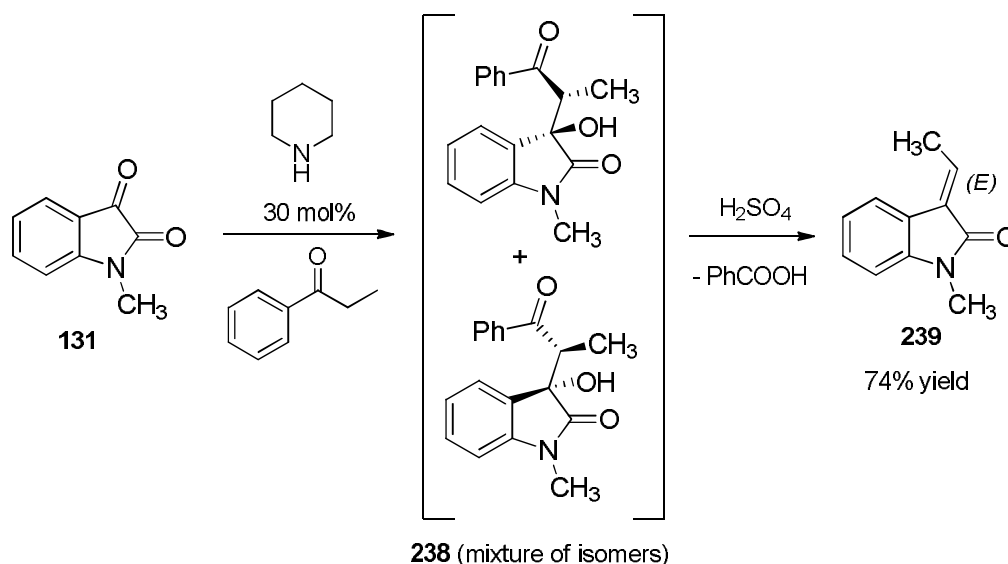
Scheme 70: synthesis of phosphonates **233-237**.

Table 10: results for HWE reaction in Scheme 70

entry	isatine	product	R ¹	R ²	time (h)	yield (%)
1	131	233	CH ₃	H	22	80
2	216	234	Ph	H	24	76
3	217	235	Bn	H	40	76
4	218	236	2,4-Cl ₂ -Bn	H	72	76
5	169	237	CH ₃	Cl	6	30

Synthesis of a substrate endowed with an electron releasing group (methyl) on the double bond instead of the second EWG

The synthesis of a substrate that features a methyl group instead of the EWG on the exocyclic double bond was accomplished following the procedure depicted in Scheme 71. A piperidine catalyzed cross-aldol condensation between phenyl ethyl ketone and isatin **131** led to a mixture of isomers **238**. The crude mixture was subsequently treated with concentrated sulphuric acid, to give the benzoic acid elimination. The known product **239**,^{81(b)} was purified *via* chromatography and isolated with a 74% overall yield.

Scheme 71: synthesis of the alkylidenoxindole **239** *via* an aldol reaction followed by elimination of benzoic acid

**3.3.8 Enlargement of the substrate scope**

The synthesized compounds, disclosed in the section above, were tested in the organocatalytic enantioselective epoxidation. To this purpose, the previously optimized reaction conditions (catalyst **A**, TBHP, hexane, room temperature) were applied.

Organocatalytic epoxidation of N-substituted 3-ylidenoxindoles, substituted on the aromatic ring

The epoxidation reaction was performed on compounds **210-215** and **224**, which are endowed with different functional groups on the nitrogen and on the aromatic ring (Scheme 72, Table 11) and unknown epoxides **240-246** were obtained. Results, depicted in Table 11, show that the diastereoisomeric ratio obtained with the *N*-methyl derivative **132** was always maintained, slightly favouring the *trans* isomer, while, steric hindrance

at the nitrogen atom seems to affect pretty much the reactivity and selectivity of the reaction; in fact lower *e.e.*s were observed in most cases for the *trans* isomer.

Scheme 72: Synthesis of *N*-alkylated ylidenoxindoles, *via* HWE reaction, starting from commercially available isatines.

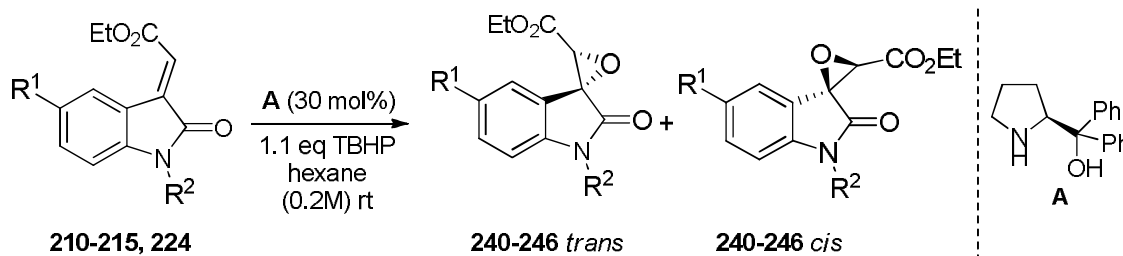


Table 11: the reaction, in Scheme 72, was performed in the optimized conditions. ^for entry 8, 2 equivalents of TBHP were used.

entry	substrate	epoxide	R ¹	R ²	time (h)	yield (%)	dr (<i>trans/cis</i>)	<i>ee trans</i> (%)	<i>ee cis</i> (%)
1	210	240	H	Ph	48	80	54/46	74	12
2	211	241	H	Bn	48	92	66/34	56	20
3	212	242	H	2,4-Cl ₂ -Bn	48	80	56/44	60	20
4	213	243	<i>i</i> -Pr	Bn	192	89	71/29	62	26
5	214	244	OCH ₃	Bn	192	80	70/30	52	16
6	215	245	OCH ₃	2-NO ₂ -Bn	190	88	70/30	78	20
7	224	246	H	Boc	114	36	66/34	93	36
8 [^]	224	246	H	Boc	24	60	66/34	92	36

On the contrary, the reaction carried on the *N*-Boc-protected substrate, **224**, led to very encouraging results, since a 93% *ee* was achieved for the *trans* epoxide. The lower reactivity for this peculiar substrate (entry 7, reaction time 144 h, yield 36%), with respect to the model compound **132**, suggested the increase of the oxidant amount to 2 equivalents. This brought to better yield (60%) in shorter time (24 h) and the *ee* was kepted (entry 8, 92% *ee*).

Organocatalytic epoxidation of 3-ylidenoxindoles bearing the free NH and substituents on the aromatic ring

In the substrates explored so far, the nitrogen atom in the oxindole ring has always been protected with an alkyl or aryl group. Then, the substrate scope was directed towards the epoxidation of *N*-unprotected ylidenoxindoles carrying different other functional groups on the aromatic ring, in positions 5 and 7. All epoxides were unknown and were isolated and characterized after being purified *via* flash chromatography. In particular, the unsubstituted substrate **223** and the halogenated compounds **225-232** have been tested (Scheme 73) and results, which are disclosed in Table 12, have been compared with those obtained with corresponding *N*-methyl-protected compounds (Table 6). Looking at the data it appears that enantiomeric excesses are generally lower than those previously observed; for instance, compound with the 7-bromine, **254**, changes its *e.e.* from 88% to 83% (Table 12, entry **8**). The diastereoisomeric ratios are generally maintained except for the iodine derivative **250** (Table 12, entry **4**), which shows an inverted dr, in favour of the *trans* isomer, low reactivity, and sensibly lower *ee*_s, compared to the corresponding methylated molecule. These experimental outcomes suggest a special role of the hydrogen of the amide in the hydrogen-bond network existing among substrate/catalyst/oxidant.

Scheme 73: free NH compounds were tested; results are reported in Table 12

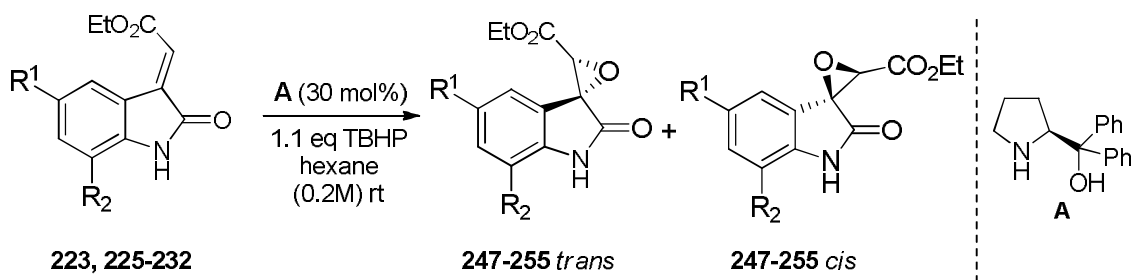
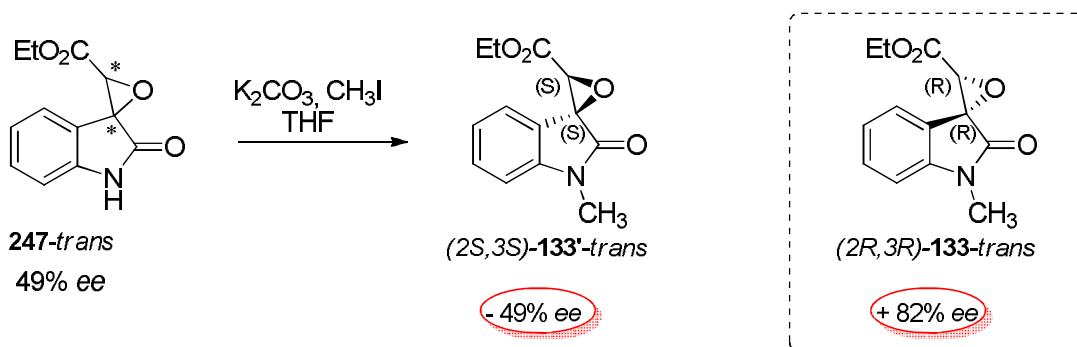


Table 12: results referred to Scheme 73

entry	substrate	epoxide	R ¹	R ²	yield	time (h)	dr (trans/cis)	ee trans (%)	ee cis (%)
1	223	247	H	H	96%	144	65/35	49	22
2	225	248	F	H	97%	43	34/66	86	22
3	226	249	Cl	H	83%	140	40/60	46	18
4	227	250	I	H	91%	170	78/22	36	18
5	228	251	OCF ₃	H	76%	96	38/62	73	32
6	229	252	H	F	93%	66	23/77	84	40
7	230	253	H	Cl	99%	48	36/64	76	24
8	231	254	H	Br	87%	16	56/44	83	29
9	232	255	Cl	Cl	42%	78	35/65	65	72

In order to understand whether the major enantiomers for NH compounds (**247-255**) were the same as for the corresponding NMe compounds (**133**, **182-191**), a new experiment was envisioned, depicted in Scheme 74. In fact, the methylation of compound **247-trans**, obtained from reaction in Scheme 73 (Table 12, entry **1**), led to a clean product (**133'-trans**), characterised by NMR spectrometry as the *N*-methyl *trans* isomer **133'-trans**. The *ee* for such product was checked under the same HPLC conditions and revealed that the major enantiomer **133'-trans** obtained from **247-trans** is the enantiomer (*2S,3S*) of the major isomer **133-trans** (*2R,3R*) obtained from **132**. Indeed, this result indicates that, at variance with the previous results on substrate **132**, the first attack on **247-trans** occurs at the *si* face of the double bond. This opens the way to other mechanistic hypothesis in which the NH function would have a key role in the selectivity induction.

Scheme 74: methylation of **247-trans** (entry 1, Table 12) bring to trans isomer with same *ee* and HPLC peaks inverted respective to same compound (**133-trans**) obtained by direct epoxidation.



Organocatalytic epoxidation of phosphonates 233-237, bearing $\text{PO}(\text{OEt})_2$ as a second EWG

The possibility of testing some phosphonate ylidenoxindoles **233-237** in the organocatalytic epoxidation, using the optimized conditions, was envisioned. The results, displayed in Table 13, show that moderate enantiomeric excess could be obtained for the *trans* isomer, exploiting the new organocatalytic enantioselective procedure (Scheme 75); as already observed of carboxylic derivatives, an halide in position 5 on the aromatic ring has the effect of inverting the diastereoisomeric ratio (entry 5). This study demonstrated that other EWG could as well be positioned on the olefinic bond, and the reaction will proceed, even though in this particular case with lower selectivity. Same reaction on a *N*-Boc protected phosphonate yielded to 58% for the *trans* isomer (by TLC scratching), which was not isolated and characterized because of a very poor conversion.

Scheme 75: epoxidation of phosphonates **233-237**

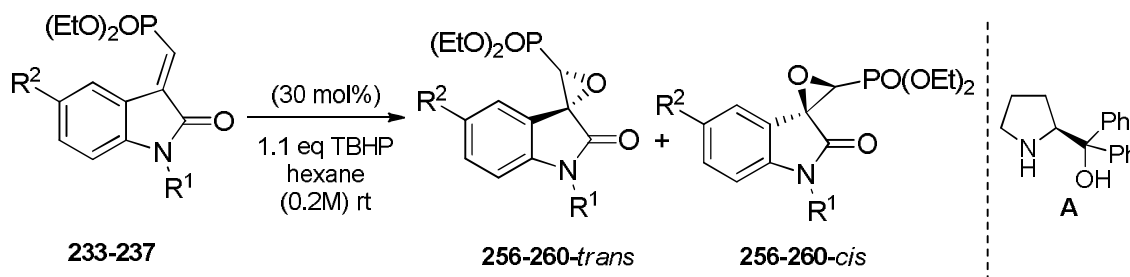


Table 13: results referred to reaction in Scheme 75

entry	substrate	epoxide	R ¹	R ²	yield	time (h)	<i>d.r.</i> (<i>trans/cis</i>)	<i>ee trans</i> (%)	<i>ee cis</i> (%)
1	233	256	CH ₃	H	80	72	56/44	60	21
2	234	257	Ph	H	95	96	60/40	58	24
3	235	258	Bn	H	80	96	56/44	48	9
4	236	259	2,4-Cl ₂ - Bn	H	83	72	65/35	44	10
5	237	260	CH ₃	Cl	65	96	40/60	53	14

In the light of the difference in reactivity between carboxylates and phosphonates in the organocatalytic epoxidation, the reaction conditions for these peculiar compounds were further tested. Therefore different solvents, oxidizing agents, and some different catalysts were explored. Results were not improved either in terms of enantioselectivity or in terms of efficiency (Scheme 76, Table 14).

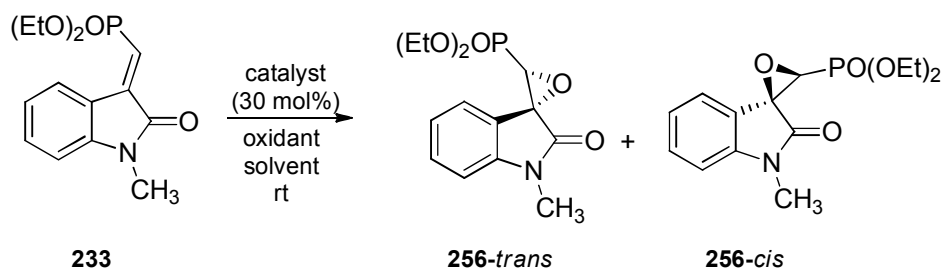
Scheme 76: conditions screening on phosphonate **231**. Conditions are reported in **Table 14**.


Table 14: The reaction on substrate **233**, **Scheme 76**, was performed in solution 0.2M, in presence of 30 mol% catalyst, 1.1 eq of oxidant, at room temperature.

entry	oxidant	catalyst	solvent	yield (%)	time (h)	d.r. (<i>trans/cis</i>)	ee <i>trans</i> (%)
1	H ₂ O ₂	A	hexane	89	0.25	91/8	1
2	H ₂ O ₂	A	hexane	80	6	94/6	3
3	CHP	A	hexane	58	23	67/33	60
4	TBHP	A	hexane	80	120	56/44	60
5	TBHP	A	CHCl ₃	traces	500	-	-
6	TBHP	A	hexane/ CHCl ₃	traces	500	-	-
7	TBHP	A	EtOH	traces	500	-	-
8	TBHP	A	toluene	traces	500	-	-
9	TBHP	B	hexane	20	96	1/1	48
10	TBHP	D	hexane	nd	96	-	-
11	TBHP	K	hexane	20	96	1/1	49

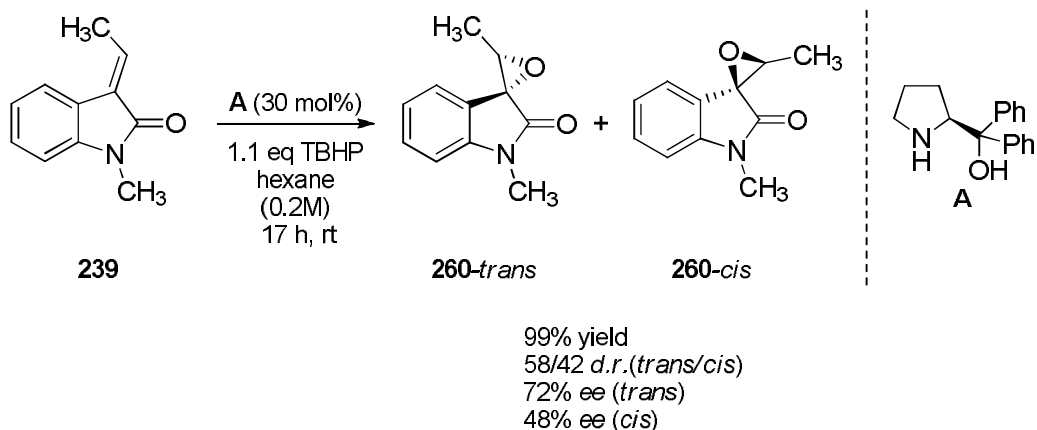
Reaction on substrate 239

In order to check the generality of this reaction and to explore the effect of the EWG on the olefin, the reaction was performed under the optimized conditions on a ylidenoxindole which featured a methyl instead of the second EWG on the double bond. A lower reactivity was expected in this case, since the lack of the second electronwithdrawing group could decrease the electrophilicity of the double bond (Scheme 77).

Surprisingly the reaction was even faster than previously observed with the model substrate, reaching complete conversion in 17 hours. Results showed poor diastereoselectivity, but moderate enantiomeric excess (72%) for the *trans* isomer; interestingly for the *cis* isomer better enantioselectivity than the previously observed was gained (48% ee). These results are quite encouraging, since the reaction is faster and could in principle be slowed performing it at lower temperature, thus probably reaching better enantiomeric excesses. Moreover this result indicates that the second electron withdrawing group on the double bond lowers the overall reactivity and the enantiomeric excess of the *cis* isomer. Furthermore, as the diastereomeric ratio is diminished favouring the *cis* isomer, probably the lack of the second electron

withdrawing group makes the carbon-carbon bond more flexible and free to rotate to give the *cis* isomer.

Scheme 77: epoxidation of the 3-ylidenoxindole **239**, which does not bear any EWG on the double bond



3.4 Conclusions

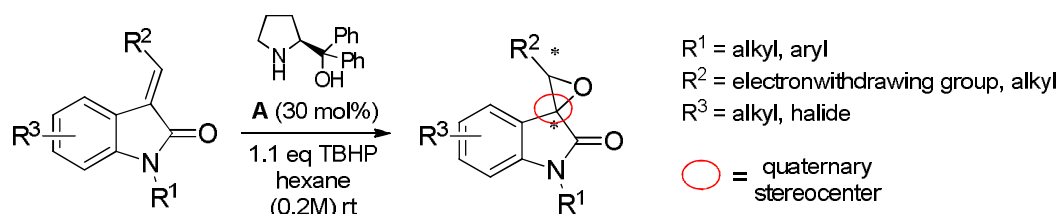
In the light of the interesting perspectives in the field of noncovalent organocatalysis and of the importance of optically pure oxindolic molecules as intermediates, this part of PhD work has been focused on applications of H-bonding bifunctional organocatalysis to the enantioselective epoxidation of electron deficient olefins, in particular 3-ylidenoxindoles (Scheme 78).

This matter was explored by:

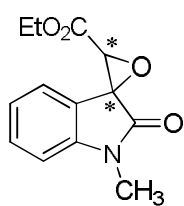
- choice of a model substrate and optimization of the reaction conditions choosing: (i) catalyst; (ii) oxidant; (iii) solvent/dilution; (iv) temperature. Different bifunctional organocatalysts were tested and the bifunctional catalyst **A** resulted to be the best one in terms of enantioselectivity and reactivity. Best conditions are depicted in Scheme 78, requiring TBHP as oxidant, in hexane, at room temperature. A 82% *ee* was achieved for the major diastereoisomer, which was supposed to have the *trans* geometry (**133-trans**, Scheme 79).
- assignment of the absolute configuration of the stereocentres and of the *cis/trans* geometry. The assignment of the stereochemistry of the two products (isomers **133-trans**, **133-cis**) was obtained *via* NOESY NMR experiments, highlighting the **133-trans** as the major product. DFT calculations and a comparison between ORD measurements and calculated ORD values indicated the (2*R*,3*R*) enantiomer as the major for the *trans* isomer.

- hypothesis for the reaction mechanism, which envisages a hydrogen bond network among the catalyst/oxidant/substrate (Scheme 80) and which takes into account the importance of using a catalyst endowed with more than one H-bonding groups.
- The epoxidation of a scope of substrates bearing different substituents on (i) aromatic ring; (ii) on the oxindolic nitrogen; (iii) on the exocyclic double bond (Scheme 79). The substrate scope studies offered the possibility of testing the generality of the organocatalytic procedure and at the same time the chance of understanding the effect of the different substituents. For instance, very good *ee*s and an interesting inversion of the diastereoisomeric ratio, ascribable to some additional interactions with the hydrogen bond network, was observed in presence of halides (**192**). Moreover a drop in *ee* and an inversion of sign, were observed for compounds bearing the unprotected NH (**254**). The effect of an electron-releasing group on the exocyclic double bond (methyl) was tested, finding moderate *ee* (**260**). A very encouraging result, was achieved with the Boc protection of the nitrogen (**246**, 92% *ee*). This result strongly suggests that the best combination could be $R^1 = \text{Boc}$, $R^2 = \text{alkyl}$ and that the scope of the substrate could be further enlarged.

Scheme 78: organocatalytic epoxidation of 3-ylidenoxindoles

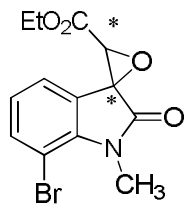


Scheme 79: results for model substrate (**133**), for substrates bearing halides, with or without N-methyl (**192**, **254**), with NBoc (**246**), and bearing different groups on the double bond (**256**, **260**)



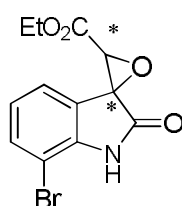
133

92% yield
64/36 *d.r.*(*trans/cis*)
82% *ee* (*trans*)
19% *ee* (*cis*)



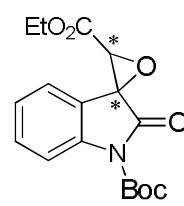
192

71% yield
30/70 *d.r.*(*trans/cis*)
88% *ee* (*trans*)
58% *ee* (*cis*)



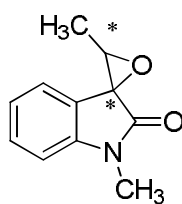
254

87% yield
56/44 *d.r.*(*trans/cis*)
(-83)% *ee* (*trans*)
29% *ee* (*cis*)



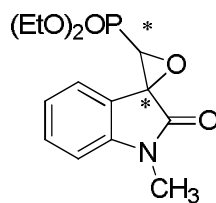
246

60% yield
66/34 *d.r.*(*trans/cis*)
92% *ee* (*trans*)
36% *ee* (*cis*)



260

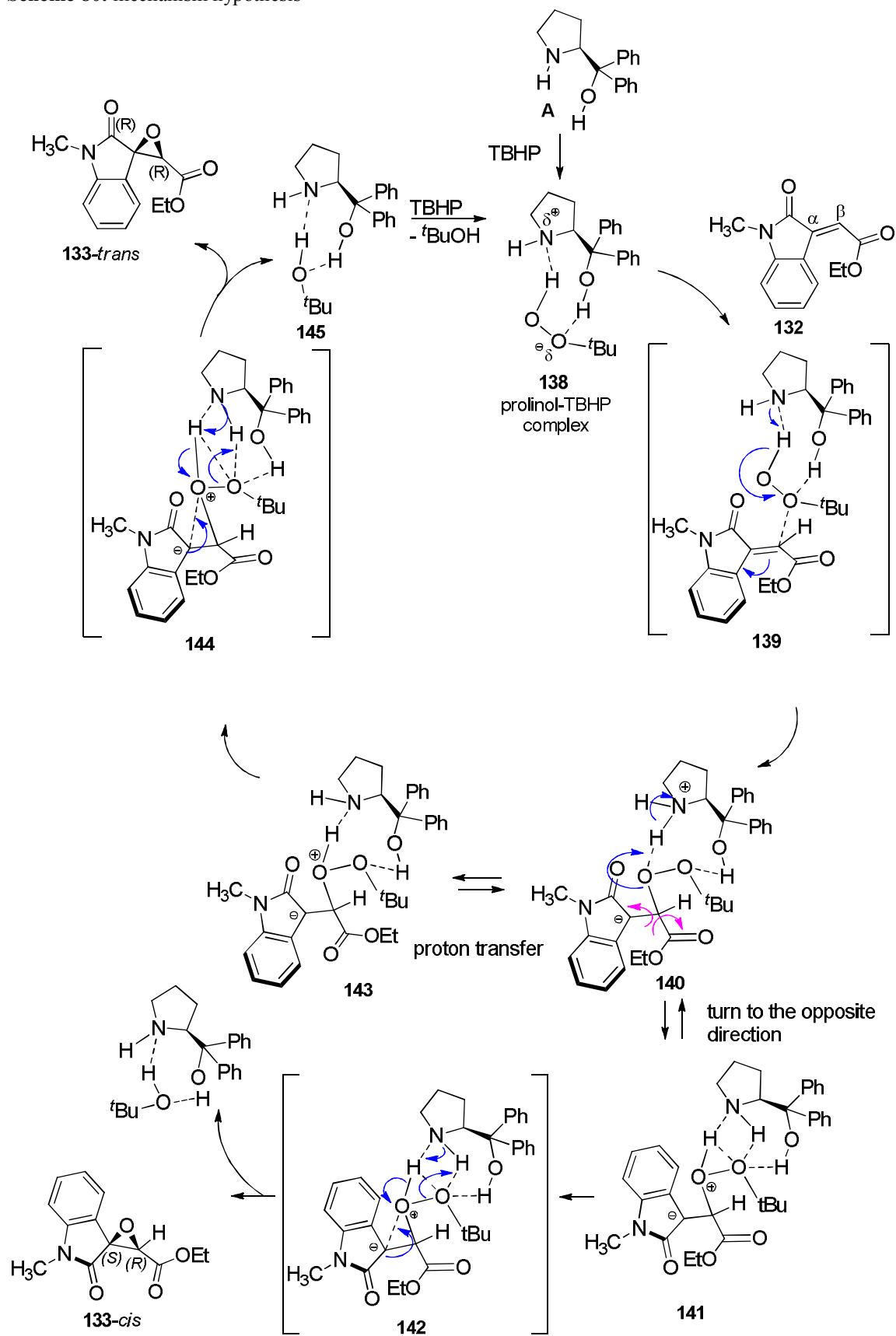
99% yield
58/42 *d.r.*(*trans/cis*)
72% *ee* (*trans*)
48% *ee* (*cis*)



256

80% yield
56/44 *d.r.*(*trans/cis*)
60% *ee* (*trans*)
21% *ee* (*cis*)

Scheme 80: mechanism hypothesis



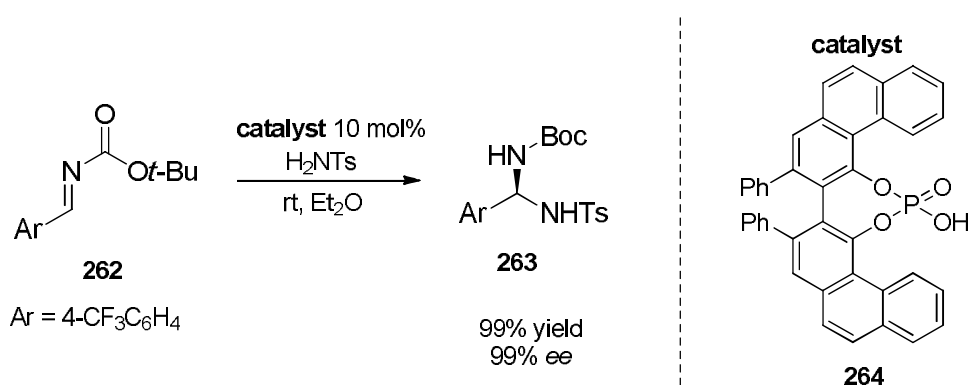
In conclusion, a promising enantioselective, organocatalytic, nucleophilic epoxidation of 3-ylidenoxindoles has been developed and applied to a broad scope of substrates. Further elucidations on the hypothesized reaction mechanism are ongoing, as well as a further enlargement of the reaction scope.

**4. KINETIC RESOLUTION OF DIOLS BEARING A
QUATERNARY STEREOCENTER *VIA* ASYMMETRIC
ACETALIZATION**

4.1 Confined Brønsted acids Organocatalysis applied to acetalization

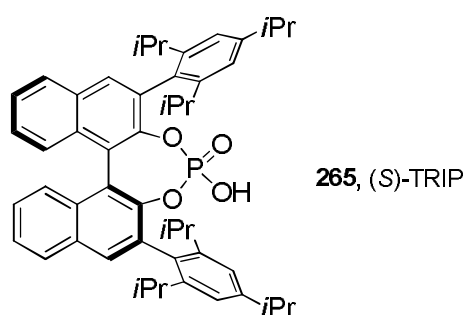
Chiral Brønsted acids have in the last decades proved to be excellent organocatalysts, since they can catalyze a number of chemical transformations, leading to highly enantioenriched products.³⁷ One of the reaction classes in which such type of asymmetric catalysis has been successfully employed is the acetalization reaction. In 2005, Antilla *et. al* reported about a Brønsted acids catalyzed amidation of imines, which in fact is a *N,N*-acetalization. The reaction, catalyzed by catalyst **264**, under mild conditions, has proved to be very efficient and selective, even though with a narrow substrate scope (Scheme 81).⁹¹

Scheme 81: Brønsted acid catalyzed imine amidation by Antilla *et al*.



Afterwards, List-group focused its attention on the chiral Brønsted acids catalysis developing a wide scope of chiral phosphoric acids, whose utility is well-known, and whose milestone is (*S*)-TRIP (Scheme 82). Such binaphthyl phosphoric acid has been employed for a broad scope of reactions and excellent results in terms of enantioselectivities have been achieved during the years, by several research groups. In the asymmetric *N,N* and *N,O*-acetalization this catalyst proved to be very efficient as well, reaching very high levels of selectivity.⁹²

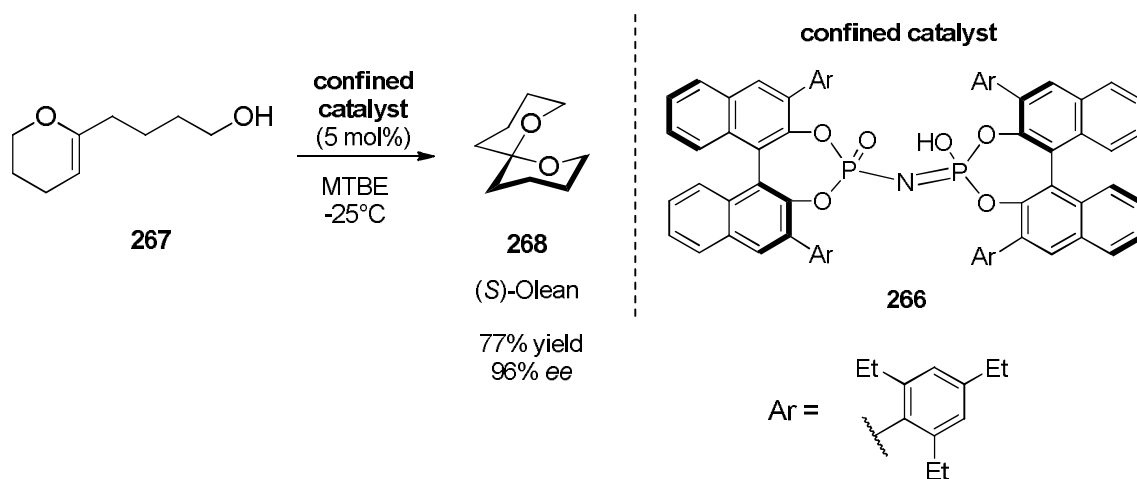
Scheme 82



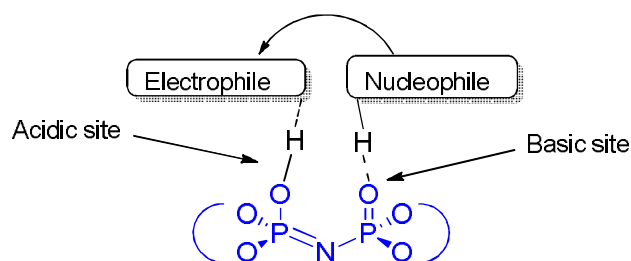
KINETIC RESOLUTION OF DIOLS BEARING A QUATERNARY STEREOCENTER VIA ASYMMETRIC ACETALIZATION

Whereas several goals have been achieved with (*S*)-TRIP and similar catalysts, substrates have always been sterically or electronically biased. In 2012 List et al. developed a new concept: confined Brønsted acids, extremely sterically demanding and bearing a chiral pocket that resemble those found in enzymes.⁹³ These catalysts have been initially used for the asymmetric spiroacetalization of unbiased compounds, to obtain biologically relevant spiro-acetals, such as Olean (Scheme 83), with very high enantiomeric excesses (96% *ee*). The new imidophosphoric acid still bears the double function, acid and base, on the two phosphosphates, allowing small and unhindered molecules to enter the active pocket and to be activated in such a peculiar environment towards the chemical transformation (Scheme 84). Afterwards enantioselective sulfoxidation and acetalization were developed by the same research group. Thus, confined acids class is starting to grow in applicability and is an evolving field.

Scheme 83: the asymmetric spiroacetalization reaction catalyzed by confined Brønsted acids (BA)



Scheme 84: bifunctional confined catalysts's pocket

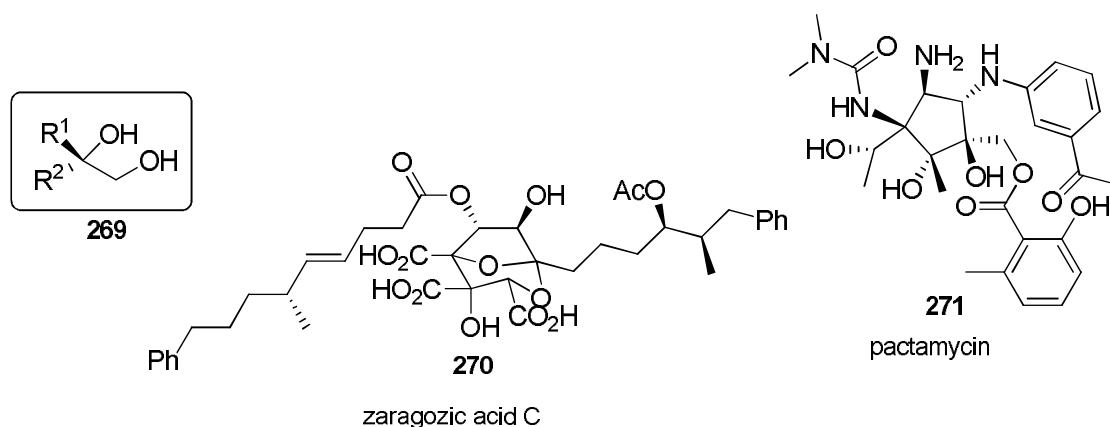


4.2 Vicinal diols bearing a quaternary stereocenter

The stereoselective synthesis of diols bearing a quaternary stereocenter is still considered a great challenge by organic chemists. Enantiopure vicinal diols are among

the most valuable and versatile synthons and intermediates towards the synthesis of biologically active molecules,⁹⁴ as pactamycin (**271**) and zaragozic acid C (**270**) (Scheme 85).⁹⁵

Scheme 85: 1,2-diols bearing a quaternary stereocenter



A few chemical approaches to the stereoselective synthesis of 1,2-diols (**269**) bearing a quaternary stereocenter are reported in literature, such as dihydroxylation of olefins, metal or organocatalyst mediated additions to ketones, pinacol couplings, and rearrangements, but none of these can be considered a real general one; some of these approaches require kinetic resolution⁹⁶ and several biochemical methods as well have recently been developed;⁹⁷ for instance an enantioselective hydrolysis of racemic epoxides catalyzed by the enzyme epoxide hydrolase have been used towards the synthesis of ibuprofen.⁹⁸

Despite the big advances in organocatalysis and the great interest of 1,2-diols, there is a lack of organocatalytic methods, even though some enantioselective organocatalytic synthesis of 1,3-diols have recently been developed.⁹⁹

4.3 Results and discussion

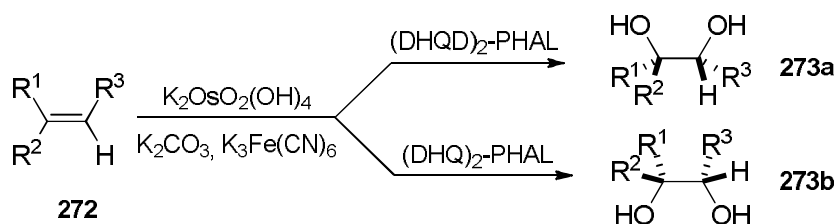
4.3.1 Sharpless approach to optically active vicinal diols: catalytic asymmetric dihydroxylation

The goal of this section, vicinal diols, had already been approached by Sharpless and Jacobsen in 1988,¹⁰⁰ *via* ligand-accelerated metal catalysis, starting from the olefins: they reported a new catalytic process towards vicinal dihydroxylation of olefins, achieving substantially improved rates and turnover numbers as well as useful levels of

**KINETIC RESOLUTION OF DIOLS BEARING A QUATERNARY STEREOCENTER
VIA ASYMMETRIC ACETALIZATION**

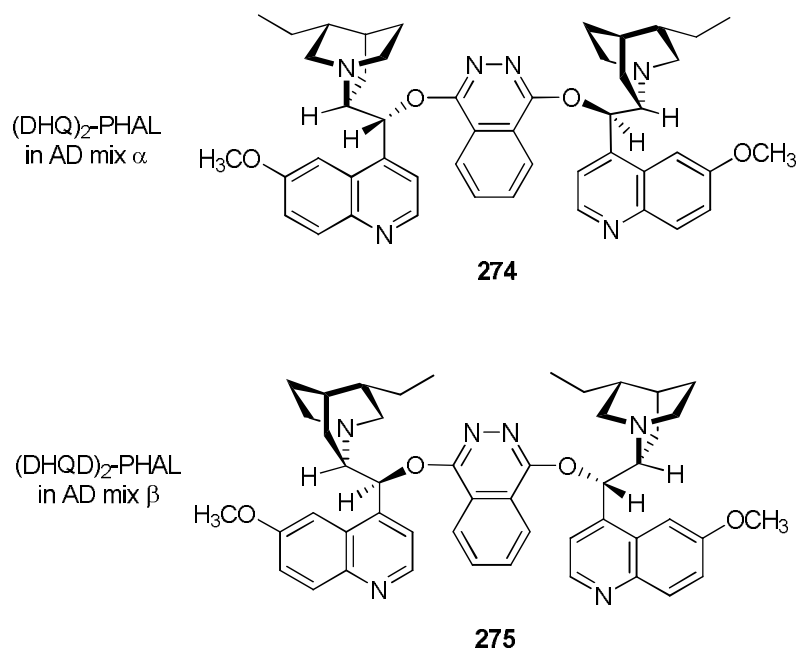
asymmetric induction with respect to the non-catalytic reaction. This osmium catalyzed reaction is in most of the cases performed in the presence of potassium osmate, potassium ferricyanide, potassium carbonate and chiral ligands, that are the constituents of the commercially available ready-mixed oxidizing system known as AD-mix (asymmetric dihydroxylation mix) (Scheme 86).¹⁰¹

Scheme 86: The Sharpless dihydroxylation



The *quasi*-enantiomeric ligand systems dihydroquinine-phtalazine ((DHQ)₂-PHAL in AD-mix α) and dihydroquinidine-phtalazine ((DHQD)₂-PHAL in AD-mix β) are constituents of the AD-mix. With the AD, Sharpless provided an useful oxidizing methodology that can be exploited with a wide range of substituted alkenes (Scheme 87).¹⁰²

Scheme 87: cinchona alkaloids-derived chiral ligands in AD-mix □□ and □

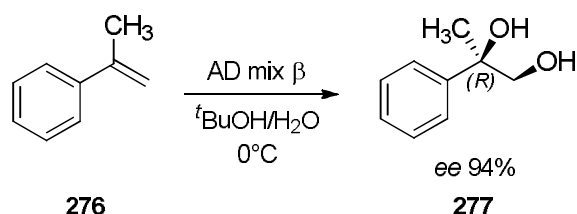


In fact this reaction, starting from alkene **276**, yield to vicinal diol **277**, with a 94% of enantiomeric excess (Scheme 88). Despite of results in terms of enantioselectivity and

KINETIC RESOLUTION OF DIOLS BEARING A QUATERNARY STEREOCENTER VIA ASYMMETRIC ACETALIZATION

broad substrate scope, this reaction still have some weakness from the green chemistry principles point of view: osmium, a toxic and expensive metal, is needed, even if in catalytic amounts.¹⁰³

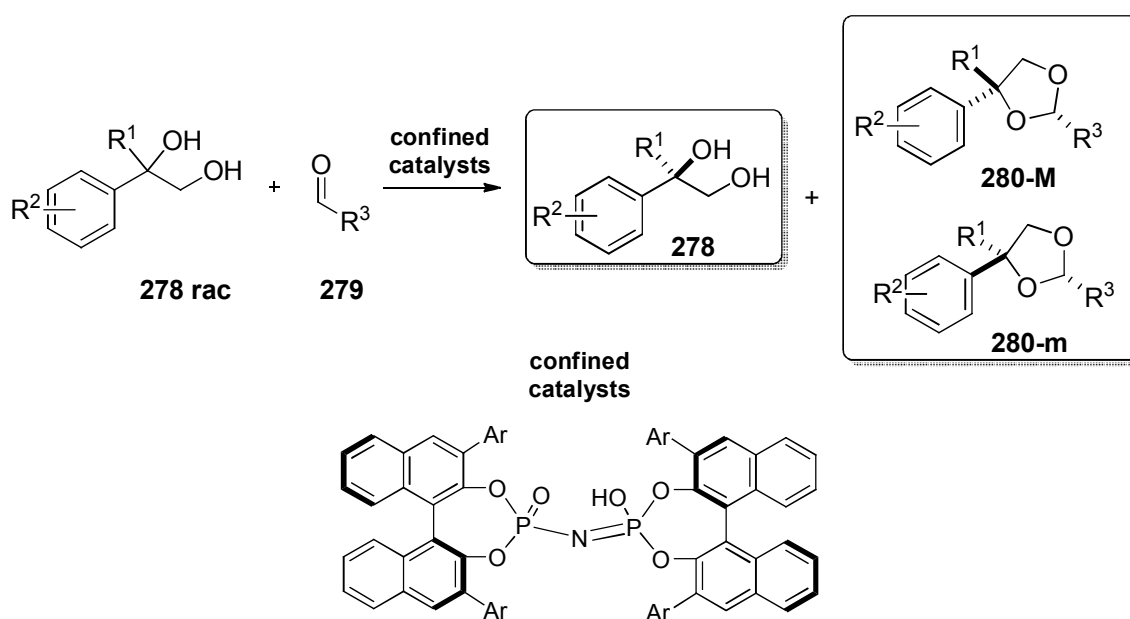
Scheme 88: application of Sharpless AD for the asymmetric synthesis of diol **277**



4.3.2 Strategy and first experiments

In the light of confined Brønsted Acids's great potential in activating sterically unbiased molecules towards chemical asymmetric transformations and of the good results in organocatalytic asymmetric acetalization of aldehydes of such kind of catalysts, a new challenge was envisioned: confined Brønsted Acids catalyzed asymmetric acetalization of aldehydes (**279**), for the kinetic resolution of 1,2-diols (**278**), bearing a quaternary stereocenter (Scheme 89).^{93, 104}

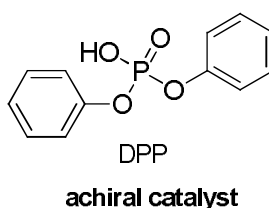
Scheme 89: kinetic resolution of 1,2-diols via asymmetric organocatalytic acetalization. Configurations of the stereocenters of substrate and product are hypothetical.



In principle this reaction could lead to two diastereoisomeric acetals (**280-M**, **280-m**) and to an enantioenriched substrate (**278**). An effective kinetic resolution should lead to a high diastereomeric ratio, a good enantiomeric ratio for the major diastereoisomer and quantitative yields both for product and recovered starting material. Moreover, an appealing feature of this reaction is that product is in principle re-convertible to reactant, this is the case of dynamic kinetic resolution. Kinetic resolution is useful if the racemate is cheap, the catalyst is highly selective for one enantiomer and effective at low loading, and if the reactant and the product are recoverable in high yields and stereoselectivities.⁵ In the light of these considerations and of confined acids catalysts potential, this new catalytic system was chosen for the challenge.

To the purpose of developing an enantioselective methodology which could easily bring to enantioenriched starting materials and products, the first experiments (reaction in Scheme 90) were carried out starting from the commercially available racemic diol **277** and two equivalents of isovaleraldehyde **280** (3-methylbutanal), using 5 mol% DPPⁿ (Figure 10) as achiral Brønsted acid catalyst, in toluene, at room temperature and in the presence of 5Å molecular sieves. This symmetric experiment would have given racemic mixture, useful for the possible subsequent asymmetric products identification; moreover a success would confirm the hypothesized reactivity. The choice of aldehyde **280** was driven by some trials with other aldehydes, like pentanal, which brought similar results.^o This first attempt was successful and it led to the desired racemic product in high yield.

Figure 10: DPP



The first asymmetric experiment was performed on **277 rac**, in the presence of thymol-derived chiral confined catalyst (catalyst **I**, 5 mol %); conditions were chosen founding on previous results in asymmetric acetalization (Scheme 90).^{93, 104a} The selected conditions required the use of molecular sieves as desiccants (in order to adsorb water).

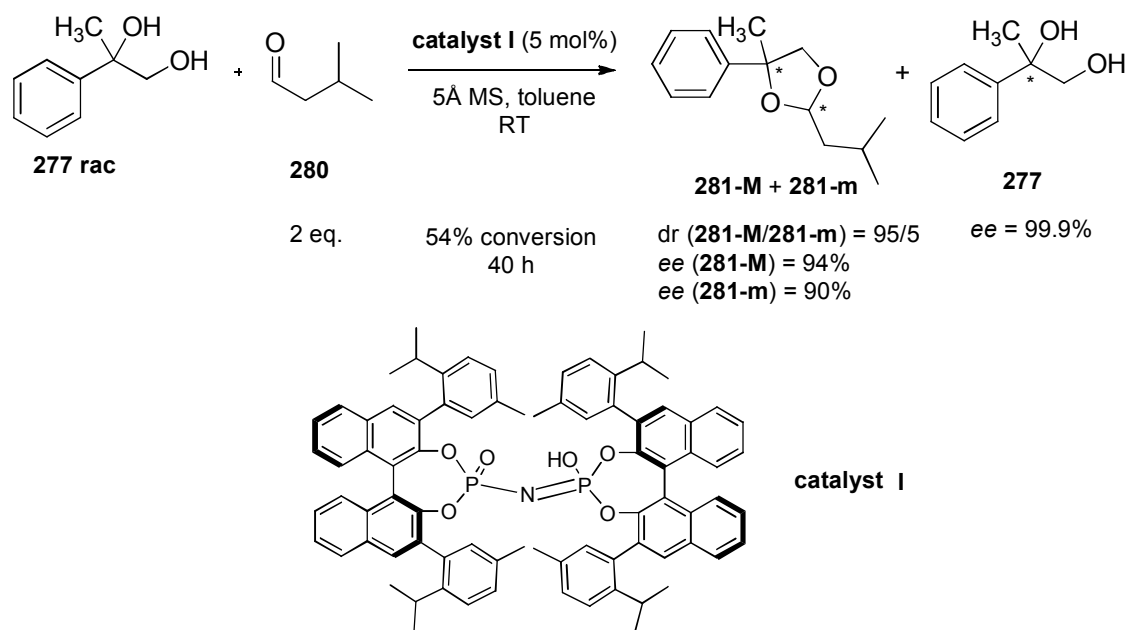
ⁿ DPP, diphenyl phosphate, commercially available.

^o Trials with other aldehydes have been performed by Ji-Hye Kim, in MPI laboratories.

KINETIC RESOLUTION OF DIOLS BEARING A QUATERNARY STEREOCENTER VIA ASYMMETRIC ACETALIZATION

Conversion was checked by TLC and HPLC and the reaction was quenched after 40 hours, close to 50% conversion, with a few drops of triethylamine. The isolation of starting material and of the mixture of the products was quite easy because of the very good separation of compounds on silica gel, even though a gradient of eluents was carefully applied because of the difference in polarity among the analytes. The mixture of product, as well as the recovered substrate, was identified by $^1\text{H-NMR}$ and $^{13}\text{C-NMR}$ spectroscopy. Chiral phase HPLC and NMR analysis revealed very good results: the unreacted diol was recovered as a single enantiomer and acetals with 95/5 dr and 94% enantiomeric excess for the major isomer (**281-M**) and 90% for the minor one (**281-m**). A sample of the same reaction was taken after only 16 hours and it showed that the starting material contained only one enantiomer. Thus, since the beginning, the new application of asymmetric acetalization appeared promising.

Scheme 90: first experiment with thymol-derived catalyst and two equivalents of isovaleraldehyde; the symmetric version of this reaction was catalyzed by DPP (Figure 10)



4.3.3 Catalyst screening

A catalyst screening was planned, in order to understand whether the thymol-derived catalyst (**I**) could be beaten by other confined BA*. To this purpose reaction in Scheme 90 was performed, under the same conditions, with catalysts differently substituted on the binol scaffold (catalysts **I-VI** in Scheme 91). Catalyst **II** (Table 15, entry **2**) led to very good diastereoselectivity and quite good enantiomeric excess both for recovered starting material and for the major diastereoisomer, despite it seemed to be less reactive

**KINETIC RESOLUTION OF DIOLS BEARING A QUATERNARY STEREOCENTER
VIA ASYMMETRIC ACETALIZATION**

than thymol-derived catalyst. Bulkier catalysts, such as **III** and **VI** showed good reactivity, good (even though lower) enantioselectivities, but lower diastereoselectivity (entries **3** and **6**); instead the 2-Ph-phenyl-substituted (**V**) and 9-anthracenyl-substituted (**IV**) led to very poor enantioselectivities, poor diastereoselectivity for the former catalyst and slow reactivity for the latter (entries **4** and **5**). In the light of these results **I** and **II** appeared the best catalysts, in terms of reactivity and selectivity.

Scheme 91: catalysts for reaction screening

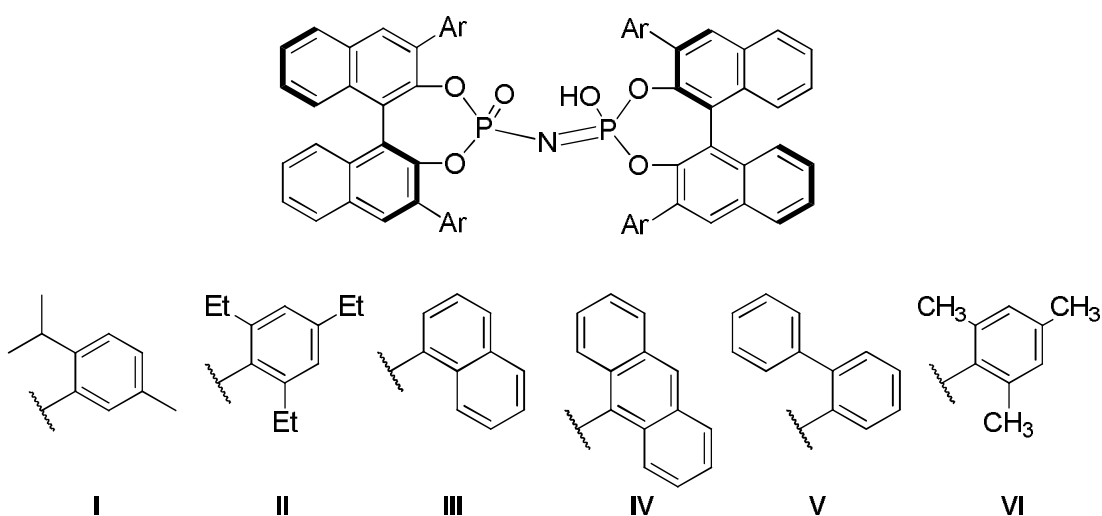


Table 15: catalyst screening; catalysts are depicted in Scheme 87; dr = **281-M/281-m**

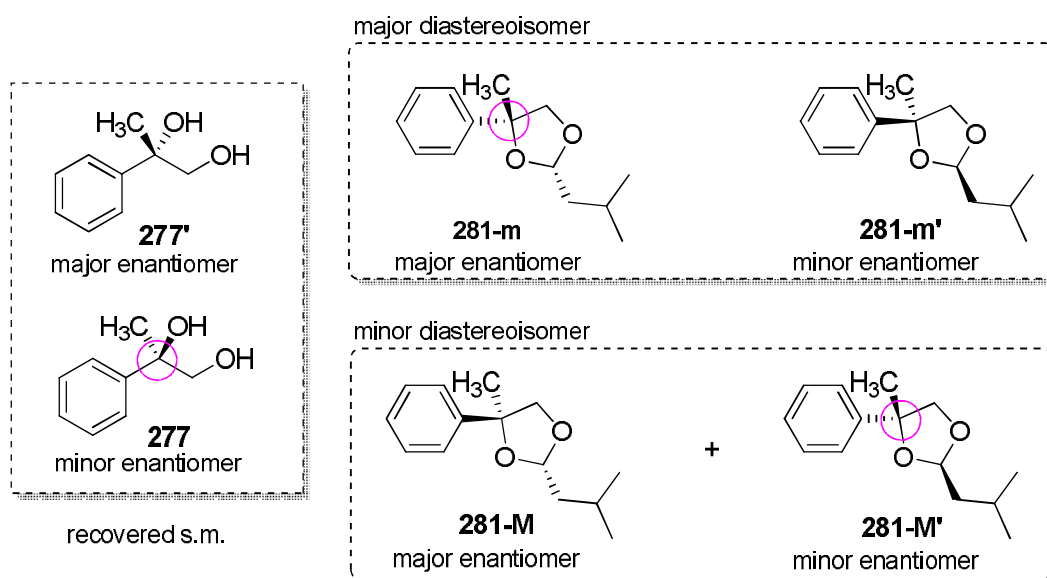
entry	catalyst	<i>ee</i> 281-M (%)	<i>ee</i> 281-m (%)	dr	<i>ee</i> 277 (%)	Conversion (time)
1	I	94	90	95/5	99.9	54% (40h)
2	II	94	67	98/2	84	49% (110h)
3	III	62	99	82/18	96	75% (60h)
4	IV	30	10	96.5/3.5	2	6% (130h)
5	V	50	99	67.5/34.5	4	92% (60h)
6	VI	91	84	92.5/7.5	90	54% (60h)

In view of lowering the catalyst loading and tuning the reaction conditions, it was necessary to point out which catalyst, between **I** and **II**, would be the best choice. To this purpose, both stereoselectivities and reactivities had to be evaluated. Therefore, two reactions were set up on larger scale, in the same conditions, in presence of catalyst **I** (reaction **a**) and **II** (reaction **b**) respectively. The reaction was checked during time in

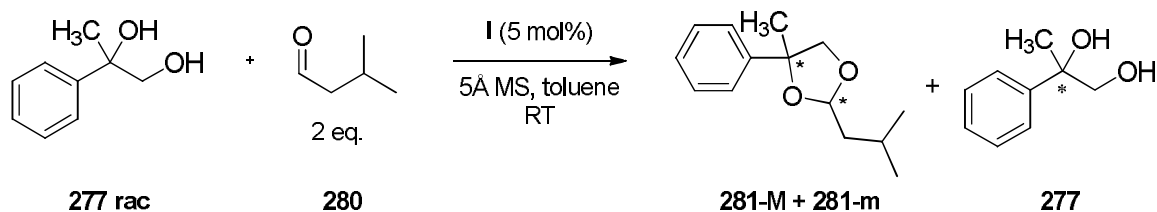
**KINETIC RESOLUTION OF DIOLS BEARING A QUATERNARY STEREOCENTER
VIA ASYMMETRIC ACETALIZATION**

terms of selectivity parameters and conversion. In this case, the possibility to compare also the theoretical enantiomeric excess of the diol coming from the products was envisioned (“theoretical product diol” in Table 17). In fact the enantiomer which reacts faster is in minority in the recovered starting material, but also, in principle, comes from the major enantiomer of **281-M** and from the minor enantiomer of **281-m** (Scheme 92). All these considerations are hypothetical.

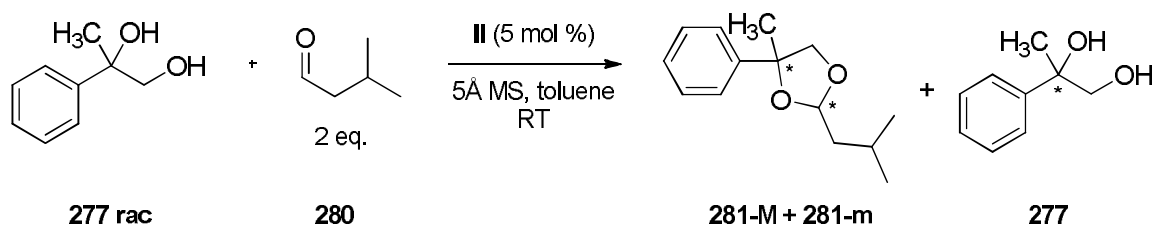
Scheme 92: hypothetical products, with relative stereochemistry. Major enantiomer of the major diastereoisomer contains the quaternary stereogenic center derived from the diol which corresponds to the minor enantiomer in the recovered starting material.



Scheme 93: reaction *a*, performed with catalyst **I**



Scheme 94: reaction *b*, performed with catalyst **II**



**KINETIC RESOLUTION OF DIOLS BEARING A QUATERNARY STEREOCENTER
VIA ASYMMETRIC ACETALIZATION**

Afterwards the reaction's screening was carried out by collecting small amounts of the reaction mixture and checking conversion and stereoselectivity parameters (Scheme 93, Scheme 94). Results are disclosed in Table 16 and Table 17. Conversion with triethyl-substituted catalyst (**II**) was pretty slow compared to reaction performed with thymol-derived catalyst (**I**). In fact, the reaction with **II** seemed to reach a *plateau* close to 48% conversion, where the reactivity was lowered, whereas with catalyst **I** reaction reached 50% conversion just after 6 hours (Graph 1). Moreover, for the reaction performed with catalyst **I**, the *ee*_s of **277** and **281-M** were always higher with respect to reaction performed with catalyst **II**. The same trend was observed for the aforementioned theoretical enantiomeric excess of the diol.

All of this points are displayed in Graph 2, which show *ee* values vs percent conversion:

- I. light blue and orange lines represent the theoretical *ee* respectively for reaction **a** and **b**: theoretical enantiomeric excess of the product diol is higher with catalyst **I**;
- II. violet and green lines stand for the *ee* of the recovered starting material respectively for reaction **a** and **b**: enantiomeric excess of **277** is higher with catalyst **I**;
- III. blue and red lines correspond to the *ee* of the major product acetal for reaction **a** and **b**: enantiomeric excess of **281-M** is higher with catalyst **I**.

In the light of this catalyst screening, catalyst **I** was chosen for the optimization of the conditions.

Table 16: reaction **a**, performed with 5% mol of catalyst **I**; * **dr** = **281-M/281-m**

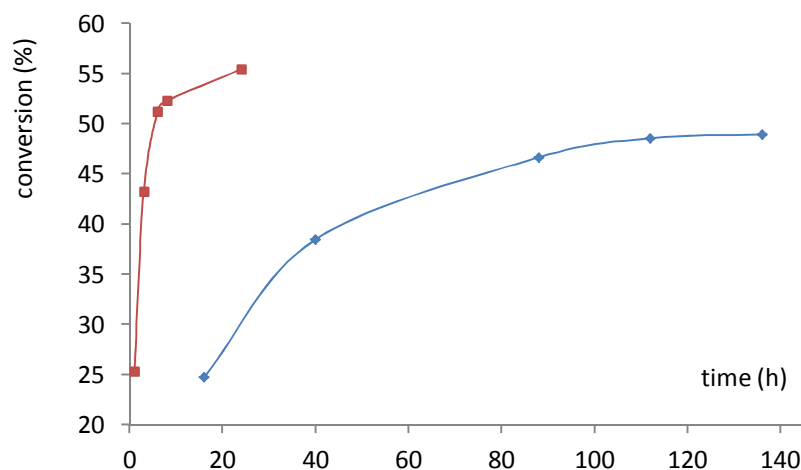
entry	<i>ee</i> 281-M (%)	<i>ee</i> 281-m (%)	<i>ee</i> 277 (%)	theoretical <i>ee</i> product diol (%)	dr *	conversion (time)
1	98	49	32	96	36	25% (1h)
2	98	49	72	96	36	43% (3h)
3	96	3	96	91	23	51% (6h)
4	95	47	99	90	30	52% (8h)
5	91	70	100	80	14	55% (24h)

**KINETIC RESOLUTION OF DIOLS BEARING A QUATERNARY STEREOCENTER
VIA ASYMMETRIC ACETALIZATION**

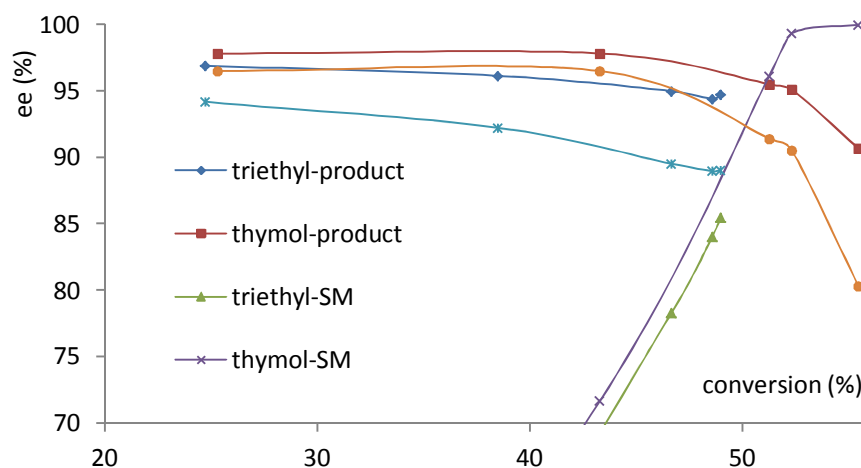
Table 17: reaction *b*, performed with 5% mol of catalyst **II**; * *dr* = 281-M/281-m

entry	<i>ee</i> 281-M (%)	<i>ee</i> 281-m (%)	<i>ee</i> 277 (%)	theoretical <i>ee</i> product diol (%)	<i>dr</i> *	Conversion (time)
1	97	87	31	94	66	24% (16h)
2	96	90	58	92	47	38% (40h)
3	95	82	78	89	32	47% (88h)
4	94	67	84	89	29	49% (112h)
5	95	75	85	89	29	49% (136h)

Graph 1: conversion (%) vs time (h) for reaction performed in presence of catalysts **I** (red line) and catalyst **II** (blue line); catalyst **I** is much more reactive.



Graph 2: *ee*_s of recovered starting material (SM = 277), of major product (product = 281-M) and theoretical *ee*_s of the product diol (theor prod diol = 281-M theoretical) for reactions performed with catalysts **I** (thymol = **I**) and **II** (triethyl = **II**).



4.3.4 Reaction conditions optimization

In order to reduce the catalyst loading, an optimization of the conditions was performed, taking into account reactivity and stereoselectivity. Lowering catalyst loadings represented an important target, since sometimes catalysts can be partially inactivated in the reaction medium. At the same time the active catalyst fraction has to be kept in order to have good outcomes. Confined Brønsted acids catalysts had previously been used at very low percent molar loading.^{104, 105}

Initially the reaction was performed at 20°C, in order to check if the system could work at controlled lower temperature without being stacked. This first trial worked similarly than at room temperature: same enantioselectivities and quite similar reaction times were observed (Scheme 95, Table 18). This meant that we could lower the reaction temperature because no sensible reactivity decrease was observed and furthermore it opened to the possibility of performing the reaction with 1 mol% **I**.

Scheme 95: reaction performed with 5 mol% catalyst **I**



Table 18: reaction in Scheme 95, results at rt and 20°C

T (°C)	ee 277 (%)	Conversion (%)	time (h)
20	96	51	6.5
RT	96	51	6

Afterwards, an increase of the amount of aldehyde was envisioned. This could in principle be useful to speed the reaction, since this had already served to the purpose in the development of asymmetric acetalization of aldehydes.^{104a} Reaction was performed with 1 mol% catalyst, in presence of 7 equivalents of isovaleraldehyde and a different behaviour of the *ee* of **281-M** was observed. It seemed to vary in a different way close to 48% conversion (Table 19 and in Graph 3; blue line in Graph 4). Moreover

the *ee* of the **277** was lower than what previously observed: at high conversion it was still 89%, and the reaction seemed to stack before 50%. In order to check whether the

**KINETIC RESOLUTION OF DIOLS BEARING A QUATERNARY STEREOCENTER
VIA ASYMMETRIC ACETALIZATION**

reactivity would increase with the temperature, reaction was checked at 30°C, but the same trend was observed (Table 20, light blue line in Graph 4). Probably in presence of such a large excess of aldehyde some other interactions could arise, leading to a reduction of reactivity close to 47% conversion and to the lowering of enantioselectivity.

Table 19 results for reaction at 20°C with 1 mol% cat* and 7 equivalents of aldehyde; dr = **281-M/281-m**

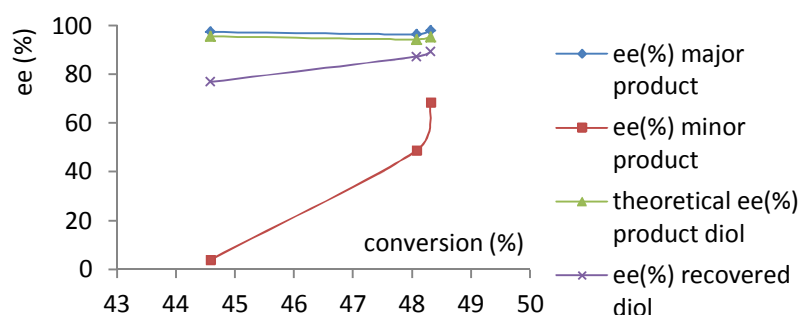
time (h)	<i>ee</i> s.m. (%)	Conversion (%)	<i>ee</i> 281a (%)	<i>ee</i> 281b (%)	theoretical <i>ee</i> diol product (%)	dr
9	77	44	97	4	95	49
22	87	48	96	49	94	67
23	89	48	98	68	95	67

Table 20 results for reaction at 20°C with 1 mol% cat* and 7 equivalents of aldehyde; dr = **281-M/281-m**

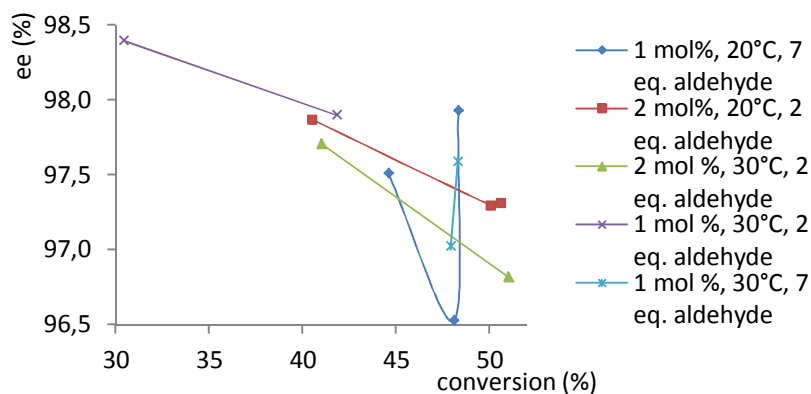
time (h)	<i>ee</i> 277 (%)	Conversion (%)	<i>ee</i> 281a (%)	<i>ee</i> 281b (%)	theoretical <i>ee</i> diol product (%)	dr
22	89	47	97	63	94	54
27	89	48	98	30	94	45

**KINETIC RESOLUTION OF DIOLS BEARING A QUATERNARY STEREOCENTER
VIA ASYMMETRIC ACETALIZATION**

Graph 3 results for reaction a at 20°C with 1 mol% **I** and 7 equivalents of aldehyde; major product = **281-M**; minor product = **281-m**; recovered diol = **277**.



Graph 4: enantiomeric excess of the major diastereoisomer product of the reaction **a**, in presence of different amounts of catalyst / aldehyde



In the light of this considerations, the reaction was performed with the same amount of **I**, at 30°C, and with only 2 equivalents of aldehyde. The attempt was not successful, since the reaction couldn't reach sufficiently high conversion. It stacked close to 40% conversion, when the *ee* of the diol was still low (Table 21; violet line in Graph 4).

Table 21 results for reaction a at 30°C with 1 mol% catalyst **I** and 2 equivalents of aldehyde; dr = **281a/281b**

time (h)	ee 277 (%)	Conversion (%)	ee 281-M (%)	ee 281-m (%)	theoretical ee diol product (%)	dr
9	39	30	98	65	97	18
22	68	42	98	8	95	34

**KINETIC RESOLUTION OF DIOLS BEARING A QUATERNARY STEREOCENTER
VIA ASYMMETRIC ACETALIZATION**

Thus the reaction was tested with 2 mol% **I**, with 2 equivalents of aldehyde, at 20°C and at 30°C. In the former case great results were achieved. Enantioselectivities were similar to the previously obtained in presence of 5 mol% catalyst: after 22 hours, 93% *ee* was measured for both **277** and the theoretical diol product. Furthermore, 97% *ee* for the major acetal and a very high diastereoisomeric ratio were achieved (Table 22 and Table 23, green and red lines in Graph 4). The increase of the temperature to 30°C led to slightly lower enantiomeric excesses for **281-M** (green line in Graph 4) and for the theoretical product diol, and it did not speed the reaction.

Table 22: results for reaction a at 20°C with 2 mol% catalyst **I** and 2 equivalents of aldehyde; dr = **281-M/281-m**

time (h)	<i>ee</i> 277 (%)	Conversion (%)	<i>ee</i> 281-M (%)	<i>ee</i> 281-m (%)	theoretical <i>ee</i> diol product (%)	dr
9	65	40	98	21	96	42
22	93	50	97	14	93	26
27	96	51	97	95	94	60

Table 23: results for reaction a at 30°C with 2 mol% cat* and 2 equivalents of aldehyde. dr = **281-M/281-m**

time (h)	<i>ee</i> 277 (%)	Conversion (%)	<i>ee</i> 281-M (%)	<i>ee</i> 281-m (%)	theoretical <i>ee</i> diol product (%)	dr
9	66	41	98	34	96	30
27	96	51	97	30	94	38

In view of achieving the same good selectivity and reactivity with the lowest amount of catalyst, the reaction was performed in the optimized conditions (20°C, 4 equivalents of **280**) with 1 mol% catalyst loading (Scheme 96). The attempt was successful, since the reaction led to 94% *ee* for the starting diol, 97% *ee* for both product acetals, very high diastereoisomeric ratio (Scheme 96, Table 24, Graph 6).

**KINETIC RESOLUTION OF DIOLS BEARING A QUATERNARY STEREOCENTER
VIA ASYMMETRIC ACETALIZATION**

Scheme 96: Reaction in best conditions.

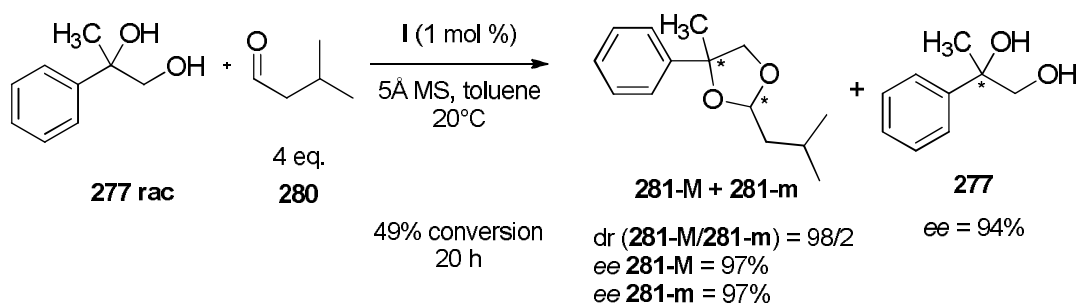
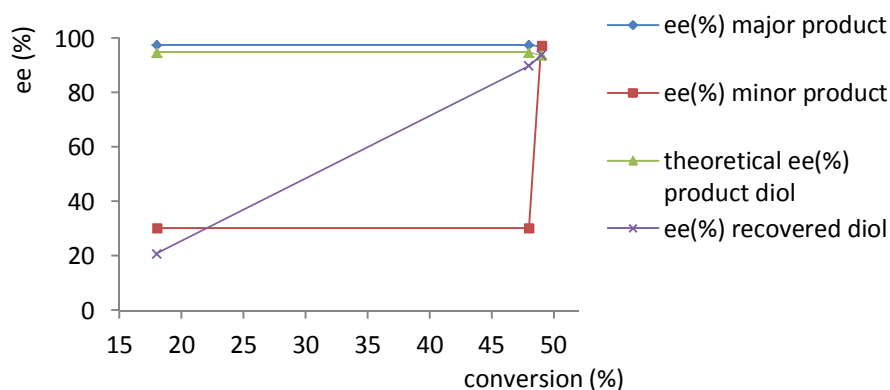


Table 24 results for reaction a at 20°C with 1 mol% I and 4 equivalents of aldehyde; dr = 281-M/281-m

time (h)	ee 277 (%)	conversion (%)	ee 281a (%)	ee 281b (%)	theoretical ee diol product (%)	dr
2	21	18	97	30	95	45
15	90	48	97	30	95	45
20	94	49	97	97	94	58

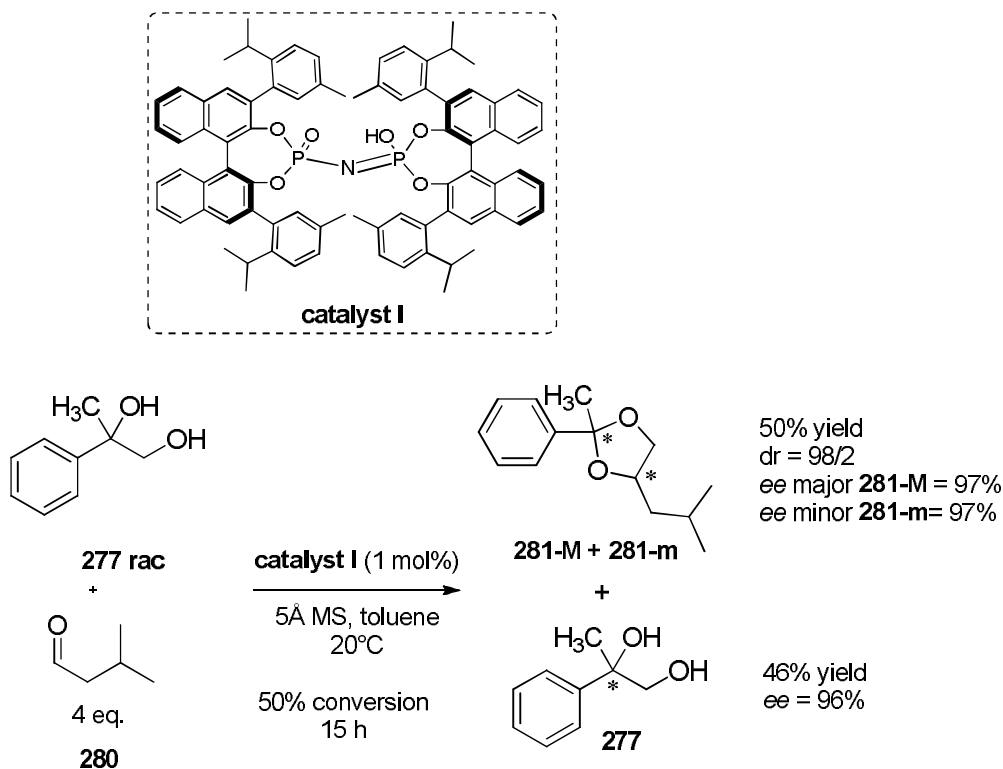
Graph 5 ee_s for reaction performed with 1 mol % catalyst 1, 4 eq. aldehyde at 20°C. Major product = 281-M; minor product = 281-m; recovered diol = 277.



The same reaction was performed in the previously optimized conditions on larger scale. Both diol and products were isolated and fully characterized after purification *via* flash chromatography. The enantioenriched starting diol **277** was recovered in 46% yield and with a 96% *ee*; the mixture of diastereoisomers was isolated in 50% yield, 58 *dr* and 97% *ee* for both products (Scheme 97). Finally this optimization served to reach

the target. The optimized procedure was subsequently used to test the kinetic resolution of other diols.

Scheme 97: reaction on the basic diol in best conditions, performed on larger scale

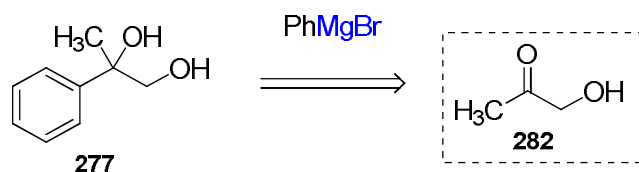


Furthermore it could be possible to separate enantioenriched starting material from the diastereomeric mixture and from the catalyst, which could be recovered and in principle employed in other catalytic cycles. The promising results achieved with the model diol, are better than those one could reach with Sharpless dihydroxylation's (*vide supra*). Indeed, dealing with a kinetic resolution, 50% yield is the best one could afford.

4.3.5 Synthesis of the diols

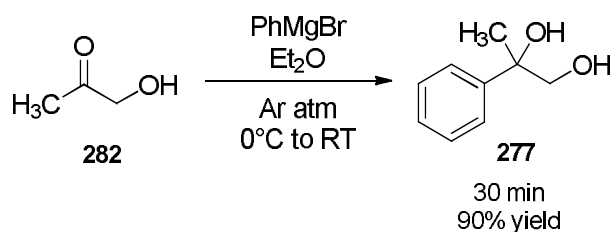
In the light of the achieved good results, the kinetic resolution could be tested on other 1,2-diols, in order to check the scope of the reaction. Thus a synthetic route was devised, that could lead as fast as possible to diols in good yields and starting from cheap materials. For the basic diol a facile one-step synthesis was considered, starting from hydroxy-aceton **282**, *via* Grignard addition with phenyl magnesium bromide (Scheme 98). Two equivalents of Grignard reagent have been used, because of the presence of the hydroxyl moiety in the substrate.

Scheme 98: single-step retrosynthesis for the diol



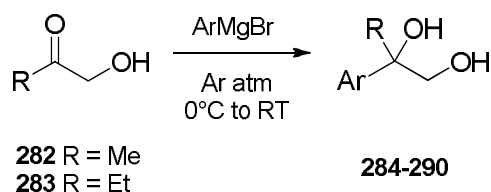
This procedure was readily, successfully, tried and in 30 minutes led to a crude mixture, giving high conversion and good purity. After purification by means of flash chromatography, the clean, desired diol was obtained in 90% yield (Scheme 99).

Scheme 99: synthesis of the basic diol.



Afterwards, the same synthesis was used to get other diols, differently substituted, which could be interesting in view of the substrate scope. Thus the Grignard addition on, variously substituted hydroxy-ketones, varying the solvent (Scheme 100, Table 26).^p The reaction worked pretty well for every substrate and all compounds **284-290** were easily obtained (reaction times between 15 min and 1.5 h) and characterized.

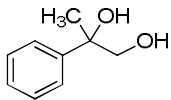
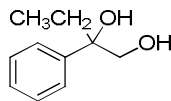
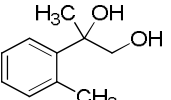
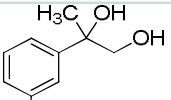
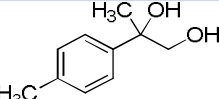
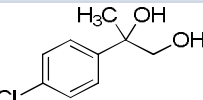
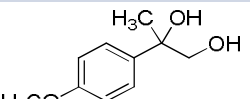
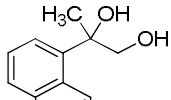
Scheme 100: synthesis of diols for substrate scope



^p For detailed procedures see experimental part.

**KINETIC RESOLUTION OF DIOLS BEARING A QUATERNARY STEREOCENTER
VIA ASYMMETRIC ACETALIZATION**

Table 25: diols obtained with one-step synthesis in Scheme 100. Commercially available Grignard reagents have been used. ^a The Grignard reagent was prepared by the general procedure reported in the experimental section.

entry	compound	solvent	time (min)	yield (%)
1	 277	Et ₂ O	30	90
2	 284	Et ₂ O	60	43
3	 285	Et ₂ O	30	88
4	 286	THF	30	70
5 ^a	 287	THF	15	50
6	 288	THF	15	65
7 ^a	 289	THF	60	60
8	 290	2MeTHF	90	80

4.3.6 Substrate scope

The substrate scope exploration for the asymmetric kinetic resolution was straightly started, in the previously optimized conditions, already successfully applied to the basic diol in larger scale. The reaction was initially tried on each diol with 1 mol% catalyst, increasing then the catalyst amount only if it was not sufficient to reach 50% conversion in short reaction time. For this small screening it was sufficient to check only the *ee* of the diols, without isolating products and starting material. This method could avoid the use of large amounts of materials.

**KINETIC RESOLUTION OF DIOLS BEARING A QUATERNARY STEREOCENTER
VIA ASYMMETRIC ACETALIZATION**

First of all diol **284 rac** was taken into account (Scheme 101). This compound, bearing an ethyl instead of the methyl group, on the quaternary stereocenter, reacted more slowly than the model diol, and conversion was too slow with 1 mol% catalyst, stacking after 20 hours. The *ee* of **284** was 81% after 24 hours and was still 80% after two days. Gratifyingly, with a 2 mol% catalyst loading, after two days, conversion was complete. Finally, quenching the reaction after 20 hours, a 96% *ee* was measured (Table 26).

Scheme 101: reaction in the optimized conditions: small screening of the catalyst loading

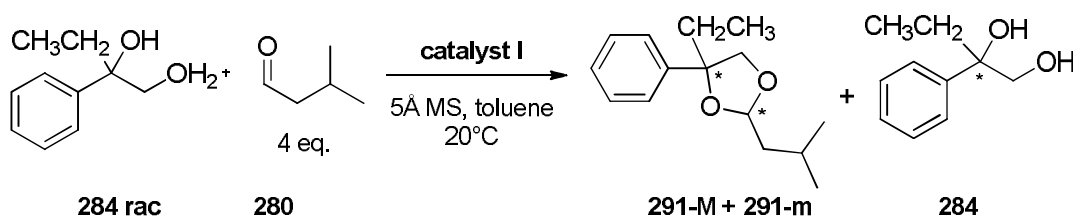


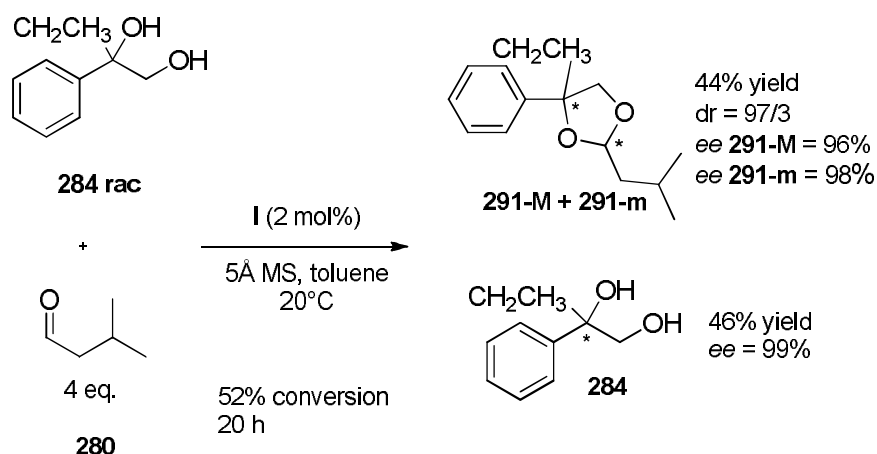
Table 26: small screening of catalyst loading for reaction in **Scheme 100**. Yields are not reported in the table, since the study of the *ee*, via HPLC, was adequate to understand the reaction trend.

catalyst loading	time (h)	<i>ee</i> 284 (%)
1 mol%	4	30
1 mol%	24	81
1 mol%	48	80
2 mol%	7	74
2 mol%	52	99
2 mol%	17	92
2 mol%	20	96

Thus the reaction was scaled up in these conditions leading to quite good results. After 20 hours, at 52% conversion, the starting diol **284** was isolated in 46% yield and 99% *ee*. The diastereoisomeric mixture of acetals was isolated in 44% yield, with a d.r. of 97/3, 96.4% *ee* for the major isomer and 98.5% *ee* for the minor (Scheme 102).

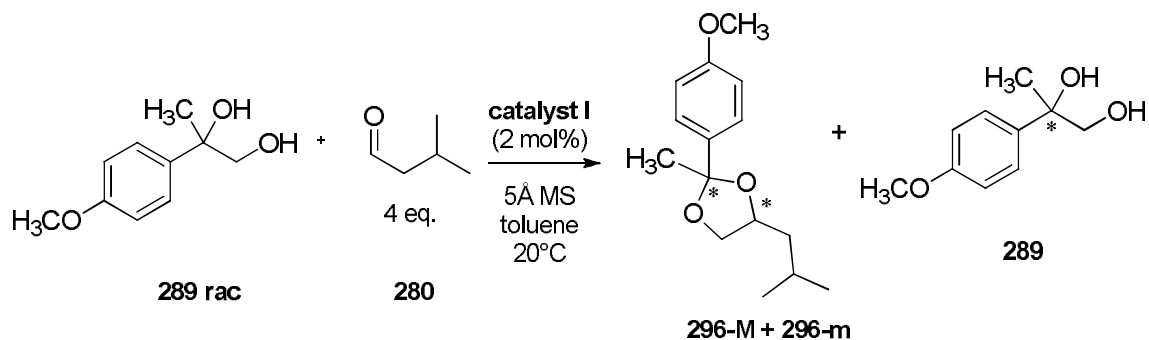
**KINETIC RESOLUTION OF DIOLS BEARING A QUATERNARY STEREOCENTER
VIA ASYMMETRIC ACETALIZATION**

Scheme 102: reaction in best conditions, with a 2 mol% **1**, performed on larger scale



Gratifyingly, for the *p*-methoxy substituted compound **289**, 2 mol% catalyst loading (Scheme 103) was sufficient to get very good results, disclosed in Table 27. Thus the scale up was readily done, quenching the reaction after 16 hours, isolating the diol in 51% yield and 92% *ee* and the diastereoisomeric mixture with a 48% yield, 98/2 *dr*, 97% *ee* for **296-M** and 96% for **296-m** (Scheme 104)

Scheme 103: reaction on **289** for a small screening of catalyst loading.

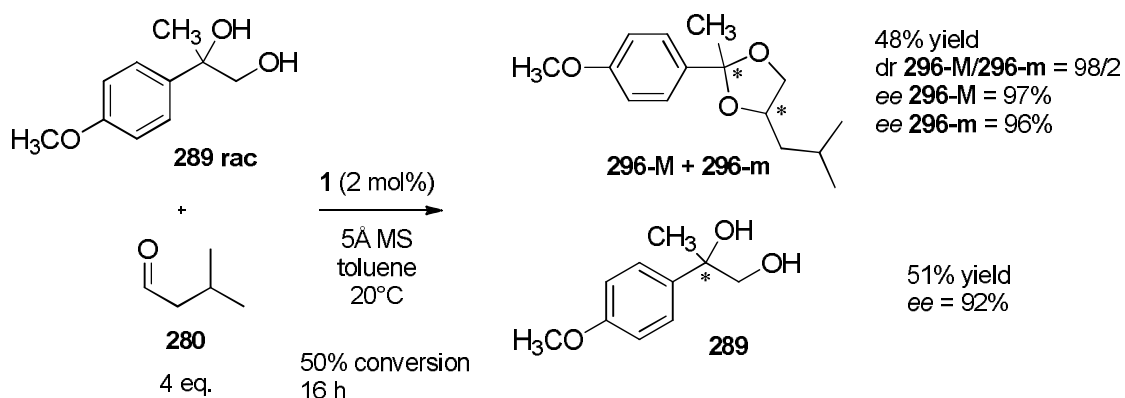


**KINETIC RESOLUTION OF DIOLS BEARING A QUATERNARY STEREOCENTER
VIA ASYMMETRIC ACETALIZATION**

Table 27 small screening of catalyst loading for reaction in Scheme 103. Yields are not reported in the table, since the study of the *ee*_s via HPLC, was adequate to understand the reaction trend.

catalyst loading	time (h)	<i>ee</i> 289 (%)
1 mol%	4	32
1 mol%	24	62
1 mol%	48	64
2 mol%	11	82
2 mol%	13	88
2 mol%	14	90
2 mol%	20	99

Scheme 104: reaction scaled up for substrate scope, in best conditions, with 2 mol% **1**



For the *p*-chlorine substituted compound, the optimization of reaction conditions (Scheme 105, Table 28) showed that such substitution did not affect the enantioselectivity of the reaction, though the reactivity required a 3 mol% catalyst loading. In this case, with 2 mol% , the *ee* of the diol stacked at 76%. Luckily with a 3 mol % loading of the catalyst, after 11 hours, a 99 % *ee* of the diol was observed. The scale up of the reaction has been performed, leading to similar good results.

**KINETIC RESOLUTION OF DIOLS BEARING A QUATERNARY STEREOCENTER
VIA ASYMMETRIC ACETALIZATION**

Scheme 105: reaction for a small screening of catalyst loading

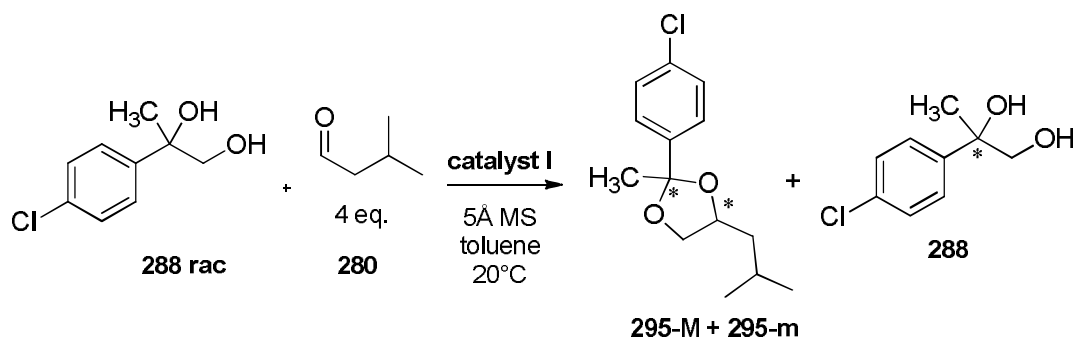


Table 28: small screening of catalyst loading for reaction in Scheme 105. Yields are not reported in the table, since the study of the *ee*, via HPLC, was adequate to understand the reaction trend.

catalyst loading	time (h)	<i>ee</i> diol (%)
1 mol %	4	28
1 mol %	24	34
1 mol %	48	33
2 mol %	7	54
2 mol %	52	76
3 mol %	11.5	99.2
3 mol %	20	99.4

4.3.7 Mechanism hypothesis and considerations on the stereochemistry assignment

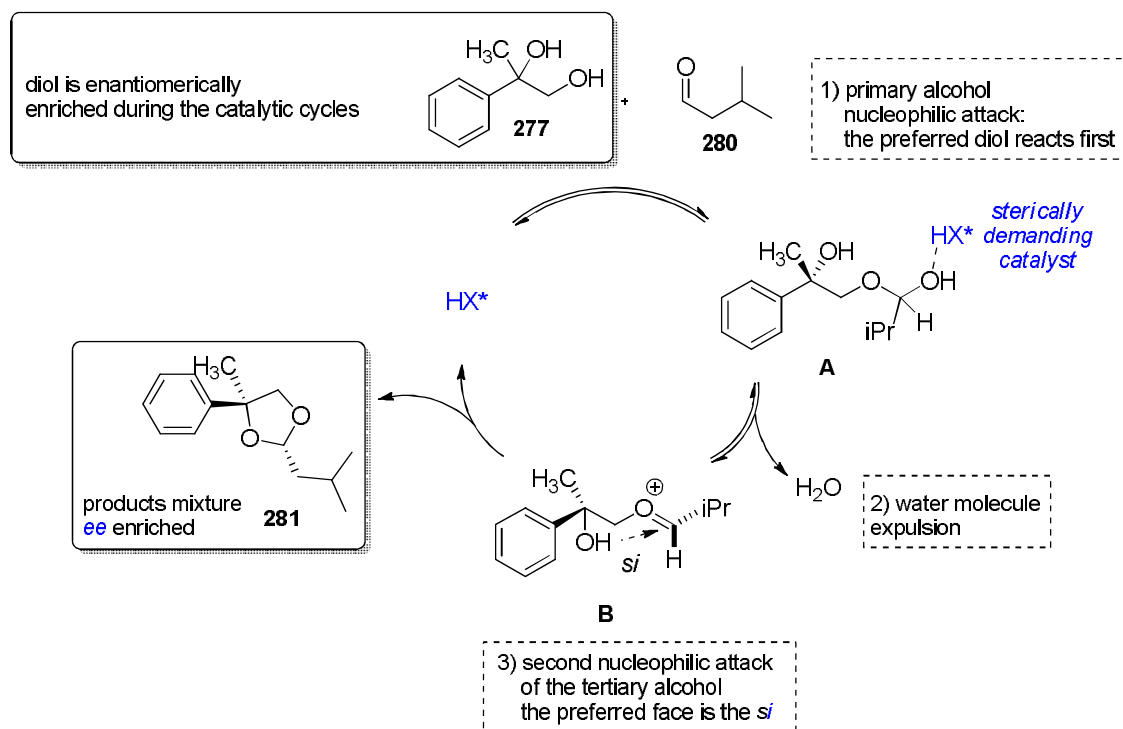
This kinetic resolution aroused as an application of the catalytic asymmetric acetalization developed by List research group, which brought to very good results in this unexplored field; the results of this kinetic resolution appear congruent to the hypothesized mechanism, which is supposed to be similar to the previously reported.^{104a} In the mechanistic hypothesis (Scheme 106), a reversible addition of the primary alcohol moiety of the **277** to the aldehyde **280** occurs; this first step is faster for one of the two enantiomers of the diol **277**, leading to an enantioenriched recovered diol during the catalytic cycles. This addition is followed by the formation of the hemiacetal intermediate **A**. Consequently, protonation of the OH by the catalyst results in the expulsion of a water molecule and formation of the oxacarbenium ion intermediate **B**, that is attacked in a stereoselective way by the second hydroxy nucleophile, leading to

KINETIC RESOLUTION OF DIOLS BEARING A QUATERNARY STEREOCENTER VIA ASYMMETRIC ACETALIZATION

the acetals **281**. Previous studies^{104a} of the acetalization mechanism, proved that the most likely intermediate is **A**, arising from the attack of the primary alcohol; moreover the *si* facial attack was verified by the absolute stereochemistry studies that had been done for the asymmetric acetalization. The asymmetry induction is clearly due to the sterically demanding catalyst pocket, in which the reaction takes place.

A confirmation of the stereochemistry assignment of this kinetic resolution will come from the optical rotatory power measurements of the recovered diols and from NMR bidimensional studies of the diastereomeric mixture of acetals. These studies are still in progress.

Scheme 106: hypothesized reaction mechanism, in the light of previous studies on asymmetric acetalization^{104a}. Configurations of the stereocenters have not been assigned yet, but a *si* attack can be hypothesized in the light of previous studies on acetalization reaction.^{104a}



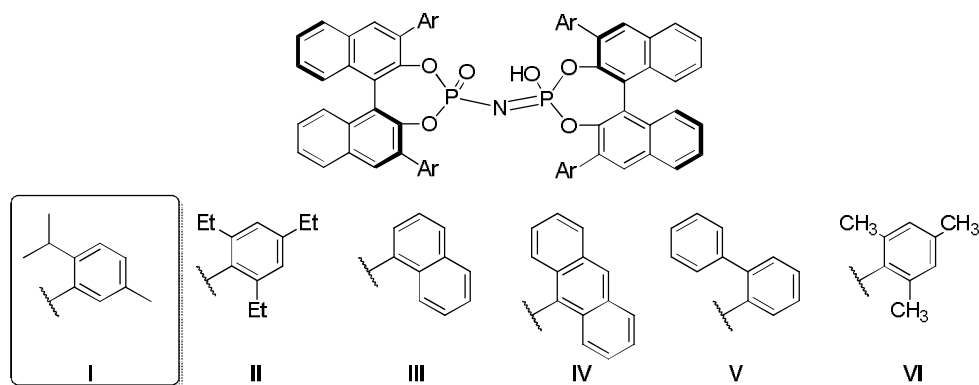
4.4 Conclusions

In conclusion, an efficient catalytic kinetic resolution of diols bearing a quaternary stereocenter have been developed, as an useful application of the catalytic asymmetric acetalization.^{104a}

KINETIC RESOLUTION OF DIOLS BEARING A QUATERNARY STEREOCENTER VIA ASYMMETRIC ACETALIZATION

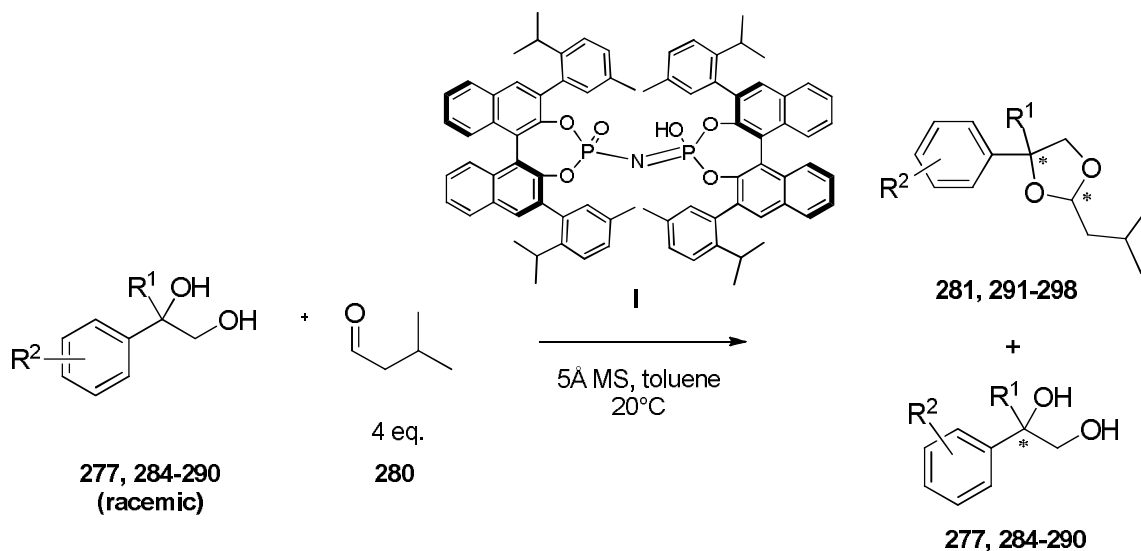
With the elected aldehyde, isovaleryc aldehyde, a catalyst screening of some confined Brønsted acids have been made, which have brought to the choice of thymol-derived catalyst (**I**) as the most efficient (Scheme 107).

Scheme 107: among the screened catalysts, **I** resulted to be the most efficient



The optimization of reaction conditions (Scheme 108) have led to the possibility of performing the reaction in a fast, mild and cheap manner. By tuning the aldehyde equivalents and the temperature, low catalyst loading (1 mol%) have been reached.

Scheme 108: kinetic resolution optimized conditions: 4 equivalents of isovaleraldehyde, catalyst **I**, 5Å molecular sieves, in toluene, at 20°C are the best conditions in order to have efficient reaction with the least amount of catalyst.



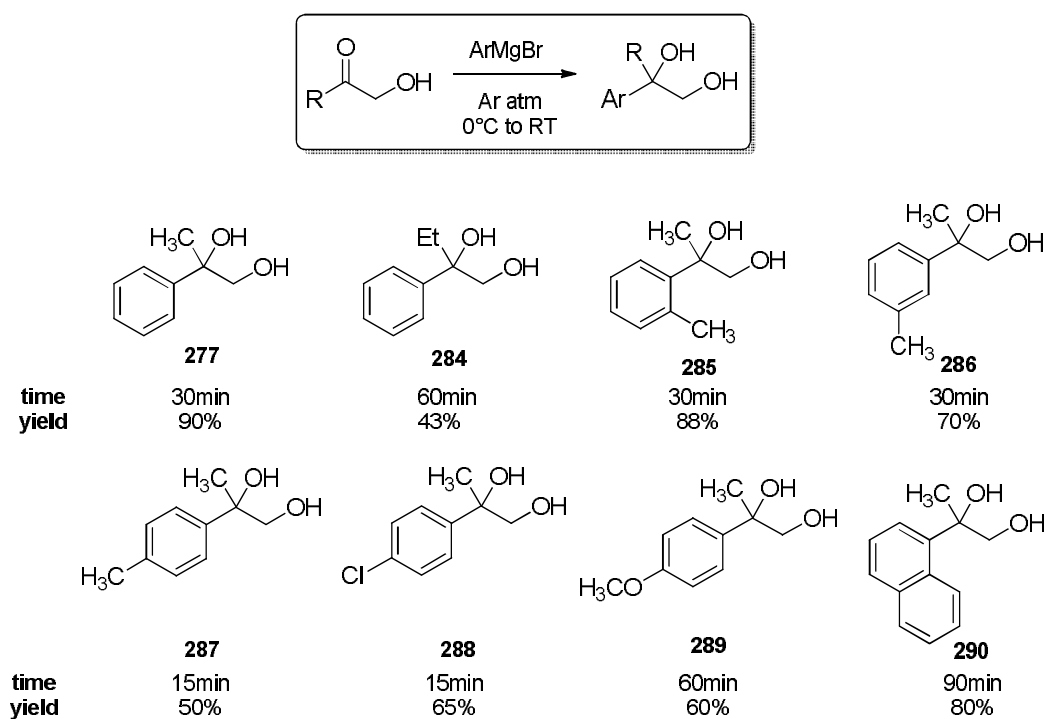
A scope of racemic diols, as starting material, have been easily synthesized, in moderate-to high yields, through a Grignard addition to corresponding hydroxy ketones (Scheme 109).

KINETIC RESOLUTION OF DIOLS BEARING A QUATERNARY STEREOCENTER VIA ASYMMETRIC ACETALIZATION

The optimized methodology have been employed to get very enantioenriched diols, with enantiomeric excess up to 99%, product acetals with a very high diastereomeric ratios (up to 98/2 dr) and enantioselectivities (up to 99% *ee*). Both products and starting diols have been isolated in good yield, keeping in mind that results are referred to a kinetic resolution (Scheme 110).

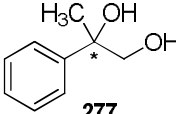
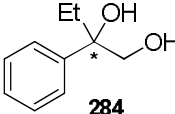
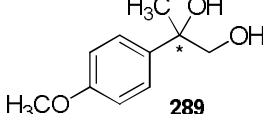
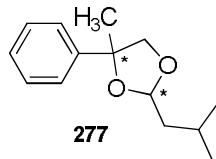
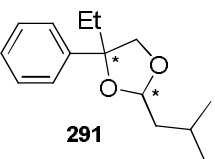
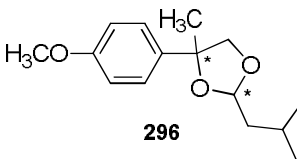
This methodology seems not to be influenced by the substitution on the aromatic ring of the diol and it represents a further improvement in the organocatalysis field, since it can reach results as good as one could do by means of metal-catalyzed processes.

Scheme 109: scope of the starting diols, synthesized by Grignard addition



**KINETIC RESOLUTION OF DIOLS BEARING A QUATERNARY STEREOCENTER
VIA ASYMMETRIC ACETALIZATION**

Scheme 110: the preliminary results for substrate scope

			
	277	284	289
conversion	50%	52%	50%
time	15h	20h	16h
yield	46%	46%	51%
ee	96%	99%	92%
			
	277	291	296
yield	50%	44%	48%
dr	98/2	97/3	98/2
ee major	97%	96%	97%
ee minor	97%	98%	96%

EXPERIMENTAL PART

General experimental

Solvents and reagents

All solvents used in the standard procedures were purified by distillation. Absolute diethyl ether, tetrahydrofuran and toluene were obtained by distillation over sodium with benzophenone as indicator; absolute chloroform and dichloromethane were obtained by distillation over calcium hydride, and ethanol, isopropanol and methanol were dried by distillation over magnesium. Commercial reagents were obtained from various sources and used without further purification.

Brønsted acid catalysts

Chiral Brønsted acid catalysts were kindly supplied by the coworkers from the List group (MPI, Mülheim an der Ruhr) and were prepared according to the literature procedures.⁹³

Inert gas atmosphere

Air and moisture sensitive reactions were conducted under an atmosphere of argon (*Air Liquide*, >99.5% purity). Unless otherwise stated, all organocatalytic reactions were performed under an ambient atmosphere without the exclusion of moisture or air.

Thin layer chromatography (TLC)

Reactions were monitored by thin layer chromatography on silica gel coated plastic sheets (0.2 mm, Machery-Nagel) or on coated aluminium Sigma-Aldrich covered with fluorescence indicator UV₂₅₄. Visualization was accomplished by irradiation with UV light at 254 nm and different staining reagents; phosphomolybdic acid (PMA) stain: PMA (10 g) in EtOH (100 ml), I₂, ninhydrin 5% in EtOH (w/w), KMnO₄ alkaline aq. solution.

Column chromatography

Column chromatography was performed under elevated pressure on silica gel (60, particle size 0.040-0.063 mm, Merck).

High pressure liquid chromatography (HPLC)

HPLC analyses on a chiral stationary phase were performed on a HPLC Thermo Spectra System SMC 1000 or on a Shimadzu LC-2010C systems, equipped with a UV detector. Commercial HPLC-grade solvents were used, and measurements were conducted at 25 °C. The chiral stationary phase of the columns is specified in each experiment. The enantiomeric ratios were determined by comparing the samples with the appropriate racemic mixtures.

Gas chromatography (GC)

GC analyses on a chiral stationary phase were performed on HP 6890 and 5890 series instruments equipped with a split-mode capillary injection system and a flame ionization detector (FID) using hydrogen as a carrier gas. Detailed conditions are given in the individual experiment. The enantiomeric ratios were determined by comparing the samples with the appropriate racemic mixtures.

Nuclear magnetic resonance spectroscopy (NMR)

Proton, carbon, and phosphorus NMR spectra were recorded on Bruker AV-500 or Bruker AV-400 or Varian "Gemini" 300 spectrometers in deuterated solvents at room temperature (298 K). Proton chemical shifts are reported in ppm (δ) relative to tetramethylsilane with the solvent resonance employed as the internal standard (C_6D_6 , δ 7.16 ppm; DMSO- d_6 , δ 2.49 ppm; $CDCl_3$, δ 7.24 ppm; acetone- d_6 , δ 2.04 ppm). Data are reported as follows: chemical shift, multiplicity (s = singlet, brs = broad singlet, d = doublet, dd = double doublet, t = triplet, q = quartet, m = multiplet), coupling constants (Hz) and integration. Slight shape deformation of the peaks in some cases due to weak coupling is not explicitly mentioned. ^{13}C chemical shifts are reported in ppm from tetramethylsilane with the solvent resonance as the internal standard (C_6D_6 , δ 128.06 ppm; DMSO- d_6 , δ 39.5 ppm; $CDCl_3$, δ 77.0 ppm; acetone- d_6 , δ 206.0, 29.8 ppm).

Infrared spectroscopy

FT-IR analysis were carried out in transmittance, in $CHCl_3$, on a Thermo Nexus spectrometer. The wave length range (4000-500 cm^{-1}) has been analyzed with 4 cm^{-1} resolution, with 32 scans.

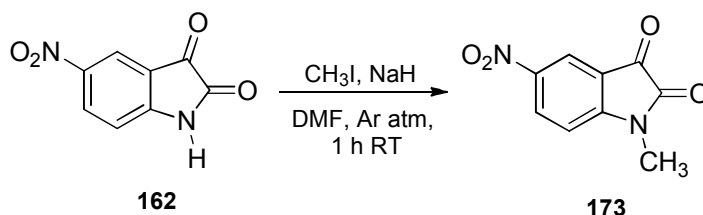
Mass spectrometry (MS)

Mass spectra were measured on a Finnigan MAT 8200 (70 eV) or MAT 8400 (70 eV) by electron ionization, chemical ionization or fast atom/ion bombardment techniques. High resolution mass spectra were obtained on a Finnigan MAT 95 or Bruker APEX III FT-MS (7 T magnet). All masses are given in atomic units/elementary charge (m/z).

Specific rotation

Optical rotations were determined with Jasco Mod. DIP-370 or Autopol IV automatic polarimeter (Rudolph Research Analytical) using a 50 mm cell with temperature control. The measurements were performed at 25°C at a wavelength $\lambda = 589$ nm (sodium D-line). Concentrations (c) are given in g/100 ml.

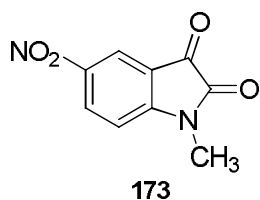
General procedure for preparing 1-methyl-indole-2,3-diones **172**, **173**.



Under an inert atmosphere of argon, to a suspension of isatin **162** (5 mmol) and sodium hydride at 60% dispersion in oil (0.17 g, 5 mmol) in DMF (10 mL) was added dropwise methyl iodide (0.7 mL, 5 mmol). After 12h under stirring at room temperature, the residue was treated with water and extracted with ethyl acetate. The organic layer was dried (MgSO_4) and the filtrate was concentrated under reduced pressure. The crude product was subsequently purified by flash chromatography on silica gel (*n*Hexane/EtOAc).¹⁰⁶

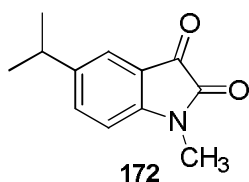
Characterization of 1-methyl-indole-2,3-diones **172**, **173**.

1-methyl-5-nitroindol-2,3-dione, **173**



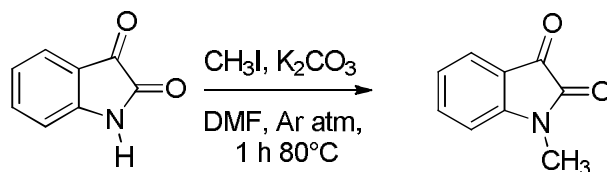
Following the above general procedure, the product **173** was obtained as an orange solid in 89% yield after purification (*n*Hexane/EtOAc=6/4). ^1H NMR (CDCl_3 , 300 MHz, 25°C): δ 3.36 (s, 3H, NCH_3); 7.06 (d, $J = 8.7$ Hz, 1H, CH_{arom}); 8.48 (d, $J = 2.3$ Hz, 1H, CH_{arom}); 8.56 (dd, $J = 8.7$ Hz, 2.3 Hz, 1H, CH_{arom}) ppm.¹⁰⁶

5-isopropyl-1-methylindol-2,3-dione, **172**



Following the above general procedure, the product **172** was obtained as a red solid in 84% yield after purification (*n*Hexane/EtOAc=7/3). ^1H NMR (CDCl_3 , 300 MHz, 25°C): δ 1.23 (d, $J = 6.9$ Hz, 6H, $(\text{CH}_3)_2\text{CHC}_{\text{arom}}$); 2.82-2.99 (m, 1H, $(\text{CH}_3)_2\text{CHC}_{\text{arom}}$); 3.22 (s, 3H, NCH_3); 6.81 (dd, $J = 7.4$ Hz, 1.3 Hz, 1H, CH_{arom}); 7.43-7.48 (m, 2H, CH_{arom}) ppm. ^{13}C NMR (CDCl_3 , 75 MHz, 25°C): 23.9 (NCH_3), 26.3 ($2\times\text{CH}_3$), 33.6 (CH), 109.9 (C_{arom}), 117.6 (C_{arom}), 123.2 (C_{arom}), 136.8 (C_{arom}), 145.0 (C_{arom}), 149.7 (C_{arom}), 158.6 ($\text{C}=\text{O}$), 183.8 ($\text{NC}=\text{O}$) ppm. HRMS: exact mass calculated for ($\text{C}_{12}\text{H}_{13}\text{NNaO}_2$) requires m/z 203.0901, found m/z 226.0903.

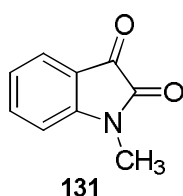
General procedure for preparing 1-methylindol-2,3-diones **131**, **168-171**, **175**, **178**



To a solution of indoline-2,3-dione (10.0 g, 68 mmol) and K_2CO_3 (18.8 g, 136 mmol) in 50 mL DMF was added CH_3I (136 mmol) dropwise slowly at room temperature. Then the mixture was stirred and monitored by TLC plates or overnight. When the reaction completed, the mixture was diluted by DCM, and water was added. The aqueous phase was extracted with DCM. The combined organic layers were then washed with saturated brine, dried over anhydrous Na_2SO_4 and concentrated under reduced pressure to give viscous oil, which was purified by chromatography on silica gel (*n*hexane/EtOAc)¹⁰⁷

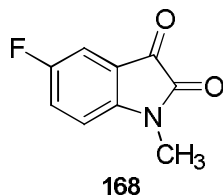
Characterization of 1-methylindol-2,3-diones **131**, **168-171**, **175**, **178**

1-methylindol-2,3-dione, **131**



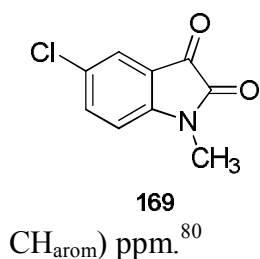
Following the above general procedure, the product **131** was obtained as a red solid in 98% yield after purification (*n*Hexane/EtOAc=6/4). 1H NMR ($CDCl_3$, 300 MHz, 25°C): δ 3.21 (s, 3H, NCH_3), 6.84 (m, 1H, CH_{arom}), 7.07 (m, 1H, CH_{arom}), 7.43-7.35 (m, 2H, CH_{arom}) ppm.⁸⁰

5-fluoro-1-methylindol-2,3-dione, **168**

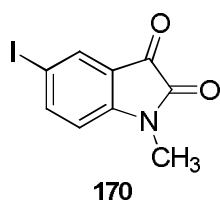


CH_{arom}) ppm.⁸⁰

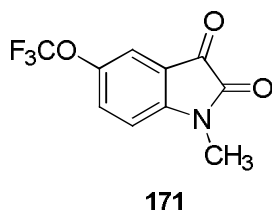
Following the above general procedure, the product **168** was obtained as a red solid in 95% yield after purification (*n*Hexane/EtOAc=7/3). 1H NMR ($CDCl_3$, 300 MHz, 25°C): δ 3.24 (s, 3H, CH_3N), 6.79-6.93 (m, 1H, CH_{arom}), 7.26-7.39 (m, 2H,

5-chloro-1-methylindol-2,3-dione, 169

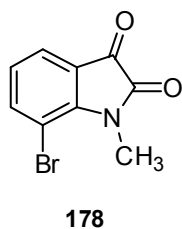
Following the above general procedure, the product **169** was obtained as a red solid in 94% yield after purification (*n*Hexane/EtOAc=7/3). ¹H NMR (CDCl₃, 300 MHz, 25°C): δ 3.24 (s, 3H, CH₃N), 6.79-6.93 (m, 1H, CH_{arom}), 7.26-7.39 (m, 2H,

5-iodo-1-methylindoline-2,3-dione, 170

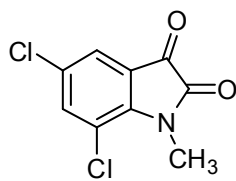
Following the above general procedure, the product **170** was obtained as a red solid in 94% yield after purification (*n*Hexane/EtOAc=6/4). ¹H NMR (DMSO-d₆, 300 MHz, 25°C): δ 3.12 (s, 3H, CH₃N), 6.98 (d, *J* = 8.8 Hz, 1H, CH_{arom}), 7.77 (s, 1H, CH_{arom}), 8.02 (d, *J*=8.8 Hz, 1H, CH_{arom}) ppm.¹⁰⁸

1-methyl-5-(trifluoromethoxy)indoline-2,3-dione, 171¹⁰⁹

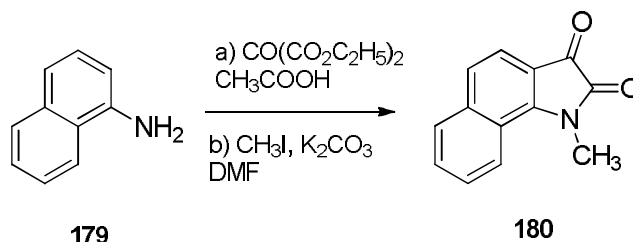
Following the above general procedure, the product **1e** was obtained as a red solid in 94% yield after purification (*n*Hexane/EtOAc=6/4). ¹H NMR (CDCl₃, 300 MHz, 25°C): δ 3.12 (s, 3H, CH₃N), 6.98 (d, *J* = 8.8 Hz, 1H, CH_{arom}), 7.77 (s, 1H, CH_{arom}), 8.02 (d, *J*=8.8 Hz, 1H, CH_{arom}) ppm.¹⁰⁸

7-bromo-1-methylindoline-2,3-dione, 178

Following the above general procedure, the product **178** was obtained as a red solid in 94% yield after purification (*n*Hexane/EtOAc=6/4). ¹H NMR (CDCl₃, 300 MHz, 25°C): δ 3.64 (s, 3H, CH₃N), 6.98 (dd, *J* = 8.0 Hz, *J* = 7.3 Hz, 1H, CH_{arom}), 7.56 (dd, *J* = 7.3 Hz, *J* = 1.3 Hz, 1H, CH_{arom}), 7.69 (dd, *J* = 8.0 Hz, *J* = 1.3 Hz, 1H, CH_{arom}) ppm.¹¹⁰

5,7-dichloro-1-methylindoline-2,3-dione, 175**175**

Following the above general procedure, the product **175** was obtained as a red solid in 92% yield after purification (*n*Hexane/EtOAc=7/3). ¹H NMR (CDCl₃, 300 MHz, 25°C): δ 3.60 (s, 3H, CH₃N), 7.47-7.52 (m, 2H, CH_{arom}) ppm. ¹³C NMR (CDCl₃, 75 MHz, 25°C): δ 29.8 (NCH₃), 118.4 (C_{arom}), 120.5 (C_{arom}), 124.1 (C_{arom}), 130.0 (C_{arom}), 139.3 (C_{arom}), 145.4 (C_{arom}), 158.0 (C=O), 181.6 (NC=O) ppm. HRMS: exact mass calculated for (C₉H₅NNaO₂) requires m/z 228.9701, found m/z 228.9705.

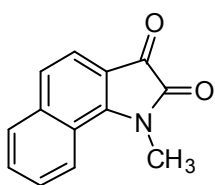
General procedure for preparing 3-ylidenoxindole 180**179****180**

a) In a round bottomed two neck flask, 24 mL acetic acid with 429mg (3mmol) of **179** are heated slowly until complete solubilisation. 0.16mL (1.06mmol) of diethylketomalonate are added drop by drop and the reaction is heated at 120°C. After 3 hours the solvent is removed in vacuo and a KOH5% solution is added to the crude. This alkaline solution is stirred to the air for 24 h, then HCl 1N is added until acidic pH. After one hour at 0°C the precipitate is filtrated and washed with acidic aqueous solution. The solid essiccated and used for the following step without further purification.

b) In a two necked flask, under Ar atmosphere, 389mg (1.88mmol) of 1H-benzo[g]indolo-2,3-dione, in 7mL DMF. Then 384 mg of K₂CO₃ (2.82 mmol) and 0,14 mL (1.86 mmol) of CH₃I are added slowly. The mixture is heated at 80°C and stirred for 30 min. Then 15mL of water are affed and the mixture is extracted with ethyl acetate (15mL x 5). The organic layers are dried over Na₂SO₄, the solvent is evaporated and the crude is purified via flash chromatography (hexane/EtOAc = 8/2). 253 mg (1.2 mmol) product are obtained as a red solid.

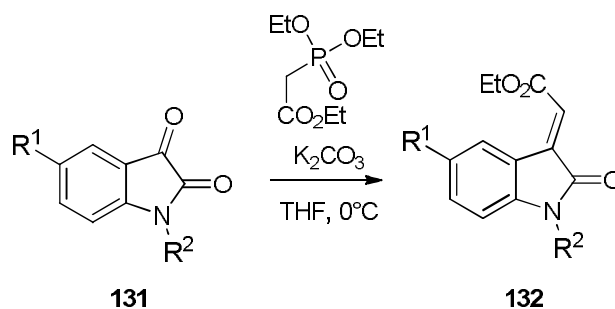
Characterization of 3-ylidenoxindole **180**

1-methyl-1H-benzo[g]indole-2,3-dione, **180**

**180**

Following the above general procedure, the product **180** was obtained as a red solid in 64% yield after purification (*n*Hexane/EtOAc=8/2). ¹H NMR (CDCl₃, 300 MHz, 25°C): δ = 3.82 (s, 3H, NCH₃), 7.44-7.71 (m, 4H, CH_{arom}), 7.85 (d, *J* = 8.1 Hz, 1H, CH_{arom}), 8.42 (d, *J* = 8.9 Hz, 1H, CH_{arom}) ppm. ¹³C NMR (CDCl₃, 75 MHz, 25°C): δ = 31.0 (NCH₃), 113.5 (C_{arom}), 119.5 (C_{arom}), 121.6 (C_{arom}), 123.9 (C_{arom}), 124.4 (C_{arom}), 127.4 (C_{arom}), 129.5 (C_{arom}), 130.1 (C_{arom}), 130.5 (C_{arom}), 140.5 (C_{arom}), 152.6 (C=O), 159.9 (NC=O) ppm. HRMS: exact mass calculated for (C₁₃H₉NNaO₂) requires *m/z* 211.0604, found *m/z* 228.0610.

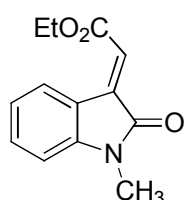
General procedure for preparing 3-ylideneoxindoles **132**, **146-150**, **154-156**, **181**, **210-215**, **223-231**



To a stirred solution of isatine (**131**) (2.7 mmol) in THF (9.0 mL) at 0 °C triethyl phosphonoacetate (3.0 mmol) and a solution of K₂CO₃ (8.7 mmol) in water (1.8 mL) were added. The mixture was stirred at 0 °C for 15 min and once reached the room temperature was kept under stirring until the reaction completion (TLC hexane /EtOAc). Afterwards, diethyl ether (50.0 mL) was added and the organic phase was washed with brine, dried with anhydrous Na₂SO₄ and concentrated under *vacuum*. The crude product **132** was subsequently purified by flash chromatography on silica gel (*n*Hexane/EtOAc).

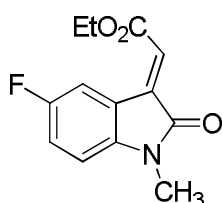
Characterization of 3-ylideneoxindoles **132**, **146-150**, **154-156**, **181**, **210-215**, **223-231**

(*E*)-ethyl 2-(1-methyl-2-oxoindolin-3-ylidene)acetate, **132**

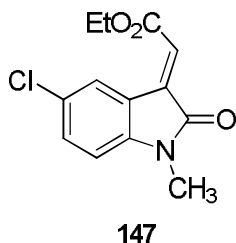
**132**

Following the above above general procedure, the single *E* diastereoisomer **132** was obtained as an orange solid in 80% yield after purification (*n*Hexane/EtOAc=7/3). IR (CHCl₃): $\tilde{\nu}$ = 3034, 3010, 1707, 1609, 1471, 1371 cm⁻¹. ¹H NMR (CDCl₃, 300 MHz, 25°C): δ 1.35 (t, *J* = 7.1 Hz, 3H, CH₃CH₂O), 3.22 (s, 3H, CH₃N), 4.31 (q, *J* = 7.1 Hz, 2H, CH₃CH₂O), 6.78 (d, *J* = 7.8 Hz, 1H, CH_{arom}), 6.89 (s, 1H, CH=C), 7.05 (dt, *J* = 7.9 Hz, 1.1 Hz, 1H, CH_{arom}), 7.35 (dt, *J* = 7.8 Hz, 1.1 Hz, 1H, CH_{arom}), 8.54 (d, *J* = 7.9 Hz, 1H, CH_{arom}) ppm. ¹³C NMR (CDCl₃, 75 MHz, 25°C): δ 14.4 (CH₃), 26.4 (NCH₃), 61.3 (CH₂), 108.3 (CH=C), 120.0 (C_{arom}), 122.6 (C_{arom}), 123.0 (C_{arom}), 128.9 (C_{arom}), 132.6 (C_{arom}), 138.0 (C=C), 146.2 (C_{arom}), 165.8 (OC=O), 167.7 (C=O) ppm. HRMS: exact mass calculated for (C₁₃H₁₃NNaO₃) requires *m/z* 254.0793, found *m/z* 254.0790.⁸⁰

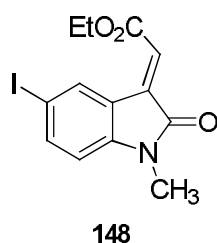
(*E*)-ethyl 2-(5-fluoro-1-methyl-2-oxoindolin-3-ylidene)acetate, **146**

**146**

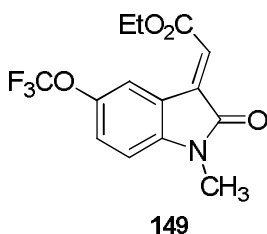
Following the above above general procedure, the single *E* diastereoisomer **146** was obtained as a red-orange solid in 60% yield after purification (*n*Hexane/EtOAc=7/3). IR (CHCl₃): $\tilde{\nu}$ = 3033, 3012, 2993, 1709, 1655, 1618, 1485, 1471, 1370, 1223 cm⁻¹. ¹H NMR (CDCl₃, 300 MHz, 25°C): δ 1.36 (t, *J* = 7.2 Hz, 3H, CH₃CH₂O), 3.21 (s, 3H, CH₃N), 4.32 (q, *J* = 7.2 Hz, 2H, CH₃CH₂O), 6.70 (dd, *J* = 8.6 Hz, 4.2 Hz, 1H, CH_{arom}), 6.93 (s, 1H, CH=C), 7.07 (dt, *J* = 8.6 Hz, 2.7 Hz, 1H, CH_{arom}), 8.36 (dd, *J* = 7.2 Hz, 1H, CH_{arom}) ppm. ¹³C NMR (CDCl₃, 75 MHz, 25°C): δ 14.3 (CH₃), 26.5 (NCH₃), 61.5 (CH₂), 108.5 [(CH=C) d, *J*_{CF} = 8.1 Hz], 116.6 [(C_{arom}), d, *J*_{CF} = 27.0 Hz], 118.7 [(C_{arom}), d, *J*_{CF} = 24.1 Hz], 120.9 [(C_{arom}), d, *J*_{CF} = 10.7 Hz], 123.9 (C_{arom}), 139.9 [(C_{arom}), d, *J*_{CF} = 239.3 Hz], 157.5 (C=C), 160.7 (C_{arom}), 165.5 (OC=O), 167.3 (C=O) ppm. HRMS: exact mass calculated for (C₁₃H₁₂FNNaO₃) requires *m/z* 272.0699, found *m/z* 272.0697.⁸⁰

(E)-ethyl 2-(5-chloro-1-methyl-2-oxoindolin-3-ylidene)acetate, 147

Following the above above general procedure, the single *E* diastereoisomer **147** was obtained as a red-orange solid in 76% yield after purification (*n*Hexane/EtOAc=9/1). IR (CHCl₃): $\tilde{\nu}$ = 3034, 3012, 2951, 1716, 1652, 1608, 1476, 1439, 1371, 1344 cm⁻¹. ¹H NMR (CDCl₃, 300 MHz, 25°C): δ 1.36 (t, *J* = 7.1 Hz, 3H, CH₃CH₂O), 3.20 (s, 3H, CH₃N), 4.32 (q, *J* = 7.1 Hz, 2H, CH₃CH₂O), 6.71 (d, *J* = 8.4 Hz, 1H, CH_{arom}), 6.92 (s, 1H, HC=), 7.33 (d, *J* = 8.4 Hz, 1H, CH_{arom}), 8.58 (s, 1H, CH_{arom}) ppm. ¹³C NMR (CDCl₃, 75 MHz, 25°C): δ 14.4 (CH₃), 26.5 (NCH₃), 61.6 (CH₂), 109.1 (CH=C), 121.1 (C_{arom}), 124.1 (C_{arom}), 128.4 (C_{arom}), 129.0 (C_{arom}), 132.2 (C_{arom}), 137.1 (C=C), 144.6 (C_{arom}), 165.5 (OC=O), 167.3 (C=O) ppm. HRMS: exact mass calculated for (C₁₃H₁₂ClNNaO₃) requires *m/z* 288.0403, found *m/z* 288.0404.⁸⁰

(E)-ethyl 2-(5-iodo-1-methyl-2-oxoindolin-3-ylidene)acetate, 148

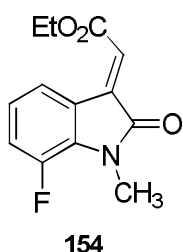
Following the above above general procedure, the single *E* diastereoisomer **148** was obtained as an orange solid in 21% yield after purification (*n*Hexane/EtOAc=8/2). IR (CHCl₃): $\tilde{\nu}$ = 3034, 3017, 3008, 1724, 1706, 1602, 1465, 1369, 1343 cm⁻¹. ¹H-NMR (CDCl₃, 300 MHz, 25°C): 1.38 (t, *J* = 7.1 Hz, 3H, CH₃CH₂O), 3.21 (s, 3H, NCH₃), 4.34 (q, *J* = 7.1 Hz, 2H, CH₃CH₂O), 6.59 (d, *J* = 8.2 Hz, 1H, CH_{arom}), 6.92 (s, 1H, CH=C), 7.69 (dd, *J* = 8.1 Hz, 1.7 Hz, 1H, CH_{arom}), 8.89 (d, *J* = 1.4 Hz, 1H, CH_{arom}) ppm. ¹³CNMR (CDCl₃, 75 MHz, 25°C): δ 14.4 (CH₃), 26.5 (NCH₃), 61.7 (CH₂), 85.5 (CH=C), 110.3 (C_{arom}), 121.9 (C_{arom}), 123.9 (C_{arom}), 136.6 (C_{arom}), 137.2 (C_{arom}), 141 (C=C), 145.6 (C_{arom}), 165.4 (OC=O), 166.8 (C=O) ppm. HRMS: exact mass calculated for (C₁₃H₁₂INNaO₃) requires *m/z* 379.9760, found *m/z* 379.9763.

(E)-ethyl 2-(1-methyl-2-oxo-5-(trifluoromethoxy)indolin-3-ylidene)acetate, 149

Following the above above general procedure, the single *E* diastereoisomer **149** was obtained as a red-orange solid in 67%

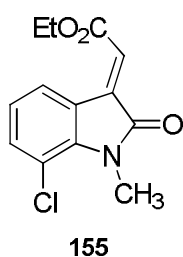
yield after purification (*n*Hexane/EtOAc=1/1). IR (CHCl₃): $\tilde{\nu}$ = 3029, 3011, 2984, 1712, 1655, 1618, 1484, 1467, 1371, 1347, 1223 cm⁻¹. ¹H NMR (CDCl₃, 300 MHz, 25°C): δ 1.36 (t, *J* = 7.1 Hz, 3H, CH₃CH₂O), 3.23 (s, 3H, CH₃N), 4.33 (q, *J* = 7.1 Hz, 2H, CH₃CH₂O), 6.77 (d, *J* = 8.5 Hz, 1H, CH_{arom}), 6.95 (s, 1H, CH=C), 7.21-7.34 (m, 1H, CH_{arom}), 8.53 (s, 1H, CH_{arom}) ppm. ¹³C NMR (CDCl₃, 75 MHz, 25°C): δ 14.3 (CH₃), 26.6 (NCH₃), 61.7 (CH₂), 108.6 (CH=C), 121.8 [(CF₃)_q, *J*_{CF} = 127.8 Hz], 122.8 (2xC_{arom}), 124.5 (C_{arom}), 125.4 (C_{arom}), 137.1 (C_{arom}), 144.7 (C=C), 144.9 (C_{arom}), 165.5 (OC=O), 167.5 (C=O) ppm. HRMS: exact mass calculated for (C₁₄H₁₂FNNaO₄) requires *m/z* 338.0616, found *m/z* 338.0617.⁸⁰

(*E*)-ethyl 2-(7-fluoro-1-methyl-2-oxoindolin-3-ylidene)acetate, 154



Following the above above general procedure, the single *E* diastereoisomer **154** was obtained as an orange-red solid in 71% yield after purification (*n*Hexane/EtOAc=95/5). IR (CHCl₃): $\tilde{\nu}$ = 3034, 3010, 2983, 1711, 1657, 1624, 1590, 1465, 1368, 1349 cm⁻¹. ¹H NMR (CDCl₃, 300 MHz, 25°C): δ 1.35 (t, *J* = 7.1 Hz, 3H, CH₃CH₂O), 3.44 (d, *J* = 2.9 Hz, 3H, CH₃N), 4.31 (q, *J* = 7.1 Hz, 2H, CH₃CH₂O), 6.88-7.02 (m, 1H, CH_{arom}), 6.93 (s, 1H, CH=C), 7.03-7.15 (m, 1H, CH_{arom}), 8.36 (d, *J* = 7.8 Hz, 1H, CH_{arom}) ppm. ¹³C NMR (CDCl₃, 75 MHz, 25°C): δ 14.3 (CH₃), 29.0 (d, *J*_{CF} = 6.2 Hz, NCH₃), 61.5 (CH₂), 120.3 [(CH=C), d, *J*_{CF} = 19.2 Hz], 122.7 [(C_{arom}), d, *J*_{CF} = 3.5 Hz], 123.3 [(C_{arom}), d, *J*_{CF} = 6.2 Hz], 124.0 (C_{arom}), 124.8 [(C_{arom}), d, *J*_{CF} = 3.1 Hz], 132.7 (C_{arom}), 137.2 (C=C), 147.8 [(C_{arom}), d, *J*_{CF} = 242.7 Hz], 165.5 (OC=O), 167.3 (C=O) ppm. HRMS: exact mass calculated for (C₁₃H₁₂FNNaO₃) requires *m/z* 272.0699, found *m/z* 272.0701.⁸⁰

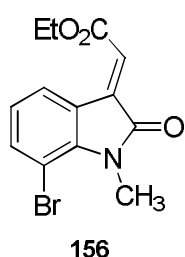
(*E*)-ethyl 2-(7-chloro-1-methyl-2-oxoindolin-3-ylidene)acetate, 155



Following the above above general procedure, the single *E* diastereoisomer **155** was obtained as a red-orange solid in 61% yield after purification (*n*Hexane/EtOAc=8/2). IR (CHCl₃): $\tilde{\nu}$ = 30334, 3002, 2951, 1710, 1649, 1601, 1455, 1366, 1346 cm⁻¹. ¹H NMR (CDCl₃, 300 MHz, 25°C): δ 1.35 (t, *J* = 7.1 Hz, 3H, CH₃CH₂O), 3.60 (s, 3H, CH₃N), 4.30 (q, *J* = 7.1 Hz, 2H, CH₃CH₂O), 6.93 (s, 1H, CH=C), 6.95 (t, *J* = 7.7 Hz, 1H, CH_{arom}), 7.26 (dd, *J* = 7.7 Hz, 0.7 Hz, 1H, CH_{arom}), 8.52

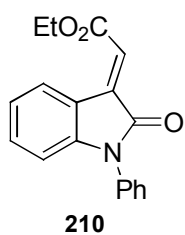
(dd, $J = 7.7$ Hz, 0.7 Hz, 1 H, CH_{arom}) ppm. ^{13}C NMR (CDCl_3 , 75 MHz, 25°C): δ 14.3 (CH_3), 30.0 (NCH_3), 61.4 (CH_2), 115.7 ($\text{CH}=\text{C}$), 122.6 (C_{arom}), 123.6 (C_{arom}), 123.8 (C_{arom}), 127.3 (C_{arom}), 134.5 (C_{arom}), 136.5 ($\text{C}=\text{C}$), 141.6 (C_{arom}), 165.4 ($\text{OC}=\text{O}$), 167.9 ($\text{C}=\text{O}$) ppm HRMS: exact mass calculated for ($\text{C}_{13}\text{H}_{12}\text{ClNNaO}_3$) requires m/z 288.0403, found m/z 288.0401.⁸⁰

(*E*)-ethyl 2-(7-bromo-1-methyl-2-oxindolin-3-ylidene)acetate, 156



Following the above above general procedure, the single *E* diastereoisomer **156** was obtained as reddish solid in 56% yield after purification (*n*Hexane/EtOAc=8/2). IR (CHCl_3): $\tilde{\nu} = 3031, 3013, 3003, 2980, 1709, 1654, 1602, 1472, 1452, 1347, 1265$ cm^{-1} . ^1H NMR (CDCl_3 , 300 MHz, 25°C): δ 1.34 (t, $J = 7.1$ Hz, 3 H, $\text{CH}_3\text{CH}_2\text{O}$), 3.61 (s, 3 H, CH_3N), 4.30 (q, $J = 7.1$ Hz, 2 H, $\text{CH}_3\text{CH}_2\text{O}$), 6.88 (t, $J = 7.9$ Hz, 1 H, CH_{arom}), 6.92 (s, 1 H, $\text{CH}=\text{C}$), 7.44 (dd, $J = 7.9$ Hz, 1.1 Hz, 1 H, CH_{arom}), 8.57 (dd, $J = 7.9$ Hz, 1.1 Hz, 1 H, CH_{arom}) ppm. ^{13}C NMR (CDCl_3 , 75 MHz, 25°C): δ 14.3 (CH_3), 30.2 (NCH_3), 61.4 (CH_2), 102.5 ($\text{CH}=\text{C}$), 122.9 (C_{arom}), 123.7 (C_{arom}), 123.9 (C_{arom}), 127.8 (C_{arom}), 136.4 (C_{arom}), 137.9 ($\text{C}=\text{C}$), 143.1 (C_{arom}), 165.4 ($\text{OC}=\text{O}$), 168.0 ($\text{C}=\text{O}$) ppm. HRMS: exact mass calculated for ($\text{C}_{13}\text{H}_{12}\text{BrNNaO}_3$) requires m/z 331.9898, found m/z 331.9896.⁸⁰

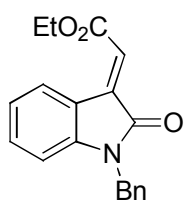
(*E*)-ethyl 2-(1-phenyl-2-oxindolin-3-ylidene)acetate, 210



Following the above above general procedure, the single *E* diastereoisomer **210** was obtained as an orange solid in 40% yield after purification (*n*Hexane/EtOAc=8/2). IR (CHCl_3): $\tilde{\nu} = 3035, 3010, 1725, 1711, 1608, 1507, 1370, 1341$ cm^{-1} . ^1H NMR (CDCl_3 , 300 MHz, 25°C): δ 1.37 (t, $J = 7.0$ Hz, 3 H, $\text{CH}_3\text{CH}_2\text{O}$), 4.33 (q, $J = 7.1$ Hz, 2 H, $\text{CH}_3\text{CH}_2\text{O}$), 6.77 (d, $J = 7.4$ Hz, 1 H, CH_{arom}), 6.98 (s, 1 H, $\text{CH}=\text{C}$), 7.08 (dt, $J = 7.7$ Hz, 0.9 Hz, 1 H, CH_{arom}), 7.27 (dt, $J = 7.8$ Hz, 1.2 Hz, 1 H, CH_{arom}), 7.35-7.45 (m, 3 H, CH_{arom}), 7.47-7.57 (m, 2 H, CH_{arom}), 8.63 (d, $J = 7.8$ Hz, 1 H, CH_{arom}) ppm. ^{13}C NMR (CDCl_3 , 75 MHz, 25°C): δ 14.4 (CH_3), 61.4 (CH_2), 109.7 ($\text{CH}=\text{C}$), 120.1 (C_{arom}), 123.2 (C_{arom}), 123.4 (C_{arom}), 126.8 (C_{arom}), 128.5 (C_{arom}), 129.1 (C_{arom}), 129.9 (C_{arom}), 132.5 (C_{arom}), 134.2 (C_{arom}), 137.8 ($\text{C}=\text{C}$), 146.2 (C_{arom}), 165.8 ($\text{OC}=\text{O}$), 167.1 ($\text{C}=\text{O}$)

ppm. HRMS: exact mass calculated for (C₁₈H₁₅NNaO₃) requires m/z 316.0950, found m/z 316.0952.⁸⁰

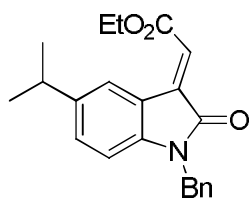
(E)-ethyl 2-(1-benzyl-2-oxoindolin-3-ylidene)acetate, 211



211

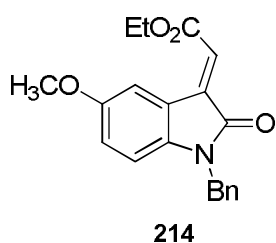
Following the above above general procedure, the single *E* diastereoisomer **211** was obtained as an orange solid in 80% yield after purification (*n*Hexane/EtOAc=7/3). IR (CHCl₃): $\tilde{\nu}$ = 3024, 3013, 1706, 1604, 1470, 1341 cm⁻¹. ¹H-NMR (CDCl₃, 300 MHz, 25°C): δ 1.36 (t, *J* = 7.6 Hz, 3H, CH₃CH₂O), 4.32 (q, *J* = 7.6 Hz, 2H, CH₃CH₂O), 4.92 (s, 2H, CH₂Ph), 6.67 (d, *J* = 7.9 Hz, 1H, CH_{arom}), 6.97 (s, 1H, HC=C), 7.01 (dt, *J* = 7.7 Hz, 1.0 Hz, 1H, CH_{arom}), 7.19-7.36 (m, 6H, CH_{arom}), 8.55 (ddd, *J* = 7.8 Hz, 0.6 Hz, 0.5 Hz, 1H, CH_{arom}) ppm. ¹³C NMR (CDCl₃, 75 MHz, 25°C): δ 14.4 (CH₃), 44.0 (C_{benz}), 61.4 (CH₂), 109.3 (CH=C), 120.2 (C_{arom}), 123.0 (C_{arom}), 123.1 (C_{arom}), 127.4 (C_{arom}), 127.9 (C_{arom}), 129.0 (C_{arom}), 129.1 (C_{arom}), 132.5 (C_{arom}), 135.6 (C_{arom}), 137.8 (C=C), 145.3 (C_{arom}), 165.8 (OC=O), 167.9 (C=O) ppm. HRMS: exact mass calculated for (C₁₉H₁₇NNaO₃) requires m/z 330.1106, found m/z 330.1102.⁸⁰

(E)-ethyl 2-(1-benzyl-5-isopropyl-2-oxoindolin-3-ylidene)acetate, 213

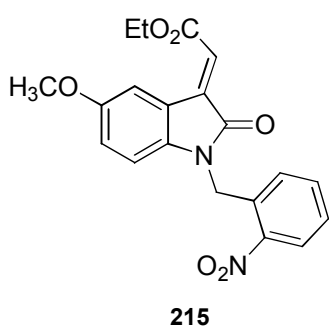


213

Following the above above general procedure, the single *E* diastereoisomer **213** was obtained as an orange solid in 67% yield after purification (*n*Hexane/EtOAc=8/2). ¹H-NMR (CDCl₃, 300 MHz, 25°C): δ 1.20 [d, *J* = 6.9 Hz, 6H, (CH₃)₂CH], 1.37 (t, *J* = 7.1 Hz, 3H, CH₃CH₂O), 2.87 [sept, *J* = 6.9 Hz, 1H, (CH₃)₂CH], 4.33 (q, *J* = 7.1 Hz, 2H, CH₃CH₂O), 4.90 (s, 2H, CH₂Ph), 6.59 (d, *J* = 8.1 Hz, 1H, CH_{arom}), 6.94 (s, 1H, HC=C), 7.10 (dd, *J* = 8.0 Hz, 1.5 Hz, 1H, CH_{arom}), 7.20-7.37 (m, 5H, CH_{arom}), 8.45 (d, *J* = 1.5 Hz, 1H, CH_{arom}) ppm. ¹³C NMR (CDCl₃, 75 MHz, 25°C): δ 14.5 (CH₃), 24.3 (2xCHCH₃), 34.1 (CHCH₃), 44.1 (CH₂_{benz}), 61.4 (CH₂), 109.1 (CH=C), 120.2 (C_{arom}), 122.7 (C_{arom}), 127.4 (C_{arom}), 127.5 (C_{arom}), 127.9 (C_{arom}), 129.0 (C_{arom}), 130.4 (C_{arom}), 135.8 (C_{arom}), 138.2 (C_{arom}), 143.4, 143.9 (C_{arom}), 166.0 (OC=O), 168.1 (C=O) ppm. HRMS: exact mass calculated for (C₂₂H₂₃NNaO₃) requires m/z 372.1576, found m/z 372.1579.⁸⁰

(E)-ethyl 2-(1-benzyl-5-methoxy-2-oxindolin-3-ylidene)acetate, 214

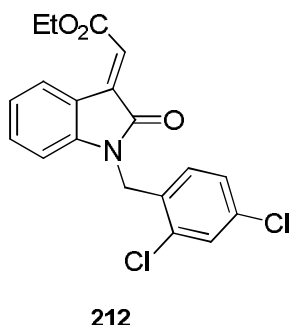
Following the above general procedure, the single *E* diastereoisomer **214** was obtained as an orange solid in 98% yield after purification (*n*Hexane/EtOAc=8/2). IR (CHCl₃): $\tilde{\nu}$ = 3027, 3009, 2987, 2963, 1729, 1708, 1650, 1612, 1594, 1483, 1345 cm⁻¹. ¹H-NMR (CDCl₃, 300 MHz, 25°C): δ 1.35 (t, *J* = 7.1 Hz, 3H, CH₃CH₂O), 3.77 (s, 3H, OCH₃), 4.31 (q, *J* = 7.1 Hz, 2H, CH₃CH₂O), 4.88 (s, 2H, CH₂Ph), 6.54 (d, *J* = 8.7 Hz, 1H, CH_{arom}), 6.79 (dd, *J* = 8.7 Hz, 2.3 Hz, 1H, CH_{arom}), 6.95 (s, 1H, HC=), 7.17–7.36 (m, 5H, CH_{arom}), 8.26 (d, *J* = 2.3 Hz, 1H, CH_{arom}) ppm. ¹³C NMR (CDCl₃, 75 MHz, 25°C): δ 14.4 (CH₃), 44.1 (CH₂benz), 56.1 (OCH₃), 61.4 (CH₂), 109.8 (CH=C), 114.8 (C_{arom}), 118.5 (C_{arom}), 120.9 (C_{arom}), 123.2 (C_{arom}), 127.4 (C_{arom}), 127.9 (C_{arom}), 129.0 (C_{arom}), 135.7 (C_{arom}), 138.4 (C_{arom}), 139.2 (C=C), 156.0 (C_{arom}), 165.8 (OC=O), 167.8 (C=O) ppm. HRMS: exact mass calculated for (C₂₀H₁₉NNaO₃) requires *m/z* 360.1212, found *m/z* 360.1210.⁸⁰

(E)-ethyl 2-(5-methoxy-1-(3-nitrobenzyl)-2-oxindolin-3-ylidene)acetate, 215

Following the above general procedure, the single *E* diastereoisomer **215** was obtained as an orange solid in 80% yield after purification (*n*Hexane/EtOAc=8/2). IR (CHCl₃): $\tilde{\nu}$ = 3034, 3009, 2952, 2922, 2852, 1718, 1700, 1650, 1593, 1482, 1371 cm⁻¹. ¹H NMR (CDCl₃, 300 MHz, 25°C): δ 1.37 (t, *J* = 7.1 Hz, 3H, CH₃CH₂O), 3.81 (s, 3H, OCH₃), 4.33 (q, *J* = 7.1 Hz, 2H, CH₃CH₂O), 5.32 (s, 2H, NCH₂), 6.45 (d, *J* = 8.5 Hz, 1H, CH_{arom}), 6.82 (dd, *J* = 8.5 Hz, 2.6 Hz, 1H, CH_{arom}), 6.98 (s, 1H, CH=C), 7.17 (d, *J* = 6.9 Hz, 1H, CH_{arom}), 7.37–7.55 (m, 2H, CH_{arom}), 8.16 (dd, *J* = 7.9 Hz, 1.6 Hz, 1H, CH_{arom}), 8.33 (d, *J* = 2.6 Hz, 1H, CH_{arom}) ppm. ¹³C NMR (CDCl₃, 75 MHz, 25°C): δ 14.4 (CH₃), 41.6 (CH₂benz), 56.1 (OCH₃), 61.5 (CH₂), 109.4 (CH=C), 115.1 (C_{arom}), 118.6 (C_{arom}), 120.9 (C_{arom}), 123.7 (C_{arom}), 125.8 (C_{arom}), 127.9 (C_{arom}), 128.7 (C_{arom}), 131.6 (C_{arom}), 134.2 (C_{arom}), 137.9 (C_{arom}), 138.5 (C_{arom}), 148.2, 156.4

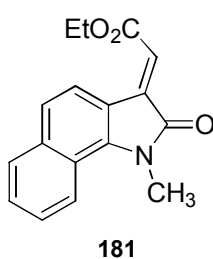
(C_{arom}), 165.7 (OC=O), 168.0 (C=O) ppm. HRMS: exact mass calculated for (C₂₀H₁₈N₂NaO₆) requires m/z 405.1063, found m/z 405.1060.⁸⁰

(E)-ethyl 2-(1-(2,4-dichlorobenzyl)-2-oxoindolin-3-ylidene)acetate, 212

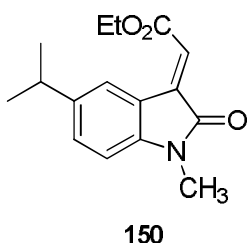


Following the above general procedure, the single *E* diastereoisomer **212** was obtained as an orange solid in 82% yield after purification (*n*Hexane/EtOAc=7/3). IR (CHCl₃): $\tilde{\nu}$ = 3032, 3010, 2397, 1709, 1698, 1609, 1470, 1372 cm⁻¹. ¹H-NMR (CDCl₃, 300 MHz, 25°C): δ 1.36 (t, *J* = 7.1 Hz, 3H, CH₃CH₂O), 4.33 (q, *J* = 7.1 Hz, 2H, CH₃CH₂O), 4.98 (s, 2H, CH₂Ph), 6.60 (d, *J* = 7.8 Hz, 1H, CH_{arom}), 6.92–7.17 (m, 4H, CH=C, CH_{arom}), 7.26 (t, *J* = 7.8 Hz, 1H, CH_{arom}), 7.40 (t, *J* = 2.1 Hz, 1H, CH_{arom}), 8.57 (d, *J* = 7.8 Hz, 1H, CH_{arom}) ppm. ¹³C NMR (CDCl₃, 75 MHz, 25°C): δ 14.4 (CH₃), 41.1 (CH₂benz), 61.5 (CH₂), 109.1 (CH=C), 120.2 (C_{arom}), 123.4 (2xC_{arom}), 127.8 (C_{arom}), 129.0 (C_{arom}), 129.1 (C_{arom}), 129.7 (C_{arom}), 131.6 (C_{arom}), 132.7 (C_{arom}), 133.7 (C_{arom}), 134.3 (C_{arom}), 137.5 (C=C), 144.7 (C_{arom}), 165.7 (OC=O), 168.0 (C=O) ppm. HRMS: exact mass calculated for (C₁₉H₁₅Cl₂NNaO₃) requires m/z 398.0327, found m/z 398.0331.⁸⁰

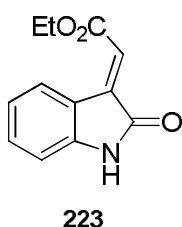
(E)-ethyl 2-(1-methyl-2-oxo-1H-benzo[*g*]indol-3(2H)-ylidene)acetate, 181



Following the above general procedure, the single *E* diastereoisomer **181** was obtained as an orange solid in 51% yield after purification (*n*Hexane/EtOAc=8/2). IR (CHCl₃): $\tilde{\nu}$ = 3038, 3027, 1710, 1644, 1620, 1590, 1466, 1377 cm⁻¹. ¹H-NMR (CDCl₃, 300 MHz, 25°C): δ 1.39 (t, *J* = 6.8 Hz, 3H, CH₃CH₂O); 3.83 (s, 3H, NCH₃); 4.35 (q, *J* = 6.8 Hz, 2H, CH₃CH₂O); 6.97 (s, 1H, CH=C); 7.42–7.53 (m, 3H, CH_{arom}); 7.82 (d, *J* = 8.2 Hz, 1H, CH_{arom}); 8.41 (d, *J* = 8.2 Hz, 1H, CH_{arom}); 8.63 (d, *J* = 8.6 Hz, 1H, CH_{arom}) ppm. ¹³C NMR (CDCl₃, 75 MHz, 25°C): δ 14.3 (CH₃), 31.1 (NCH₃), 61.4 (CH₂), 115.9 (CH=C), 120.9 (C_{arom}), 122.6 (C_{arom}), 122.8 (C_{arom}), 122.9 (C_{arom}), 124.2 (C_{arom}), 126.1 (C_{arom}), 127.6 (C_{arom}), 129.5 (C_{arom}), 137.0 (C_{arom}), 137.3 (C=C), 143.5 (C_{arom}), 165.9 (OC=O), 169.4 (C=O) ppm. HRMS: exact mass calculated for (C₁₇H₁₅NNaO₃) requires m/z 304.0950, found m/z 304.0971.

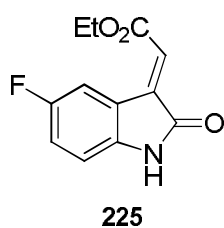
(E)-ethyl 2-(5-isopropyl-1-methyl-2-oxoindolin-3-ylidene)acetate, 150

Following the above general procedure, the single *E* diastereoisomer **150** was obtained as an orange solid in 63% yield after purification (*n*Hexane/EtOAc=8/2). IR (CHCl₃): $\tilde{\nu}$ = 3025, 3020, 3011, 1722, 1712, 1612, 1490, 1370 cm⁻¹. ¹H-NMR (CDCl₃, 300 MHz, 25°C): δ 1.26 (d, *J* = 7.0 Hz, 6H, (CH₃)₂CH); 1.38 (t, *J* = 7.1 Hz, 3H, CH₃CH₂O); 2.88–2.98 (m, 1H, (CH₃)₂CHC); 3.22 (s, 3H, NCH₃); 4.34 (q, *J* = 7.0 Hz, 2H, CH₃CH₂O); 6.72 (d, *J* = 7.9 Hz, 1H, CH_{arom}); 6.89 (s, 1H, CH=C); 7.24 (d, *J* = 7.9 Hz, 1H, CH_{arom}); 8.47 (s, 1H, CH_{arom}) ppm. ¹³CNMR (CDCl₃, 75 MHz, 25°C): δ 14.3 (CH₃), 24.3 (2xCHCH₃), 26.4 (NCH₃), 34.0 (CHCH₃), 61.2 (CH₂), 108.0 (CH=C), 119.9 (C_{arom}), 122.2 (C_{arom}), 127.2 (C_{arom}), 130.3 (C_{arom}), 138.3 (C_{arom}), 143.7 (C=C), 144.1 (C_{arom}), 165.8 (OC=O), 167.7 (C=O) ppm. HRMS: exact mass calculated for (C₁₆H₁₉NNaO₃) requires *m/z* 296.1263, found *m/z* 296.1265.

(E)-ethyl 2-(2-oxoindolin-3-ylidene)acetate, 223

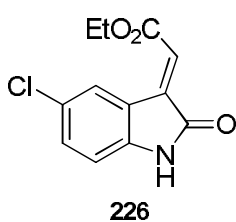
Following the above general procedure, the single *E* diastereoisomer **223** was obtained as an orange solid in 74% yield after purification (*n*Hexane/EtOAc=7/3). IR (CHCl₃): $\tilde{\nu}$ = 3034, 3010, 1707, 1609, 1471, 1371 cm⁻¹. ¹H-NMR (CDCl₃, 300 MHz, 25°C): δ 1.37 (t, *J* = 7.1 Hz, 3H, CH₃CH₂O); 4.31-4.36 (q, *J* = 7.1 Hz, 2H, CH₃CH₂O); 6.86-6.87 (m, 2H, CH=C, CH_{arom}); 7.04 (t, *J* = 7.7 Hz, 1H, CH_{arom}); 7.31 (t, *J* = 7.7 Hz, 1H, CH_{arom}); 8.53 (d, *J* = 7.8 Hz, 1H, CH_{arom}); 8.74 (bs, 1H, NH) ppm. ¹³CNMR (CDCl₃, 75 MHz, 25°C): δ 14.3 (CH₃), 61.4 (CH₂), 110.3 (CH=C), 120.5 (C_{arom}), 122.8 (C_{arom}), 123.0 (C_{arom}), 129.2 (C_{arom}), 132.7 (C_{arom}), 138.3 (C=C), 143.5 (C_{arom}), 165.7 (OC=O), 169.5 (C=O) ppm. HRMS: exact mass calculated for (C₁₉H₁₅Cl₂NNaO₃) requires *m/z* 398.0327, found *m/z* 398.0331.¹⁰⁷

(E)-ethyl 2-(5-fluoro-2-oxoindolin-3-ylidene)acetate, 225



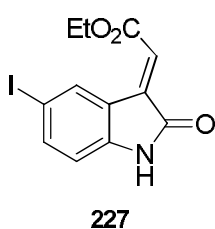
Following the above general procedure, the single *E* diastereoisomer **225** was obtained as an orange solid in 54% yield after purification (*n*Hexane/EtOAc=8/2). IR (CHCl₃): $\tilde{\nu}$ = 3429, 3028, 3017, 1709, 1655, 1618, 1485, 1471, 1370 cm⁻¹. ¹H-NMR (CDCl₃, 300 MHz, 25°C): δ 1.38 (t, *J* = 7.1 Hz, 3H, CH₃CH₂O), 4.34 (q, *J* = 7.0 Hz, 2H, CH₃CH₂O), 6.71–6.83 (m, 1H, CH_{arom}), 6.91 (s, 1H), 7.05 (t, *J* = 8.1 Hz, 1H, CH_{arom}), 8.23 (bs, 1H, NH), 8.37 (d, *J*_{HF} = 9.0 Hz, 1H, CH_{arom}) ppm. ¹³CNMR (CDCl₃, 75 MHz, 25°C): δ 14.3 (CH₃), 61.6 (CH₂), 110.6 [(CH=C), d, *J*_{C-F} = 7.9 Hz], 116.7 [(C_{arom}), d, *J*_{C-F} = 26.8 Hz], 118.6 (C_{arom}), 119.0 [(C_{arom}), d, *J*_{C-F} = 24.7 Hz], 124.2 (C_{arom}), 133.8 (C_{arom}), 139.4 (C=C), 158.9 [(C_{arom}), d, *J*_{C-F} = 243.7 Hz], 165.4 (OC=O), 168.2 (C=O) ppm. HRMS: exact mass calculated for (C₁₂H₁₀FNNaO₃) requires *m/z* 258.0542, found *m/z* 258.0544.¹¹¹

(*E*)-ethyl 2-(5-chloro-2-oxoindolin-3-ylidene)acetate, 226



Following the above general procedure, the single *E* diastereoisomer **226** was obtained as an orange solid in 80% yield after purification (*n*Hexane/EtOAc=7/3). IR (CHCl₃): $\tilde{\nu}$ = 3443, 3034, 3012, 1716, 1649, 1608, 1476, 1439, 1368, 1343 cm⁻¹. ¹H-NMR (CDCl₃, 300 MHz, 25°C): δ 1.38 (t, *J* = 7.0 Hz, 3H, CH₃CH₂O), 4.35 (q, *J* = 7.0 Hz, 2H, CH₃CH₂O), 6.79 (d, *J* = 8.4 Hz, 1H, CH_{arom}), 6.91 (s, 1H), 7.31 (d, *J* = 8.4 Hz, 1H, CH_{arom}), 7.90 (bs, 1H, NH), 8.61 (s, 1H, CH_{arom}) ppm. ¹³CNMR (CDCl₃, 75 MHz, 25°C): δ 14.3 (CH₃), 61.7 (CH₂), 111.0 (CH=C), 121.8 (C_{arom}), 124.4 (C_{arom}), 128.5 (C_{arom}), 129.3 (C_{arom}), 131.2 (C_{arom}), 132.4 (C_{arom}), 137.2 (C=C), 141.6 (C_{arom}), 165.4 (OC=O), 168.5 (C=O) ppm. HRMS: exact mass calculated for (C₁₂H₁₀ClNNaO₃) requires *m/z* 274.0247, found *m/z* 274.0244.¹¹¹

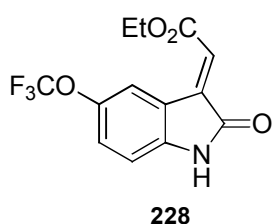
(*E*)-ethyl 2-(5-iodo-2-oxoindolin-3-ylidene)acetate, 227



Following the above general procedure, the single *E* diastereoisomer **227** was obtained as an orange solid in 70% yield after purification (*n*Hexane/EtOAc=7/3). IR (CHCl₃): $\tilde{\nu}$ 3443, 3034, 3012, 1716, 1649, 1608, 1476, 1439, 1368, 1343 cm⁻¹. ¹H-NMR (CDCl₃, 300 MHz, 25°C): δ 1.38 (t, *J* = 7.0 Hz, 3H, CH₃CH₂O), 4.35 (q, *J* = 7.0 Hz, 2H, CH₃CH₂O), 6.64 (d, *J* = 8.4 Hz, 1H, CH_{arom}), 6.89

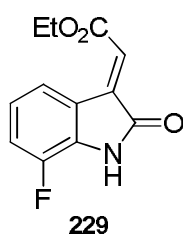
(s, 1H), 7.63-7.68 (m, 2H, CH_{arom}), 8.90 (bs, 1H, NH) ppm. ¹³CNMR (CDCl₃, 75 MHz, 25°C): δ 14.4 (CH₃), 61.7 (CH₂), 112.1 (CH=C), 122.6 (C_{arom}), 124.3 (C_{arom}), 134.2 (C_{arom}), 137.7 (C_{arom}), 140.0 (C_{arom}), 141.1 (C=C), 142.7 (C_{arom}), 165.4 (OC=O), 168.2 (C=O) ppm. HRMS: exact mass calculated for (C₁₂H₁₀INNaO₃) requires m/z 365.9603, found m/z 365.9607.

(E)-ethyl 2-(5-trifluoromethoxy-2-oxoindolin-3-ylidene)acetate, 228

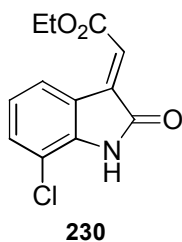


Following the above general procedure, the single *E* diastereoisomer **228** was obtained as an orange solid in 44% yield after purification (*n*Hexane/EtOAc=7/3). IR (CHCl₃): $\tilde{\nu}$ = 3443, 3026, 3020, 1724, 1709, 1617, 1470, 1375 cm⁻¹. ¹H-NMR (CDCl₃, 300 MHz, 25°C): δ 1.38 (t, *J* = 7.1 Hz, 3H, CH₃CH₂O), 4.35 (q, *J* = 7.1 Hz, 2H, CH₃CH₂O), 6.85 (d, *J* = 9.1 Hz, 1H, CH_{arom}), 6.94 (s, 1H), 7.22 (d, *J* = 7.8 Hz, 1H, CH_{arom}), 7.80 (bs, 1H, NH), 8.55 (s, 1H) ppm. ¹³CNMR (CDCl₃, 75 MHz, 25°C): δ 14.3 (CH₃), 61.7 (CH₂), 110.5 (CH=C), 120.7 (q, *J*_{CF} = 256.9 Hz, OCF₃), 121.5 (C_{arom}), 123.0 (C_{arom}), 124.7 (C_{arom}), 125.7 (C_{arom}), 137.3 (C_{arom}), 141.8 (C=C), 144.8 (C_{arom}), 165.3 (CO₂), 168.8 (C=O) ppm. HRMS: exact mass calculated for (C₁₃H₁₀F₃NNaO₅) requires m/z 324.0460, found m/z 324.0465.

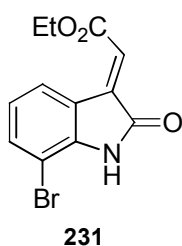
(E)-ethyl 2-(7-fluoro-2-oxoindolin-3-ylidene)acetate, 229



Following the above general procedure, the single *E* diastereoisomer **229** was obtained as an orange solid in 80% yield after purification (*n*Hexane/EtOAc=8/2). IR (CHCl₃): $\tilde{\nu}$ = 3433, 3029, 3020, 2983, 1711, 1657, 1626, 1455, 1358 cm⁻¹. ¹H-NMR (CDCl₃, 300 MHz, 25°C): δ 1.38 (t, *J* = 7.0 Hz, 3H, CH₃CH₂O), 4.34 (q, *J* = 7.0 Hz, 2H, CH₃CH₂O), 6.94 (s, 1H), 6.97–7.04 (m, 1H, CH_{arom}), 7.12 (t, *J* = 8.3 Hz, 1H, CH_{arom}), 7.82 (bs, 1H, NH), 8.37 (d, *J* = 8.3 Hz, 1H, CH_{arom}) ppm. ¹³CNMR (CDCl₃, 75 MHz, 25°C): δ 14.3 (CH₃), 61.5 (CH₂), 119.4 [d, *J*_{CF} = 16.9 Hz, (CH=C)], 122.9 (d, *J*_{CF} = 3.7 Hz, C_{arom}), 123.3 (d, *J*_{CF} = 5.7 Hz, C_{arom}), 124.4 (HC=C), 124.9 (d, *J*_{CF} = 3.3 Hz, C_{arom}), 130.7 (d, *J*_{CF} = 12.5 Hz, C_{arom}), 137.5 (d, *J*_{CF} = 3.4 Hz, C=C), 147.1 (d, *J*_{CF} = 243.3 Hz, C_{arom}), 165.4 (OC=O), 168.5 (C=O) ppm. HRMS: exact mass calculated for (C₁₂H₁₀FNNaO₃) requires m/z 258.0542, found m/z 258.0545.¹¹²

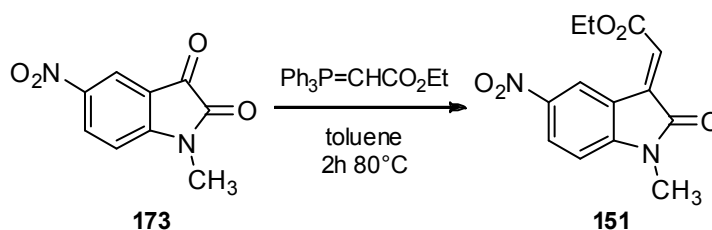
(E)-ethyl 2-(7-chloro-2-oxoindolin-3-ylidene)acetate, 230

Following the above general procedure, the single *E* diastereoisomer **230** was obtained as an orange solid in 42% yield after purification (*n*Hexane/EtOAc=8/2). IR (CHCl₃): $\tilde{\nu}$ = 3445, 3030, 3020, 1710, 1649, 1601, 1455, 1366, 1346 cm⁻¹. ¹H-NMR (CDCl₃, 300 MHz, 25°C): δ 1.37 (t, *J* = 7.0 Hz, 3H, CH₃CH₂O), 4.33 (q, *J* = 7.0 Hz, 2H, CH₃CH₂O), 6.93 (s, 1H, HC=C); 6.99 (t, 1H, *J* = 7.7 Hz, CH_{arom}); 7.30 (d, *J* = 7.7 Hz, 1H, CH_{arom}), 8.46 (d, *J* = 7.7 Hz, 1H, CH_{arom}) 8.65 (bs, 1H, NH), ppm. ¹³CNMR (CDCl₃, 75 MHz, 25°C): δ 14.3 (CH₃), 61.6 (CH₂), 115.5 (HC=C), 121.9 (C_{arom}), 123.0 (C_{arom}), 127.4 (C_{arom}), 127.7 (C_{arom}), 134.1 (C_{arom}), 137.9 (C_{arom}), 141.1 (C=C), 165.4 (OC=O), 168.3 (C=O) ppm. HRMS: exact mass calculated for (C₁₂H₁₀ClNNaO₃) requires *m/z* 274.0247, found *m/z* 274.0249.¹¹²

(E)-ethyl 2-(7-bromo-2-oxoindolin-3-ylidene)acetate, 231

Following the above general procedure, the single *E* diastereoisomer **231** was obtained as an orange solid in 50% yield after purification (*n*Hexane/EtOAc=7/3). IR (CHCl₃): $\tilde{\nu}$ = 3440, 3027, 3016, 2980, 1709, 1654, 1615, 1472, 1452, 1347 cm⁻¹. ¹H-NMR (CDCl₃, 300 MHz, 25°C): δ 1.37 (t, *J* = 7.1 Hz, 3H, CH₃CH₂O), 4.33 (q, *J* = 7.1 Hz, 2H, CH₃CH₂O), 6.91 (s, 1H, C-(9)), 6.96 (t, *J* = 7.7 Hz, 1H, CH_{arom}), 7.45 (d, *J* = 8.5 Hz, 1H, CH_{arom}), 7.75 (bs, 1H, NH), 8.52 (d, *J* = 8.5 Hz, 1H, CH_{arom}) ppm. ¹³CNMR (CDCl₃, 75 MHz, 25°C): δ 14.3 (CH₃), 61.5 (CH₂), 103.3 (HC=C), 121.8 (C_{arom}), 124.0 (C_{arom}), 124.5 (C_{arom}), 127.9 (C_{arom}), 134.9 (C_{arom}), 138.2 (C_{arom}), 142.6 (C=C), 165.3 (OC=O), 167.9 (C=O) ppm. HRMS: exact mass calculated for (C₁₂H₁₀BrNNaO₃) requires *m/z* 317.9742, found *m/z* 317.9739.

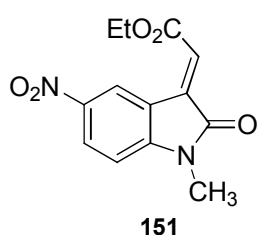
General procedure for preparing 3-ylideneoxindoles **151**, **152**



To a solution of the corresponding isatin (5 mmol, 1 equiv) in toluene (30 mL) was added the Wittig reagent (5 mmol, 1 equiv) and the mixture was stirred at reflux. After the reaction was complete, the solution was removed under reduced pressure and the residue was purified by flash chromatography directly to afford the purified product.

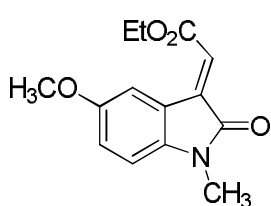
Characterization of 3-ylideneoxindoles **151**, **152**

(*E*)-ethyl 2-(1-methyl-5-nitro-2-oxindolin-3-ylidene)acetate, **151**



Following the above general procedure, the single *E* diastereoisomer **151** was obtained as an orange solid in 58% yield after purification (*n*Hexane/EtOAc=6/4). IR (CHCl₃): $\tilde{\nu}$ = 3025, 3020, 3011, 1724, 1715, 1613, 1523, 1366, 1340 cm⁻¹. ¹H-NMR (CDCl₃, 300 MHz, 25°C): δ 1.41 (t, *J* = 7.1 Hz, 3H, CH₃CH₂O); 3.32 (s, 3H, NCH₃); 4.39 (q, *J* = 7.1 Hz, 2H, CH₃CH₂O); 6.91 (d, *J* = 8.7 Hz, 1H, CH_{arom}); 7.04 (s, 1H, CH=C); 8.35 (dd, *J* = 8.7, 2.3 Hz, 1H, CH_{arom}); 9.48 (d, *J* = 2.3 Hz, 1H, CH_{arom}) ppm. ¹³CNMR (CDCl₃, 75 MHz, 25°C): δ 14.3 (CH₃), 26.9 (NCH₃), 62.1 (CH₂), 108.0 (CH=C), 120.1 (C_{arom}), 124.6 (C_{arom}), 126.0 (C_{arom}), 128.7 (C_{arom}), 135.6 (C_{arom}), 143.8 (C=C), 150.7 (C_{arom}), 165.0 (OC=O), 167.7 (C=O) ppm. HRMS: exact mass calculated for (C₁₃H₁₂N₂NaO₅) requires *m/z* 299.0644, found *m/z* 299.0646.¹¹³

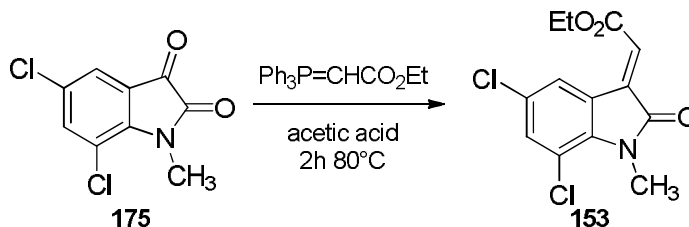
(*E*)-ethyl 2-(5-methoxy-1-methyl-2-oxindolin-3-ylidene)acetate, **152**¹¹⁴



Following the above general procedure, the single *E* diastereoisomer **152** was obtained as an orange solid in 90% yield after purification (*n*Hexane/EtOAc=6/4). IR (CHCl₃): $\tilde{\nu}$ = 3019, 2942, 2819, 1708, 1597, 1479, 1368, 1344, 1029, 772 cm⁻¹. ¹H-NMR (CDCl₃, 300 MHz, 25°C): δ 1.37 (t, *J* = 7.2 Hz, 3H, CH₃CH₂O); 3.21 (s, 3H,

NCH₃), 3.84 (s, 3H, OCH₃), 4.33 (q, $J = 7.2$ Hz, 2H, CH₃CH₂O), 6.69 (d, $J = 10.0$ Hz, 1H, CH_{arom}), 6.91 (s, 1H, CH=C), 6.91-6.96 (m, 1H, CH_{arom}), 8.28 (s, 1H, CH_{arom}) ppm.

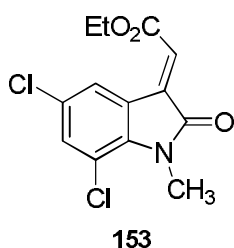
General procedure for preparing 3-ylideneoxindoles 153, 232



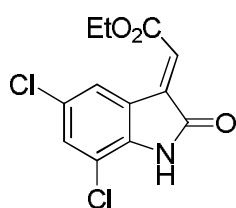
In a round bottomed flask 150 mg (0,65 mmol) of isatin were stirred in 1mL of acetic acid. After the addition of 226 mg (0,65 mmol) of phosphorane, the mixture was stirred at 80°C for two hours. Then the solvent was removed in vacuo and the crude was purified *via* flash column chromatography (eluent 8/2 hexane/EtOAc), leading to 172 mg (0,56 mmol) of pure product.

Characterization of 3-ylideneoxindoles 153, 232

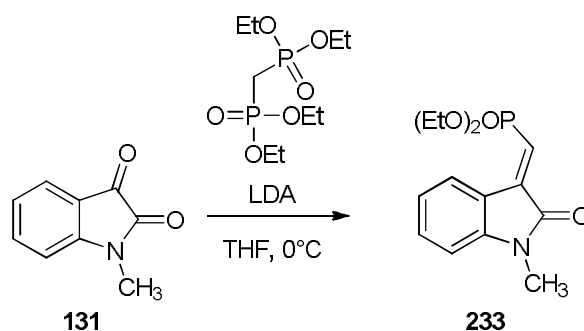
(*E*)-ethyl 2-(5,7-dichloro-1-methyl-2-oxoindolin-3-ylidene)acetate, 153



Following the above general procedure, the single *E* diastereoisomer **153** was obtained as an orange solid in 89% yield after purification (*n*Hexane/EtOAc=8/2). IR (CHCl₃): $\tilde{\nu} = 3029, 3016, 1726, 1714, 1574, 1453, 1374, 1339$ cm⁻¹. ¹H-NMR (CDCl₃, 300 MHz, 25°C): δ 1.36 (t, $J = 6.9$ Hz, 3H, CH₃CH₂O); 3.54 (s, 3H, NCH₃); 4.31 (q, $J = 6.9$ Hz, 2H, CH₃CH₂O); 6.90 (s, 1H, CH=C); 7.23 (s, 1H, CH_{arom}); 8.51 (s, 1H, CH_{arom}) ppm. ¹³CNMR (CDCl₃, 75 MHz, 25°C): δ 14.4 (CH₃), 30.0 (NCH₃), 61.9 (CH₂), 116.1 (CH=C), 123.3 (C_{arom}), 125.4 (C_{arom}), 127.6 (C_{arom}), 128.4 (C_{arom}), 133.7 (C_{arom}), 135.7 (C=C), 140.3 (C_{arom}), 165.2 (OC=O), 167.5 (C=O) ppm. HRMS: exact mass calculated for (C₁₇H₁₅NNaO₃) requires m/z 322.0014, found m/z 322.0017.

(E)-ethyl 2-(5,7-dichloro-2-oxoindolin-3-ylidene)acetate, 232**232**

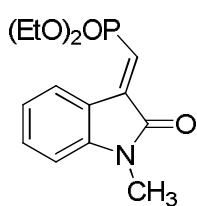
Following the above general procedure, the single *E* diastereoisomer **232** was obtained as an orange solid in 70% yield after purification (*n*Hexane/EtOAc=7/3). IR (CHCl₃): $\tilde{\nu}$ = 430, 3029, 3010, 1736, 1710, 1612, 1450, 1291 cm⁻¹. ¹H-NMR (CDCl₃, 300 MHz, 25°C): δ 1.38 (t, *J* = 6.6 Hz, 3H, CH₃CH₂O), 4.35 (m, 2H, CH₃CH₂O), 6.96 (s, 1H, CH=C); 7.35 (s, 1H, CH_{arom}); 8.16 (bs, 1H, NH); 8.54 (s, 1H, CH_{arom}) ppm. ¹³CNMR (CDCl₃, 75 MHz, 25°C): δ 14.3 (CH₃), 61.9 (CH₂), 115.7 (HC=C), 122.4 (C_{arom}), 125.9 (C_{arom}), 127.7 (C_{arom}), 128.6 (C_{arom}), 131.6 (C_{arom}), 137.0 (C_{arom}), 139.5 (C_{arom}), 165.1 (OC=O), 167.6 (C=O) ppm. HRMS: exact mass calculated for (C₁₂H₉Cl₂NNaO₃) requires *m/z* 307.9857, found *m/z* 307.9859.¹¹⁵

General procedure for preparing 3-ylideneoxindoles 233-237

To a stirred solution of tetraethyl methylenebis(phosphonate) (2.6 mmol, 749 mg) in anhydrous THF (2 mL) under Ar at 0 °C, LDA (2 m in THF, 1.43 mL, 2.86 mmol) was added dropwise. After 30 min, the mixture was warmed to room temp., stirred for an additional 30 min and cooled again to 0 °C. At this temperature, a solution of isatine 7 (2 mmol) in anhydrous THF (8 mL) was slowly added. The reaction mixture was allowed to reach room temp., and stirred until complete (monitored by TLC; hexane/ethyl acetate). Saturated aqueous NH₄Cl solution was slowly added, and the aqueous layer was extracted with ethyl acetate (3x50 mL). The combined organic phases were dried with anhydrous Na₂SO₄ and concentrated under reduced pressure to give the crude product, which was subsequently purified by flash chromatography on silica gel (hexane/ethyl acetate).

Characterization of 3-ylideneoxindoles 233-237

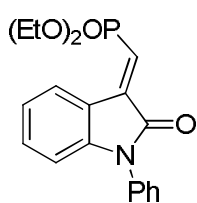
(*E*)-diethyl ((1-methyl-2-oxoindolin-3-ylidene)methyl)phosphonate, 233



233

Following the above general procedure¹, the single *E* diastereoisomer **233** was obtained as a pale orange solid in 66% yield after purification (*n*Hexane/EtOAc=1/1). ¹H-NMR (CDCl₃, 300 MHz, 25°C): δ 1.33 (t, *J* = 7.1 Hz, 3H, CH₃CH₂O), 1.34 (t, *J* = 7.1 Hz, 3H, CH₃CH₂O), 3.22 (s, 3H, CH₃N), 4.06–4.23 [m, 4H, (CH₃CH₂O)₂P], 6.78 (d, *J* = 7.6 Hz, 1H, CH_{arom}), 6.80 (d, *J*_{HP} = 13.4 Hz, 1H, CHP=O), 7.06 (dt, *J* = 7.6, 1.1 Hz, 1H, CH_{arom}), 7.36 (m, 1H, CH_{arom}), 8.45 (d, *J* = 7.6 Hz, 1H, CH_{arom}) ppm.

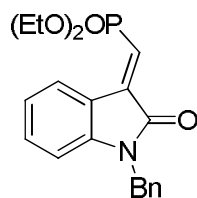
(*E*)-diethyl ((2-oxo-1-phenylindolin-3-ylidene)methyl)phosphonate, 234



234

Following the above general procedure¹, the single *E* diastereoisomer **234** was obtained as a pale orange solid in 76% yield after purification (*n*Hexane/EtOAc=1/1). ¹H-NMR (CDCl₃, 300 MHz, 25°C): δ 1.21 [t, *J* = 7.1 Hz, 6H, (CH₃CH₂O)₂P], 4.13–4.28 [m, 4H, (CH₃CH₂O)₂P], 6.78 (d, *J* = 7.9 Hz, 1H, CH_{arom}), 6.91 (d, *J*_{HP} = 13.1 Hz, 1H, CHP=O), 7.10 (dt, *J* = 7.7, 1.0 Hz, 1H, CH_{arom}), 7.24–7.33 (m, 1H, CH_{arom}), 7.37–7.46 (m, 3H, CH_{arom}), 7.49–7.58 (m, 2H, CH_{arom}), 8.55 (d, *J* = 7.7 Hz, 1H, ArH) ppm.

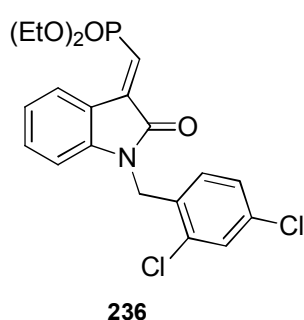
(*E*)-diethyl ((2-oxo-1-benzylindolin-3-ylidene)methyl)phosphonate, 235



235

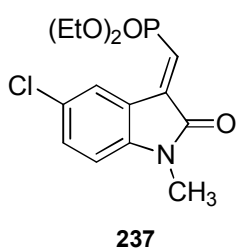
Following the above general procedure¹, the single *E* diastereoisomer **235** was obtained as a pale orange solid in 56% yield after purification (*n*Hexane/EtOAc=1/1). ¹H-NMR (CDCl₃, 300 MHz, 25°C): δ 1.36 [t, *J* = 7.0 Hz, 6H, (CH₃CH₂O)₂P], 4.07–4.26 [m, 4H, (CH₃CH₂O)₂P], 4.93 (s, 2H, CH₂N), 6.69 (d, *J* = 7.9 Hz, 1H, CH_{arom}), 6.88 (d, *J*_{HP} = 13.3 Hz, 1H, CHP=O), 7.04 (dt, *J* = 7.7, 0.96 Hz, 1H, CH_{arom}), 7.21–7.34 (m, 6H, CH_{arom}), 8.47 (d, *J* = 7.7 Hz, 1H, CH_{arom}) ppm.

(*E*)-diethyl ((1-(2,4-dichlorobenzyl)-2-oxoindolin-3-ylidene)methyl)phosphonate, 236



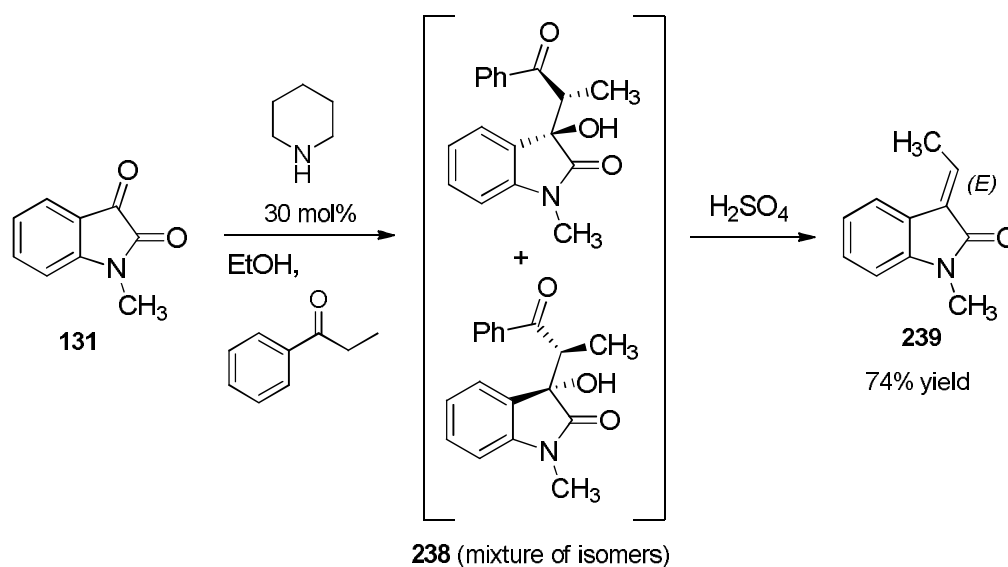
Following the above general procedure¹, the single *E* diastereoisomer **236** was obtained as a pale orange solid in 72% yield after purification (*n*Hexane/EtOAc=1/1). ¹H-NMR (CDCl₃, 300 MHz, 25°C): δ 1.37 [t, *J* = 7.1 Hz, 6H, (CH₃CH₂O)₂P], 4.10–4.27 [m, 4H, (CH₃CH₂O)₂P], 5.00 (s, 2H, CH₂N), 6.62 (d, *J* = 7.8 Hz, 1H, CH_{arom}), 6.89 (d, *J*_{HP} = 13.0 Hz, 1H, CHP=O), 7.01–7.18 (m, 4H, CH_{arom}), 7.23–7.32 (m, 1H, CH_{arom}), 8.51 (d, *J* = 7.6 Hz, 1H, CH_{arom}) ppm.

(*E*)-diethyl ((5-chloro-1-methyl-2-oxoindolin-3-ylidene)methyl)phosphonate, 237



Following the above general procedure, the single *E* diastereoisomer **237** was obtained as an orange amorphous solid in 30% yield after purification (*n*Hexane/EtOAc=6/4). IR (CHCl₃): $\tilde{\nu}$ = 1727, 1606 cm⁻¹. ¹H-NMR (CDCl₃, 300 MHz, 25°C): δ 1.34 [t, *J* = 7.0 Hz, 6H, (CH₃CH₂O)₂P], 3.20 (s, 3H, CH₃N), 4.12–4.21 [m, 4H, (CH₃CH₂O)₂P], 6.71 (d, *J* = 8.2 Hz, 1H, CH_{arom}), 6.85 (d, *J*_{HP} = 13.0 Hz, 1H, CHP=O), 7.31 (d, *J* = 8.2 Hz, 1H, CH_{arom}), 8.49 (s, 1H, CH_{arom}) ppm. ¹³CNMR (CDCl₃, 75 MHz, 25°C): δ 16.4 (CH₃), 26.5 (NCH₃), 62.7 (d, *J*_{CP} = 5.6 Hz, 2xCH₂), 109.2 (HC=C), 121.1 (d, *J*_{CP} = 7.0 Hz, C_{arom}), 121.4 (C_{arom}, d, *J*_{CP} = 189.5 Hz), 128.0 (C_{arom}), 128.5 (C_{arom}), 132.0 (C_{arom}), 140.5 (C_{arom}, d, *J*_{CP} = 4.9 Hz), 144.2 (C_{benz}), 166.2 [(C=O), d, *J*_{C-P} = 25.7 Hz] ppm. HRMS: exact mass calculated for (C₁₄H₁₇ClNNaO₄P) requires *m/z* 352.0627, found *m/z* 352.0631.

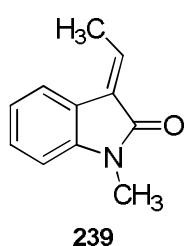
Procedure for preparing 3-ylideneoxindole **239**



In a round bottomed flask, isatine **131** (800 mg), phenyl ethyl ketone (0.7 mL), and a 30 mol% of piperidine (0.4 mL) were stirred in EtOH, at room temperature, for 24 hours. The solvent was evaporated *in vacuo*, then the crude was then treated with concentrated sulphuric acid (4 mL) and stirred for 10 minutes. The reaction mixture was slowly poured in cold water and extracted with DCM. The organic layers were dried over anhydrous Na₂SO₄ and concentrated under reduced pressure. Purification *via* flash chromatography yielded to the product **239** as a pale yellow solid.

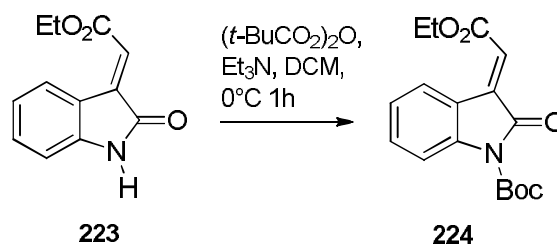
Characterization of 3-ylideneoxindole **239**

(*E*)-3-ethylidene-1-methylindol-2-one, **239**



Following the above procedure, the single *E* diastereoisomer **239** was obtained as an orange solid in 74% yield after purification (DCM/Et₂O = 95/5). ¹H-NMR (CDCl₃, 300 MHz, 25°C): δ 1.37 (t, *J* = 7.1 Hz, 3H, CH₃CH₂O); 4.31-4.36 (q, *J* = 7.1 Hz, 2H, CH₃CH₂O); 6.86-6.87 (m, 2H, CH=C, CH_{arom}); 7.04 (t, *J* = 7.7 Hz, 1H, CH_{arom}); 7.31 (t, *J* = 7.7 Hz, 1H, CH_{arom}); 8.53 (d, *J* = 7.8 Hz, 1H, CH_{arom}); 8.74 (bs, 1H, NH) ppm.²

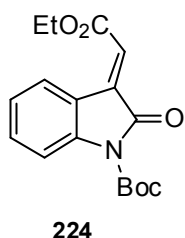
Procedure for preparing 3-ylideneoxindole 224



In a round bottomed flask, 262mg of Boc_2O were added drop by drop to a solution of 223 (217 mg, 1 mmol) and DMAP (12 mg, 0.1 mmol) in CH_3CN (10mL). The solution was stirred at room temperature overnight. The solvent was removed under reduced pressure and the crude was purified *via* flash chromatography, yielding 314 mg (0.99 mmol) of clean product as a yellow solid.

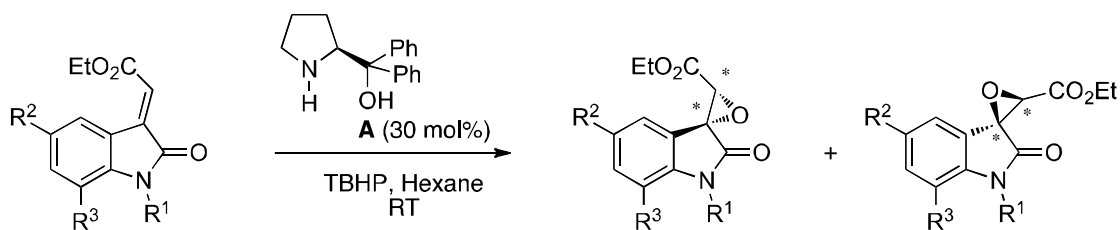
Characterization of 3-ylideneoxindole 224

(*E*)-tert-butyl 3-(2-ethoxy-2-oxoethylidene)-2-oxoindoline-1-carboxylate, 224



Following the above procedure, the single *E* diastereoisomer **224** was obtained as an orange solid in 99% yield after purification (*n*Hexane/EtOAc=9/1). IR (CHCl_3): $\tilde{\nu} = 2979, 1757, 1728, 1600, 1462, 1368, 1328, 1303 \text{ cm}^{-1}$. $^1\text{H-NMR}$ (CDCl_3 , 300 MHz, 25°C): δ 1.38 (t, $J = 7.2 \text{ Hz}$, 3H, $\text{CH}_3\text{CH}_2\text{O}$), 1.65 (s, 9H, $(\text{CH}_3)_3\text{C}$), 4.33 (q, $J = 7.2 \text{ Hz}$, 2H, OCH_2CH_3), 6.91 (s, 1H, $\text{CH}=\text{C}$), 7.17-7.31 (m, 2H, CH_{arom}), 7.41-7.45 (m, 1H, CH_{arom}), 8.67-8.69 (m, 1H, CH_{arom}). $^{13}\text{CNMR}$ (CDCl_3 , 75 MHz, 25°C): $\delta = 14.0$ (CH_3), 27.8 ($3 \times \text{CH}_3$), 61.0 (CH_2), 84.2 (CH_3C), 114.6 ($\text{HC}=\text{C}$), 119.7 (C_{arom}), 122.7 (C_{arom}), 124.2 (C_{arom}), 128.1 (C_{arom}), 132.4 (C_{arom}), 136.1 (C_{arom}), 141.5 (C_{arom}), 148.5 ($t\text{BuCOC}=\text{O}$), 164.9 ($\text{OC}=\text{O}$), 165.3 ($\text{NC}=\text{O}$) ppm.¹⁰⁷

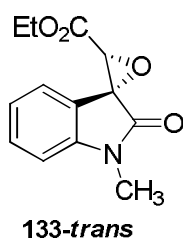
General procedure for the Asymmetric Epoxidation



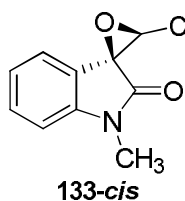
To a solution of the catalyst **A** (38 mg, 0.15 mmol) and *trans*-3-ylideneoxindoles (0.5 mmol) in *n*Hexane for HPLC grade (2.7 mL) was added TBHP (5.5 M in decane solution, 0.6 mmol, 0.11 mL) at room temperature (25°C). The resultant heterogeneous mixture was maintained under stirring until the reaction completion (TLC *n*Hexane/EtOAc). Afterwards, the crude reaction mixture was purified *via* flash chromatography on silica gel (*n*Hexane/EtOAc) to furnish the epoxy oxindoles *trans* and *cis*.

Characterization of epoxides 133, 182-193, 240-260

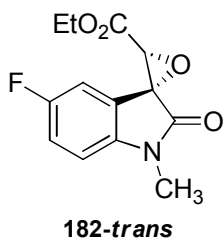
(2'*R*,3'*R*)-ethyl 1-methyl-2-oxospiro[indoline-3,2'-oxirane]-3'-carboxylate, 133-*trans*



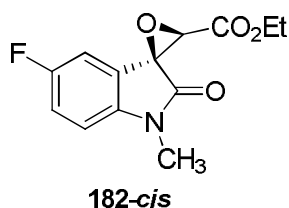
Following the above general procedure, *trans* diastereoisomer **133-*trans*** was obtained as a whitish solid in 61% yield after purification (*n*Hexane/EtOAc=7/3). IR (CHCl₃): $\tilde{\nu}$ = 3033, 3010, 2984, 1736, 1709, 1618, 1495, 1473, 1376, 1347 cm⁻¹. ¹H-NMR (CDCl₃, 300 MHz, 25°C): δ 1.26 (t, *J* = 7.2 Hz, 3H, CH₃CH₂O), 3.25 (s, 3H, CH₃N), 4.18 (s, 1H, OCH), 4.24 (dq, *J* = 10.9 Hz, 7.2 Hz, 1H, CH₃CHHO), 4.29 (dq, *J* = 10.9 Hz, 7.2 Hz, 1H, CH₃CHHO), 6.89 (ddd, *J* = 7.9 Hz, 0.9 Hz, 0.6 Hz, 1H, CH_{arom}), 7.04 (dt, *J* = 7.7 Hz, 0.9 Hz, 1H, CH_{arom}), 7.39 (dt, *J* = 7.9 Hz, 1.3 Hz, 1H, CH_{arom}), 7.45 (ddd, *J* = 7.7 Hz, 1.3 Hz, 0.6 Hz, 1H, CH_{arom}) ppm. ¹³C-NMR (CDCl₃, 75 MHz, 25°C): δ 14.3 (CH₃), 27.0 (NCH₃), 60.0 (CH₂), 60.3 (CO), 62.4 (OCH), 109.1 (C_{arom}), 119.5 (C_{arom}), 123.3 (C_{arom}), 125.0 (C_{arom}), 131.3 (C_{arom}), 145.9 (C_{arom}), 165.9, 170.1 (C=O) ppm. HRMS: exact mass calculated for (C₁₃H₁₃NNaO₄) requires *m/z* 270.0742, found *m/z* 270.0741. Chiral-phase HPLC analysis: [Daiacel Chiralpack IC 5 μ , λ =254 nm, *n*Hexane/EtOH=7/3, flow rate 1.0mL/min]: *T*_{major} = 11.91 min, *T*_{minor} = 14.97 min *ee* = 82%. [α]_D = -93 (*c* = 1.6 g/cm³ in CH₂Cl₂).

(2'S,3'R)-ethyl 1-methyl-2-oxospiro[indoline-3,2'-oxirane]-3'-carboxylate, 133-cis

Following the above general procedure, *cis* diastereoisomer **133-cis** was obtained as a pale yellow solid in 34% yield after purification (*n*Hexane/EtOAc=7/3). IR (CHCl₃): $\tilde{\nu}$ = 3034, 3010, 2933, 1759, 1733, 1621, 1472, 1375, 1345 cm⁻¹. ¹H NMR (CDCl₃, 300 MHz, 25°C): δ 1.35 (t, *J* = 7.2 Hz, 3H, CH₃CH₂O), 3.22 (s, 3H, CH₃N), 4.15 (s, 1H, OCH), 4.34 (q, *J* = 7.2 Hz, 2H, CH₃CH₂O), 6.89 (dd, *J* = 7.8 Hz, 0.5 Hz, 1H, CH_{arom}), 7.04-7.14 (m, 2H, CH_{arom}), 7.40 (ddd, *J* = 7.9 Hz, 6.2 Hz, 2.8 Hz, 1H, CH_{arom}) ppm. ¹³C NMR (CDCl₃, 75 MHz, 25°C): δ 14.3 (CH₃), 26.9 (NCH₃), 60.3 (CH₂), 60.4 (CO), 62.3 (OCH), 109.2 (C_{arom}), 121.4 (C_{arom}), 122.6 (C_{arom}), 123.2 (C_{arom}), 131.4 (C_{arom}), 145.5 (C_{arom}), 165.0, 169.0 (C=O) ppm. HRMS: exact mass calculated for (C₁₃H₁₃NNaO₄) requires *m/z* 270.0742, found *m/z* 270.0739. Chiral-phase HPLC analysis: [Daiacel Chiralpack IC 5 μ , λ =254 nm, *n*Hexane/EtOH=7/3, flow rate 1.0mL/min]: *T*_{major} = 14.60 min, *T*_{minor} = 19.82 min, *ee* = 19%. [α]_D = -105 (*c* = 0.035 g/cm³ in CHCl₃).

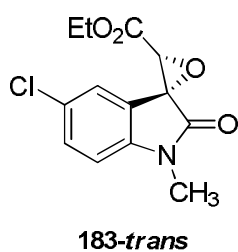
(2'R,3'R)-ethyl 5-fluoro-1-methyl-2-oxospiro[indoline-3,2'-oxirane]-3'-carboxylate, 182-trans

Following the above general procedure, *trans* diastereoisomer **182-trans** was obtained as a whitish solid in 36% yield after purification (*n*Hexane/EtOAc=8/2). IR (CHCl₃): $\tilde{\nu}$ = 3032, 3009, 2952, 2925, 1756, 1735, 1612, 1579, 1461, 1367, 1338 cm⁻¹. ¹H-NMR (CDCl₃, 300 MHz, 25°C): δ 1.29 (t, *J* = 7.1 Hz, 3H, CH₃CH₂O), 3.25 (s, 3H, CH₃N), 4.19 (s, 1H, OCH), 4.22-4.36 (m, 2H, CH₃CH₂O), 6.82 (dd, *J* = 8.6 Hz, 4.4 Hz, 1H, CH_{arom}), 7.10 (dt, *J* = 8.6 Hz, 2.7 Hz, 1H, CH_{arom}), 7.26 (dd, *J* = 8.6 Hz, 2.7 Hz, 1H, CH_{arom}) ppm. ¹³C-NMR (CDCl₃, 75 MHz, 25°C): δ 14.3 (CH₃), 27.1 (NCH₃), 60.0 (CH₂), 60.2 (CO), 62.6 (OCH), 109.6 (d, *J*_{CF} = 8 Hz, CH_{arom}), 113.5 (d, *J*_{CF} = 27 Hz, CH_{arom}), 117.7 (d, *J*_{CF} = 24 Hz, CH_{arom}), 121.2 (d, *J*_{CF} = 9 Hz, CH_{arom}), 141.9 (d, *J*_{CF} = 2 Hz, CH_{arom}), 159.5 (d, *J*_{CF} = 242 Hz, CH_{arom}), 165.6, 169.9 (C=O) ppm. HRMS: exact mass calculated for (C₁₃H₁₂FNNaO₄) requires *m/z* 288.0648, found *m/z* 288.0647. Chiral-phase HPLC analysis: [Daiacel Chiralpack IC 5 μ , λ =254 nm, *n*Hexane/EtOH=7/3, flow rate 1.0mL/min]: *T*_{major} = 12.10 min, *T*_{minor} = 9.10 min *ee* = 84%. [α]_D = -211 (*c* = 0.0052 g/cm³ in CHCl₃).

(2'*S*,3'*R*)-ethyl 5-fluoro-1-methyl-2-oxospiro[indoline-3,2'-oxirane]-3'-carboxylate, 182-*cis*

Following the above general procedure, *cis* diastereoisomer **182-*cis*** was obtained as a pale yellow solid in 39% yield after purification (*n*Hexane/EtOAc=8/2). IR (CHCl₃): $\tilde{\nu}$ = 3030, 3010, 2985, 1764, 1735, 1613, 1581, 1461, 1367, 1333 cm⁻¹.

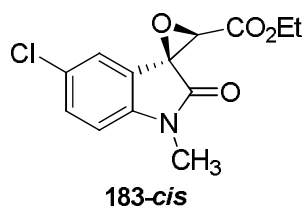
¹H-NMR (CDCl₃, 300 MHz, 25°C): δ 1.35 (t, *J* = 7.1 Hz, 3H, CH₃CH₂O), 3.22 (s, 3H, CH₃N), 4.13 (s, 1H, OCH), 4.34 (q, *J* = 7.1 Hz, 2H, CH₃CH₂O), 6.80 (m, 2H, CH_{arom}), 7.10 (dt, *J* = 8.8 Hz, 2.6 Hz, 1H, CH_{arom}) ppm. ¹³C-NMR (CDCl₃, 75 MHz, 25°C): δ 14.3 (CH₃), 27.0 (NCH₃), 60.0 (CO), 60.4 (CH₂), 62.4 (OCH), 109.9 (d, *J*_{CF} = 8 Hz, CH_{arom}), 110.8 (d, *J*_{CF} = 26 Hz, CH_{arom}), 117.8 (d, *J*_{CF} = 23 Hz, CH_{arom}), 123.0 (d, *J*_{CF} = 9 Hz, CH_{arom}), 141.4 (C_{arom}), 159.5 (d, *J*_{CF} = 243 Hz, CH_{arom}), 164.6, 168.7 (C=O) ppm. HRMS: exact mass calculated for (C₁₃H₁₂FNNaO₄) requires *m/z* 288.0648, found *m/z* 288.0650. Chiral-phase HPLC analysis: [Daiacel Chiralpack IC 5 μ , λ =254 nm, *n*Hexane/EtOH=7/3, flow rate 1.0mL/min]: *T*_{major} = 14.15 min, *T*_{minor} = 15.85 min, *ee* = 30%. [α]_D = -131 (*c* = 0.0084 g/cm³ in CHCl₃).

(2'*R*,3'*R*)-ethyl 5-chloro-1-methyl-2-oxospiro[indoline-3,2'-oxirane]-3'-carboxylate, 183-*trans*

Following the above general procedure, *trans* diastereoisomer **183-*trans*** was obtained as a whitish solid in 37% yield after purification (*n*Hexane/EtOAc=85/15). IR (CHCl₃): $\tilde{\nu}$ = 3033, 3006, 2980, 1754, 1751, 1615, 1496, 1466, 1440 cm⁻¹. ¹H-NMR (CDCl₃, 300 MHz, 25°C): δ 1.30 (t, *J* = 7.1 Hz, 3H, CH₃CH₂O),

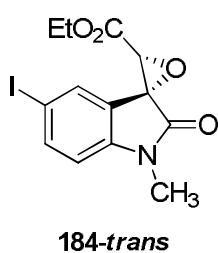
3.25 (s, 3H, CH₃N), 4.18 (s, 1H, OCH), 4.22-4.43 (m, 2H, CH₃CH₂O), 6.83 (d, *J* = 8.4 Hz, 1H, CH_{arom}), 7.37 (dd, *J* = 8.4 Hz, 2.2 Hz, 1H, CH_{arom}), 7.47 (d, *J* = 2.2 Hz, 1H, CH_{arom}) ppm. ¹³C-NMR (CDCl₃, 75 MHz, 25°C): δ 14.3 (CH₃), 27.0 (NCH₃), 59.9 (CH₂), 60.0 (CO), 62.6 (OCH), 110.0 (C_{arom}), 121.2 (C_{arom}), 125.5 (C_{arom}), 128.9 (C_{arom}), 131.1 (C_{arom}), 144.4 (C_{arom}), 165.5, 169.6 (C=O) ppm. HRMS: exact mass calculated for (C₁₃H₁₂ClNNaO₄) requires *m/z* 304.0353, found *m/z* 304.0355. Chiral-phase HPLC analysis: [Daiacel Chiralpack IC 5 μ , λ =254 nm, *n*Hexane/EtOH=7/3, flow rate 1.0mL/min]: *T*_{major} = 12.97 min, *T*_{minor} = 9.68 min *ee* = 76%. [α]_D = -62 (*c* = 0.0091 g/cm³ in CHCl₃).

(2'*S*,3'*R*)-ethyl 5-chloro-1-methyl-2-oxospiro[indoline-3,2'-oxirane]-3'-carboxylate, 183-*cis*



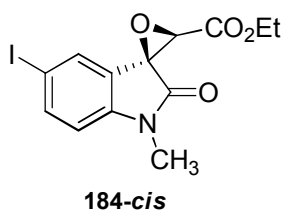
Following the above general procedure, *cis* diastereoisomer **183-*cis*** was obtained as a pale yellow solid in 55% yield after purification (*n*Hexane/EtOAc=7/3). IR (CHCl₃): $\tilde{\nu}$ = 3032, 3009, 2331, 1758, 1735, 1618, 1495, 1466, 1359, 1343 cm⁻¹. ¹H-NMR (CDCl₃, 300 MHz, 25°C): δ 1.35 (t, *J* = 7.2 Hz, 3H, CH₃CH₂O), 3.22 (s, 3H, CH₃N), 4.13 (s, 1H, OCH), 4.34 (q, *J* = 7.2 Hz, 2H, CH₃CH₂O), 6.82 (d, *J* = 8.3 Hz, 1H, CH_{arom}), 7.07 (d, *J* = 2.1 Hz, 1H, CH_{arom}), 7.37 (dd, *J* = 8.3 Hz, 2.1 Hz, 1H, CH_{arom}) ppm. ¹³C NMR (CDCl₃, 75 MHz, 25°C): δ 14.3 (CH₃), 27.0 (NCH₃), 59.9 (CO), 60.4 (CH₂), 62.4 (OCH), 110.2 (C_{arom}), 123.0 (C_{arom}), 123.1 (C_{arom}), 128.9 (C_{arom}), 131.3 (C_{arom}), 143.9 (C_{arom}), 164.5, 168.6 (C=O) ppm. HRMS: exact mass calculated for (C₁₃H₁₂ClNNaO₄) requires *m/z* 304.0353, found *m/z* 304.0352. Chiral-phase HPLC analysis: [Daiacel Chiralpack IC 5 μ , λ =254 nm, *n*Hexane/EtOH=7/3, flow rate 1.0mL/min]: *T*_{major} = 14.46 min, *T*_{minor} = 17.91 min, *ee* = 42%. [α]_D = -61 (*c* = 0.0070 g/cm³ in CHCl₃).

(2'*R*,3'*R*)-ethyl 5-iodo-1-methyl-2-oxospiro[indoline-3,2'-oxirane]-3'-carboxylate 184-*trans*



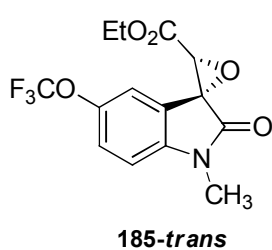
Following the above general procedure, *trans* diastereoisomer **184-*trans*** was obtained as a pale yellow solid in 32% yield after purification (*n*Hexane/EtOAc=7/3). IR (CHCl₃): $\tilde{\nu}$ = 3028, 3017, 3008, 1736, 1727, 1611, 1535, 1486, 1358, 1340 cm⁻¹. ¹H-NMR (CDCl₃, 300 MHz, 25°C): 1.33 (t, *J* = 7.1 Hz, 3H, CH₃CH₂O); 3.24 (s, 3H, NCH₃); 3.94-4.41 (m, 3H, CH₃CH₂O, OCH); 6.69 (t, *J* = 8.2 Hz, 1H, CH_{arom}); 6.68-6.78 (m, 2H, CH_{arom}) ppm. ¹³CNMR (CDCl₃, 75 MHz, 25°C): 14.3 (CH₃), 27.0 (NCH₃), 59.6 (CO), 60.0 (CH₂), 62.6 (OCH), 85.6 (C_{arom}), 111.0 (C_{arom}), 121.7 (C_{arom}), 133.6 (C_{arom}), 140.0 (C_{arom}), 145.4 (C_{arom}), 165.5, 169.3 (C=O) ppm. HRMS: exact mass calculated for (C₁₃H₁₂INNaO₄) requires *m/z* 395.9709, found *m/z* 395.9712. Chiral-phase HPLC analysis: [Daiacel Chiralpack IC 5 μ , λ =254 nm, *n*Hexane/EtOH=70/30, flow rate 1.0mL/min]: *T*_{major} = 13.04 min, *T*_{minor} = 10.19 min *ee* = 61%. [α]_D = -9 (*c* = 0.0140 g/cm³ in CHCl₃)

(2'S,3'R)-ethyl 5-iodo-1-methyl-2-oxospiro[indoline-3,2'-oxirane]-3'-carboxylate
184-cis

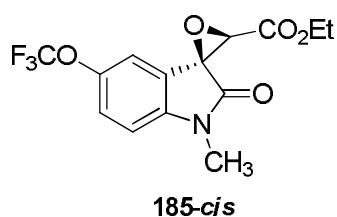


Following the above general procedure, *cis* diastereoisomer **184-cis** was obtained as a pale yellow solid in 32% yield after purification (*n*Hexane/EtOAc=7/3). IR (CHCl₃): $\tilde{\nu}$ = 3025, 3017, 3008, 1753, 1736, 1611, 1486, 1465, 1430, 1340 cm⁻¹. ¹H-NMR (CDCl₃, 300 MHz, 25°C): 1.35 (t, *J* = 7.1 Hz, 3H, CH₃CH₂O); 3.21 (s, 3H, NCH₃); 4.14 (s, 1H, OCH); 4.35 (dq, *J* = 9.8 Hz, 7.1 Hz, 1H, CH₃CHHO); 4.38 (dq, *J* = 9.8 Hz, 7.1 Hz, 1H, CH₃CHHO); 6.69 (d, *J* = 8.2 Hz, 1H, CH_{arom}); 7.37 (s, 1H, CH_{arom}); 7.71 (dd, *J* = 8.2 Hz, 1.5 Hz, 1H, CH_{arom}) ppm. ¹³C-NMR (CDCl₃, 75 MHz, 25°C): 14.3 (CH₃), 27.0 (NCH₃), 59.6 (CO), 60.0 (CH₂), 62.6 (OCH), 85.6 (C_{arom}), 111.0 (C_{arom}), 121.7 (C_{arom}), 133.6 (C_{arom}), 140.0 (C_{arom}), 145.4 (C_{arom}), 165.5, 169.3 (C=O) ppm. HRMS: exact mass calculated for (C₁₃H₁₂INNaO₄) requires *m/z* 395.9709, found *m/z* 395.9712. Chiral-phase HPLC analysis: [Daiacel Chiralpack IC 5μ, λ=254 nm, *n*Hexane/EtOH=70/30, flow rate 1.0mL/min]: *T*_{major} = 14.94 min, *T*_{minor} = 19.58 min *ee* = 61%. [α]_D = -9 (*c* = 0.0140 g/cm³ in CHCl₃)

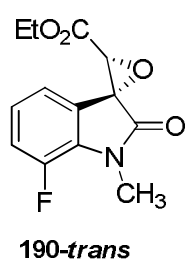
(2'R,3'R)-ethyl 1-methyl-2-oxo-5-(trifluoromethoxy)spiro[indoline-3,2'-oxirane]-3'-carboxylate, 185-trans



Following the above general procedure, *trans* diastereoisomer **185-trans** was obtained as a whitish solid in 28% yield after purification (*n*Hexane/EtOAc=7/3). IR (CHCl₃): $\tilde{\nu}$ = 3038, 3010, 2986, 1757, 1739, 1626, 1492, 1470, 1369, 1348 cm⁻¹. ¹H-NMR (CDCl₃, 300 MHz, 25°C): δ 1.28 (t, *J* = 7.1 Hz, 3H, CH₃CH₂O), 3.27 (s, 3H, CH₃N), 4.20 (s, 1H, OCH), 4.27 (q, *J* = 7.1 Hz, 2H, CH₃CH₂O), 6.89 (d, *J* = 8.5 Hz, 1H, CH_{arom}), 7.19-7.33 (m, 1H, CH_{arom}), 7.40 (s, 1H, CH_{arom}) ppm. ¹³C-NMR (CDCl₃, 75 MHz, 25°C): δ 14.3 (CH₃), 27.1 (NCH₃), 59.9 (CO), 60.1 (CH₂), 62.7 (OCH), 109.6 (C_{arom}), 119.3 (C_{arom}), 120.7 [(OCF₃), q, *J*_{CF} = 277.4 Hz], 121.1 (C_{arom}), 124.5 (C_{arom}), 144.5 (C_{arom}), 145.2 (C_{arom}), 165.5, 169.9 (C=O) ppm. HRMS: exact mass calculated for (C₁₄H₁₂F₃NNaO₅) requires *m/z* 354.0565, found *m/z* 354.0566. Chiral-phase HPLC analysis: [Daiacel Chiralpack IC 5μ, λ=254 nm, *n*Hexane/EtOH=7/3, flow rate 1.0mL/min]: *T*_{major} = 7.73 min, *T*_{minor} = 6.05 min *ee* = 78%. [α]_D = -171 (*c* = 0.0033 g/cm³ in CHCl₃)

(2'S,3'R)-ethyl 1-methyl-2-oxo-5-(trifluoromethoxy)spiro[indoline-3,2'-oxirane]-3'-carboxylate, 185-cis

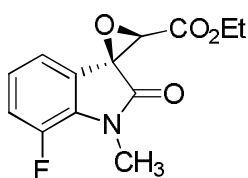
Following the above general procedure, *cis* diastereoisomer **185-cis** was obtained as a pale yellow solid in 42% yield after purification (*n*Hexane/EtOAc=7/3). IR (CHCl₃): $\tilde{\nu}$ = 3030, 3009, 2983, 1761, 1735, 1628, 1495, 1469, 1372, 1349 cm⁻¹. ¹H NMR (CDCl₃, 300 MHz, 25°C): δ 1.35 (t, *J* = 7.1 Hz, 3H, CH₃CH₂O), 3.24 (s, 3H, CH₃N), 4.15 (s, 1H, OCH), 4.34 (q, *J* = 7.1 Hz, 2H, CH₃CH₂O), 6.89 (d, *J* = 8.4 Hz, 1H, CH_{arom}), 6.99 (s, 3H, CH_{arom}), 7.19 -7.36 (m, 1H, CH_{arom}) ppm. ¹³C-NMR (CDCl₃, 75 MHz, 25°C): δ 14.3 (CH₃), 27.1 (NCH₃), 59.9 (CO), 60.5 (CH₂), 62.4 (OCH), 109.9 (C_{arom}), 116.6 (C_{arom}), 120.7 [(OCF₃), q, *J*_{CF} = 257.5 Hz], 123.0 (C_{arom}), 124.5 (C_{arom}), 144.1 (C_{arom}), 145.3 (C_{arom}), 164.4, 168.8 (C=O) ppm. HRMS: exact mass calculated for (C₁₄H₁₂F₃NNaO₅) requires *m/z* 354.0565, found *m/z* 354.0563. Chiral-phase HPLC analysis: [Daiacel Chiralpack IC 5 μ , λ =254 nm, *n*Hexane/EtOH=7/3, flow rate 1.0mL/min]: *T*_{major} = 7.43 min, *T*_{minor} = 8.53 min, *ee* = 30%. [α]_D = -101 (*c* = 0.0056 g/cm³ in CHCl₃).

(2'R,3'R)-ethyl 7-fluoro-1-methyl-2-oxospiro[indoline-3,2'-oxirane]-3'-carboxylate, 190-trans

Following the above general procedure, *trans* diastereoisomer **190-trans** was obtained as a whitish solid in 29% yield after purification (*n*Hexane/EtOAc=8/2). IR (CHCl₃): $\tilde{\nu}$ = 3042, 3016, 2987, 1743, 1703, 1636, 1601, 1493, 1479, 1373, 1341, 1226 cm⁻¹. ¹H NMR (CDCl₃, 300 MHz, 25°C): δ 1.35 (t, *J* = 7.2 Hz, 3H, CH₃CH₂O), 3.43 (d, *J*_{HF} = 2.7 Hz, 3H, CH₃N), 4.13 (s, 1H, OCH), 4.34 (q, *J* = 7.2 Hz, 2H, CH₃CH₂O), 6.88 (dd, *J* = 7.3 Hz, 1.1 Hz, 1H, CH_{arom}), 6.97-7.21 (m, 2H, CH_{arom}) ppm. ¹³C-NMR (CDCl₃, 75 MHz, 25°C): δ 14.3 (CH₃), 29.7 (NCH₃, d, *J*_{CF} = 5.9 Hz), 60.1 (CO), 60.3 (CH₂), 62.5 (OCH), 119.4 [(C_{arom}), d, *J*_{CF} = 19.1 Hz], 120.9 [(C_{arom}), d, *J*_{CF} = 3.4 Hz], 122.5 [(C_{arom}), d, *J*_{CF} = 3.4 Hz], 124.0 [(C_{arom}), d, *J*_{CF} = 6.4 Hz], 132.4 [(C_{arom}), d, *J*_{CF} = 8.9 Hz], 148.3 [(C_{arom}), d, *J*_{CF} = 244.4 Hz], 165.5, 169.9 (C=O) ppm. HRMS: exact mass calculated for (C₁₃H₁₃FNNaO₄) requires *m/z* 288.0648, found *m/z* 288.0646. Chiral-phase HPLC analysis: [Daiacel Chiralpack IC 5 μ , λ =254 nm,

*n*Hexane/EtOH=7/3, flow rate 1.0mL/min]: $T_{major} = 11.67$ min, $T_{minor} = 10.47$ min $ee = 80\%$. $[\alpha]_D = -60$ ($c = 0.0230$ g/cm³ in CHCl₃).

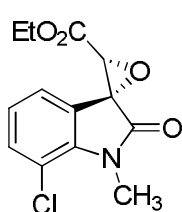
(2'S,3'R)-ethyl 7-fluoro-1-methyl-2-oxospiro[indoline-3,2'-oxirane]-3'-carboxylate, 190-*cis*



190-*cis*

Following the above general procedure, *cis* diastereoisomer **190-*cis*** was obtained as a pale yellow solid in 56% yield after purification (*n*Hexane/EtOAc=8/2). IR (CHCl₃): $\tilde{\nu} = 3033, 3004, 2985, 1759, 1738, 1636, 1604, 1484, 1372, 1338$ cm⁻¹. ¹H NMR (CDCl₃, 300 MHz, 25°C): δ 1.35 (t, $J = 7.1$ Hz, 3H, CH₃CH₂O), 3.43 (d, $J_{HF} = 7.3$ Hz, 3H, CH₃N), 4.13 (s, 1H, OCH), 4.34 (q, $J = 7.2$ Hz, 2H, CH₃CH₂O), 6.82-7.21 (m, 3H, CH_{arom}) ppm. ¹³C NMR (CDCl₃, 75 MHz, 25°C): δ 14.2 (CH₃), 29.4 (NCH₃, d, $J_{CF} = 5.6$ Hz), 59.9 (CO), 60.6 (CH₂), 62.3 (OCH), 118.3 [(C_{arom}), d, $J_{CF} = 3.4$ Hz], 119.4 [(C_{arom}), d, $J_{CF} = 19.4$ Hz], 123.9 [(C_{arom}), d, $J_{CF} = 6.3$ Hz], 124.3 [(C_{arom}), d, $J_{CF} = 3.6$ Hz], 131.8 (C_{arom}), 148.1 [(C_{arom}), d, $J_{CF} = 245.2$ Hz], 164.5, 168.7 (C=O) ppm. HRMS: exact mass calculated for (C₁₃H₁₂FNNaO₄) requires m/z 288.0648, found m/z 288.0645. Chiral-phase HPLC analysis: [Daiacel Chiralpack IC 5 μ , $\lambda=254$ nm, *n*Hexane/EtOH=7/3, flow rate 1.0mL/min]: $T_{major} = 11.83$ min, $T_{minor} = 14.18$ min, $ee = 32\%$. $[\alpha]_D = -18$ ($c = 0.0610$ g/cm³ in CHCl₃).

(2'R,3'R)-ethyl 7-chloro-1-methyl-2-oxospiro[indoline-3,2'-oxirane]-3'-carboxylate, 191-*trans*

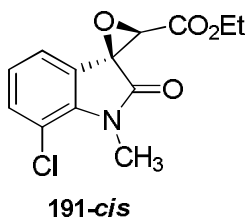


191-*trans*

Following the above general procedure, *trans* diastereoisomer **191-*trans*** was obtained as a whitish solid in 22% yield after purification (*n*Hexane/EtOAc=8/2). IR (CHCl₃): $\tilde{\nu} = 3029, 3002, 2989, 1755, 1738, 1613, 1464, 1359, 1338, 1250$ cm⁻¹. ¹H-NMR (CDCl₃, 300 MHz, 25°C): δ 1.26 (t, $J = 7.1$ Hz, 3H, CH₃CH₂O), 3.63 (s, 3H, CH₃N), 4.15-4.38 (m, 2H, CH₃CH₂O), 4.19 (s, 1H, OCH), 6.95 (t, $J = 7.7$ Hz, 1H, CH_{arom}), 7.30 (d, $J = 7.7$ Hz, 1H, CH_{arom}), 7.34 (d, $J = 7.7$ Hz, 1H, CH_{arom}), ppm. ¹³C-NMR (CDCl₃, 75 MHz, 25°C): δ 14.3 (CH₃), 30.5 (NCH₃), 59.7 (CO), 60.6 (CH₂), 62.5 (OCH), 116.7 (C_{arom}), 122.5 (C_{arom}), 123.4 (C_{arom}), 124.0 (C_{arom}), 133.6 (C_{arom}), 141.5 (C_{arom}), 165.4, 170.5 (C=O) ppm. HRMS: exact mass calculated for (C₁₃H₁₂ClNNaO₄) requires m/z 304.0353, found m/z 304.0352. Chiral-phase HPLC analysis: [Daiacel

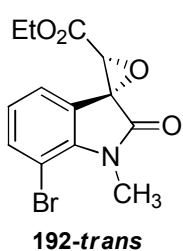
Chiralpack IC 5 μ , λ =254 nm, *n*Hexane/EtOH=7/3, flow rate 1.0mL/min]: T_{major} = 12.63 min, T_{minor} = 11.17 min *ee* = 82%. $[\alpha]_D = -200$ ($c = 0.0198$ g/cm³ in CHCl₃)

(2'*S*,3'*R*)-ethyl 7-chloro-1-methyl-2-oxospiro[indoline-3,2'-oxirane]-3'-carboxylate, 191-*cis*



Following the above general procedure, *cis* diastereoisomer **191-*cis*** was obtained as a pale yellow solid in 66% yield after purification (*n*Hexane/EtOAc=8/2). IR (CHCl₃): $\tilde{\nu} = 3043, 3012, 2974, 1759, 1730, 1618, 1589, 1467, 1369, 1336, 1261$ cm⁻¹. ¹H NMR (CDCl₃, 300 MHz, 25°C): δ 1.35 (t, $J = 7.2$ Hz, 3H, CH₃CH₂O), 3.59 (s, 3H, CH₃N), 4.11 (s, 1H, OCH), 4.34 (q, $J = 7.2$ Hz, 2H, CH₃CH₂O), 6.92-7.11 (m, 2H, CH_{arom}), 7.32 (dd, $J = 7.5$ Hz, 1.8 Hz, 1H, CH_{arom}) ppm. ¹³C NMR (CDCl₃, 75 MHz, 25°C): δ 14.1 (CH₃), 30.1 (NCH₃), 59.4 (CO), 60.7 (CH₂), 62.2 (OCH), 116.6 (C_{arom}), 120.9 (C_{arom}), 124.1 (C_{arom}), 133.4 (C_{arom}), 141.0 (C_{arom}), 164.3, 169.2 (C=O) ppm. HRMS: exact mass calculated for (C₁₃H₁₂CINNaO₄) requires m/z 304.0353, found m/z 304.0355. Chiral-phase HPLC analysis: [Daiacel Chiralpack IC 5 μ , λ =254 nm, *n*Hexane/EtOH=7/3, flow rate 1.0mL/min]: T_{major} = 13.28 min, T_{minor} = 14.08 min, *ee* = 32%. $[\alpha]_D = -116$ ($c = 0.0140$ g/cm³ in CHCl₃).

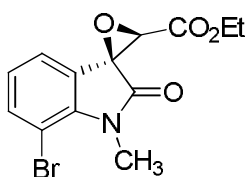
(2'*R*,3'*R*)-ethyl 7-bromo-1-methyl-2-oxospiro[indoline-3,2'-oxirane]-3'-carboxylate, 192-*trans*



Following the above general procedure, *trans* diastereoisomer **192-*trans*** was obtained as a whitish solid in 21% yield after purification (*n*Hexane/EtOAc=9/1). IR (CHCl₃): $\tilde{\nu} = 3032, 3009, 2951, 2925, 1756, 1735, 1612, 1578, 1461, 1367, 1338$ cm⁻¹. ¹H-NMR (CDCl₃, 300 MHz, 25°C): δ 1.26 (t, $J = 7.2$ Hz, 3H, CH₃CH₂O), 3.64 (s, 3H, CH₃N), 4.15□4.40 (m, 2H, CH₃CH₂O), 4.19 (s, 1H, OCH), 6.88 (t, $J = 7.6$ Hz, 1H, CH_{arom}), 7.39 (d, $J = 7.6$ Hz, 1H, CH_{arom}), 7.48 (d, $J = 7.6$ Hz, 1H, CH_{arom}) ppm. ¹³C-NMR (CDCl₃, 75 MHz, 25°C): δ 14.3 (CH₃), 30.7 (NCH₃), 59.7 (CO), 60.7 (CH₂), 62.5 (OCH), 103.4 (C_{arom}), 122.8 (C_{arom}), 123.9 (C_{arom}), 124.4 (C_{arom}), 136.9 (C_{arom}), 143.0 (C_{arom}), 165.4, 170.8 (C=O) ppm. HRMS: exact mass calculated for (C₁₃H₁₂BrNNaO₄) requires m/z 347.9847, found m/z 347.9846. Chiral-phase HPLC analysis: [Daiacel

Chiralpack IC 5 μ , λ =254 nm, *n*Hexane/EtOH=7/3, flow rate 1.0mL/min]: T_{major} = 12.08 min, T_{minor} = 10.57 min *ee* = 88%. $[\alpha]_D = -200$ ($c = 0.0119$ g/cm³ in CHCl₃)

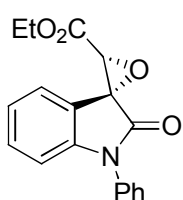
(2'*S*,3'*R*)-ethyl 7-bromo-1-methyl-2-oxospiro[indoline-3,2'-oxirane]-3'-carboxylate, 192-*cis*



192-*cis*

Following the above general procedure, *cis* diastereoisomer **192-*cis*** was obtained as a pale yellow solid in 50% yield after purification (*n*Hexane/EtOAc=9/1). IR (CHCl₃): $\tilde{\nu} = 3030, 3008, 2985, 1764, 1735, 1612, 1581, 1461, 1367, 1333$ cm⁻¹. ¹H NMR (CDCl₃, 300 MHz, 25°C): δ 1.34 (t, $J = 7.1$ Hz, 3H, CH₃CH₂O), 3.60 (s, 3H, CH₃N), 4.11 (s, 1H, OCH), 4.33 (q, $J = 7.1$ Hz, 2H, CH₃CH₂O), 6.88-7.03 (m, 2H, CH_{arom}), 7.49 (dd, $J = 8.0$ Hz, 1.3 Hz, 1H, CH_{arom}), ppm. ¹³C NMR (CDCl₃, 75 MHz, 25°C): δ 14.3 (CH₃), 30.4 (NCH₃), 59.6 (CO), 60.9 (CH₂), 62.4 (OCH), 103.6 (C_{arom}), 121.5 (C_{arom}), 124.3 (C_{arom}), 124.6 (C_{arom}), 137.0 (C_{arom}), 142.7 (C_{arom}), 164.5, 169.5 (C=O) ppm. HRMS: exact mass calculated for (C₁₃H₁₂BrNNaO₄) requires m/z 347.9847, found m/z 347.9844. Chiral-phase HPLC analysis: [Daiacel Chiralpack IC 5 μ , λ =254 nm, *n*Hexane/EtOH=7/3, flow rate 1.0mL/min]: T_{major} = 14.35 min, T_{minor} = 16.40 min, *ee* = 58%. $[\alpha]_D = -92$ ($c = 0.0043$ g/cm³ in CHCl₃).

(2'*R*,3'*R*)-ethyl 1-phenyl-2-oxospiro[indoline-3,2'-oxirane]-3'-carboxylate, 240-*trans*

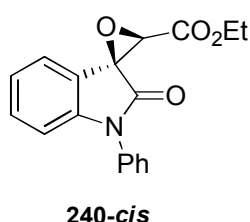


240-*trans*

Following the above general procedure, *trans* diastereoisomer **240-*trans*** was obtained as a whitish solid in 43% yield after purification (*n*Hexane/EtOAc=8/2). IR (CHCl₃): $\tilde{\nu} = 3034, 3010, 2981, 1742, 1732, 1619, 1598, 1508, 1468, 1376$ cm⁻¹. ¹H NMR (CDCl₃, 300 MHz, 25°C): δ 1.31 (t, $J = 7.1$ Hz, 3H, CH₃CH₂O), 4.22-4.42 (m, 2H, CH₃CH₂O), 4.28 (s, 1H, OCH), 6.87 (dd, $J = 8.0$ Hz, 0.6 Hz, 1H, CH_{arom}), 7.05 (dt, $J = 7.6$ Hz, 1.0 Hz, 1H, CH_{arom}), 7.31 (dt, $J = 7.9$ Hz, 1.3 Hz, 1H, CH_{arom}), 7.28-7.31 (m, 3H, CH_{arom}), 7.48-7.59 (m, 3H, CH_{arom}) ppm. ¹³C NMR (CDCl₃, 75 MHz, 25°C): δ 14.4 (CH₃), 60.5 (CH₂, CO), 62.5 (OCH), 110.5 (C_{arom}), 119.4 (C_{arom}), 123.8 (C_{arom}), 125.3 (C_{arom}), 126.7 (C_{arom}), 128.8 (C_{arom}), 130.0 (C_{arom}), 131.2 (C_{arom}), 134.0 (C_{arom}), 146.0 (C_{arom}), 165.8, 169.5 (C=O) ppm. HRMS: exact mass calculated for (C₁₈H₁₅NNaO₄)

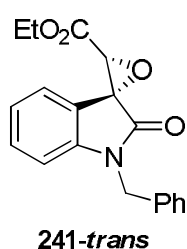
requires m/z 332.0899, found m/z 332.0897. Chiral-phase HPLC analysis: [Daiacel Chiralpack IC 5 μ , λ =254 nm, n Hexane/EtOH=7/3, flow rate 1.0mL/min]: T_{major} =17.28 min, T_{minor} = 10.28 min, ee = 74%. $[\alpha]_D$ = -172 (c = 0.0110 g/cm³ in CHCl₃).

(2'S,3'R)-ethyl 1-phenyl-2-oxospiro[indoline-3,2'-oxirane]-3'-carboxylate, 240-*cis*



Following the above general procedure, *cis* diastereoisomer **240-*cis*** was obtained as a whitish solid in 37% yield after purification (n Hexane/EtOAc=8/2). IR (CHCl₃): $\tilde{\nu}$ = 3037, 3006, 2399, 1734, 1717, 1620, 1470, 1358 cm⁻¹. ¹H-NMR (CDCl₃, 300 MHz, 25°C): δ 1.33 (t, J = 7.1 Hz, 3H, CH₃CH₂O), 4.24 (s, 1H, OCH), 4.33 (q, J = 7.1 Hz, 2H, CH₃CH₂O), 6.89 (d, J = 8.0 Hz, 1H, CH_{arom}), 7.07-7.21 (m, 2H, CH_{arom}) 7.33 (dt, J = 7.6 Hz, 1.6 Hz, 1H, CH_{arom}), 7.36-7.59 (m, 5H, CH_{arom}) ppm. ¹³C-NMR (CDCl₃, 75 MHz, 25°C): δ 14.3 (CH₃), 60.4 (CO), 60.8 (CH₂), 62.4 (OCH), 110.5 (C_{arom}), 121.2 (C_{arom}), 122.9 (C_{arom}), 123.8 (C_{arom}), 126.6 (C_{arom}), 128.7 (C_{arom}), 130.0 (C_{arom}), 131.4 (C_{arom}), 134.0 (C_{arom}), 145.6 (C_{arom}), 164.9, 168.5 (C=O) ppm. HRMS: exact mass calculated for (C₁₈H₁₅NNaO₄) requires m/z 332.0899, found m/z 332.0903. Chiral-phase HPLC analysis: [Daiacel Chiralpack IC 5 μ , λ =254 nm, n Hexane/*i*PrOH=7/3, flow rate 1.0mL/min]: T_{major} = 12.90 min, T_{minor} = 10.62 min, ee = 12%. $[\alpha]_D$ = +309 (c = 0.0030 g/cm³ in CHCl₃)

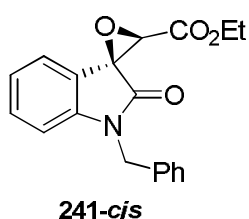
(2'R,3'R)-ethyl 1-benzyl-2-oxospiro[indoline-3,2'-oxirane]-3'-carboxylate, 241-*trans*



Following the above general procedure, *trans* diastereoisomer **241-*trans*** was obtained as a pale yellow solid in 61% yield after purification (n Hexane/EtOAc=8/2). IR (CHCl₃): $\tilde{\nu}$ = 3055, 3035, 3003, 1735, 1689, 1601 cm⁻¹. ¹H NMR (CDCl₃, 300 MHz, 25°C): δ 1.28 (t, J = 7.2 Hz, 3H, CH₃CH₂O), 4.18-4.40 (m, 2H, CH₃CH₂O), 4.26 (s, 1H, OCH), 4.90 (d, J = 15.6 Hz, 1H, CHHPh), 4.96 (d, J = 15.6 Hz, 1H, CHHPh), 6.80 (dd, J = 7.9 Hz, 0.6 Hz 1H, CH_{arom}), 6.85 (dt, J = 7.7 Hz, 0.6 Hz, 1H, CH_{arom}), 7.22-7.35 (m, 6H, CH_{arom}), 7.45 (dd, J = 7.7 Hz, 0.8 Hz 1H, CH_{arom}) ppm. ¹³C-NMR (CDCl₃, 75 MHz, 25°C): δ 14.3 (CH₃), 44.7 (CH₂_{benz}), 60.1 (CH₂), 60.3 (CO),

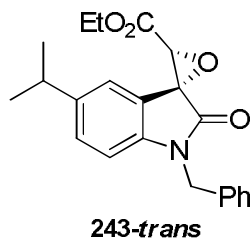
62.4 (OCH), 110.1 (C_{arom}), 119.6 (C_{arom}), 123.3 (C_{arom}), 125.1 (C_{arom}), 127.6 (C_{arom}), 128.1 (C_{arom}), 129.1 (C_{arom}), 131.2 (C_{arom}), 135.2 (C_{arom}), 145.1 (C_{arom}), 165.8, 170.3 (C=O) ppm. HRMS: exact mass calculated for (C₁₉H₁₇NNaO₄) requires m/z 346.1055, found m/z 346.1058. Chiral-phase HPLC analysis: [Daiacel Chiralpack IC 5 μ , λ =254 nm, *n*Hexane/EtOH=7/3, flow rate 1.0 mL/min]: T_{major} = 11.13 min, T_{minor} = 8.38 min, *ee* = 56%. [α]_D = -110 (*c* = 0.0290 g/cm³ in CHCl₃).

(2'*S*,3'*R*)-ethyl 1-benzyl-2-oxospiro[indoline-3,2'-oxirane]-3'-carboxylate, 241-*cis*



Following the above general procedure, *cis* diastereoisomer **241-*cis*** was obtained as a pale yellow solid in 31% yield after purification (*n*Hexane/EtOAc=8/2). IR (CHCl₃): $\tilde{\nu}$ = 3037, 3007, 2399, 1734, 1709, 1610, 1470, 1358 cm⁻¹. ¹H NMR (CDCl₃, 300 MHz, 25°C): δ 1.36 (t, *J* = 7.2 Hz, 3H, CH₃CH₂O), 4.19 (s, 1H, OCH), 4.29-4.47 (m, 2H, CH₃CH₂O), 4.86 (d, *J* = 15.6 Hz, 1H, CHHPh), 4.95 (d, *J* = 15.6 Hz, 1H, CHHPh), 6.74 (d, *J* = 7.9 Hz, 1H, CH_{arom}), 6.99-7.14 (m, 2H, CH_{arom}), 7.21-7.38 (m, 6H, CH_{arom}) ppm. ¹³C NMR (CDCl₃, 75 MHz, 25°C): δ 14.3 (CH₃), 44.5 (CH₂benz), 60.6 (CO), 60.8 (CH₂), 62.3 (OCH), 110.2 (C_{arom}), 121.4 (C_{arom}), 122.6 (C_{arom}), 123.3 (C_{arom}), 127.6 (C_{arom}), 128.1 (C_{arom}), 129.1 (C_{arom}), 131.3 (C_{arom}), 135.3 (C_{arom}), 144.6 (C_{arom}), 164.9, 169.3 (C=O) ppm. HRMS: exact mass calculated for (C₁₉H₁₇NNaO₄) requires m/z 346.1055, found m/z 346.1053. Chiral-phase HPLC analysis: [Daiacel Chiralpack IB 5 μ , λ =254 nm, *n*Heptane/EtOH/DEA=70/30/0.1, flow rate 1.0 mL/min]: T_{major} = 12.43 min, T_{minor} = 14.59 min, *ee* = 20%. [α]_D = -62 (*c* = 0.0150 g/cm³ in CHCl₃).

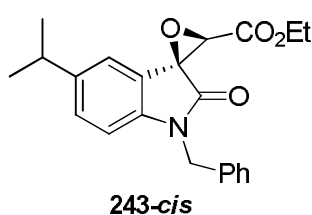
(2'*R*,3'*R*)-ethyl 1-benzyl-5-isopropyl-2-oxospiro[indoline-3,2'-oxirane]-3'-carboxylate, 243-*trans*



Following the above general procedure, *trans* diastereoisomer **243-*trans*** was obtained as a pale yellow solid in 63% yield after purification (*n*Hexane/EtOAc=9/1). IR (CHCl₃): $\tilde{\nu}$ = 3027, 3009, 2959, 2927, 1747, 1729, 1625, 1491, 1371 cm⁻¹. ¹H NMR (CDCl₃, 300 MHz, 25°C): δ 1.15 (d, *J* = 6.9 Hz, 3H, CH₃CHCH₃), 1.16 (d, *J* = 6.9 Hz, 3H, CH₃CHCH₃), 1.30 (t, *J* = 7.1 Hz, 3H, CH₃CH₂O), 2.81 (sept, *J* = 6.9 Hz, 1H, CH₃CHCH₃), 4.19-4.36 (m, 2H, CH₃CH₂O), 4.26 (s, 1H, OCH), 4.88 (d, *J* = 15.5

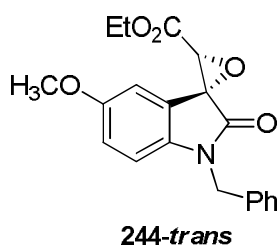
Hz, 1H, *CHHPh*), 4.95 (d, $J = 15.5$ Hz, 1H, *CHHPh*), 6.72 (d, $J = 8.1$ Hz, 1H, CH_{arom}), 7.11 (dd, $J = 8.1$ Hz, 1.9 Hz, 1H, CH_{arom}), 7.20–7.37 (m, 6H, CH_{arom}) ppm. ^{13}C NMR (CDCl_3 , 75 MHz, 25°C): δ 14.4 (CH_3), 24.0 (CHCH_3), 24.3 (CHCH_3), 34.0 (CHCH_3), 44.8 ($\text{CH}_{2\text{benz}}$), 60.1 (CH_2), 60.4 (CO), 62.4 (OCH), 109.9 (C_{arom}), 119.5 (C_{arom}), 123.2 (C_{arom}), 127.7 (C_{arom}), 128.1 (C_{arom}), 129.0 (C_{arom}), 129.1 (C_{arom}), 135.4 (C_{arom}), 142.9 (C_{arom}), 144.3 (C_{arom}), 165.9, 170.4 (C=O) ppm. HRMS: exact mass calculated for ($\text{C}_{22}\text{H}_{23}\text{NNaO}_4$) requires m/z 388.1525, found m/z 388.1521. Chiral-phase HPLC analysis: [Daiacel Chiralpack IC 5 μ , $\lambda=254$ nm, $n\text{Hexane}/\text{EtOH}=7/3$, flow rate 1.0mL/min]: $T_{\text{major}} = 10.60$ min, $T_{\text{minor}} = 6.83$ min, $ee = 62\%$. $[\alpha]_{\text{D}} = -90$ ($c = 0.0560$ g/cm³ in CHCl_3).

(2'*S*,3'*R*)-ethyl 1-benzyl-5-isopropyl-2-oxospiro[indoline-3,2'-oxirane]-3'-carboxylate, 243-*cis*



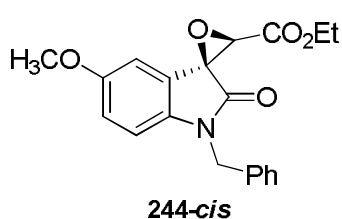
Following the above general procedure, *cis* diastereoisomer **243-*cis*** was obtained as a pale yellow solid in 26% yield after purification ($n\text{Hexane}/\text{EtOAc}=9/1$). IR (CHCl_3): $\tilde{\nu} = 3063, 3037, 2964, 2928, 2872, 1759, 1731, 1628, 1603, 1492$ cm⁻¹. ^1H NMR (CDCl_3 , 300 MHz, 25°C): δ 1.17 [d, $J = 6.9$ Hz, 6H, (CH_3)₂CH], 1.36 (t, $J = 7.2$ Hz, 3H, $\text{CH}_3\text{CH}_2\text{O}$), 2.82 [sept, $J = 6.9$ Hz, 1H, (CH_3)₂CH], 4.19 (s, 1H, OCH), 4.28–4.44 (m, $J = 7.2$ Hz, 2H, $\text{CH}_3\text{CH}_2\text{O}$), 4.84 (d, $J = 15.5$ Hz, 1H, *CHHPh*), 4.94 (d, $J = 15.5$ Hz, 1H, *CHHPh*), 6.69 (d, $J = 8.1$ Hz, 1H, CH_{arom}), 6.96 (d, $J = 1.8$ Hz, 1H, CH_{arom}), 7.12 (dd, $J = 8.1$ Hz, 1.8 Hz, 1H, CH_{arom}), 7.20–7.35 (m, 5H, CH_{arom}) ppm. ^{13}C NMR (CDCl_3 , 75 MHz, 25°C): δ 14.3 (CH_3), 24.1 (CHCH_3), 24.2 (CHCH_3), 33.9 (CHCH_3), 44.5 ($\text{CH}_{2\text{benz}}$), 60.5 (CO), 60.6 (CH_2), 62.2 (OCH), 110.0 (C_{arom}), 120.7 (C_{arom}), 121.2 (C_{arom}), 127.6 (C_{arom}), 128.0 (C_{arom}), 129.0 (C_{arom}), 129.2 (C_{arom}), 135.4 (C_{arom}), 142.4 (C_{arom}), 144.3 (C_{arom}), 164.9, 169.3 (C=O) ppm. HRMS: exact mass calculated for ($\text{C}_{22}\text{H}_{23}\text{NNaO}_4$) requires m/z 388.1525, found m/z 388.1527. Chiral-phase HPLC analysis: [Daiacel Chiralpack IC 5 μ , $\lambda=254$ nm, $n\text{Hexane}/\text{EtOH}=7/3$, flow rate 1.0mL/min]: $T_{\text{major}} = 9.84$ min, $T_{\text{minor}} = 9.21$ min, $ee = 26\%$. $[\alpha]_{\text{D}} = -37$ ($c = 0.0390$ g/cm³ in CHCl_3)

(2'*R*,3'*R*)-ethyl 1-benzyl-5-methoxy-2-oxospiro[indoline-3,2'-oxirane]-3'-carboxylate, 244-*trans*



Following the above general procedure, *trans* diastereoisomer **244-*trans*** was obtained as a pale yellow solid in 56% yield after purification (*n*Hexane/EtOAc=8/2). IR (CHCl₃): $\tilde{\nu}$ = 3091, 3067, 2988, 2960, 2837, 1731, 1690, 1602, 1490, 1474, 1456, 1370 cm⁻¹. ¹H NMR (CDCl₃, 300 MHz, 25°C): δ 1.30 (t, *J* = 7.1 Hz, 3H, CH₃CH₂O), 3.71 (s, 3H, OCH₃), 4.16-4.41 (m, 2H, CH₃CH₂O), 4.26 (s, 1H, OCH), 4.88 (d, *J* = 15.7 Hz, 1H, CHHPh), 4.94 (d, *J* = 15.7 Hz, 1H, CHHPh), 6.68 (d, *J* = 8.4 Hz, 1H, CH_{arom}), 6.79 (dd, *J* = 8.4 Hz, 2.7 Hz, 1H, CH_{arom}), 7.11 (d, *J* = 2.7 Hz, 1H, CH_{arom}), 7.20–7.38 (m, 5H, CH_{arom}) ppm. ¹³C NMR (CDCl₃, 75 MHz, 25°C): δ 14.4 (CH₃), 44.8 (CH₂benz), 56.0 (OCH₃), 60.2 (CH₂), 60.5 (CO), 62.5, 110.7 (C_{arom}), 111.7 (C_{arom}), 116.5 (C_{arom}), 120.7 (C_{arom}), 127.7 (C_{arom}), 128.1 (C_{arom}), 129.1 (C_{arom}), 135.3 (C_{arom}), 138.3 (C_{arom}), 156.4 (C_{arom}), 165.9, 170.1 (C=O) ppm. HRMS: exact mass calculated for (C₂₀H₁₉NNaO₅) requires *m/z* 376.1161, found *m/z* 376.1163. Chiral-phase HPLC analysis: [Daiacel Chiralpack IC 5 μ , λ =254 nm, *n*Hexane/EtOH=7/3, flow rate 1.0mL/min]: *T*_{major} = 14.49 min, *T*_{minor} = 10.21 min, *ee* = 52%. [α]_D = +21 (*c* = 0.0100 g/cm³ in CHCl₃).

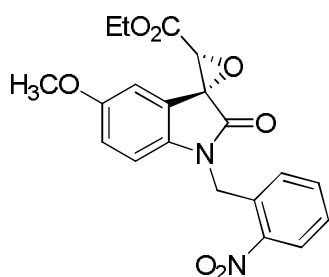
(2'*S*,3'*R*)-ethyl 1-benzyl-5-methoxy-2-oxospiro[indoline-3,2'-oxirane]-3'-carboxylate, 244-*cis*



Following the above general procedure, *cis* diastereoisomer **244-*cis*** was obtained as a pale yellow solid in 24% yield after purification (*n*Hexane/EtOAc=8/2). IR (CHCl₃): $\tilde{\nu}$ = 3079, 3024, 2986, 2962, 2939, 1758, 1731, 1605, 1495, 1477, 1437, 1370 cm⁻¹. ¹H NMR (CDCl₃, 300 MHz, 25°C): δ 1.39 (t, *J* = 7.2 Hz, 3H, CH₃CH₂O), 3.75 (s, 3H, OCH₃), 4.19 (s, 1H, OCH), 4.29-4.54 (m, 2H, CH₃CH₂O), 4.85 (d, *J* = 15.7 Hz, 1H, NCHH), 4.97 (d, *J* = 15.7 Hz, 1H, NCHH), 6.62-6.91 (m, 3H, CH_{arom}), 7.23–7.42 (m, 5H, CH_{arom}) ppm. ¹³C NMR (CDCl₃, 75 MHz, 25°C): δ 14.3 (CH₃), 44.6 (CH₂benz), 56.1 (OCH₃), 60.6 (CO), 60.7 (CH₂), 62.3 (OCH), 109.5 (C_{arom}), 110.9 (C_{arom}), 116.1 (C_{arom}), 122.5 (C_{arom}), 127.6 (C_{arom}), 128.1 (C_{arom}), 129.1 (C_{arom}), 135.3 (C_{arom}), 137.8 (C_{arom}), 156.6 (C_{arom}), 164.8, 169.0 (C=O) ppm. HRMS: exact mass

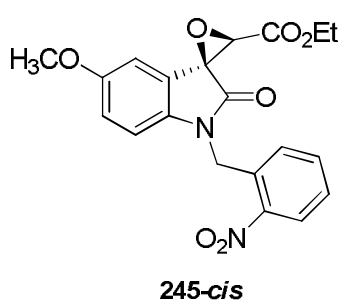
calculated for (C₂₀H₁₉NNaO₅) requires m/z 376.1161, found m/z 376.1162 Chiral-phase HPLC analysis: [Daiacel Chiralpack IC 5 μ , λ =254 nm, *n*Hexane/EtOH=7/3, flow rate 1.0mL/min]: T_{major} = 14.38 min, T_{minor} = 10.11 min, *ee* = 16%. [α]_D = -180 (*c* = 0.0090 g/cm³ in CHCl₃).

(2'*R*,3'*R*)-ethyl 5-methoxy-1-(2-nitrobenzyl)-2-oxospiro[indoline-3,2'-oxirane]-3'-carboxylate, 245-*trans*

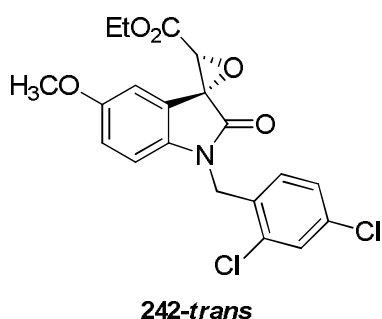


245-*trans*

Following the above general procedure, *trans* diastereoisomer **245-*trans*** was obtained as a pale yellow solid in 55% yield after purification (*n*Hexane/EtOAc=7/3). IR (CHCl₃): $\tilde{\nu}$ = 3049, 3004, 2987, 2958, 2929, 1736, 1701, 1601, 1529, 1491, 1474, 1371 cm⁻¹. ¹H NMR (CDCl₃, 300 MHz, 25°C): δ 1.32 (t, *J* = 7.1 Hz, 3H, CH₃CH₂O), 3.74 (s, 3H, OCH₃), 4.23-4.42 (m, 2H, CH₂CH₂O), 4.28 (s, 1H, OCH), 5.33 (d, *J* = 18.2 Hz, 1H, NCHH), 5.38 (d, *J* = 18.2 Hz, 1H, NCHH), 6.56 (d, *J* = 8.5 Hz, 1H, CH_{arom}), 6.81 (dd, *J* = 8.5 Hz, 2.6 Hz, 1H, CH_{arom}), 7.17 (d, *J* = 2.5 Hz, 1H, CH_{arom}), 7.20–7.28 (m, 1H, CH_{arom}), 7.46 (dt, *J* = 7.9 Hz, 1.3 Hz, 1H, CH_{arom}), 7.55 (dt, *J* = 7.9 Hz, 1.3 Hz, 1H, CH_{arom}), 8.17 (dd, *J* = 7.9 Hz, 1.3 Hz, 1H, CH_{arom}) ppm. ¹³C NMR (CDCl₃, 75 MHz, 25°C): δ 14.4 (CH₃), 42.2 (CH₂benz), 56.1 (OCH₃), 60.3 (CH₂), 60.5 (CO), 62.6 (OCH), 110.4 (C_{arom}), 112.1 (C_{arom}), 116.7 (C_{arom}), 120.7 (C_{arom}), 125.8 (C_{arom}), 128.1 (C_{arom}), 128.9 (C_{arom}), 131.1 (C_{arom}), 134.4 (C_{arom}), 137.8 (C_{arom}), 148.2 (C_{arom}), 156.8 (C_{arom}), 165.7, 170.5 (C=O) ppm. HRMS: exact mass calculated for (C₂₀H₁₈N₂NaO₇) requires m/z 421.1012, found m/z 421.1013. Chiral-phase HPLC analysis: [Daiacel Chiralpack IC 5 μ , λ =254 nm, *n*Hexane/EtOH=7/3, flow rate 1.0mL/min]: T_{major} = 24.70 min, T_{minor} = 23.14 min, *ee* = 78%. [α]_D = -105 (*c* = 0.0060 g/cm³ in CHCl₃).

(2'*S*,3'*R*)-ethyl 5-methoxy-1-(2-nitrobenzyl)-2-oxospiro[indoline-3,2'-oxirane]-3'-carboxylate, 245-*cis*

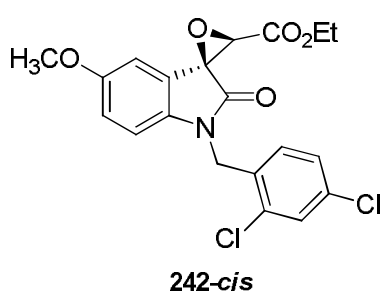
Following the above general procedure, *cis* diastereoisomer **245-*cis*** was obtained as a pale yellow solid in 26% yield after purification (*n*Hexane/EtOAc=7/3). IR (CHCl₃): $\tilde{\nu}$ = 3030, 3016, 2928, 2957, 2853, 1759, 1734, 1607, 1530, 1496, 1437 cm⁻¹. ¹H NMR (CDCl₃, 300 MHz, 25°C): δ 1.34 (t, *J* = 7.1 Hz, 3H, CH₃CH₂O), 3.76 (s, 3H, OCH₃), 4.22 (s, 1H, OCH), 4.34 (q, *J* = 7.1 Hz, 2H, CH₃CH₂O), 5.27 (d, *J* = 18.0 Hz, 1H, NCHH), 5.38 (d, *J* = 18.0 Hz, 1H, NCHH), 6.58 (d, *J* = 8.5 Hz, 1H, CH_{arom}), 6.73-6.88 (m, 2H, CH_{arom}), 7.18-7.28 (m, 1H, CH_{arom}), 7.38-7.61 (m, 2H, CH_{arom}), 8.15 (d, *J* = 7.4 Hz, 1H, CH_{arom}) ppm. ¹³C NMR (CDCl₃, 75 MHz, 25°C): δ 14.3 (CH₃), 41.9 (CH₂benz), 56.1 (OCH₃), 60.6 (CH₂), 60.8 (CO), 62.5 (OCH), 109.8 (C_{arom}), 110.6 (C_{arom}), 116.3 (C_{arom}), 116.6 (C_{arom}), 122.4 (C_{arom}), 125.8 (C_{arom}), 128.0 (C_{arom}), 128.9 (C_{arom}), 131.1 (C_{arom}), 134.4 (C_{arom}), 137.3 (C_{arom}), 157.0 (C_{arom}), 164.7, 169.4 (C=O) ppm. HRMS: exact mass calculated for (C₂₀H₁₈N₂NaO₇) requires *m/z* 421.1012, found *m/z* 421.1010. Chiral-phase HPLC analysis: [Daiacel Chiralpack IA 5 μ , λ =254 nm, *n*Heptane/EtOH/DEA =70/30/0.1, flow rate 1.0mL/min]: *T*_{major} = 17.20 min, *T*_{minor} = 18.05 min, *ee* = 20%. [α]_D = +125 (*c* = 0.0020 g/cm³ in CHCl₃).

(2'*R*,3'*R*)-ethyl 1-(2,4-dichlorobenzyl)-2-oxospiro[indoline-3,2'-oxirane]-3'-carboxylate, 242-*trans*

Following the above general procedure, *trans* diastereoisomer **242-*trans*** was obtained as a pale yellow solid in 49% yield after purification (*n*Hexane/EtOAc=8/2). IR (CHCl₃): $\tilde{\nu}$ = 3012, 1767, 1739, 1603, 1472 cm⁻¹. ¹H-NMR (CDCl₃, 300 MHz, 25°C): δ 1.29 (t, *J* = 7.1 Hz, 3H, CH₃CH₂O), 4.19-4.39 (m, 2H, CH₃CH₂O), 4.26 (s, 1H, OCH), 4.98 (d, *J* = 17.7 Hz, 1H, NCHH), 5.04 (d, *J* = 17.7 Hz, 1H, NCHH), 6.74 (d, *J* = 7.8 Hz, 1H, CH_{arom}), 7.05 (dt, *J* = 7.7 Hz, 0.9 Hz, 1H, CH_{arom}), 7.08 (d, *J* = 8.6 Hz, 1H, CH_{arom}), 7.16 (dd, *J* = 8.6 Hz, 2.0 Hz, 1H, CH_{arom}), 7.29 (dt, *J* = 7.8 Hz, 1.3 Hz, 1H, CH_{arom}), 7.41 (d, *J* = 2.0 Hz, 1H, CH_{arom}), 7.48 (ddd, *J*

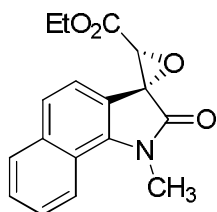
= 7.7 Hz, 1.3 Hz, 0.9 Hz 1H, CH_{arom}) ppm. ¹³C NMR (CDCl₃, 75 MHz, 25°C): δ = 14.3 (CH₃), 41.6 (CH₂benz), 60.2 (OCH₃, OCH), 62.5 (CO), 110.0 (C_{arom}), 119.5 (C_{arom}), 123.7 (C_{arom}), 125.3 (C_{arom}), 127.9 (C_{arom}), 129.4 (C_{arom}), 129.8 (C_{arom}), 131.2 (C_{arom}), 131.4 (C_{arom}), 133.8 (C_{arom}), 134.6 (C_{arom}), 144.5 (C_{arom}), 165.7, 170.6 (C=O) ppm. HRMS: exact mass calculated for (C₁₉H₁₅Cl₂NNaO₄) requires m/z 414.0276, found m/z 414.0279. Chiral-phase HPLC analysis: [Daiacel Chiralpack IC 5μ, λ=254 nm, *n*Hexane/EtOH=7/3, flow rate 1.0mL/min]: T_{major} = 10.83 min, T_{minor} = 8.47 min, *ee* = 60%. [α]_D = -127 (*c* = 0.0260 g/cm³ in CHCl₃).

(2'*S*,3'*R*)-ethyl 1-(2,4-dichlorobenzyl)-2-oxospiro[indoline-3,2'-oxirane]-3'-carboxylate, 242-*cis*



Following the above general procedure, *cis* diastereoisomer **242-*cis*** was obtained as a pale yellow solid in 35% yield after purification (*n*Hexane/EtOAc=8/2). IR (CHCl₃): $\tilde{\nu}$ = 3022, 3012, 2399, 1745, 1737, 1602, 1472, 1357cm⁻¹. ¹H NMR (CDCl₃, 300 MHz, 25°C): δ 1.34 (t, *J* = 7.1 Hz, 3H, CH₃CH₂O), 4.22 (s, 1H, OCH), 4.29-4.41 (m, *J* = 7.1 Hz, 2H, CH₃CH₂O) 4.96 (d, *J* = 17.1 Hz, 1H, NCHH), 5.02 (d, *J* = 17.1 Hz, 1H, NCHH), 6.73 (d, *J* = 7.9 Hz, 1H, CH_{arom}), 7.03-7.18 (m, 4H, CH_{arom}), 7.33 (dt, *J* = 7.8 Hz, 1.6 Hz, 1H, CH_{arom}), 7.40 (d, *J* = 2.0 Hz, 1H, CH_{arom}) ppm. ¹³C NMR (CDCl₃, 75 MHz, 25°C): δ 14.4 (CH₃), 41.4 (CH₂benz), 60.6 (CO), 60.7 (OCH), 62.4 (OCH₃), 110.1 (C_{arom}), 121.3 (C_{arom}), 122.8 (C_{arom}), 123.7 (C_{arom}), 128.0 (C_{arom}), 129.4 (C_{arom}), 129.8 (C_{arom}), 131.2 (C_{arom}), 131.5 (C_{arom}), 133.8 (C_{arom}), 134.6 (C_{arom}), 144.1 (C_{arom}), 164.7, 169.5 (C=O) ppm. HRMS: exact mass calculated for (C₁₉H₁₅Cl₂NNaO₄) requires m/z 414.0276, found m/z 414.0277. Chiral-phase HPLC analysis: [Daiacel Chiralpack IC 5μ, λ=254 nm, *n*Heptane/DCM/EtOH/DEAH=50/50/1/0.1, flow rate 1.0mL/min]: T_{major} = 7.00 min, T_{minor} = 9.00 min, *ee* = 20%. [α]_D = -274 (*c* = 0.014 g/cm³ in CHCl₃).

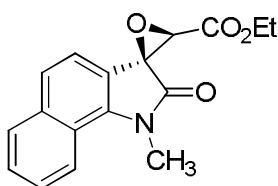
(2'R,3'R)-ethyl 1-methyl-2-oxo-1,2-dihydrospiro[benzo[g]indole-3,2'-oxirane]-3'-carboxylate 193-trans



193-trans

Following the above general procedure, *trans* diastereoisomer **193-trans** was obtained as a pale red solid in 50% yield after purification (*n*Hexane/EtOAc=8/2). ¹H-NMR (CDCl₃, 300 MHz, 25°C): □ 1.26-1.30 (m, 3H, CH₃CH₂O); 3.88 (s, 3H, NCH₃); 4.21-4.31 (m, 3H, OCH, CH₃CH₂O), 7.50-7.55 (m, 4H, CH_{arom}); 7.86-7.88 (m, 1H, CH_{arom}), 8.40-8.43 (m, 1H, CH_{arom}) ppm. HRMS: exact mass calculated for (C₁₇H₁₅NNaO₄) requires *m/z* 320.0899, found *m/z* 320.0701. Chiral-phase HPLC analysis: [Daiacel Chiralpack IC 5μ, λ=254 nm, *n*Hexane/EtOH=70/30, flow rate 1.0mL/min]: T_{major} = 18.48 min, T_{minor} = 13.56 min *ee* = 82%. [α]_D = -20.15 (*c* = 0.0059 g/cm³ in CHCl₃)

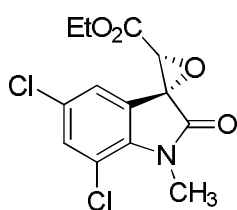
(2'S,3'R)-ethyl 1-methyl-2-oxo-1,2-dihydrospiro[benzo[g]indole-3,2'-oxirane]-3'-carboxylate 193-cis



193-cis

Following the above general procedure, *cis* diastereoisomer **193-cis** was obtained as a pale red solid in 48% yield after purification (*n*Hexane/EtOAc=8/2). ¹H-NMR (CDCl₃, 300 MHz, 25°C): □ 1.39 (t, *J* = 7.0 Hz, 3H, CH₃CH₂O); 3.83 (s, 3H, NCH₃); 4.27 (s, 1H, OCH), 4.39 (q, *J* = 7.0 Hz, 2H, CH₃CH₂O), 7.16 (d, *J* = 8.1 Hz, 1H, CH_{arom}), 7.51-7.54 (m, 1H, CH_{arom}); 7.60 (d, *J* = 8.2 Hz, 1H, CH_{arom}), 7.87-7.90 (m, 1H, CH_{arom}); 8.38-8.41 (m, 1H, CH_{arom}) ppm. HRMS: exact mass calculated for (C₁₁H₁₁NNaO₂) requires *m/z* 320.0899, found *m/z* 320.0701. Chiral-phase HPLC analysis: [Daiacel Chiralpack IB 5μ, λ=254 nm, *n*Heptane/EtOH/DEA=70/30/0.1, flow rate 1.0mL/min]: T_{major} = 8.91 min, T_{minor} = 9.71 min *ee* = 10%.

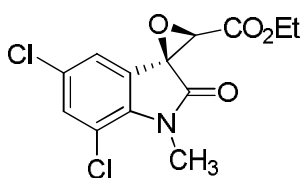
(trans)-(2'R,3'R)-ethyl 5,7-dichloro-1-methyl-2-oxospiro[indoline-3,2'-oxirane]-3'-carboxylate 189-trans



189-trans

Following the above general procedure, *trans* diastereoisomer **189-trans** was obtained as a pale red solid in 29% yield after purification (*n*Hexane/EtOAc=8/2). IR (CHCl₃): $\tilde{\nu}$ = 3031, 3006, 1740, 1729, 1578, 1463, 1337, 1309 cm⁻¹. ¹H-NMR (CDCl₃, 300 MHz, 25°C): 1.31 (t, *J* = 7.1 Hz, 3H, CH₃CH₂O); 3.62 (s, 3H, NCH₃); 4.18–4.40 (m, 3H, CH₃CH₂O, OCH); 7.34 (s, 1H, CH_{arom}); 7.40 (s, 1H, CH_{arom}) ppm. ¹³CNMR (CDCl₃, 75 MHz, 25°C): 14.3 (CH₃), 30.5 (NCH₃), 59.4, 60.6, 62.8, 117.0 (C_{arom}), 123.6 (C_{arom}), 124.0 (C_{arom}), 129.0 (C_{arom}), 132.9 (C_{arom}), 140.2 (C_{arom}), 165.1, 170.1 (C=O) ppm. HRMS: exact mass calculated for (C₁₃H₁₁Cl₂NNaO₄) requires *m/z* 337.9963, found *m/z* 337.9961. Chiral-phase HPLC analysis: [Daiacel Chiralpack IC 5μ, λ=254 nm, *n*Hexane/EtOH=70/30, flow rate 1.0mL/min]: *T*_{major} = 11.74 min, *T*_{minor} = 9.48 min *ee* = 85%. [α]_D = -96 (*c* = 0.0160 g/cm³ in CHCl₃)

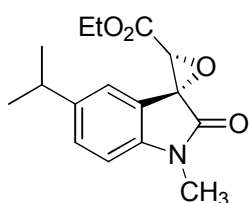
(cis)-(2'S,3'R)-ethyl 5,7-dichloro-1-methyl-2-oxospiro[indoline-3,2'-oxirane]-3'-carboxylate 189-cis



189-cis

Following the above general procedure, *cis* diastereoisomer **189-cis** was obtained as a pale red solid in 50% yield after purification (*n*Hexane/EtOAc=8/2). IR (CHCl₃): $\tilde{\nu}$ = 3034, 3003, 1759, 1740, 1583, 1463, 1334, 1306 cm⁻¹. ¹H-NMR (CDCl₃, 300 MHz, 25°C): 1.36 (t, *J* = 7.1 Hz, 3H, CH₃CH₂O); 3.59 (s, 3H, NCH₃); 4.12 (s, 1H, OCH); 4.35 (q, *J* = 7.1 Hz, 2H, CH₃CH₂O); 6.97 (s, 1H, CH_{arom}); 7.35 (s, 1H, CH_{arom}) ppm. ¹³CNMR (CDCl₃, 75 MHz, 25°C): 14.2 (CH₃), 30.2 (NCH₃), 59.2, 60.7, 62.5, 117.1 (C_{arom}), 121.4 (C_{arom}), 125.3 (C_{arom}), 128.9 (C_{arom}), 132.8 (C_{arom}), 139.7 (C_{arom}), 164.0, 168.8 (C=O) ppm. HRMS: exact mass calculated for (C₁₃H₁₁Cl₂NNaO₄) requires *m/z* 337.9963, found *m/z* 337.9961. Chiral-phase HPLC analysis: [Daiacel Chiralpack IC 5μ, λ=254 nm, *n*Hexane/EtOH=70/30, flow rate 1.0mL/min]: *T*_{major} = 21.69 min, *T*_{minor} = 20.20 min *ee* = 53%. [α]_D = -42 (*c* = 0.0220 g/cm³ in CHCl₃)

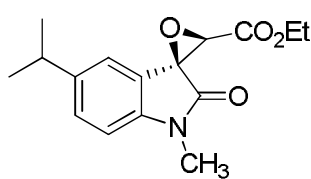
(*trans*)-(2'R,3'R)-ethyl 5,7-dichloro-1-methyl-2-oxospiro[indoline-3,2'-oxirane]-3'-carboxylate 186-*trans*



186-*trans*

Following the above general procedure, *trans* diastereoisomer **186-*trans*** was obtained as a pale yellow solid in 38% yield after purification (*n*Hexane/EtOAc=8/2). IR (CHCl₃): $\tilde{\nu}$ = 3025, 3011, 2959, 1739, 1727, 1625, 1494, 1471, 1369, 1346 cm⁻¹. ¹H-NMR (CDCl₃, 300 MHz, 25°C): δ 1.20 (d, *J* = 6.8 Hz, 6H, (CH₃)₂CHC_{arom}); 1.29 (t, *J* = 7.1 Hz, 3H, CH₃CH₂O); 2.80–2.95 (m, 1H, (CH₃)₂CHC_{arom}); 3.26 (s, 3H, NCH₃); 4.18–4.40 (m, 3H, CH₃CH₂O, OCH); 6.84 (d, *J* = 7.9 Hz, 1H, CH_{arom}); 7.24 (d, *J* = 7.9 Hz, 1H, CH_{arom}); 7.33 (m, 2H, CH_{arom}) ppm. ¹³CNMR (CDCl₃, 75 MHz, 25°C): δ 14.3 (CH₃), 24.2 (2xCH₃), 26.9 (NCH₃), 34.0 (CHCH₃), 59.9, 60.3, 62.3, 108.9 (C_{arom}), 119.3 (C_{arom}), 123.0 (C_{arom}), 129.0 (C_{arom}), 143.6 (C_{arom}), 144.3 (C_{arom}), 165.9, 170.0 (C=O) ppm. HRMS: exact mass calculated for (C₁₆H₁₉NNaO₄) requires *m/z* 312.1212, found *m/z* 312.1215. Chiral-phase HPLC analysis: [Daiacel Chiralpack IC 5 μ , λ =254 nm, *n*Hexane/EtOH=70/30, flow rate 1.0mL/min]: *T*_{major} = 14.85 min, *T*_{minor} = 8.42 min *ee* = 78%. [α]_D = -79 (*c* = 0.0220 g/cm³ in CHCl₃)

(*cis*)-(2'S,3'R)-ethyl 5,7-dichloro-1-methyl-2-oxospiro[indoline-3,2'-oxirane]-3'-carboxylate 186-*cis*

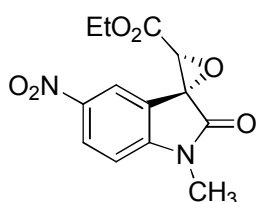


186-*cis*

Following the above general procedure, *cis* diastereoisomer **186-*cis*** was obtained as a pale yellow solid in 52% yield after purification (*n*Hexane/EtOAc=8/2). IR (CHCl₃): $\tilde{\nu}$ = 3025, 3011, 2959, 1739, 1727, 1625, 1494, 1471, 1369, 1346 cm⁻¹. ¹H-NMR (CDCl₃, 300 MHz, 25°C): δ 1.22 (d, *J* = 6.8 Hz, 6H, (CH₃)₂CHC_{arom}); 1.36 (t, *J* = 7.1 Hz, 3H, CH₃CH₂O); 2.80–2.95 (m, 1H, (CH₃)₂CHC_{arom}); 3.23 (s, 3H, NCH₃); 4.18 (s, 1H, OCH); 4.30–4.40 (m, 3H, CH₃CH₂O, OCH); 6.83 (d, *J* = 7.9 Hz, 1H, CH_{arom}); 6.98 (s, 1H, CH_{arom}); 7.28 (d, *J* = 7.9 Hz, 1H, CH_{arom}) ppm. ¹³CNMR (CDCl₃, 75 MHz, 25°C): δ 14.2 (CH₃), 24.2 (2xCH₃), 26.8 (NCH₃), 33.9 (CHCH₃), 60.2, 60.3, 62.1, 109.0 (C_{arom}), 120.5 (C_{arom}), 121.1 (C_{arom}), 129.2 (C_{arom}), 143.2 (C_{arom}), 144.3 (C_{arom}), 164.9, 168.9 (C=O) ppm. HRMS: exact mass calculated for (C₁₆H₁₉NNaO₄) requires *m/z* 312.1212, found *m/z* 312.1215. Chiral-phase HPLC analysis: [Daiacel Chiralpack IC 5 μ , λ =254 nm,

*n*Hexane/EtOH=70/30, flow rate 1.0mL/min]: $T_{major} = 13.73$ min, $T_{minor} = 15.19$ min *ee* = 79%. $[\alpha]_D = -33$ ($c = 0.0250$ g/cm³ in CHCl₃)

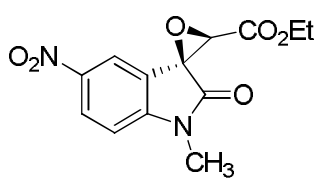
(*trans*)- (2'R,3'R)-ethyl 1-methyl-5-nitro-2-oxospiro[indoline-3,2'-oxirane]-3'-carboxylate 187-*trans*



187-*trans*

Following the above general procedure, *trans* diastereoisomer **187-*trans*** was obtained as a pale yellow solid in 19% yield after purification (DCM 100%). IR (CHCl₃): $\tilde{\nu} = 3031, 3017, 3009, 1754, 1743, 1617, 1533, 1494, 1340$ cm⁻¹. ¹H-NMR (CDCl₃, 300 MHz, 25°C): δ 1.34 (t, $J = 7.1$ Hz, 3H, CH₃CH₂O); 3.35 (s, 3H, NCH₃); 4.23–4.42 (m, 3H, CH₃CH₂O, OCH); 7.03 (d, $J = 8.9$ Hz, 1H, CH_{arom}); 8.37 (d, $J = 7.4$ Hz, 2H, CH_{arom}) ppm. ¹³CNMR (CDCl₃, 75 MHz, 25°C): δ 14.2 (CH₃), 27.4 (NCH₃), 59.4, 60.1, 62.9, 108.9 (C_{arom}), 120.4 (C_{arom}), 121.1 (C_{arom}), 128.0 (C_{arom}), 143.8 (C_{arom}), 150.9 (C_{arom}), 165.1, 170.1 (C=O) ppm. HRMS: exact mass calculated for (C₁₃H₁₂N₂NaO₆) requires m/z 315.0593, found m/z 315.0596. Chiral-phase HPLC analysis: [Daiacel Chiralpack IC 5 μ , λ =254 nm, *n*Hexane/EtOH=70/30, flow rate 1.0mL/min]: $T_{major} = 23.13$ min, $T_{minor} = 22.02$ min *ee* = 70%. $[\alpha]_D = -29$ ($c = 0.0180$ g/cm³ in CHCl₃)

(*cis*)- (2'S,3'R)-ethyl 1-methyl-5-nitro-2-oxospiro[indoline-3,2'-oxirane]-3'-carboxylate 187-*cis*

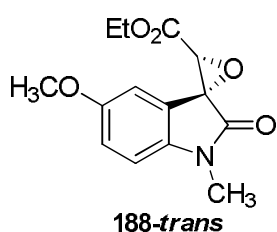


187-*cis*

Following the above general procedure, *cis* diastereoisomer **187-*cis*** was obtained as a pale yellow solid in 53% yield after purification (DCM 100%). IR (CHCl₃): $\tilde{\nu} = 3029, 3017, 3009, 1754, 1729, 1630, 1527, 1494, 1463, 1340$ cm⁻¹. ¹H-NMR (CDCl₃, 300 MHz, 25°C): δ 1.37 (t, $J = 7.1$ Hz, 3H, CH₃CH₂O); 3.33 (s, 3H, NCH₃); 4.29 (s, 1H, OCH); 4.36 (dq, $J = 9.2$ Hz, 7.1 Hz, 1H, CH₃CHHO); 4.38 (dq, $J = 9.2$ Hz, 7.1 Hz, 1H, CH₃CHHO); 7.03 (d, $J = 8.9$ Hz, 1H, CH_{arom}); 8.02 (d, $J = 1.9$ Hz, 1H, CH_{arom}); 8.39 (dd, $J = 8.7$ Hz, 2.2 Hz, 1H, CH_{arom}) ppm. ¹³CNMR (CDCl₃, 75 MHz, 25°C): δ 14.1 (CH₃), 27.3 (NCH₃), 59.2 (CO), 60.4 (CH₂), 62.5 (CH), 109 (C_{arom}), 118.5 (C_{arom}), 122.2 (C_{arom}), 128.1 (C_{arom}), 143.2 (C_{arom}), 150.5 (C_{arom}), 163.9, 169.1 (C=O) ppm. HRMS: exact mass calculated for (C₁₃H₁₂N₂NaO₆) requires m/z 315.0593, found m/z 315.0596. Chiral-phase HPLC

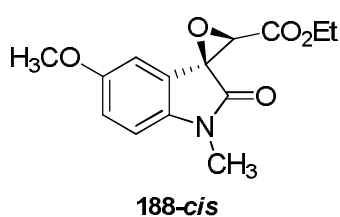
analysis: [Daiacel Chiralpack IB 5 μ , λ =254 nm, *n*Heptane/EtOH/DEA=70/30/0.1, flow rate 1.0mL/min]: T_{major} = 12.89 min, T_{minor} = 14.80 min ee = 12%. $[\alpha]_D = -29$ ($c = 0.0160$ g/cm³ in CHCl₃)

(2'R,3'R)-ethyl 5-methoxy-1-methyl-2-oxospiro[indoline-3,2'-oxirane]-3'-carboxylate 188-trans

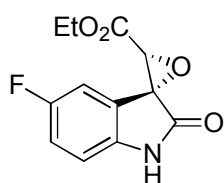


Following the above general procedure, *trans* diastereoisomer **188-trans** was obtained as a pale yellow solid in 50% yield after purification (hexane/EtOAc = 8/2). IR (CHCl₃): $\tilde{\nu} = 1735, 1734, 1614, 1492, 1467, 1358, 1260$ cm⁻¹. ¹H-NMR (CDCl₃, 300 MHz, 25°C): δ 1.28 (t, $J = 7.1$ Hz, 3H, CH₃CH₂O); 3.23 (s, 3H, NCH₃); 3.75 (s, 3H, OCH₃); 4.18 (s, 1H, OCH); 4.22-4.25 (m, 2H, CH₃CH₂O); 6.80 (d, $J = 8.5$ Hz, 1H, CH_{arom}); 6.92 (d, $J = 8.5$ Hz, 1H, CH_{arom}); 7.09 (s, 1H, CH_{arom}) ppm. ¹³CNMR (CDCl₃, 75 MHz, 25°C): δ 14.3 (CH₃), 26.9 (NCH₃), 56.0, 59.9, 62.3, 120.5 (C_{arom}), 139.1 (C_{arom}), 156.3 (C_{arom}), 165.8 (C_{arom}), 169.8 (C=O) ppm. HPLC analysis: [Daiacel Chiralpack IC 5 μ , λ =254 nm, *n*Heptane/EtOH=70/30, flow rate 1.0mL/min]: T_{major} = 16.33 min, T_{minor} = 11.45 min ee = 80%. $[\alpha]_D = -10$ ($c = 0.0451$ g/cm³ in CHCl₃)

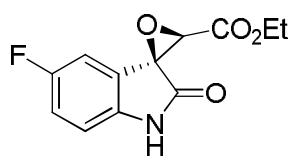
(2'S,3'R)-ethyl 5-methoxy-1-methyl-2-oxospiro[indoline-3,2'-oxirane]-3'-carboxylate 188-cis



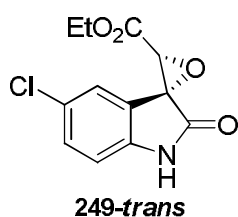
Following the above general procedure, *trans* diastereoisomer **188-cis** was obtained as a pale yellow solid in 50% yield after purification (hexane/EtOAc = 8/2). IR (CHCl₃): $\tilde{\nu} = 1763, 1603, 1502, 1367, 1290$ cm⁻¹. ¹H-NMR (CDCl₃, 300 MHz, 25°C): δ 1.34 (t, $J = 7.2$ Hz, 3H, CH₃CH₂O); 3.18 (s, 3H, NCH₃); 3.75 (s, 3H, OCH₃); 4.12 (s, 1H, OCH); 4.33 (q, $J = 7.2$ Hz, 2H, CH₃CH₂O); 6.69 (s, 1H, CH_{arom}); 6.69 (d, $J = 8.5$ Hz, 1H, CH_{arom}); 6.90 (d, $J = 8.5$ Hz, 1H, CH_{arom}) ppm. ¹³CNMR (CDCl₃, 75 MHz, 25°C): δ 14.1 (CH₃), 26.7 (NCH₃), 56.0, 60.3, 62.1, 109.4 (C_{arom}), 109.7 (C_{arom}), 122.4 (C_{arom}), 138.6 (C_{arom}), 156.5 (C_{arom}), 164.8 (C_{arom}), 168.6 (C=O) ppm. HPLC analysis: [Daiacel Chiralpack IC 5 μ , λ =254 nm, *n*Heptane/EtOH=70/30, flow rate 1.0mL/min]: T_{major} = 16.35 min, T_{minor} = 19.33 min ee = 24%. $[\alpha]_D = -4$ ($c = 0.0390$ g/cm³ in CHCl₃)

(2'R,3'R)-ethyl 5-fluoro-2-oxospiro[indoline-3,2'-oxirane]-3'-carboxylate, 248-trans**248-trans**

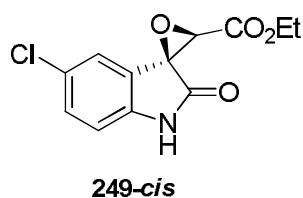
Following the above general procedure, *trans* diastereoisomer **248-trans** was obtained as a white solid in 32% yield after purification (*n*Hexane/EtOAc=7/3). IR (CHCl₃): $\tilde{\nu}$ = 3429, 3207, 3031, 2979, 1715, 1767, 1752, 1630, 1481, 1319, 1231, 1204 cm⁻¹. ¹H-NMR (CDCl₃, 300 MHz, 25°C): δ 1.32 (t, 3H, *J* = 7.1 Hz, CH₃CH₂O); 4.19 (s, 1H, OCH); 4.26-4.36 (m, 2H, CH₃CH₂O); 6.88 (m, 1H, CH_{arom}); 7.06 (t, 1H, *J* = 8.4 Hz, CH_{arom}); 7.24 (m, 1H, CH_{arom}); 8.66 (s, 1H, NH) ppm. ¹³CNMR (CDCl₃, 75 MHz, 25°C): δ 14.3 (CH₃), 60.0 (CO), 60.5 (CH₂), 62.7 (CH), 111.9 (d, *J*_{CF} = 7.9 Hz, C_{arom}), 113.5 (d, *J*_{CF} = 26.7 Hz, C_{arom}), 117.9 (d, *J*_{CF} = 23.9 Hz, C_{arom}), 121.3 (d, *J*_{CF} = 9.1 Hz, C_{arom}), 138.8 (C_{arom}), 159.3 (d, *J*_{CF} = 242.2 Hz, C_{arom}), 165.4 (OC=O), 172.3 (C=O) ppm. HRMS: exact mass calculated for (C₁₂H₁₀FNNaO₄) requires *m/z* 274.0492, found *m/z* 274.0497. Chiral-phase HPLC analysis: [Daiacel Chiralpack IC 5 μ , λ =254 nm, *n*Hexane/EtOH=90/10, flow rate 1.0mL/min]: *T*_{major} = 10.44 min, *T*_{minor} = 9.05 min *ee* = 86%. [α]_D = -132 (*c* = 0.0155 g/cm³ in CHCl₃)

(2'S,3'R)-ethyl 5-fluoro-2-oxospiro[indoline-3,2'-oxirane]-3'-carboxylate, 248-cis**248-cis**

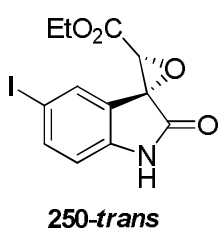
Following the above general procedure, *cis* diastereoisomer **248-cis** was obtained as a white solid in 58% yield after purification (*n*Hexane/EtOAc=7/3). IR (CHCl₃): $\tilde{\nu}$ = 3429, 3207, 3031, 2979, 1715, 1767, 1752, 1630, 1481, 1319, 1231, 1204 cm⁻¹. ¹H-NMR (CDCl₃, 300 MHz, 25°C): δ 1.35 (t, 3H, *J* = 7.0 Hz, CH₃CH₂O); 4.15 (s, 1H, OCH); 4.35 (q, 2H, *J* = 7.0 Hz, CH₃CH₂O); 6.84–6.93 (m, 2H, CH_{arom}); 7.07 (t, 1H, *J* = 8.6 Hz, CH_{arom}); 8.44 (s, 1H, NH) ppm. ¹³CNMR (CDCl₃, 75 MHz, 25°C): δ 14.3 (CH₃), 60.0 (CH₂), 60.5 (CO), 62.7 (CH), 111.9 (d, *J*_{CF} = 7.9 Hz, C_{arom}), 113.5 (d, *J*_{CF} = 26.7 Hz, C_{arom}), 117.9 (d, *J*_{CF} = 23.9 Hz, C_{arom}), 121.3 (d, *J*_{CF} = 9.1 Hz, C_{arom}), 138.8 (C_{arom}), 159.3 (d, *J*_{CF} = 242.2 Hz, C_{arom}), 165.4 (OC=O), 172.3 (C=O) ppm. HRMS: exact mass calculated for (C₁₂H₁₀FNNaO₄) requires *m/z* 274.0492, found *m/z* 274.0497. Chiral-phase HPLC analysis: [Daiacel Chiralpack IB 5 μ , λ =254 nm, *n*Heptane/EtOH/DEA=70/30/0.1, flow rate 1.0mL/min]: *T*_{major} = 5.22 min, *T*_{minor} = 5.97 min *ee* = 22%. [α]_D = -381 (*c* = 0.0221 g/cm³ in CHCl₃)

(2'R,3'R)-ethyl 5-chloro-2-oxospiro[indoline-3,2'-oxirane]-3'-carboxylate, 249-trans

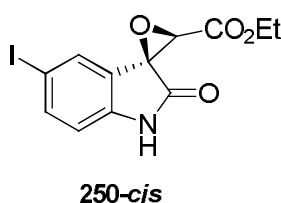
Following the above general procedure, *trans* diastereoisomer **249-trans** was obtained as a white solid in 33% yield after purification (*n*Hexane/EtOAc=1/1). IR (CHCl₃): $\tilde{\nu}$ = 3433, 3213, 3021, 1764, 1755, 1602, 1441, 1240, 1228, 1213 cm⁻¹. ¹H-NMR (CDCl₃, 300 MHz, 25°C): □ 1.32 (t, 3H, *J* = 7.1 Hz, CH₃CH₂O); 4.19 (s, 1H, OCH); 4.26-4.36 (m, 2H, CH₃CH₂O); 6.88 (m, 1H, CH_{arom}); 7.06 (t, 1H, *J* = 8.4 Hz, CH_{arom}); 7.24 (m, 1H, CH_{arom}); 8.66 (s, 1H, NH) ppm. ¹³CNMR (CDCl₃, 75 MHz, 25°C): □ 14.3 (CH₃), 60.0 (CH₂), 60.5 (CO), 62.7 (CH), 112.1 (C_{arom}), 123.3 (C_{arom}), 125.9 (C_{arom}), 129.0 (C_{arom}), 131.3 (C_{arom}), 140.3 (C_{arom}), 165.4 (OC=O), 171.8 (C=O) ppm. HRMS: exact mass calculated for (C₁₂H₁₀ClNNaO₄) requires *m/z* 290.0196, found *m/z* 290.0198. Chiral-phase HPLC analysis: [Daiacel Chiralpack IC 5μ, λ=254 nm, *n*Hexane/EtOH=70/30, flow rate 1.0mL/min]: *T*_{major} = 5.15 min, *T*_{minor} = 4.66 min *ee* = 86%. [α]_D = -43 (*c* = 0.0108 g/cm³ in CHCl₃)

(2'S,3'R)-ethyl 5-chloro-2-oxospiro[indoline-3,2'-oxirane]-3'-carboxylate, 249-cis

Following the above general procedure, *cis* diastereoisomer **249-cis** was obtained as a white solid in 50% yield after purification (*n*Hexane/EtOAc=1/1). IR (CHCl₃): $\tilde{\nu}$ = 3433, 3265, 3024, 1761, 1733, 1633, 1481, 1277, 1200 cm⁻¹. ¹H-NMR (CDCl₃, 300 MHz, 25°C): □□ 1.34 (t, 3H, *J* = 7.2 Hz, CH₃CH₂O); 4.16 (s, 1H, OCH); 4.34 (q, 2H, *J* = 7.2 Hz, CH₃CH₂O); 6.92 (d, 1H, *J* = 8.3 Hz, CH_{arom}); 7.08 (s, 1H, CH_{arom}); 7.33 (d, 1H, *J* = 8.3 Hz, CH_{arom}); 8.65 (s, 1H, NH) ppm. ¹³CNMR (CDCl₃, 75 MHz, 25°C): □ 14.2 (CH₃), 60.1 (CO), 60.5 (CH₂), 62.4 (CH), 112.4 (C_{arom}), 123.3 (C_{arom}), 128.9 (C_{arom}), 131.3 (C_{arom}), 131.4 (C_{arom}), 140.9 (C_{arom}), 164.2 (OC=O), 170.7 (C=O) ppm. HRMS: exact mass calculated for (C₁₂H₁₀ClNNaO₄) requires *m/z* 290.0196, found *m/z* 290.0198. Chiral-phase HPLC analysis: [Daiacel Chiralpack IC 5μ, λ=254 nm, *n*Heptane/EtOH/DEA=70/30/0.1, flow rate 1.0mL/min]: *T*_{major} = 5.30 min, *T*_{minor} = 6.13 min *ee* = 18%. [α]_D = -29 (*c* = 0.0164 g/cm³ in CHCl₃)

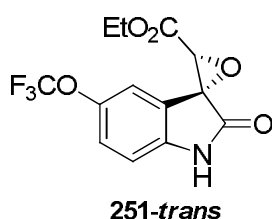
(2'R,3'R)-ethyl 5-iodo-2-oxospiro[indoline-3,2'-oxirane]-3'-carboxylate, 250-trans

Following the above general procedure, *trans* diastereoisomer **250-trans** was obtained as a white solid in 71% yield after purification (*n*Hexane/EtOAc=1/1). IR (CHCl₃): $\tilde{\nu}$ = 1765, 1760, 1602, 1441, 1240, 1228 cm⁻¹. ¹H-NMR (CDCl₃, 300 MHz, 25°C): □ 1.34 (t, 3H, *J* = 7.0 Hz, CH₃CH₂O); 4.17-4.40 (m, 3H, CHO, CH₃CH₂O); 6.76 (d, 1H, *J* = 8.3 Hz, CH_{arom}); 7.67 (d, 1H, *J* = 8.3 Hz, CH_{arom}); 7.76 (s, 1H, CH_{arom}), 8.73 (bs, 1H, NH) ppm. ¹³CNMR (CDCl₃, 75 MHz, 25°C): □ □ 14.4 (CH₃), 59.8 (CO), 60.1 (CH₂), 62.7 (CH), 85.6 (C_{arom}), 113.0 (C_{arom}), 122.0 (C_{arom}), 134.2 (C_{arom}), 140.1 (C_{arom}), 142.4 (C_{arom}), 165.4 (OC=O), 171.2 (C=O) ppm. HRMS: exact mass calculated for (C₁₂H₁₀INNaO₄) requires *m/z* 381.9552, found *m/z* 381.9555. Chiral-phase HPLC analysis: [Daiacel Chiralpack IC 5μ, λ=254 nm, *n*Hexane/EtOH=90/10, flow rate 1.0mL/min]: τ_{major} = 11.56 min, τ_{minor} = 9.81 min *ee* = 36%. [α]_D = -23 (*c* = 0.0120 g/cm³ in CHCl₃)

(2'S,3'R)-ethyl 5-iodo-2-oxospiro[indoline-3,2'-oxirane]-3'-carboxylate, 250-cis

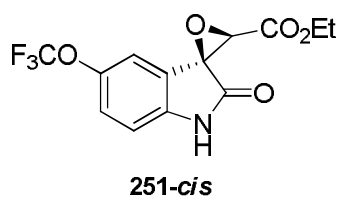
Following the above general procedure, *cis* diastereoisomer **250-cis** was obtained as a white solid in 20% yield after purification (*n*Hexane/EtOAc=1/1). ¹H-NMR (CDCl₃, 300 MHz, 25°C): □ □ 1.35 (t, 3H, *J* = 7.1 Hz, CH₃CH₂O); 4.18 (s, 1H, OCH); 4.25-4.43 (m, 2H, CH₃CH₂O); 6.77 (d, 1H, *J* = 8.2 Hz, CH_{arom}); 7.67 (d, 1H, *J* = 8.2 Hz, CH_{arom}); 7.76 (s, 1H, CH_{arom}); 8.81 (s, 1H, NH) ppm. ¹³CNMR (CDCl₃, 75 MHz, 25°C): □ □ 14.2 (CH₃), 60.1 (CO), 60.5 (CH₂), 62.4 (CH), 112.4 (C_{arom}), 123.3 (C_{arom}), 128.9 (C_{arom}), 131.3 (C_{arom}), 131.4 (C_{arom}), 140.9 (C_{arom}), 164.2 (OC=O), 170.7 (C=O) ppm. HRMS: exact mass calculated for (C₁₂H₁₀INNaO₄) requires *m/z* 381.9552, found *m/z* 381.9555. Chiral-phase HPLC analysis: [Daiacel Chiralpack IB 5μ, λ=254 nm, *n*Heptane/EtOH/DEA=70/30/0.1, flow rate 1.0mL/min]: τ_{major} = 5.46 min, τ_{minor} = 6.43 min *ee* = 18%. [α]_D = -2 (*c* = 0.0101 g/cm³ in CHCl₃)

(2'R,3'R)-ethyl 2-oxo-5-(trifluoromethoxy)spiro[indoline-3,2'-oxirane]-3'-carboxylate, 251-trans

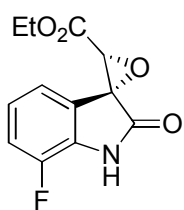


Following the above general procedure, *trans* diastereoisomer **251-trans** was obtained as a white solid in 29% yield after purification (*n*Hexane/EtOAc=7/3). IR (CHCl₃): $\tilde{\nu}$ = 3433, 3210, 3028, 1764, 1724, 1630, 1478, 1371, 1234, 1197 cm⁻¹. ¹H-NMR (CDCl₃, 300 MHz, 25°C): δ 1.31 (t, 3H, *J* = 7.0 Hz, CH₃CH₂O); 4.20 (s, 1H, OCH); 4.31 (q, 2H, *J* = 7.0 Hz, CH₃CH₂O); 6.97 (d, 1H, *J* = 8.4 Hz, CH_{arom}); 7.22-7.26 (m, 1H, CH_{arom}); 7.41 (s, 1H, CH_{arom}); 8.41 (bs, 1H, NH) ppm. ¹³CNMR (CDCl₃, 75 MHz, 25°C): δ 14.2 (CH₃), 60.1 (CO), 60.0 (CH₂), 62.7 (CH), 111.6 (C_{arom}), 119.6 (C_{arom}), 120.6 (q, *J*_{CF} = 256.0 Hz, CF₃), 121.3 (C_{arom}), 124.6 (C_{arom}), 141.3 (C_{arom}), 145.1 (C_{arom}), 165.3 (OC=O), 171.7 (C=O) ppm. HRMS: exact mass calculated for (C₁₃H₁₀F₃NNaO₅) requires *m/z* 340.0409, found *m/z* 340.0410. Chiral-phase HPLC analysis: [Daiacel Chiralpack IC 5 μ , λ =254 nm, *n*Hexane/EtOH=95/5, flow rate 1.0mL/min]: τ_{major} = 12.04 min, τ_{minor} = 9.15 min *ee* = 73%. [α]_D = -56.53 (*c* = 0.0168 g/cm³ in CHCl₃)

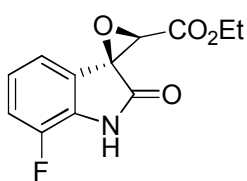
(2'S,3'R)-ethyl 2-oxo-5-(trifluoromethoxy)spiro[indoline-3,2'-oxirane]-3'-carboxylate, 251-cis



Following the above general procedure, *cis* diastereoisomer **251-cis** was obtained as a white solid in 47% yield after purification (*n*Hexane/EtOAc=7/3). IR (CHCl₃): $\tilde{\nu}$ = 3433, 3207, 3015, 1764, 1724, 1636, 1584, 1487, 1264, 1234 cm⁻¹. ¹H-NMR (CDCl₃, 300 MHz, 25°C): δ 1.35 (t, 3H, *J* = 7.0 Hz, CH₃CH₂O); 4.19 (s, 1H, OCH); 4.35 (q, 2H, *J* = 7.0 Hz, CH₃CH₂O); 6.99-7.01 (m, 2H, CH_{arom}); 7.23 (s, 1H, CH_{arom}); 8.57 (bs, 1H, NH) ppm. ¹³CNMR (CDCl₃, 75 MHz, 25°C): δ 14.2 (CH₃), 60.3 (CO), 60.5 (CH₂), 62.5 (CH), 112.4 (C_{arom}), 116.6 (C_{arom}), 120.6 (q, *J*_{CF} = 257.3 Hz, CF₃), 122.3 (C_{arom}), 124.7 (C_{arom}), 141.3 (C_{arom}), 145.1 (C_{arom}), 164.3 (OC=O), 171.3 (C=O) ppm. HRMS: exact mass calculated for (C₁₃H₁₀F₃NNaO₅) requires *m/z* 340.0409, found *m/z* 340.0410. Chiral-phase HPLC analysis: [Daiacel Chiralpack IB 5 μ , λ =254 nm, *n*Heptane/EtOH/DEA=70/30/0.1, flow rate 1.0mL/min]: τ_{major} = 4.44 min, τ_{minor} = 5.31 min *ee* = 32%. [α]_D = -20.7 (*c* = 0.0133 g/cm³ in CHCl₃)

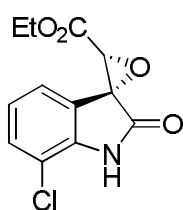
(2'R,3'R)-ethyl 7-fluoro-2-oxospiro[indoline-3,2'-oxirane]-3'-carboxylate, 252-trans**252-trans**

Following the above general procedure, *trans* diastereoisomer **252-trans** was obtained as a white solid in 21% yield after purification (*n*Hexane/EtOAc=8/2). IR (CHCl₃): $\tilde{\nu}$ = 3433, 3031, 2976, 2930, 1752, 1737, 1639, 1493, 1234, 1228 cm⁻¹. ¹H-NMR (CDCl₃, 300 MHz, 25°C): \square 1.30 (t, 3H, *J* = 7.0 Hz, CH₃CH₂O); 4.20 (s, 1H, OCH); 4.25-4.30 (m, 2H, CH₃CH₂O); 7.01-7.05 (m, 1H, CH_{arom}); 7.14 (t, 1H, *J* = 9.2 Hz, CH_{arom}); 7.28 (d, 1H, *J* = 9.2 Hz, CH_{arom}); 7.84 (s, 1H, NH) ppm. ¹³CNMR (CDCl₃, 75 MHz, 25°C): \square 14.3 (CH₃), 60.0 (CO), 60.1 (CH₂), 62.5 (CH), 118.4 (d, *J*_{CF} = 17 Hz, C_{arom}), 121.1 (d, *J*_{CF} = 3.6 Hz, C_{arom}), 122.2 (C_{arom}), 124.0 (d, *J*_{CF} = 5.9 Hz, C_{arom}), 129.9 (C_{arom}), 147.4 (d, *J*_{CF} = 244.7 Hz, C_{arom}), 165.3 (OC=O), 170.5 (C=O) ppm. HRMS: exact mass calculated for (C₁₂H₁₀FNNaO₄) requires *m/z* 274.0492, found *m/z* 274.0493. Chiral-phase HPLC analysis: [Daiacel Chiralpack IC 5 μ , λ =254 nm, *n*Hexane/EtOH=8/2, flow rate 1.0mL/min]: τ_{major} = 7.88 min, τ_{minor} = 8.60 min *ee* = 84%. [α]_D = -63.2 (*c* = 0.0150 g/cm³ in CHCl₃)

(2'S,3'R)-ethyl 7-fluoro-2-oxospiro[indoline-3,2'-oxirane]-3'-carboxylate, 252-cis**252-cis**

Following the above general procedure, *cis* diastereoisomer **252-cis** was obtained as a white solid in 72% yield after purification (*n*Hexane/EtOAc=8/2). IR (CHCl₃): $\tilde{\nu}$ = 3433, 3201, 3056, 2988, 1773, 1761, 1605, 1328, 1252 cm⁻¹. ¹H-NMR (CDCl₃, 300 MHz, 25°C): $\square\square$ 1.36 (t, 3H, *J* = 7.1 Hz, CH₃CH₂O); 4.18 (s, 1H, OCH); 4.36 (q, 2H, *J* = 7.1 Hz, CH₃CH₂O); 6.92 (d, 1H, *J* = 7.4 Hz, CH_{arom}); 7.01-7.17 (m, 2H, CH_{arom}); 8.42 (s, 1H, NH) ppm. ¹³CNMR (CDCl₃, 75 MHz, 25°C): \square 14.1 (CH₃), 60.3 (CO), 60.5 (CH₂), 62.4 (CH), 118.4 (d, *J*_{CF} = 8.6 Hz, C_{arom}), 118.6 (d, *J*_{CF} = 5.1 Hz, C_{arom}), 124.0 (C_{arom}), 124.2 (d, *J*_{CF} = 3.5 Hz, C_{arom}), 129.8 (d, *J*_{CF} = 13.2 Hz, C_{arom}), 147.5 (d, *J*_{CF} = 246.1 Hz, C_{arom}), 164.5 (OC=O), 170.6 (C=O) ppm. HRMS: exact mass calculated for (C₁₂H₁₀FNNaO₄) requires *m/z* 274.0492, found *m/z* 274.0493. Chiral-phase HPLC analysis: [Daiacel Chiralpack IB 5 μ , λ =254 nm, *n*Heptane/EtOH/DEA=70/30/0.1, flow rate 1.0 mL/min]: τ_{major} = 5.08 min, τ_{minor} = 5.78 min *ee* = 40%. [α]_D = -44.4 (*c* = 0.0291 g/cm³ in CHCl₃)

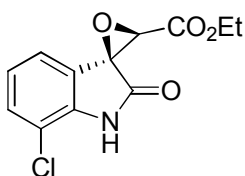
(2'R,3'R)-ethyl 7-chloro-2-oxospiro[indoline-3,2'-oxirane]-3'-carboxylate, 253-*trans*



253-*trans*

Following the above general procedure, *trans* diastereoisomer **253-*trans*** was obtained as a white solid in 35% yield after purification (*n*Hexane/EtOAc=7/3). IR (CHCl₃): $\tilde{\nu}$ = 3420, 3177, 3009, 1764, 1749, 1624, 1478, 1316, 1234, 1189 cm⁻¹. ¹H-NMR (CDCl₃, 300 MHz, 25°C): δ 1.29 (t, 3H, *J* = 6.8 Hz, CH₃CH₂O); 4.20-4.31 (m, 2H, CH₃CH₂O, OCH); 7.01 (t, 1H, *J* = 8.1 Hz, CH_{arom}); 7.36 (t, 2H, *J* = 8.1 Hz, CH_{arom}); 8.14 (s, 1H, NH) ppm. ¹³CNMR (CDCl₃, 75 MHz, 25°C): δ 14.2 (CH₃), 60.1 (CH₂), 60.7 (CO), 62.5 (CH), 116.3 (C_{arom}), 121.3 (C_{arom}), 123.6 (C_{arom}), 124.1 (C_{arom}), 131.1 (C_{arom}), 140.4 (C_{arom}), 165.3 (OC=O), 171.2 (C=O) ppm. HRMS: exact mass calculated for (C₁₂H₁₀ClNNaO₄) requires *m/z* 290.0196, found *m/z* 290.0197. Chiral-phase HPLC analysis: [Daiacel Chiralpack IC 5 μ , λ =254 nm, *n*Hexane/EtOH=8/2, flow rate 1.0mL/min]: τ_{major} = 7.72 min, τ_{minor} = 10.00 min *ee* = 76%. [α]_D = -186.6 (*c* = 0.0220 g/cm³ in CHCl₃)

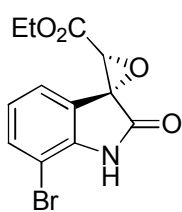
(2'S,3'R)-ethyl 7-chloro-2-oxospiro[indoline-3,2'-oxirane]-3'-carboxylate, 253-*cis*



253-*cis*

Following the above general procedure, *cis* diastereoisomer **253-*cis*** was obtained as a white solid in 63% yield after purification (*n*Hexane/EtOAc=7/3). IR (CHCl₃): $\tilde{\nu}$ = 3426, 3201, 3003, 1764, 1736, 1627, 1478, 1328, 1237, 1200 cm⁻¹. ¹H-NMR (CDCl₃, 300 MHz, 25°C): δ 1.35 (t, 3H, *J* = 7.1 Hz, CH₃CH₂O); 4.16 (s, 1H, OCH); 4.38 (q, 2H, *J* = 7.1 Hz, CH₃CH₂O); 7.03-7.05 (m, 2H, CH_{arom}); 7.35 (d, 1H, *J* = 7.4 Hz, CH_{arom}); 8.02 (s, 1H, NH) ppm. ¹³CNMR (CDCl₃, 75 MHz, 25°C): δ 14.2 (CH₃), 60.5 (CH₂), 60.6 (CO), 62.4 (CH), 116.4 (C_{arom}), 121.0 (C_{arom}), 123.1 (C_{arom}), 124.1 (C_{arom}), 131.2 (C_{arom}), 140.0 (C_{arom}), 164.3 (OC=O), 170.2 (C=O) ppm. HRMS: exact mass calculated for (C₁₂H₁₀ClNNaO₄) requires *m/z* 290.0196, found *m/z* 290.0197. Chiral-phase HPLC analysis: [Daiacel Chiralpack IB 5 μ , λ =254 nm, *n*Heptane/EtOH/DEA=70/30/0.1, flow rate 1.0mL/min]: τ_{major} = 5.24 min, τ_{minor} = 5.67 min *ee* = 24%. [α]_D = -27.9 (*c* = 0.0168 g/cm³ in CHCl₃)

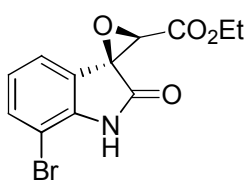
(2'R,3'R)-ethyl 7-bromo-2-oxospiro[indoline-3,2'-oxirane]-3'-carboxylate, 254-*trans*



254-*trans*

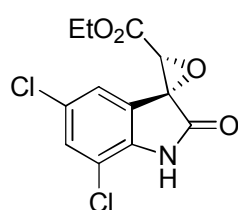
Following the above general procedure, *trans* diastereoisomer **254-*trans*** was obtained as a white solid in 49% yield after purification (*n*Hexane/EtOAc=7/3). IR (CHCl₃): $\tilde{\nu}$ = 3414, 3210, 3006, 1742, 1730, 1621, 1444, 1316, 1234 cm⁻¹. ¹H-NMR (CDCl₃, 300 MHz, 25°C): δ 1.29 (t, 3H, *J* = 7.1 Hz, CH₃CH₂O); 4.20 (s, 1H, OCH); 4.23-4.37 (m, 2H, CH₃CH₂O); 6.96 (t, 1H, *J* = 7.9 Hz, CH_{arom}); 7.42 (d, 1H, *J* = 7.9 Hz, CH_{arom}); 7.48 (d, 1H, *J* = 7.9 Hz, CH_{arom}); 8.06 (s, 1H, NH) ppm. ¹³CNMR (CDCl₃, 75 MHz, 25°C): δ 14.3 (CH₃), 60.1 (CH₂), 61.0 (CO), 62.6 (CH), 104.1 (C_{arom}), 121.4 (C_{arom}), 124.3 (C_{arom}), 124.5 (C_{arom}), 133.9 (C_{arom}), 141.9 (C_{arom}), 165.3 (OC=O), 170.5 (C=O) ppm. HRMS: exact mass calculated for (C₁₂H₁₀BrNNaO₄) requires *m/z* 333.9691, found *m/z* 333.9693. Chiral-phase HPLC analysis: [Daiacel Chiralpack IC 5 μ , λ =254 nm, *n*Hexane/EtOH=7/3, flow rate 1.0mL/min]: τ_{major} = 6.14 min, τ_{minor} = 7.18 min *ee* = 83%. [α]_D = -15.85 (*c* = 0.0132 g/cm³ in CHCl₃)

(2'S,3'R)-ethyl 7-bromo-2-oxospiro[indoline-3,2'-oxirane]-3'-carboxylate, 254-*cis*

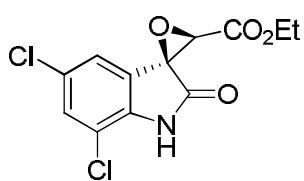


254-*cis*

Following the above general procedure, *cis* diastereoisomer **254-*cis*** was obtained as a white solid in 38% yield after purification (*n*Hexane/EtOAc=7/3). IR (CHCl₃): $\tilde{\nu}$ = 3414, 3210, 3006, 1742, 1730, 1621, 1444, 1316, 1234 cm⁻¹. ¹H-NMR (CDCl₃, 300 MHz, 25°C): δ 1.35 (t, 3H, *J* = 6.9 Hz, CH₃CH₂O); 4.16 (s, 1H, OCH); 4.36 (q, 2H, *J* = 6.9 Hz, CH₃CH₂O); 6.97-7.07 (m, 2H, CH_{arom}); 7.49 (d, 1H, *J* = 7.8 Hz, CH_{arom}); 7.66 (s, 1H, NH) ppm. ¹³CNMR (CDCl₃, 75 MHz, 25°C): δ 14.2 (CH₃), 60.7 (CH₂), 60.9 (CO), 62.4 (CH), 104.2 (C_{arom}), 121.7 (C_{arom}), 123.2 (C_{arom}), 124.4 (C_{arom}), 134.0 (C_{arom}), 141.6 (C_{arom}), 164.2 (OC=O), 169.5 (C=O) ppm. HRMS: exact mass calculated for (C₁₂H₁₀BrNNaO₄) requires *m/z* 333.9691, found *m/z* 333.9693. Chiral-phase HPLC analysis: [Daiacel Chiralpack IC 5 μ , λ =254 nm, *n*Hexane/EtOH=8/2, flow rate 1.0mL/min]: τ_{major} = 13.98 min, τ_{minor} = 12.80 min *ee* = 29%. [α]_D = -32.92 (*c* = 0.0120 g/cm³ in CHCl₃)

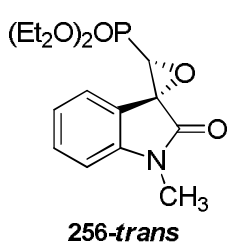
(2'R,3'R)-ethyl 5,7-dichloro-2-oxospiro[indoline-3,2'-oxirane]-3'-carboxylate, 255-*trans***255-*trans***

Following the above general procedure, *trans* diastereoisomer **255-*trans*** was obtained as a white solid in 27% yield after purification (*n*Hexane/EtOAc=7/3). IR (CHCl₃): $\tilde{\nu}$ = 3423, 3031, 3009, 1757, 1743, 1463, 1323, 1290 cm⁻¹. ¹H-NMR (CDCl₃, 300 MHz, 25°C): □□ 1.32 (t, *J* = 7.0 Hz, 3H, CH₃CH₂O); 4.18-4.36 (m, 3H, CH₃CH₂O, OCH); 7.38 (s, 1H, CH_{arom}); 7.42 (s, 1H, CH_{arom}); 8.09 (s, 1H, NH) ppm. ¹³CNMR (CDCl₃, 75 MHz, 25°C): □ 14.3 (CH₃), 60.1 (CH₂), 60.4 (CO), 62.9 (CH), 116.6 (C_{arom}), 122.4 (C_{arom}), 124.4 (C_{arom}), 129.3 (C_{arom}), 130.8 (C_{arom}), 138.9 (C_{arom}), 165.1 (OC=O), 170.1 (C=O) ppm. HRMS: exact mass calculated for (C₁₂H₉Cl₂NNaO₄) requires *m/z* 323.9806, found *m/z* 323.9808. Chiral-phase HPLC analysis: [Daiacel Chiralpack IC 5μ, λ=254 nm, *n*Hexane/EtOH=7/3, flow rate 1.0mL/min]: τ_{major} = 5.52 min, τ_{minor} = 6.34 min *ee* = 65%. [α]_D = +137 (*c* = 0.0090 g/cm³ in CHCl₃)

(2'S,3'R)-ethyl 5,7-dichloro-2-oxospiro[indoline-3,2'-oxirane]-3'-carboxylate, 255-*cis***255-*cis***

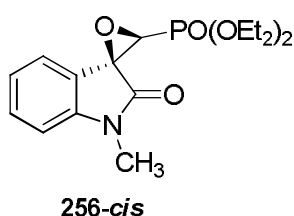
Following the above general procedure, *cis* diastereoisomer **255-*cis*** was obtained as a white solid in 51% yield after purification (*n*Hexane/EtOAc=7/3). IR (CHCl₃): $\tilde{\nu}$ = 3423, 3031, 3003, 1765, 1740, 1706, 1633, 1469, 1315 cm⁻¹. ¹H-NMR (CDCl₃, 300 MHz, 25°C): □□ 1.35 (t, *J* = 7.2 Hz, 3H, CH₃CH₂O); 4.16 (s, OCH); 4.35 (q, *J* = 6.6 Hz, 2H, CH₃CH₂O); 7.01 (s, 1H, CH_{arom}); 7.37 (s, 1H, CH_{arom}); 8.31 (s, 1H, NH) ppm. ¹³CNMR (CDCl₃, 75 MHz, 25°C): □□ 14.2 (CH₃), 60.1 (CH₂), 60.6 (CO), 62.6 (CH), 116.8 (C_{arom}), 121.8 (C_{arom}), 124.4 (C_{arom}), 129.2 (C_{arom}), 130.9 (C_{arom}), 138.6 (C_{arom}), 163.8 (OC=O), 169.3 (C=O) ppm. HRMS: exact mass calculated for (C₁₂H₉Cl₂NNaO₄) requires *m/z* 323.9806, found *m/z* 323.9808. Chiral-phase HPLC analysis: [Daiacel Chiralpack IC 5μ, λ=254 nm, *n*Hexane/EtOH=9/1, flow rate 1.0mL/min]: τ_{major} = 20.84 min, τ_{minor} = 19.81 min *ee* = 72%. [α]_D = +10 (*c* = 0.0100 g/cm³ in CHCl₃)

diethyl ((2'S,3'S)-1-methyl-2-oxospiro[indoline-3,2'-oxiran]-3'-yl)phosphonate, 256-trans



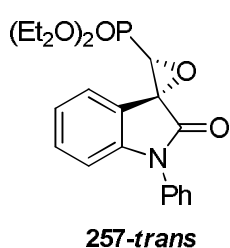
Following the above general procedure, *trans* diastereoisomer **256-trans** was obtained as a pale yellow solid in 45% yield after purification (*n*Hexane/EtOAc=4/6).¹ IR (CHCl₃): $\tilde{\nu}$ = 1725, 1236 cm⁻¹. ¹H-NMR (CDCl₃, 300 MHz, 25°C): δ 1.21 [t, *J* = 7.0 Hz, 3H, (CH₃CH₂O)₂P], 1.41 [t, *J* = 7.1 Hz, 3H, (CH₃CH₂O)₂P], 3.26 (s, 3H, NCH₃), 3.73 (d, *J*_{HP} = 27.6 Hz, 1H, OCH), 3.95–4.14 [m, 2H, (CH₃CH₂O)₂P], 4.20–4.37 [m, 2H, (CH₃CH₂O)₂P], 6.90 (d, *J* = 7.9 Hz, 1H, CH_{arom}), 7.1 (dt, *J* = 7.7, 1.0 Hz, 1H, CH_{arom}), 7.39 (dt, *J* = 7.9, 1.3 Hz, 1H, CH_{arom}), 7.99 (d, *J* = 7.7 Hz, 1H, CH_{arom}) ppm. Chiral-phase HPLC analysis: [Daiacel Chiralpack IB 5 μ , λ =254 nm, *n*Hexane/*i*PrOH=9/1, flow rate 1.0mL/min]: *T*_{major} = 42.20 min, *T*_{minor} = 23.60 min *ee* = 60%. [α]_D = -2 (*c* = 0.0101 g/cm³ in CHCl₃)

diethyl ((2'S,3'R)-1-methyl-2-oxospiro[indoline-3,2'-oxiran]-3'-yl)phosphonate, 256-cis



Following the above general procedure, *cis* diastereoisomer **256-cis** was obtained as a pale yellow solid in 35% yield after purification (*n*Hexane/EtOAc=4/6).¹ ¹H-NMR (CDCl₃, 300 MHz, 25°C): δ 1.35–1.43 [m, 6H, (CH₃CH₂O)₂P], 3.26 (s, 3H, NCH₃), 3.71 (d, *J*_{H,P} = 27.4 Hz, 1H, OCH), 4.18–4.48 [m, 4H, (CH₃CH₂O)₂P], 6.89 (d, *J* = 7.9 Hz, 1H, CH_{arom}), 7.04–7.08 (m, 2H, CH_{arom}), 7.35–7.44 (m, 1H, CH_{arom}) ppm. Chiral-phase HPLC analysis: [Daiacel Chiralpack IB 5 μ , λ =254 nm, *n*Hexane/*i*PrOH=9/1, flow rate 1.0mL/min]: *T*_{major} = 16.50 min, *T*_{minor} = 12.80 min *ee* = 21%. [α]_D = -19.45 (*c* = 0.0098 g/cm³ in CHCl₃)

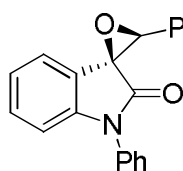
diethyl ((2'S,3'S)-1-phenyl-2-oxospiro[indoline-3,2'-oxiran]-3'-yl)phosphonate, 257-trans



Following the above general procedure, *trans* diastereoisomer **257-trans** was obtained as a pale yellow solid in 57% yield after purification (*n*Hexane/EtOAc=1/1).¹ IR (CHCl₃): $\tilde{\nu}$ = 1716, 1265 cm⁻¹. ¹H-NMR (CDCl₃, 300 MHz, 25°C): δ 1.18 [t, *J* = 7.1 Hz,

3H, (CH₃CH₂O)₂P], 1.34 [t, *J* = 7.1 Hz, 3H, (CH₃CH₂O)₂P], 3.76 (d, *J*_{H,P} = 27.6 Hz, 1H, OCH), 4.00–4.08 [m, 2H, (CH₃CH₂O)₂P], 4.18–4.33 [m, 2H, (CH₃CH₂-O)₂P], 6.77 (d, *J* = 7.6 Hz, 1H, CH_{arom}), 7.05 (t, *J* = 7.6 Hz, 1H, CH_{arom}), 7.22 (t, *J* = 7.6 Hz, 1H, CH_{arom}), 7.35–7.46 (m, 5H, CH_{arom}), 7.96 (d, *J* = 7.6 Hz, 1H, CH_{arom}) ppm. Chiral-phase HPLC analysis: [Daiacel Chiralpack IB 5μ, λ = 254 nm, *n*Hexane/*i*PrOH = 9/1, flow rate 1.0 mL/min]: *T*_{major} = 39.90 min, *T*_{minor} = 17.50 min *ee* = 58%. [α]_D = -6.7 (*c* = 0.0122 g/cm³ in CHCl₃)

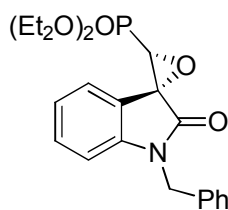
diethyl ((2'S,3'R)-1-phenyl-2-oxospiro[indoline-3,2'-oxiran]-3'-yl)phosphonate, 257-*cis*



257-*cis*

Following the above general procedure, *cis* diastereoisomer **257-*cis*** was obtained as a pale yellow solid in 36% yield after purification (*n*Hexane/EtOAc = 1/1).¹ ¹H-NMR (CDCl₃, 300 MHz, 25°C): □□ 1.33–1.42 [m, 6H, (CH₃CH₂O)₂P], 3.79 (d, *J*_{H,P} = 27.3 Hz, 1H, OCH), 4.18–4.45 [m, 4H, (CH₃CH₂O)₂P], 6.86 (d, *J* = 7.9 Hz, 1H, CH_{arom}), 7.05–7.14 (m, 2H, CH_{arom}), 7.28–7.39 (m, 1H, CH_{arom}), 7.40–7.57 (m, 5H, CH_{arom}) ppm. Chiral-phase HPLC analysis: [Daiacel Chiralpack IB 5μ, λ = 254 nm, *n*Hexane/*i*PrOH = 9/1, flow rate 1.0 mL/min]: *T*_{major} = 12.40 min, *T*_{minor} = 9.29 min *ee* = 24%. [α]_D = -20.5 (*c* = 0.0047 g/cm³ in CHCl₃)

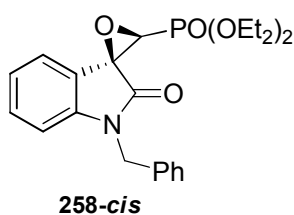
diethyl ((2'S,3'S)-1-benzyl-2-oxospiro[indoline-3,2'-oxiran]-3'-yl)phosphonate, 258-*trans*



258-*trans*

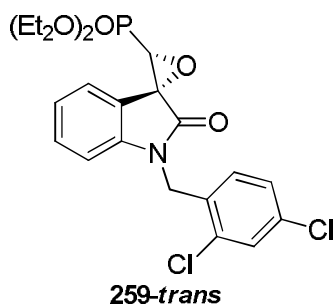
Following the above general procedure, *trans* diastereoisomer **258-*trans*** was obtained as a yellow solid in 45% yield after purification (*n*Hexane/EtOAc = 1/1).¹ IR (CHCl₃): $\tilde{\nu}$ = 1731, 1262 cm⁻¹. ¹H-NMR (CDCl₃, 300 MHz, 25°C): □ 1.22 [t, *J* = 7.1 Hz, 3H, (CH₃CH₂O)₂P], 1.43 [t, *J* = 7.1 Hz, 3H, (CH₃CH₂O)₂P], 3.81 (d, *J*_{H,P} = 27.4 Hz, 1H, OCH), 4.02–4.14 [m, 2H, (CH₃CH₂O)₂P], 4.24–4.39 [m, 2H, (CH₃CH₂-O)₂P], 4.96 (s, 2H, CH₂N), 6.81 (d, *J* = 7.6 Hz, 1H, CH_{arom}), 7.07 (t, *J* = 7.6 Hz, 1H, CH_{arom}), 7.24–7.36 (m, 6H, CH_{arom}), 8.00 (d, *J* = 7.6 Hz, 1H, CH_{arom}) ppm. Chiral-phase HPLC analysis: [Daiacel Chiralpack IB 5μ, λ = 254 nm, *n*Hexane/*i*PrOH = 9/1, flow rate 1.0 mL/min]: *T*_{major} = 39.90 min, *T*_{minor} = 17.50 min *ee* = 58%. [α]_D = -6.7 (*c* = 0.0122 g/cm³ in CHCl₃)

diethyl ((2'S,3'R)-1-benzyl-2-oxospiro[indoline-3,2'-oxiran]-3'-yl)phosphonate, 258-*cis*



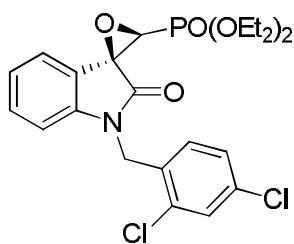
Following the above general procedure, *cis* diastereoisomer **258-*cis*** was obtained as a yellow solid in 35% yield after purification (*n*Hexane/EtOAc=1/1).¹ ¹H-NMR (CDCl₃, 300 MHz, 25°C): □ 1.33 [t, *J* = 7.1 Hz, 6H (CH₃CH₂O)₂P], 3.69 (d, *J*_{H,P} = 27.6 Hz, 1H, OCH), 4.14–4.40 [m, 4H, (CH₃CH₂O)₂P], 4.90 (s, 2H, CH₂N), 6.71 (d, *J* = 7.8 Hz, 1H, CH_{arom}), 6.92–7.02 (m, 2H, CH_{arom}), 7.16–7.30 (m, 6H, CH_{arom}) ppm. Chiral-phase HPLC analysis: [Daiacel Chiralpack IB 5μ, λ=254 nm, *n*Hexane/*i*PrOH=9/1, flow rate 1.0mL/min]: *T*_{major} = 10.00 min, *T*_{minor} = 12.10 min *ee* = 9%. [α]_D = -10.7 (*c* = 0.0053 g/cm³ in CHCl₃)

(2'S,3'S)-1-(2,4-dichlorobenzyl)-2-oxospiro[indoline-3,2'-oxiran]-3'-yl)phosphonate, 259-*trans*



Following the above general procedure, *trans* diastereoisomer **259-*trans*** was obtained as a pale yellow solid in 54% yield after purification (*n*Hexane/EtOAc=1/1).¹ IR (CHCl₃): $\tilde{\nu}$ = 1733, 1253 cm⁻¹. ¹H-NMR (CDCl₃, 300 MHz, 25°C): □□ 1.23 [t, *J* = 7.1 Hz, 3H, (CH₃CH₂O)₂P], 1.42 [t, *J* = 7.1 Hz, 3H, (CH₃CH₂O)₂P], 3.81 (d, *J*_{H,P} = 27.4 Hz, 1H, OCH), 3.97–4.19 [m, 2H, (CH₃CH₂O)₂P], 4.22–4.39 [m, 2H, (CH₃CH₂O)₂P], 5.03 (s, 2H, CH₂N), 6.73 (d, *J* = 7.9 Hz, 1H, CH_{arom}), 7.05–7.20 (m, 3H, CH_{arom}), 7.30–7.34 (m, 3H, CH_{arom}), 7.43 (d, *J* = 1.9 Hz, 1H, CH_{arom}), 8.00 (d, *J* = 7.6 Hz, 1H, CH_{arom}) ppm. Chiral-phase HPLC analysis: [Daiacel Chiralpack IB 5μ, λ=254 nm, *n*Hexane/*i*PrOH=9/1, flow rate 1.0mL/min]: *T*_{major} = 26.20 min, *T*_{minor} = 16.80 min *ee* = 44%. [α]_D = -20.4 (*c* = 0.0091 g/cm³ in CHCl₃)

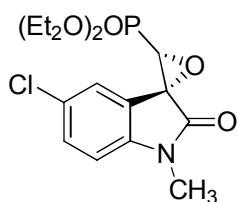
(2'S,3'R)-1-(2,4-dichlorobenzyl)-2-oxospiro[indoline-3,2'-oxiran]-3'-yl)phosphonate, 259-cis



259-cis

Following the above general procedure, *cis* diastereoisomer **259-cis** was obtained as a pale yellow solid in 29% yield after purification (*n*Hexane/EtOAc=1/1).¹ ¹H-NMR (CDCl₃, 300 MHz, 25°C): □□ 1.50 [t, *J* = 7.1 Hz, 6H (CH₃CH₂O)₂P], 3.87 (d, *J*_{H,P} = 27.6 Hz, 1H, OCH), 4.21–4.57 [m, 4H, (CH₃CH₂O)₂P], 5.15 (s, 2H, CH₂N), 6.83 (d, *J* = 7.2 Hz, 1H, CH_{arom}), 7.14–7.52 (m, 6H, CH_{arom}) ppm. Chiral-phase HPLC analysis: [Daiacel Chiralpack IB 5μ, λ=254 nm, *n*Hexane/*i*PrOH=9/1, flow rate 1.0mL/min]: *T*_{major} = 11.00 min, *T*_{minor} = 9.90 min *ee* = 10%. [α]_D = -5.32 (*c* = 0.0064 g/cm³ in CHCl₃)

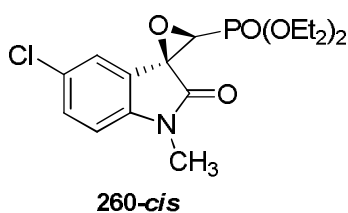
(2'S,3'S)-5-chloro-1-methyl-2-oxospiro[indoline-3,2'-oxiran]-3'-yl)phosphonate, 260-trans



260-trans

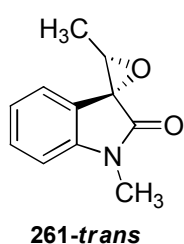
Following the above general procedure, *trans* diastereoisomer **260-trans** was obtained as a white solid in 38% yield after purification (*n*Hexane/EtOAc=1/1). IR (CHCl₃): $\tilde{\nu}$ = 1734, 1260 cm⁻¹. ¹H-NMR (CDCl₃, 300 MHz, 25°C): □ 1.26 [t, *J* = 7.0 Hz, 3H, (CH₃CH₂O)₂P], 1.42 [t, *J* = 7.0 Hz, 3H, (CH₃CH₂O)₂P], 3.26 (s, 3H, NCH₃); 3.73 (d, *J*_{HP} = 26.6 Hz, 1H, OCH), 4.05–4.18 [m, 2H, (CH₃CH₂O)₂P], 4.25–4.34 [m, 2H, (CH₃CH₂-O)₂P], 6.83 (d, *J* = 8.3 Hz, 1H, CH_{arom}), 7.38 (d, *J* = 8.3 Hz, 1H, CH_{arom}), 8.02 (s, 2H, CH_{arom}) ppm. ¹³CNMR (CDCl₃, 75 MHz, 25°C): □□ 16.4 [(CH₃), d, *J*_{CP} = 5.9 Hz], 16.6 (d, *J*_{CP} = 5.6 Hz), 27.1 (NCH₃), 58.1 (d, *J*_{CP} = 203.4 Hz), 59.9, 63.3 (d, *J*_{CP} = 6.3 Hz), 63.8 (d, *J*_{CP} = 6.1 Hz), 109.8 (C_{arom}), 121.2 (C_{arom}), 127.5 (C_{arom}), 128.8 (C_{arom}), 131.0 (C_{arom}), 144.3 (C_{arom}), 170.4 (C=O) ppm. HRMS: exact mass calculated for (C₁₄H₁₇ClNNaO₅P) requires *m/z* 368.0431, found *m/z* 368.0433. Chiral-phase HPLC analysis: [Daiacel Chiralpack IC 5μ, λ=254 nm, *n*Hexane/EtOH=9/1, flow rate 1.0mL/min]: *T*_{major} = 18.92 min, *T*_{minor} = 17.56 min *ee* = 52%. [α]_D = +4 (*c* = 0.0170 g/cm³ in CHCl₃)

(2'S,3'R)- 5-chloro-1-methyl-2-oxospiro[indoline-3,2'-oxiran]-3'-yl)phosphonate, 260-cis

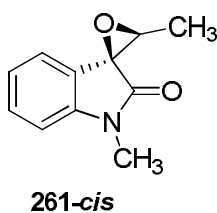


Following the above general procedure, *cis* diastereoisomer **260-cis** was obtained as a pale yellow solid in 58% yield after purification (*n*Hexane/EtOAc=1/1). IR (CHCl₃): $\tilde{\nu}$ = 1752, 1258 cm⁻¹. ¹H-NMR (CDCl₃, 300 MHz, 25°C): δ 1.59-1.65 [m, 6H (CH₃CH₂O)₂P], 3.48 (s, 3H, NCH₃); 3.92 (d, *J*_{H,P} = 27.0 Hz, 1H, OCH), 4.44–4.68 [m, 4H, (CH₃CH₂O)₂P], 7.05 (d, *J* = 7.9 Hz, 1H, CH_{arom}), 7.50–7.60 (m, 2H, CH_{arom}) ppm. ¹³CNMR (CDCl₃, 75 MHz, 25°C): δ 16.4 [(CH₃), t, *J*_{CP} = 6.3 Hz], 27.0 (NCH₃), 60.0 (d, *J*_{CP} = 200.7 Hz), 60.6, 62.8 (d, *J*_{CP} = 6.5 Hz), 64.4 (d, *J*_{CP} = 6.6 Hz), 122.5 (C_{arom}), 125.8 [(C_{arom}), d, *J*_{CP} = 27.0 Hz], 126.5 [(C_{arom}), d, *J*_{CP} = 9.2 Hz], 128.2 [(C_{arom}), d, *J*_{CP} = 20.0 Hz], 131.0 (C_{arom}), 143.7 (C_{arom}), 168.5 (C=O) ppm. HRMS: exact mass calculated for (C₁₄H₁₇CINNaO₅P) requires *m/z* 368.0431, found *m/z* 368.0433. Chiral-phase HPLC analysis: [Daiacel Chiralpack IC 5 μ , λ =254 nm, *n*Hexane/EtOH=85/15, flow rate 1.0mL/min]: *T*_{major} = 32.17 min, *T*_{minor} = 30.15 min *ee* = 10%. [α]_D = -1 (*c* = 0.0060 g/cm³ in CHCl₃)

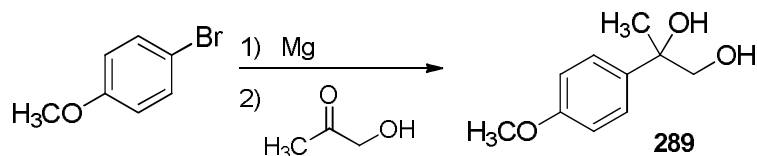
(2'R,3'S)-1,3'-dimethylspiro[indoline-3,2'-oxiran]-2-one, 261-trans



Following the above general procedure, *trans* diastereoisomer **261-trans** was obtained as a pale yellow oil in 57% yield after purification (*n*Hexane/EtOAc=8/2). IR (CHCl₃): $\tilde{\nu}$ = 1725, 1617, 1469, 1374, 1258 cm⁻¹. ¹H-NMR (CDCl₃, 300 MHz, 25°C): δ 1.60 (d, *J* = 5.0 Hz, 3H, CH₃CH); 3.27 (s, 3H, NCH₃); 3.77 (q, *J* = 5.0 Hz, 1H, OCH), 6.94 (d, *J* = 7.9 Hz, 1H, CH_{arom}), 7.10 (d, *J* = 7.7 Hz, 1H, CH_{arom}), 7.40 (t, *J* = 7.5 Hz, 1H, CH_{arom}) ppm. ¹³CNMR (CDCl₃, 75 MHz, 25°C): δ 13.8 (CH₃), 26.7 (NCH₃), 60.6, 61.5, 108.9 (C_{arom}), 121.6 (C_{arom}), 122.6 (C_{arom}), 124.1 (C_{arom}), 130.1 (C_{arom}), 145.5 (C_{arom}), 172.7 (C=O) ppm. HRMS: exact mass calculated for (C₁₁H₁₁NNaO₂) requires *m/z* 212.0687, found *m/z* 212.0689. Chiral-phase HPLC analysis: [Daiacel Chiralpack IC 5 μ , λ =254 nm, *n*Hexane/EtOH=70/30, flow rate 1.0mL/min]: *T*_{major} = 10.61 min, *T*_{minor} = 9.90 min *ee* = 72%. [α]_D = -1 (*c* = 0.0133 g/cm³ in CHCl₃)

(2'S,3'S)-1,3'-dimethylspiro[indoline-3,2'-oxiran]-2-one, 261-*cis*

Following the above general procedure, *cis* diastereoisomer **261-*cis*** was obtained as a pale yellow oil in 42% yield after purification (*n*Hexane/EtOAc=8/2). IR (CHCl₃): $\tilde{\nu}$ = 1725, 1618, 1465, 1377, 1224 cm⁻¹. ¹H-NMR (CDCl₃, 300 MHz, 25°C): δ 1.73 (d, *J* = 5.1 Hz, 3H, CH₃CH); 3.27 (s, 3H, NCH₃); 3.75 (q, *J* = 4.8 Hz, 1H, OCH), 6.90 (d, *J* = 7.7 Hz, 1H, CH_{arom}), 7.07-7.08 (m, 2H, CH_{arom}), 7.34-7.39 (m, 1H, CH_{arom}) ppm. ¹³CNMR (CDCl₃, 75 MHz, 25°C): 12.4 (CH₃), 26.8 (NCH₃), 59.9, 63.4, 108.7 (C_{arom}), 121.8 (C_{arom}), 122.9 (C_{arom}), 124.3 (C_{arom}), 130.1 (C_{arom}), 144.6 (C_{arom}), 171.8 (C=O) ppm. HRMS: exact mass calculated for (C₁₁H₁₁NNaO₂) requires *m/z* 212.0687, found *m/z* 212.0689. Chiral-phase HPLC analysis: [Daiacel Chiralpack IB 5 μ , λ =254 nm, *n*Hexane/EtOH=90/10, flow rate 1.0mL/min]: *T*_{major} = 7.86 min, *T*_{minor} = 7.23 min *ee* = 48%. [α]_D = +1 (*c* = 0.0054 g/cm³ in CHCl₃)

General procedure for the synthesis of 1,2-diols 277, 284-290 (procedure 1)**1) Preparation of the Grignard reagent**

A solution of 4-Bromoanisole (3.74 g, 20.0 mmol) in dry THF (2 ml) was added to activated magnesium turnings^a (0.48 g, 20 mmol) under dry atmosphere. The exothermic reaction mixture was kept at room temperature.^b After heat development ceased, the mixture was diluted with dry THF (8 ml) and the resulting solution (calculated ca. 2 mmol/ml) was used immediately.

2) Addition to hydroxyketones

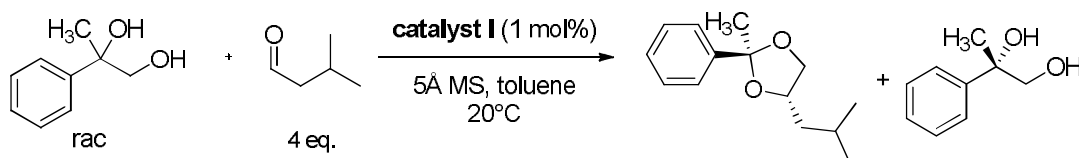
A solution of Grignard reagent prepared above (2 mL, 4 mmol) was added dropwise to an ice-cooled solution of hydroxyketone in THF (8 mL, 2 mmol). The reaction mixture was allowed to reach room temperature and after completion^c was quenched at 0 °C with concentrated aqueous NH₄Cl (2 ml). The aqueous phase was extracted with ethyl acetate (4 x 20 ml); the combined organic extracts were dried over MgSO₄, filtered and concentrated under reduced pressure directly before purification. Flash chromatography

on silica gel yielded pure products, which were stored at -20 °C or directly used for the kinetic resolution.

Notes:

- Activation was performed with a few drops of 1,2-dibromoethane.
- If there is no exothermic reaction at this point, initiation is performed by adding more 1,2-dibromoethane and fast heating (with a heat gun) and cooling to 25 °C (repeated until reaction becomes exothermic after cooling).
- completion was observed through TLC visualization: UV (254 nm) and/or PMA stain.

General procedure for kinetic resolution of diols (procedure 2)



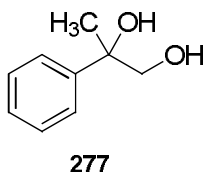
Isovaleraldehyde (0.8 mmol) was added dropwise to the solution of diol (0.2 mmol), molecular sieves (20 mg) and catalyst (0.002 mmol) in dry toluene (2 mL) and stirred at 20 °C. Then Et₃N (28mL) was added to the reaction mixture near 50% conversion of the starting material (in most cases within 6-20 h).^a The reaction mixture was concentrated under reduced pressure and purified via flash chromatography eluting with a gradient 1% EtOAc/Hexane to 40% EtOAc/Hexane, to isolate the product and the starting material.

Note:

For small scale reaction, conversion was observed through TLC visualization: UV (254 nm) and/or PMA stain and checked by measuring enantiomeric excess of the diol during time. For larger scale reactions, the reaction was performed in a vial with septum and directly quenched after a pre-determined time.

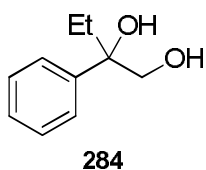
Characterization of diols 277, 284-290

2-Phenylpropane-1,2-diol, 277



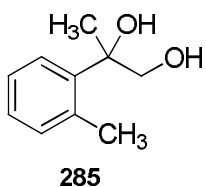
Following the above general procedure (procedure 1), **277** was obtained as a pale yellow oil in 90% yield after purification (DCM/MeOH=98/2) following procedure 1.¹¹⁶ ¹H NMR (500 MHz, CDCl₃) δ 1.52 (s, 3H, CH₃), 2.01 (brs, 1H, OH), 2.70 (brs, 1H, OH), 3.70 (m, 2H, CH₂), 7.27 (t, *J* = 7.3 Hz, 1 H, CH_{arom}), 7.36 (m, 2H, CH_{arom}), 7.45 (d, *J* = 7.3 Hz, 2H, CH_{arom}) ppm. ¹³C NMR (500 MHz, CDCl₃): □ 26.1 (CH₃), 71.1 (CH₂), 74.8 (C), 125.1 (C_{arom}), 127.2 (C_{arom}), 128.4 (C_{arom}), 144.9 (C_{arom}) ppm. MS: *m/z*=152.1 [M⁺]. Enantioenriched diol was obtained following procedure 2. Chiral-phase HPLC analysis: [Column OD3, 5μ, λ=210 nm, *n*Heptane/*i*PrOH=95/5, flow rate 1.0mL/min]: *T*_{major} = 10.03 min, *T*_{minor} = 9.36 min, *ee* = 96%.

2-Phenylbutane-1,2-diol, 284



Following the above general procedure (procedure 1), **284** was obtained as a colourless oil in 43% yield after purification (hexane/EtOAc=1/1).¹¹⁷ ¹H NMR (500 MHz, C₆D₆) δ 0.73 (t, *J* = 7.43 Hz, 3H, CH₃), 0.97 (brs, 1H, OH), 2.24 (s, 1H, OH), 3.40 (m, 2H, (CH₂), 7.08 (t, *J*=7.29 Hz, 1H, CH_{arom}), 7.17 (t, *J* = 7.3 Hz, 2H, CH_{arom}), 7.29 (d, *J* = 7.3 Hz, 2H, CH_{arom}); ¹³C NMR (500 MHz, C₆D₆): □ 17.6 (CH₃), 31.44 (CH₃CH₂), 70.6 (C), 77.1 (CH₂), 126.0 (C_{arom}), 126.9 (C_{arom}), 128.4 (C_{arom}), 144.2 (C_{arom}) ppm. Enantioenriched diol was obtained following procedure 2. Chiral-phase HPLC analysis: [Column OD3, 5μ, λ=210 nm, *n*Heptane/*i*PrOH=95/5, flow rate 1.0mL/min]: *T*_{major} = 8.09 min, *T*_{minor} = 7.42 min, *ee* = 99%. [α]_D = -1.87 (*c* = 0.0220 g/cm³ in CHCl₃)

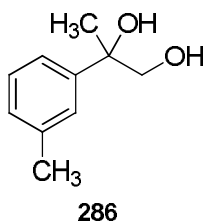
2-(2-methylphenyl)-propane-1,2-diol, 285



Following the above general procedure (procedure 1), **285** was obtained as a colourless oil in 88% yield after purification (hexane/EtOAc=1/1).¹¹⁸ ¹H NMR (500 MHz, CDCl₃) δ 1.61 (s, 3H, CH₃), 1.83 (brs, 1H, OH), 2.56 (s, 3H, CH₃), 3.87 (m, 2H, CH₂), 7.18 (m, 3H, CH_{arom}), 7.45 (m, 1H, CH_{arom}); MS: *m/z*=166.2 [M⁺]. Enantioenriched diol was obtained following procedure 2. Chiral-phase HPLC analysis: [Column OD3, 5μ, λ=210

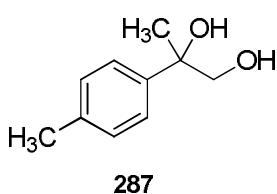
nm, *n*Heptane/*i*PrOH=95/5, flow rate 1.0mL/min]: $T_{major} = 9.15$ min, $T_{minor} = 8.32$ min, $ee = 96\%$.

2-(3-methylphenyl)-propane-1,2-diol, **286**



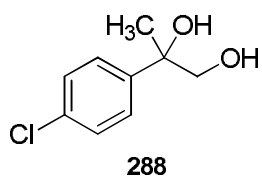
Following the above general procedure (procedure 1), **286** was obtained as a colourless oil in 70% yield after purification (hexane/EtOAc=1/1).¹¹⁹ ^1H NMR (500 MHz, CDCl_3) δ 1.53 (s, 3H, CH_3), 1.70 (brs, 1H, OH), 2.38 (s, 3H, CH_3), 2.51 (brs, 1H, OH), 3.72 (m, 2H, CH_2), 7.10 (d, $J = 6.8$ Hz, 1H, CH_{arom}), 7.26 (m, 3H, CH_{arom}); MS: $m/z=166.2$ [M^+]. Enantioenriched diol was obtained following procedure 2. Chiral-phase HPLC analysis: [Column OD3, 5μ , $\lambda=210$ nm, *n*Heptane/*i*PrOH=95/5, flow rate 1.0mL/min]: $T_{major} = 8.04$ min, $T_{minor} = 7.45$ min, $ee = 94\%$

2-(4-methylphenyl)-propane-1,2-diol, **287**

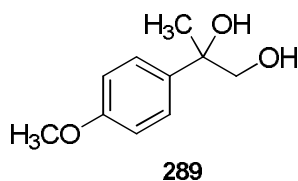


Following the above general procedure (procedure 1), **287** was obtained as a colourless oil in 50% yield after purification (hexane/EtOAc=4/6). ^1H NMR (500 MHz, CDCl_3) δ 1.53 (s, 3H, CH_3), 1.74 (brs, 2H, 2xOH), 2.35 (s, 3H, CH_3), 3.71 (m, 2H, CH_2), 7.19 (d, $J = 8.1$ Hz, 2H, CH_{arom}), 7.35 (d, $J = 7.8$ Hz, 2H, CH_{arom}); MS: $m/z=166.2$ [M^+] Enantioenriched diol was obtained following procedure 2. Chiral-phase HPLC analysis: [Column OD3, 5μ , $\lambda=210$ nm, *n*Heptane/*i*PrOH=95/5, flow rate 1.0mL/min]: $T_{major} = 9.98$ min, $T_{minor} = 9.14$ min, $ee = 96\%$.

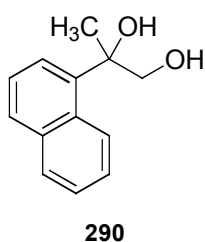
2-(4-chlorophenyl)-propane-1,2-diol, **288**



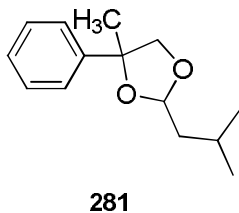
Following the above general procedure, **288** was obtained as a colourless oil in 65% yield after purification (DCM/MeOH=95/5).¹²⁰ ^1H NMR (500 MHz, CDCl_3) δ 1.47 (s, 3H, CH_3), 2.43 (t, 1H, OH), 2.97 (brs, 1H, OH), 3.62 (m, 2H, CH_2); 7.26 (d, $J = 8.6$ Hz, 2H, CH_{arom}), 7.44 (d, $J = 8.6$ Hz, 2H, CH_{arom}); ^{13}C NMR (500 MHz, CDCl_3) \square 26.2 (CH_3), 70.9 (C), 74.7 (CH_2), 126.7 (C_{arom}), 128.5 (C_{arom}), 133.2 (C_{arom}), 143.7 (C_{arom}) ppm; MS: $m/z=186.0$ [M^+].

2-(4-methoxyphenyl)-propane-1,2-diol, 289

Following the above general procedure (procedure 1), **289** was obtained as a colourless oil in 60% yield after purification (hexane/EtOAc = 1/1). ^1H NMR (500 MHz, DMSO- d_6) δ 1.35 (s, 3H, CH₃), 3.35 (m, 2H, CH₂), 3.72 (s, 3H, CH₃), 4.61 (t, J = 4.6 Hz, 1H, OH), 4.75 (s, 1H, OH), 6.83 (m, 2H, CH_{arom}), 7.34 (m, 2H, CH_{arom}) ppm; ^{13}C NMR (500 MHz, DMSO- d_6) \square 26.1 (CH₃), 55.0 (CH₃), 70.6 (CH₂), 73.3 (C), 112.9 (C_{arom}), 126.6 (C_{arom}), 139.5 (C_{arom}), 157.7 (C_{arom}) ppm; MS: m/z =182.2 [M^+]. Enantioenriched diol was obtained following procedure 2. Chiral-phase HPLC analysis: [Column OD3, 5 μ , λ =210 nm, *n*Heptane/*i*PrOH=95/5, flow rate 1.0mL/min]: T_{major} = 17.28 min, T_{minor} = 13.44 min, ee = 99%. $[\alpha]_{\text{D}}$ = +8.635 (c = 0.0170 g/cm³ in CHCl₃)

2-(1-naphthalenyl)-propane-1,2-diol, 290

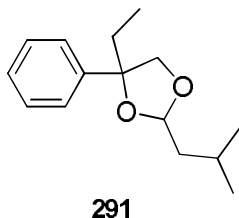
Following the above general procedure (procedure 1), **290** was obtained as a colourless solid in 80% yield after purification (hexane/EtOAc = 6/4). ^{121}H NMR (500 MHz, CDCl₃) δ 1.83 (s, 3H, CH₃), 1.86 (brs, 1H, OH), 2.82 (brs, 1H, OH), 4.11 (m, 2H, CH₂), 7.47 (m, 3H, CH_{arom}), 7.64 (d, J = 7.3 Hz, 1H, CH_{arom}), 7.80 (d, J = 8.4 Hz, 1H, CH_{arom}), 7.88 (d, J = 7.4 Hz, 1H, CH_{arom}), 8.66 (d, J = 8.4 Hz, 1H, CH_{arom}) ppm; MS: m/z =202.3 [M^+].

Characterization of acetals 281, 291, 296**4-isobutyl-2-methyl-2-phenyl-1,3-dioxolane, 281**

281 was obtained following the above general procedure (procedure 2), quenching reaction at 50% conversion after 15 h; purification: gradient hexane 100% to hexane/EtOAc = 1/1. Colourless oil, 0.022 g (from 0.2 mmol of diol), 50%. GC (Column: 25 m Lipodex G, G566); detector: FID; temperature: injector 220 °C, detector 125 °C, oven 220°C; gas: 0.5 bar H₂), t_{major} = 21.05 min, t_{minor} = 21.42 min, minor diastereomer (t_{major} = 20.04 min, t_{minor} = 19.72 min); ee = 97%; dr = 98:2; ^1H NMR (500 MHz, C₆D₆) δ 0.94 (m, 6H), 1.39 (s, 3H), 1.76 (m, 2H), 1.96 (m, 2H), 3.75 (m, 2H), 5.26 (t, J = 5.23 Hz, 1H), 7.08 (t, J = 7.35 Hz, 1H), 7.18 (t, J = 7.5

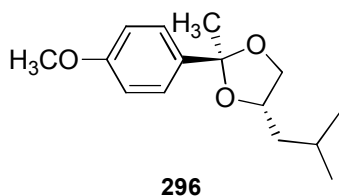
Hz, 2H), 7.37 (d, $J = 7.2$ Hz, 2H); ^{13}C NMR (500 MHz, C_6D_6) δ 23.1, 23.2, 25.1, 26.3, 43.6, 77.5, 81.7, 104.5, 125.2, 127.1, 128.4, 146.7; MS: $m/z=220.3$ [M^+].

4-isobutyl-2-ethyl-2-phenyl-1,3-dioxolane, 291



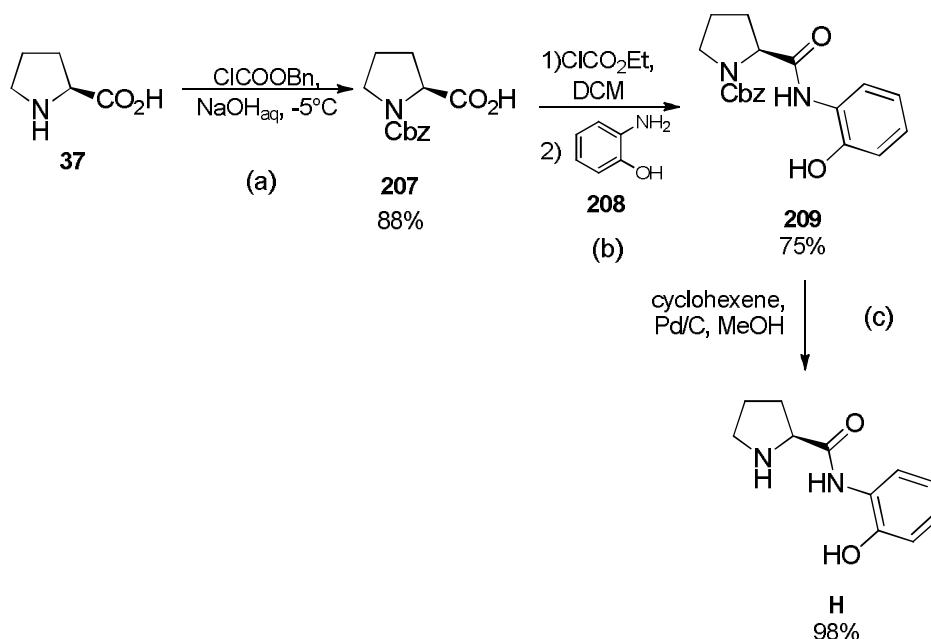
291 was obtained following procedure 2, quenching the reaction at 52% conversion after 20 h; purification: gradient hexane 100% to hexane/EtOAc = 1/1. Colourless oil, 0.021 g (from 0.2 mmol of diol), 44%. GC (Column: 25 m Lipodex G, G566); detector: FID; temperature: injector 220 °C, detector 320°C, oven 110 to 220°C; gas: 0.5 bar H_2), $t_{\text{major}} = 30.75$ min, $t_{\text{minor}} = 31.45$ min, minor diastereomer ($t_{\text{major}} = 29.17$ min, $t_{\text{minor}} = 28.42$ min) $ee = 96\%$; $dr = 97:3$; ^1H NMR (500 MHz, C_6D_6) δ 0.94 (t, $J = 7.56$ Hz, 6H), 1.39 (s, 3H), 1.63 (m, 1H), 1.75 (m, 3H), 1.95 (m, 1H), 3.82 (m, 2H), 5.25 (t, $J = 5.24$ Hz, 1H), 7.08 (t, $J = 6.94$ Hz, 1H), 7.19 (t, $J = 7.53$ Hz, 2H), 7.32 (d, $J = 8.08$ Hz, 2H); ^{13}C NMR (500 MHz, C_6D_6) δ 8.62, 23.12, 23.20, 32.27, 40.05, 43.70, 76.69, 104, 29, 125.68, 126.94, 145.00, 128.50; MS: $m/z=234.3$ [M^+]. $[\alpha]_{\text{D}} = -50.73$ ($c = 0.0110$ g/ cm^3 in CHCl_3)

4-isobutyl-2-(4-methoxyphenyl)-2-methyl-1,3-dioxolane, 296



Compound **296** was obtained following procedure 2, quenching the reaction at 50% conversion after 16 h; purification: gradient hexane 100% to hexane/EtOAc = 1/1. Colourless oil, 0.024 g (from 0.2 mmol of diol), 48%. GC (Column: 25 m Lipodex G, G566); detector: FID; temperature: injector 220 °C, detector 320°C, oven 145 to 220°C; gas: 0.5 bar H_2), $t_{\text{major}} = 45.80$ min, $t_{\text{minor}} = 44.23$ min, minor diastereomer ($t_{\text{major}} = 41.12$ min, $t_{\text{minor}} = 42.19$ min). $ee = 96.9\%$; $dr = 98:2$; ^1H NMR (500 MHz, C_6D_6) δ 0.96 (m, 6H), 1.43 (s, 3H), 1.78 (m, 2H), 1.98 (m, 1H), 3.32 (s, 3H), 3.77 (m, 2H), 5.29 (t, $J = 5.2$ Hz, 1H), 6.81 (d, $J = 8.72$ Hz, 2H), 7.31 (d, $J = 8.75$ Hz, 2H); ^{13}C NMR (500 MHz, C_6D_6) δ 23.19, 23.21, 25.07, 43.72, 54.81, 77.69, 81.51, 103.99, 113.88, 126.38, 138.73, 159.19; MS: $m/z=250.3$ [M^+]. $[\alpha]_{\text{D}} = -41.58$ ($c = 0.0215$ g/ cm^3 in CHCl_3)

General procedure for preparing catalyst **H**



Catalyst **H** was prepared following the above reaction scheme.

(a) In a refrigerated flask (-5°C through ice/ NaCl bath) 575 mg (5 mmol) (*S*)-proline **37** were stirred for ten minutes in 2.5 mL NaOH 2M. Afterwards 1 mL (7 mmol) di benzyl chloroformate and 1.75 mL of NaOH 4M are added drop by drop, in 30 minutes. The reaction was then stirred at 0°C for one hour and then washed with Et_2O (2x1.5 mL). Then the reaction mixture was acidified to pH 2 with HCl 6M and then saturated with anhydrous sodium sulphate. Solvent was evaporated *in vacuo* yielding 1.1 g **207** (88% yield) as a colourless oil, which was used for next step without further purification.

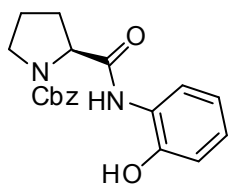
(b) To a solution of 249 mg *N*-Cbz-(*S*)-proline **207** in 2 mL dry DCM , stirred at 0°C , were added 305 μL triethylamine (2.2 mmol) and 105 μL (1.1 mmol) ethyl chloroformate. The reaction was stirred at 0°C for 30 minutes and 109 mg (1 mmol) of **208** were added. The mixture was stirred overnight at room temperature, then 2 mL HCl were added and the reaction was extracted with DCM (2x2 mL). Organic layers were dried over anhydrous Na_2SO_4 and solvent was evaporated *in vacuo*. Purification *via* flash chromatography led to 255 mg of clean product **209** (0.75 mmol).

(c) 157 mg (0.46 mmol) of **209** were dissolved in 3 mL of MeOH under Ar atmosphere together with 8 mg of Pd/C (10% Pd/C). The reaction was heated to reflux and 286 μL of cyclohexene were added. After one hour the mixture was filtrated on Celite and

solvent was evaporated in vacuo. Purification (CHCl₃/MeOH) *via* flash chromatography led to 93 mg of clean product **H** (98%).

Characterization of **209** and **H**

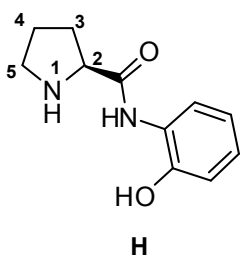
(*S*)-benzyl 2-((2-hydroxyphenyl)carbamoyl)pyrrolidine-1-carboxylate, **209**



209

Following the above procedure, compound **209** was purified via flash chromatography (hexane/acetate = 9/1) and isolated in 75% yield as a pale yellow oil. ¹H-NMR (CDCl₃, 300 MHz, 25°C): δ = 10.00 (bs, 1H, NH_{amide}), 7.43-7.35 (m, 4H, CH_{arom}), 7.11 (t, *J* = 7.6 Hz, 1H, CH), 7.01 (d, *J* = 8.1 Hz, 1H, CH), 6.91 (d, *J* = 6.8 Hz, 1H, CH), 6.83 (t, *J* = 7.4 Hz, 1H, CH), 5.33 (s, 2H, CH₂Ph), 4.40 (m, 1H, CH), 3.64-3.44 (m, 2H, CH), 2.32-1.84 (m, 4H, 2xCH).

(*S*)-*N*-(2-hydroxyphenyl)pyrrolidine-2-carboxamide, **H**



H

Following the above procedure, compound **209** was purified via flash chromatography (hexane/acetate = 9/1) and isolated in 75% yield as a pale yellow oil. ¹H-NMR (CDCl₃, 300 MHz, 25°C): δ = 9.99 (bs, 1H, NH_{amide}), 7.11 (t, *J* = 7.6 Hz, 1H, H⁴), 7.01 (d, *J* = 8.1 Hz, 1H, H⁶), 6.91 (d, *J* = 6.8 Hz, 1H, H³), 6.83 (t, *J* = 7.4 Hz, 1H, H⁵), 3.94 (dd, *J* = 9.4, 5.0 Hz, 1H, H²), 3.07 (m, *J* = 16.4, 10.1, 6.5 Hz, 2H, H^{5'}), 2.75 (bs, 1H, OH), 2.25 (m, *J* = 16.8, 7.5 Hz, 1H, H⁴), 2.06 (m, *J* = 19.3, 6.4 Hz, 1H, H^{4'}), 1.79 (m, *J* = 13.6, 6.6 Hz, 2H, H³), 1.72-1.52 (m, 1H, NH_{amine}) ppm. ¹³C-NMR (75 MHz, CDCl₃): δ = 175.5 (CON), 149.3 (C^{4'}), 127.3 (C^{6'}), 125.3 (C^{3'}), 122.2 (C^{5'}), 120.2 (C^{1'}), 120.2 (C^{2'}), 60.5 (C²), 47.6 (C⁵), 31.1 (C³), 26.5 (C⁴) ppm.

Assignment of configurations of epoxides

General Information

NOESY experiments were recorded with a Bruker AC 300 spectrometer. All calculations were carried out on a simple PC endowed with a Intel(R) Xeon Quadcore E5420 at 2.50 GHz. Optical rotation analyses were carried out on a Jasco DIP-370 digital polimeter using a Na-lamp. The starting geometries were generated by conformational analysis with the SPARTAN02 software,^q using molecular mechanics (MMFF94s force field) and retaining all the structures differing by 4 kcal/mol by most stable conformer. All these geometries were fully optimized at the DFT/B3LYP/6-31G* and 6-31++G (2d,2p) level in the gas phase as implemented in the GAUSSIAN09 package.^f In all cases, the free energy values at T = 298K were employed to calculate the population of each conformer, using the Boltzmann's statistics. The calculations of the Optical Rotation Dispersion (ORD) were carried out at TDDFT/B3LYP/6-31G* level in the gas phase. The theoretical ORD values (to be compared with the experimental ones) were obtained as weighted averages on the Boltzmann's populations calculated in the gas phase or in the selected solvents.

Configuration Assignment

NOESY Spectroscopy Data

The *trans* and *cis* configuration assignments of the obtained spiro-epoxyoxiranes **133-trans** and **133-cis** were unambiguously determined by comparing the NOESY spectroscopic data reported below. Indeed:

- in the NOESY spectrum of **133-cis** [Figure 1' (a)] cross-peaks were found between the aromatic 4-H atom [δ 7.04-7.14 (m, 2H, CH_{arom}) ppm] and the epoxide proton [δ 4.15 (s, 1H, OCH) ppm], due the spatial proximity of these nuclei, unequivocally proving the *cis* configuration of the minor diastereoisomer **133-cis**. Moreover, further cross-peaks are generated by the spatial interaction between the H atom

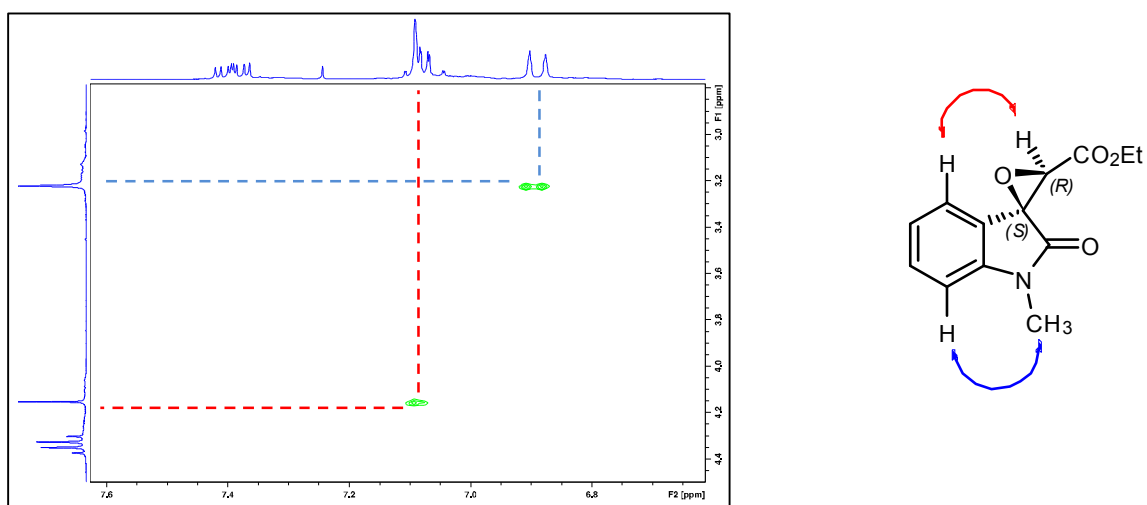
^q SPARTAN '02; Wavefunction Inc.: Irvine, CA. <http://www.wavefunction.com>

^f Frisch, M.J.; Trucks, G.W.; Schlegel, H.B.; Scuseria, G.E.; Robb, M.A.; Cheeseman, J.R.; Scalmani, G.; Barone, V.; Mennucci, B.; Petersson, G.A.; Nakatsuji, H.; Caricato, M.; Li, X.; Hratchian, H.P.; Izmaylov, A.F.; Bloino, J.; Zheng, G.; Sonnenberg, J.L.; Hada, M.; Ehara, M.; Toyota, K.; Fukuda, R.; Hasegawa, J.; Ishida, M.; Nakajima, T.; Honda, Y.; Kitao, O.; Nakai, H.; Vreven, T.; Montgomery, Jr., J.A.; Peralta, J.E.; Ogliaro, F.; Bearpark, M.; Heyd, J.J.; Brothers, E.; Kudin, K.N.; Staroverov, V.N.; Kobayashi, R.; Normand, J.; Raghavachari, K.; Rendell, A.; Burant, J.C.; Iyengar, S.S.; Tomasi, J.; Cossi, M.; Rega, N.; Millam, J.M.; Klene, M.; Knox, J.E.; Cross, J.E.; Bakken, V.; Adamo, C.; Jaramillo, J.; Gomperts, R.; Stratmann, R.E.; Yazyev, O.; Austin, A.J.; Cammi, R.; Pomelli, C.; Ochterski, J.W.; Martin, R.L.; Morokuma, K.; Zakrzewski, V.G.; Voth, G.A.; Salvador, P.; Dannenberg, J.J.; Dapprich, S.; Daniels, A.D.; Farkas, O.; Foresman, J.B.; Ortiz, J.V.; Cioslowski, J.; Fox, D.J. GAUSSIAN 09, Revision A.02; Gaussian, Inc.: Wallingford, CT, 2009

belonging to the $N\text{-CH}_3$ [δ 3.22 (s, 3H, CH_3N) ppm] group and 7-H atom on the aromatic ring [δ 6.89 (dd, $J = 7.8\text{Hz}$, 0.5Hz , 1H, CH_{arom}) ppm].

- b. conversely, no NOESY cross peaks for the epoxide proton were found in the major isomer **133-trans** [Fig. 1 (b)], although the through-space connectivity between the $N\text{-CH}_3$ group [δ 3.25 (s, 3H, CH_3N) ppm] and the aromatic 7-H atom [δ 6.89 (ddd, $J = 7.9\text{Hz}$, 0.9Hz , 0.6Hz , 1H, CH_{arom}) ppm] is clearly still present.

(a) (2'S,3'R)-ethyl 1-methyl-2-oxospiro[indoline-3,2'-oxirane]-3'-carboxylate **133-cis**



(b) (2'R,3'R)-ethyl 1-methyl-2-oxospiro[indoline-3,2'-oxirane]-3'-carboxylate **133-trans**

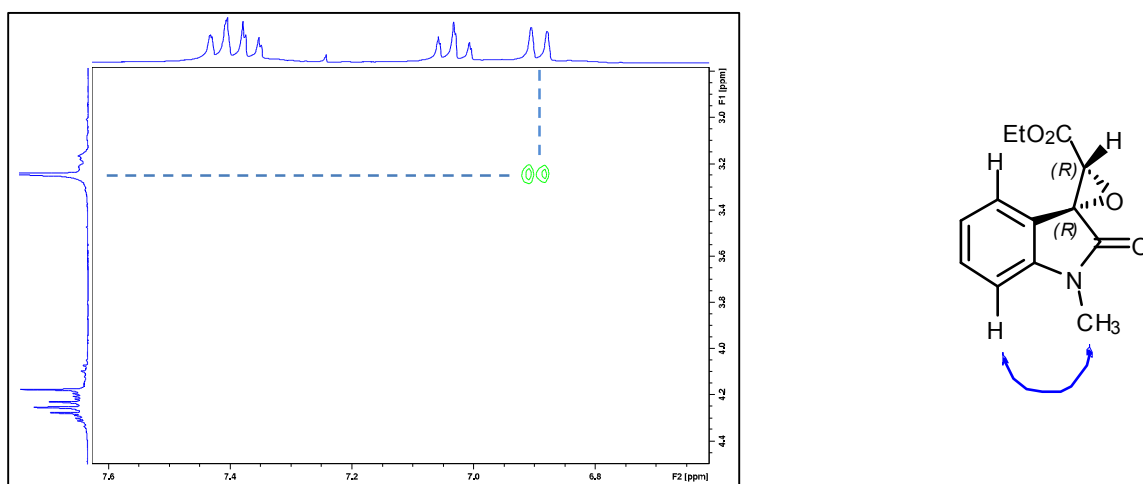


Figure 1'

Optical Rotation Dispersion Data: comparison between calculated and experimental values.

ORD values of **133-trans** were calculated by means of the Time-Dependent Density Functional Theory (TDDFT) method, using B3LYP functional,^s which, with the 6-31G* (or higher) basis sets is wide used by the experimental organic chemists to assign the absolute configuration of new synthetic and natural compounds.^t The (2'R,3'R) configuration was arbitrarily fixed at two newly formed stereogenic centers. Molecular mechanics provided six conformers, then fully optimized at DFT/B3LYP/6-31G* level of calculation. Calculated conformers free energies were used to carry out Boltzmann's populations distribution. In Figure 2' the most stable conformer (2'R,3'R)-**133-trans-A** structure is reported.

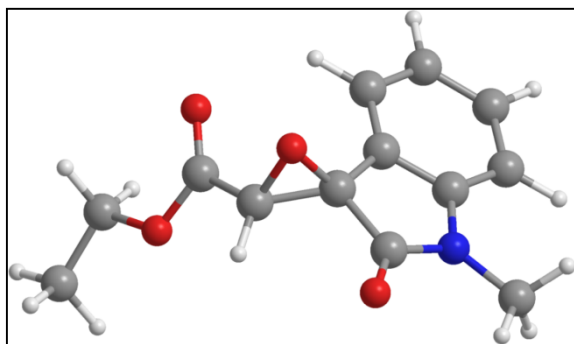


Figure 2' The most stable conformer (2'R,3'R)-**2aA** calculated at DFT/B3LYP/6-31G* level of theory.

All optimized conformers differ each other by the orientation of the ester moiety (Figure 3').

^s (a) Becke, A.D. *J. Chem. Phys.*, **1993**, *98*, 5648. (b) Lee, C.; Yang, W.; Parr, R.G. *Phys. Rev. B*, **1998**, *37*, 785

^t Synthetic compounds: (a) Xu, D.; Wang, Y.; Luo, S.; Zhong, A.; Chen, H.; Xu, Z. *Adv. Synth. Cat.* **2008**, *350*, 2610. (b) Gioia, C.; Fini, F.; Mazzanti, A.; Bernardi, L.; Ricci, A. *J. Am. Chem. Soc.*, **2009**, *131*, 9614. Natural products: (c) Ge, H.M.; Zhu, C.H.; Da, H.S.; Zhang, L.D.; Xie, D.Q.; Yang, J.; Ng, S.W.; Tan, R.X. *Chem. Eur. J.*, **2008**, *14*, 376. See also: (d) Bringmann, G.; Gulder, T.A.M.; Reichert, M.; Gulder, T. *Chirality*, **2008**, *20*, 628. (e) Bringmann, G.; Bruhn, T.; Maksimenka, K.; Hemberger, Y. *Eur. J. Org. Chem.*, **2009**, 2717 and references cited therein.

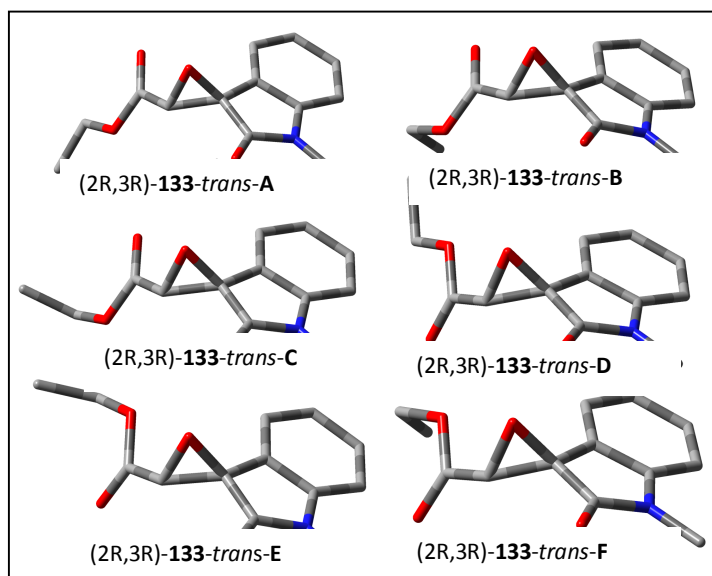


Figure 3' Structures of the most stable conformers of ($2'R,3'R$)-**2a** optimized at the DFT/B3LYP/6-31G*

The calculated optical rotatory power at four different wavelengths (589.3, 546, 435 and 405 nm), calculated at the TDDFT/B3LYP/6-31G*, relative free energies, conformers Boltzmann populations for all optimized conformers of ($2'R,3'R$)-**2a** and comparison with the experimental ORD ($c = 0.55 \text{ g/cm}^3$ in CH_2Cl_2) are shown in Table 1. Results strongly supports ($2'R,3'R$)-**2a** absolute configuration.

Table 1'. Relative-free energies with respect to the most stable conformer, populations, ORD values (deg [dm g/cm³]⁻¹) obtained at TDDFT/B3LYP/6-31G* level for each conformer and experimental ORD in CH₂Cl₂

Conformers	ΔG (kcal/mol)	% pop	$[\alpha]_D$	$[\alpha]_{546}$	$[\alpha]_{435}$	$[\alpha]_{405}$
133-trans-A	0.0	45.9	-101	-127	-294	-419
133-trans-B	0.4	24.3	-51	-64	-153	-220
133-trans-C	0.5	21.4	-75	-92	-193	-262
133-transD	1.4	4.7	-15	-18	-37	-50
133-trans-E	1.7	2.7	-7	-8	-18	-25
133-trans-F	2.2	1.0	-2	-2	-6	-8
Total Calc.ORD			-250	-312	-701	-984
Experimental ORD			-101	-134	-295	-395

The sign, the order of magnitude and the uniform trend in the experimental ORD have been correctly reproduced by the calculations, despite the fact that the Boltzmann averaged ORD values are about twice higher than the experimental ones. Such difference may result from basis set calculation errors in overestimating ORD. Nevertheless, it is important to notice that all calculated conformers OR are negative. In facts problems may arise in the case of flexible molecule having many conformers with opposite-signed OR in order to get a more accurate geometries, populations and OR computational analysis achieving a reliable absolute configuration assignment.^u In any case we also performed a geometry conformers optimization at DFT/B3LYP/6-31++G(2d,2p), and a ORD calculation at TDDFT/B3LYP/6-31G* level of theory, in

^u Mazzeo, G.; Giorgio, E.; Zanasi, R.; Berova, N.; Rosini, C. *J. Org. Chem.*, **2010**, *75*, 4600.

order to check if significantly changes may occur in the theoretical predictions of respective conformers and/or in the conformational distribution, which could become more significant as in the present case where several conformers are involved. Then no significant differences were reported (Table 2).

Table 2. Relative-free energies with respect to the most stable conformer, populations, ORD values ($\text{deg} [\text{dm g/cm}^3]^{-1}$) obtained at TDDFT/B3LYP/6-31++G(2d,2p) level for each conformer and experimental ORD in CH_2Cl_2

Conformers	ΔG (kcal/mol)	% pop	$[\alpha]_D$	$[\alpha]_{546}$	$[\alpha]_{435}$	$[\alpha]_{405}$
133-trans-A	0.0	53.9	-115	-145	-337	-478
133-trans-B	0.6	18.6	-39	-49	-116	-167
133-trans-C	0.7	17.2	-57	-71	-149	-202
133-transD	1.3	6.4	-20	-25	-51	-68
133-trans-E	1.8	2.7	-6	-8	-17	-24
133-trans-F	2.3	1.1	-2	-3	-6	-9
Total						
Calc.ORD			-240	-301	-677	-948
Experimental (CH_2Cl_2)	ORD		-101	-134	-295	-395

In conclusion we got a satisfactory agreement between experimental and calculated ORD avoiding large basis set such as aug-cc-pVDZ or 6-311++G** calculations and saving more computational efforts.

Likewise, the (2'S,3'R) configuration to the major enantiomer of *cis*-**3a** has been assigned by exploiting the same quantum mechanics protocol. In particular, the experimental optical rotation value at $\lambda = 589.3 \text{ nm}$ for the (2'S,3'R)- **3a** is $[\alpha]_D = -105$

($c = 0.035 \text{ g/cm}^3$ in CHCl_3) which has to be compared with the *ab initio* calculated one
 $[\alpha]_{\text{D}} = -258 \text{ [deg (dm g/cm}^3\text{)}^{-1}$.

References

1. Aitken, R. A.; Kilényi, S. N., *Asymmetric synthesis*, CRC Press, **1992**.
2. Keith, John M.; Larrow, Jay F.; Jacobsen, Eric N., *Adv. Synth. Catal.* **2001**, *343*, 5-26.
3. (a) Holton, R. A.; Somoza, C.; Kim, H. B.; Liang, F.; Biediger, R. J.; Boatman, P. D.; Shindo, M.; Smith, C. C.; Kim, S., *J. Am. Chem. Soc.* **1994**, *116* (4), 1597-1598; (b) Holton, R. A.; Kim, H. B.; Somoza, C.; Liang, F.; Biediger, R. J.; Boatman, P. D.; Shindo, M.; Smith, C. C.; Kim, S. *J. Am. Chem. Soc.* **1994**, *116*, 1599-1600.
4. (a) Wang, Z.-M.; Kolb, H. C.; Sharpless, K. B., *J. Org. Chem.* **1994**, *59*, 5104-5105; (b) Deng, L.; Jacobsen, E. N. *J. Org. Chem.* **1992**, *57*, 4320-4323.
5. Keith, M. K.; Jacobsen, E. N. *Adv. Synth. Catal.* **2000**, *343*.
6. Jacques, A. C. *Enantiomers, Racemates, and Resolutions*, Krieger, **1981**.
7. Robertson, D. W.; Krushinski, Jr.; Joseph H, 3-aryloxy-3-substituted propanamines, US5023269 A, **1990**.
8. Toda, F., *Enantiomer separation*, Kluwer Academic Publishers, **2004**.
9. (a) Porter, W. H. *Pure & Appl. Chem* **1991**, *63*; (b) Wistuba, D. S., Volker *J. Chrom. A* **2000**, *875*.
10. Jakubetz, H.; Czesla, H.; Schurig, V. *J. Microcolumn Sep.* **1997**, *9*, 421-431.
11. Marckwald, W.; Kenzie, A. M. *Ber. Dtsch. Chem. Ges.* **1899**, *32* (2), 2130-2136.
12. May, O.; Verseck, S.; Bommarius, A.; Drauz, K. *Org. Process Res. Dev.* **2002**, *6*, 452-457.
13. Moss, G. P. *Pure Appl. Chem.* **1996**, *68*.
14. Gawley, J. A., *Principles of Asymmetric Synthesis*, 2nd ed, Elsevier, **2012**.
15. Nicolaou, K. C. S. *Classics in Total Synthesis: Targets, Strategies, Methods*, Wiley: **1996**.
16. Nicolaou, K. C.; Li, A.; Ellery, S. P.; Edmonds, D. J. *Angew. Chem. Int. Ed.* **2009**, *48*, 6293-6295.
17. Drauz, K., *Enzyme Catalysis in Organic Synthesis: A Comprehensive Handbook*, Wiley-VCH, **2012**.
18. List, B.; Lerner, R. A.; Barbas, C. F., *J. Am. Chem. Soc.* **2000**, *122*, 2395-2396.
19. (a) Ahrendt, K. A.; Borths, C. J.; MacMillan, D. W. C., *J. Am. Chem. Soc.* **2000**, *122*, 4243-4244; (b) MacMillan, D. W. C. *Nature* **2008**, *455*, 304-308; (c) Jen, W. S.; Wiener, J. J. M.; MacMillan, D. W. C. *J. Am. Chem. Soc.* **2000**, *122*, 9874-9875.
20. Krautwald, S.; Sarlah, D.; Schafroth, M. A.; Carreira, E. M., *Science* **2013**, *340*, 1065-1068.
21. Bredig, G.; Fiske, P., *Biochem. Z.* **1912**, *46*, 7-23.
22. Pracejus, H., *Justus Liebigs Ann. Chem.* **1960**, *634*, 23-29.
23. Hajos, Z. G.; Parrish, D. R. *J. Org. Chem.* **1974**, *39*, 1615-1621.
24. Seayad, J.; List, B., *Org. Biom. Chem.* **2005**, *3*, 719-724.
25. Berkessel, A., *Asymmetric Organocatalysis (Topics in Current Chemistry)*, Springer, **2009**.
26. Knowles, R. R.; Jacobsen, E. N., *Proc. Nat. Acad. Sci.* **2010**, *107*, 20678-20685.
27. Schreiner, P. R.; Wittkopp, A. *Org. Lett.* **2002**, *4*, 217-220.
28. (a) Vakulya, B.; Varga, S.; Csámpai, A.; Soós, T., *Org. Lett.* **2005**, *7*, 1967-1969; (b) Lattanzi, A., *Adv. Synth. Catal.* **2006**, *348*, 339-346.
29. Sigman, M. S.; Vachal, P.; Jacobsen, E. N., *Angew. Chem. Int. Ed.* **2000**, *39*, 1279-1281.
30. (a) Pihko, P. M., *Angew. Chem. Int. Ed.* **2004**, *43* (16), 2062-2064; (b) Ema, T.; Tanida, D.; Matsukawa, T.; Sakai, T., *Chem. Comm.* **2008**, 957-959.
31. (a) Schreiner, P. R., *Chem. Soc. Rev.* **2003**, *32*, 289-296; (b) Taylor, M. S.; Jacobsen, E. N. *Angew. Chem. Int. Ed.* **2006**, *45*, 1520-1543.

32. Uyeda, C.; Jacobsen, E. N., *J. Am. Chem. Soc.* **2008**, *130*, 9228-9229.
33. Raheem, I. T.; Thiara, P. S.; Peterson, E. A.; Jacobsen, E. N., *J. Am. Chem. Soc.* **2007**, *129*, 13404-13405.
34. Zuend, S. J.; Jacobsen, E. N. *J. Am. Chem. Soc.* **2009**, *131*, 15358-15374.
35. Fleischmann, M.; Drettwan, D.; Sugiono, E.; Rueping, M.; Gschwind, R. M., *Angew. Chem. Int. Ed.* **2011**, *50*, 6364-6369.
36. Akiyama, T.; Itoh, J.; Yokota, K.; Fuchibe, K. *Angew. Chem. Int. Ed.* **2004**, *43*, 1566-1568.
37. Kampen, D.; Reisinger, C.; List, B., *Chiral Brønsted Acids for Asymmetric Organocatalysis*. In *Asymmetric Organocatalysis*, Springer, **2009**.
38. Čorić, I.; Vellalath, S.; List, B., *J. Am. Chem. Soc.* **2010**, *132*, 8536-8537.
39. Bergonzini, G.; Gramigna, L.; Mazzanti, A.; Fochi, M.; Bernardi, L.; Ricci, A., *Chem. Comm.* **2010**, *46*, 327-329.
40. Čorić, I.; Kim, J. H.; Vlaar, T.; Patil, M.; Thiel, W.; List, B. *Angew. Chem. Int. Ed.* **2013**, *52*, 3490-3493.
41. Duce, S.; Pesciaioli, F.; Gramigna, L.; Bernardi, L.; Mazzanti, A.; Ricci, A.; Bartoli, G.; Bencivenni, *Adv. Synth. Catal.* **2011**, *353*, 860-864.
42. (a) Lifchits, O.; Reisinger, C. M.; List, B., *C. J. Am. Chem. Soc.* **2010**, *132*, 10227-10229; (b) *Science*, **2013**, *340*, 180-182.
43. Aggarwal, V. K.; Charmant, J. P. H.; Fuentes, D.; Harvey, J. N.; Hynd, G.; Ohara, D.; Picoul, W.; Robiette, R.; Smith, C.; Vasse, J.-L.; Winn, C. L., *J. Am. Chem. Soc.* **2006**, *128*, 2105-2114.
44. Katsuki, T.; Martin, V., *Asymmetric Epoxidation of Allylic Alcohols: the Katsuki–Sharpless Epoxidation Reaction*. In *Organic Reactions*, John Wiley & Sons, Inc.: **2004**.
45. Zhang, W.; Loebach, J. L.; Wilson, S. R.; Jacobsen, E. N. *J. Am. Chem. Soc.* **1990**, *112*, 2801-2803.
46. Srour, H.; Le Maux, P.; Chevance, S.; Simonneaux, G., *Coord. Chem. Rev.* **2013**, *257*, 3030-3050.
47. Berkessel, A.; Günther, T.; Wang, Q.; Neudörfl, J.-M., T. *Angew. Chem. Int. Ed.* **2013**, *52*, 8467-8471.
48. Wu, X. Y.; She, X. G.; Shi, Y. A., *J. Am. Chem. Soc.* **2002**, *124*, 8792-8793.
49. Porter, M. J.; Skidmore, J., *Asymmetric Epoxidation of Electron-Deficient Alkenes*. In *Organic Reactions*, John Wiley & Sons, Inc.: **2004**.
50. Christmann, M., *Asymmetric Synthesis: The Essentials*, Wiley-VCH, **2008**.
51. Wang, Z., *Weitz-Scheffer Epoxidation*. In *Comprehensive Organic Name Reactions and Reagents*, John Wiley & Sons, **2010**.
52. Banfi, S.; Colonna, S.; Molinari, H.; Julia, S.; Guixer, J., *Tetrahedron* **1984**, *40*, 5207-5211.
53. Berkessel, A.; Gasch, N.; Glaubitz, K.; Koch, C. *Org. Lett.* **2001**, *3*, 3839-3842.
54. Lygo, B.; Gardiner, S. D.; McLeod, M. C.; To, D. C., *Org. Biomol. Chem.* **2007**, *5*, 2283-2290.
55. (a) Wang, X.; Reisinger, C. M.; List, B. *J. Am. Chem. Soc.* **2008**, *130*, 6070-6075; (b) Lifchits, O.; Mahlau, M.; Reisinger, C. M.; Lee, A.; Farès, C.; Polyak, I.; Gopakumar, G.; Thiel, W.; List, B. *J. Am. Chem. Soc.* **2013**, *135*, 6677-6693.
56. (a) Marigo, M.; Franzen, J.; Poulsen, T. B.; Zhuang, W.; Jorgensen, K. A. *J. Am. Chem. Soc.* **2005**, *127*, 6964-6965; (b) Bondzic, B. P.; Urushima, T.; Ishikawa, H.; Hayashi, Y., *Org. Lett.* **2010**, *12*, 5434-5437.
57. (a) Lattanzi, A. *Org. Lett.* **2005**, *7*, 2579-2582; (b) Lattanzi, A. *Chem. Comm.* **2009**, 1452-1463.
58. Wu, S.; Pan, D.; Cao, C.; Wang, Q.; Chen, F.-X., *Adv. Synth. Catal.* **2013**, *355*, 1917-1923.
59. Russo, A.; Galdi, G.; Croce, G.; Lattanzi, A. *Chem. Eur. J.* **2012**, *18*, 6152-6157.
60. (a) 1. Baeyer, A., *Ber. Dtsch. Chem. Ges.* **1900**, *33*; (b) Zhang, S.-J.; Zhang, J.; Zhou, Q.-Q.; Dong, L.; Chen, Y.-C. *Org. Lett.* **2013**, *15*, 968-971.

61. Galliford, C. V. S. *Angew. Chem. Int. Ed.* **2007**, *46*.
62. Jiang, K.; Tiwari, B.; Chi, Y. R. *Org. Lett.* **2012**, *14*, 2382-2385.
63. Tan, W.; Zhu, X.-T.; Zhang, S.; Xing, G.-J.; Zhu, R.-Y.; Shi, F. *RSC Advances* **2013**, *3*, 10875-10886.
64. Miyamoto, H.; Hirano, T.; Okawa, Y.; Nakazaki, A.; Kobayashi, S. *Tetrahedron* (0).
65. Christoffers, J.; Baro, A. *Angew. Chem.* **2003**, *115*, 1726-1728.
66. Hong, L.; Wang, R., *Adv. Synth. Catal.* **2013**, *355*, 1023-1052.
67. Kato, S.; Kanai, M.; Matsunaga, S. *Chem. Asian J.* **2013**, (0).
68. Li, Y.-M.; Li, X.; Peng, F.-Z.; Li, Z.-Q.; Wu, S.-T.; Sun, Z.-W.; Zhang, H.-B.; Shao, Z.-H. *Org. Lett.* **2011**, *13* (23), 6200-6203.
69. Pesciaoli, F.; Righi, P.; Mazzanti, A.; Bartoli, G.; Bencivenni, G. *Chem. Eur J.* **2011**, *17*, 2842-2845.
70. Anthony, W. C. *J. Org. Chem.* **1966**, *31*, 77-81.
71. (a) Dandia, A.; Singh, R.; Bhaskaran, S. *Ultrason. Sonochem.* **2011**, *18*, 1113-1117; (b) Dandia, A.; Singh, R.; Saha, M.; Shivpuri, A. *Pharmazie* **2002**, *57*, 602-605.
72. Basavaiah, D.; Badsara, S. S.; Sahu, B. C. *Chem. Eur J.* **2013**, *19*, 2961-2965.
73. Schulz, V.; Davoust, M.; Lemarié, M.; Lohier, J.-F.; Sopkova de Oliveira Santos, J.; Metzner, P.; Brière, J.-F. *Org. Lett.* **2007**, *9*, 1745-1748.
74. Ammetto, I.; Gasperi, T.; Loreto, M. A.; Migliorini, A.; Palmarelli, F.; Tardella, P. A. *Eur. J. Org. Chem.* **2009**, *2009*, 6189-6197.
75. Gasperi, T.; Loreto, M. A.; Migliorini, A.; Ventura, C. *Eur. J. Org. Chem.* **2011**, 385-391.
76. Falagas, M. E.; Giannopoulou, K. P.; Kokolakis, G. N.; Rafailidis, P. I. *Clinical Infectious Diseases* **2008**, *46*, 1069-1077.
77. Russo, A.; Capobianco, A.; Perfetto, A.; Lattanzi, A.; Peluso, A. *Eur. J. Org. Chem.* **2011**, 1922-1931.
78. Lattanzi, A. *Org. Lett.* **2005**, *7*, 2579-2582.
79. Palumbo, C., *Un nuovo approccio organocatalitico per la sintesi stereoselettiva di spiroepossi-ossindoli*, Master Thesis, **2010**.
80. Palumbo, C.; Mazzeo, G.; Mazziotta, A.; Gambacorta, A.; Loreto, M. A.; Migliorini, A.; Superchi, S.; Tofani, D.; Gasperi, T. *Org. Lett.* **2011**, *13*, 6248-6251.
81. (a) Bruice, T. C. *J. Am. Chem. Soc.* **1957**, *79*, 702. (b) Goehring, R. R.; Sachdeva, Y. P.; Pisipati, J. S.; Sleevi, M. C.; Wolfe, J. F. *J. Am. Chem. Soc.* **1985**, *107*, 435-444. (c) Savitha, G.; Niveditha, S. K.; Muralidharan, D.; Perumal, P. T. *Tetrahedron Lett.* **2007**, *48* (16), 2943-2947; (d) Jiang, K.; Jia, Z.-J.; Chen, S.; Wu, L.; Chen, Y.-C. *Chem. Eur. J.* **2010**, *16*, 2852-2856.
82. Nising, C. F.; Brase, S., *Chem. Soc. Rev.* **2012**, *41*, 988-999.
83. Lee, S. I.; Hwang, G.-S.; Ryu, D. H., *Catalytic J. Am. Chem. Soc.* **2013**, *135*, 7126-7129.
84. (a) Corey, E.; Shibata, S.; Bakshi, R. K. *J. Org. Chem.* **1988**, *53*, 2861-2863; (b) Saha, S.; Moorthy, J. N. *J. Org. Chem.* **2010**, *76*, 396-402; (c) Berkessel, A.; Harnying, W.; Duangdee, N.; Neudörfl, J.-M.; Gröger, H. *Org. Process Res. Dev.* **2011**, *16*, 123-128.
85. Cao, C.-L.; Ye, M.-C.; Sun, X.-L.; Tang, Y. *Org. Lett.* **2006**, *8*, 2901-2904.
86. (a) Bartoli, G.; Bosco, M.; Dalpozzo, R.; Giuliani, A.; Marcantoni, E.; Mecozzi, T.; Sambri, L.; Torregiani, E. *J. Org. Chem.* **2002**, *67*, 9111-9114; (b) Shen, Z.; Mang, Y.; Jiao, C.; Li, B.; Ding, J.; Zhang, Y. *Chirality* **2007**, *19*, 307-312.
87. Vakulya, B.; Varga, S.; Csampai, A.; Soos, T. *Org. Lett.* **2005**, *7*, 1967-1969.
88. (a) Berkessel, A.; Harnying, W.; Duangdee, N.; Neudörfl, J.-M.; Gröger, H. *Org. Process Res. Dev.* **2012**, *16*, 123-128; (b) Corey, E. J.; Shibata, S.; Bakshi, R. K. *J. Org. Chem.* **1988**, *53*, 2861-2863.

89. Bencivenni, G.; Wu, L.-Y.; Mazzanti, A.; Giannichi, B.; Pesciaioli, F.; Song, M.-P.; Bartoli, G.; Melchiorre, P. *Angew. Chem. Int. Ed.* **2009**, *48*, 7200-7203.
90. Liu, T.-L.; Xue, Z.-Y.; Tao, H.-Y.; Wang, C.-J. *Org. Biomol. Chem.* **2011**, *9*, 1980-1986.
91. Rowland, G. B.; Zhang, H.; Rowland, E. B.; Chennamadhavuni, S.; Wang, Y.; Antilla, J. C. *J. Am. Chem. Soc.* **2005**, *127*, 15696-15697.
92. (a) Vellalath, S.; Čorić, I.; List, B. *Angew. Chem. Int. Ed.* **2010**, *122*, 9943-9946; (b) Cheng, X.; Vellalath, S.; Goddard, R.; List, B. *J. Am. Chem. Soc.* **2008**, *130*, 15786-15787.
93. Coric, I.; List, B. *Nature* **2012**, *483*, 315-319.
94. Mills, J.; Gibson, W. R.; Swanson, E. E. *Proc. Soc. Exp. Biol. Med.* **1957**, *96*, 100-2.
95. Loertscher, B. M.; Young, P. R.; Evans, P. R.; Castle, S. L. *Org. Lett.* **2013**, *15*, 1930-1933.
96. Theil, F. *Chem. Rev.* **1995**, *95*, 2203-2227.
97. (a) Liu, W.; Lau, F.; Liu, K.; Wood, H. B.; Zhou, G.; Chen, Y.; Li, Y.; Akiyama, T. E.; Castriota, G.; Einstein, M.; Wang, C.; McCann, M. E.; Doebber, T. W.; Wu, M.; Chang, C. H.; McNamara, L.; McKeever, B.; Mosley, R. T.; Berger, J. P.; Meinke, P. T. *J. Med. Chem.* **2011**, *54*, 8541-8554; (b) Kourist, R.; Domínguez de María, P.; Bornscheuer, U. T. *Chem. Bio. Chem.* **2008**, *9*, 491-498.
98. Cleij, M.; Archelas, A.; Furstoss, R. *J. Org. Chem.* **1999**, *64*, 5029-5035.
99. (a) Andersen, N. R.; Hansen, S. G.; Bertelsen, S.; Jørgensen, K. A., *Adv. Synth. Catal.* **2009**, *351*, 3193-3198; (b) Díaz-de-Villegas, M. D.; Gálvez, J. A.; Badorrey, R.; López-Ram-de-Víu, M. P. *Chem. Eur. J.* **2012**, *18*, 13920-13935.
100. Jacobsen, E. N.; Marko, I.; Mungall, W. S.; Schroeder, G.; Sharpless, K. B. *J. Am. Chem. Soc.* **1988**, *110*, 1968-1970.
101. Kolb, H. C.; VanNieuwenhze, M. S.; Sharpless, K. B. *Chem. Rev.* **1994**, *94*, 2483-2547.
102. (a) Crispino, G. A.; Jeong, K. S.; Kolb, H. C.; Wang, Z. M.; Xu, D.; Sharpless, K. B. *J. Org. Chem.* **1993**, *58*, 3785-3786; (b) Sharpless, K. B.; Amberg, W.; Bennani, Y. L.; Crispino, G. A.; Hartung, J.; Jeong, K. S.; Kwong, H. L.; Morikawa, K.; Wang, Z. M. *J. Org. Chem.* **1992**, *57*, 2768-2771.
103. Branco, L. C.; Ferreira, F. C.; Santos, J. L.; Crespo, J. G.; Afonso, C. A. M.; Sharpless, K. B. *Adv. Synth. Catal.* **2008**, *350*, 2086-2098.
104. (a) Kim, J. H.; Čorić, I.; Vellalath, S.; List, B. *Angew. Chem. Int. Ed.* **2013**, *52*, 4474-4477; (b) Liao, S.; Čorić, I.; Wang, Q.; List, B. *J. Am. Chem. Soc.* **2012**, *134*, 10765-10768.
105. Čorić, I.; List, B. *Nature* **2012**, *483*, 315-319.
106. Beauchard, A.; Ferandin, Y.; Frère, S.; Lozach, O.; Blairvacq, M.; Meijer, L.; Thiéry, V.; Besson, T. *Bioorg. Med. Chem.* **2006**, *14*, 6434-6443.
107. Cao, S.-H.; Zhang, X.-C.; Wei, Y.; Shi, M. *Eur. J. Org. Chem.* **2011**, 2668-2672.
108. Zhou, L.; Liu, Y.; Zhang, W.; Wei, P.; Huang, C.; Pei, J.; Yuan, Y.; Lai, L. *J. Med. Chem.* **2006**, *49*, 3440-3443.
109. Jiang, X.; Cao, Y.; Wang, Y.; Liu, L.; Shen, F.; Wang, R. *J. Am. Chem. Soc.* **2010**, *132*, 15328-15333.
110. Ferandin, Y.; Bettayeb, K.; Kritsanida, M.; Lozach, O.; Polychronopoulos, P.; Magiatis, P.; Skaltsounis, A.-L.; Meijer, L. *J. Med. Chem.* **2006**, *49*, 4638-4649.
111. Malhotra, S.; Balwani, S.; Dhawan, A.; Singh, B. K.; Kumar, S.; Thimmulappa, R.; Biswal, S.; Olsen, C. E.; Van der Eycken, E.; Prasad, A. K.; Ghosh, B.; Parmar, V. S. *Med. Chem. Comm.* **2011**, *2*, 743-751.
112. Singh, A.; Loomer, A. L.; Roth, G. P. *Org. Lett.* **2012**, *14*, 5266-5269.
113. Cao, Y.; Jiang, X.; Liu, L.; Shen, F.; Zhang, F.; Wang, R. *Angew. Chem. Int. Ed.* **2011**, *50*, 9124-9127.
114. Wu, H.; Zhang, L.-L.; Tian, Z.-Q.; Huang, Y.-D.; Wang, Y.-M. *Chem. Eur. J.* **2013**, *19*, 1747-1753.

-
115. Brandman, H. A. *J. Heter. Chem.* **1973**, *10*, 383-384.
 116. Hu, W.-X.; Li, P.-R.; Jiang, G.; Che, C.-M.; Chen, J. *Adv. Synth. Catal.* **2010**, *352*, 3190-3194.
 117. Vanhessche, K. P. M.; Sharpless, K. B. *J. Org. Chem.* **1996**, *61*, 7978-7979.
 118. Mills, J.; Gibson, W. R.; Swanson, E. E. *Proc. Soc. Exp. Biol. Med.* **1957**, *96*, 100-2.
 119. Liu, W.; Lau, F.; Liu, K.; Wood, H. B.; Zhou, G.; Chen, Y.; Li, Y.; Akiyama, T. E.; Castriota, G.; Einstein, M.; Wang, C.; McCann, M. E.; Doebber, T. W.; Wu, M.; Chang, C. H.; McNamara, L.; McKeever, B.; Mosley, R. T.; Berger, J. P.; Meinke, P. T. *J. Med. Chem.* **2011**, *54*, 8541-8554.
 120. Cleij, M.; Archelas, A.; Furstoss, R. *J. Org. Chem.* **1999**, *64*, 5029-5035.
 121. Fujisawa, T.; Watai, T.; Sugiyama, T.; Ukaji, Y. *Chem. Lett.* **1989**, *18*, 2045-2048.